UCLA

UCLA Electronic Theses and Dissertations

Title

Redesign of metabolic pathways for photosynthetic production of n-butanol using cyanobacteria

Permalink

https://escholarship.org/uc/item/3nr53271

Author

Lan, Ethan I.

Publication Date

2013

Peer reviewed|Thesis/dissertation

UNIVERSITY OF CALIFORNIA

Los Angeles

Redesign of metabolic pathways for photosynthetic

production of *n*-butanol using cyanobacteria

A dissertation submitted in partial satisfaction of the

requirements for the degree Doctor of Philosophy

in Biomedical Engineering

by

Ethan I Lan

2013

ABSTRACT OF THE DISSERTATION

Redesign of metabolic pathways for photosynthetic

production of *n*-butanol using cyanobacteria

by

Ethan I Lan

Doctor of Philosophy in Biomedical Engineering

University of California, Los Angeles, 2013

Professor James C. Liao, Chair

As world population increases and fossil fuel-based resource depletes, production of renewable chemical and fuel using microorganisms is an attractive approach to solving both energy and environmental problems. *n*-Butanol has received increasing attention because it is both a potential fuel substitute and an important chemical feedstock, and has been produced by microorganisms from sugars or biomass. However, direct conversion of carbon dioxide into *n*-butanol has never been accomplished. Metabolic engineering of cyanobacteria is often challenging because of their incompletely characterized physiology, limited genetic tools, and a relatively low growth rate. In particular, pathways originating from anaerobes are sometimes difficult to express in cyanobacteria due to enzyme oxygen sensitivity and the difference in their redox environment. As such, no one has demonstrated production of *n*-butanol directly from CO_2

using any microorganism, including cyanobacteria. In this work, we first constructed an *n*-butanol biosynthesis pathway in cyanobacteria and demonstrated the first production of n-butanol from CO_2. However, the production requires anoxic treatment in dark and the inhibition of photosystem II in light (Chapter 2). This difficulty turns out to be originated in both the lack of driving force and the oxygen sensitivity of the key CoA-acylating aldehyde dehydrogenase. We overcomed this difficulty of *n*-butanol production in cyanobacteria by redesigning the pathway with ATP expenditure as a driving force (Chapter 3) and expressing an oxygen tolerant enzyme for converting butyryl-CoA to butyraldehyde (Chapter 4). Instead of using direct acetyl-CoA condensation to synthesize acetoacetyl-CoA, which is the initial metabolite to *n*-butanol synthesis, we redesigned the pathway through using malonyl-CoA with the help of ATP. The final synthetic pathway was constructed using enzymes from five different organisms and accomplished direct photosynthetic *n*-butanol production up to 400 mg/L. These results demonstrate both the feasibility of direct *n*-butanol production from CO_2 and the importance of redesigning pathways according to the characteristics of host metabolism.

With the above success, the next bottleneck resides in the malonyl-CoA synthesis, which is highly regulated across all organisms. Despite several previous attempts in boosting malonyl-CoA synthesis, the results were at best moderately successful. To solve this problem, we redesigned malonyl-CoA biosynthesis (Chapter 6) by constructing pathways that are independent of acetyl-CoA carboxylase, which is used universally for malonyl-CoA synthesis and is highly regulated. We designed several novel pathways, and experimentally demonstrated one route for malonyl-CoA biosynthesis *in vitro* from oxaloacetate in four enzymatic steps: aspartate aminotransferase, aspartate α-decarboxylase, β-alanine aminotransferase, and malonyl-CoA reductase. In particular, the pathway was further improved by using a pyridoxal-5-phosphate-

dependent aspartate α-decarboxylase. This result presents a novel method for engineering malonyl-CoA availablility, which is crucial for the production of fatty acids, polyketides, and flavonoids. In vivo construction of this pathway is currently on-going in our laboratory.

Building on the success of the *n*-butanol pthway in cyanobacteria, we also expand the chemical diversity of microbial products. To test the feasibility of the pathways, we constructed a synthetic recursive chain elongation by expanding on the CoA-dependent pathway in *E. coli*. We further integrated it with acetone biosynthesis and metabolically engineered *E. coli* for production of 2-pentanone (Chapter 5), a methyl ketone with five carbons used as a solvent and flavor additive. The resulting *E. coli* strain produced over 240 mg/L of 2-pentanone.

Together, this work presents a collection of metabolic engineering design principles which enhances our understanding of fundamental evolution of natural pathways and our ability to design new metabolic pathways for the green production of desirable compounds.

The dissertation of Ethan I Lan is approved.

Tatiana Segura

Yi Tang

Todd Yeates

James C. Liao, Committee Chair

University of California, Los Angeles

2013

DEDICATION

This work is dedicated to my parents, Yow-lih Lan and Gillian C. Lan, my lovely wife, Claire R.

Shen, and the rest of my family for their guidance and support. Without them, this would not

have been possible.

TABLE OF CONTENTS

ix

LIST OF FIGURES

LIST OF TABLES

ACKNOWLEDGEMENTS

I would like to thank my advisor Professor James C. Liao for giving me the opportunity to demonstrate myself and for his patience, guidance, and help throughout my Ph.D career. I would also like to thank the other members of my committee, Professors Tatiana Segura, Yi Tang, and Todd Yeates, for their support and advice.

I would like to acknowledge the following people for either their help in developing my skill and mind set as a researcher or their technical assistance.

VITA

2009	B.S., Chemistry University of Maryland, College Park College Park, MD
2007 - 2008	Teaching Assistant Department of Chemistry University of Maryland, College Park
2009 - 2013	Graduate Student Researcher Department of Chemical & Biomolecular Engineering University of California, Los Angeles

PUBLICATIONS AND PRESENTATIONS

Publications

2013
1. Lan, E.I., Ro, S.Y., Liao, J.C., 2013. Oxygen-tolerant Coenzyme A-acylating aldehyde dehydrogenase facilitates efficient photosynthetic *n*-butanol biosynthesis in cyanobacteria. Energy Environ Sci. 6, 2672-2681

2. Lan, E.I., Dekishima, Y., Chuang, D.S., Liao, J.C., 2013. Metabolic engineering of 2-pentanone synthesis in Escherichia coli. AICHE J. 59, 3167-3175.

2012
3. Lan, E.I., Liao, J.C., 2012. Microbial synthesis of *n*-butanol, isobutanol, and other higher alcohols from diverse resources. Bioresour Technol., 135, 339-349.

4. Machado, H.B., Dekishima, Y., Luo, H., Lan, E.I., Liao, J.C., 2012. A selection platform for carbon chain elongation using the CoA-dependent pathway to produce linear higher alcohols. Metab Eng 14, 504-511.

5. Lan, E.I., Liao, J.C., 2012. ATP drives direct photosynthetic production of 1-butanol in cyanobacteria. Proc. Natl. Acad. Sci. USA 109, 6018-6023

2011
6. Dekishima, Y., Lan, E.I., Shen, C.R., Cho, K.M., Liao, J.C., 2011. Extending Carbon Chain Length of 1-Butanol Pathway for 1-Hexanol Synthesis from Glucose by Engineered Escherichia coli. J. Am. Chem. Soc. 133, 11399-11401

7. Lan, E.I., Liao, J.C., 2011. Metabolic engineering of cyanobacteria for 1-butanol production from carbon dioxide. Metab. Eng. 13, 353-363

8. Shen, C.R., Lan, E.I., Dekishima, Y., Baez, A., Cho, K.M., Liao, J.C., 2011. Driving forces enable high-titer anaerobic 1-butanol synthesis in Escherichia coli. Appl. Environ. Microbiol. 77, 2905-2915

Presentations

Lan, E.I., Liao, J.C., Driving Force and Oxygen Tolerance As Design Principles to Enable Efficient Photosynthetic *n*-Butanol Biosynthesis in Cyanobacteria. (Oral presentation). AIChE Annual Meeting, San Francisco, California, USA. Nov. 7, 2013.

Lan, E.I., Shen, C.R., Li, H., Liao, J.C., Direct conversion of CO_2 to fuels and chemicals. (Poster Presentation). University of California, Los Angeles, Henry Samueli School of Engineering and Applied Science Annual Tech Forum, Los Angeles, California, USA. May 8, 2013.

Li, H., Lan, E.I., Liao, J.C., Direct biofuel production from carbon dioxide. (Oral presentation). 245th ACS National Meeting, New Orleans, Louisiana, USA. Apr. 7, 2013.

Lan, E. I., Liao, J.C, ATP driving force as a design principle for photosynthetic production of *n*-butanol. (Poster Presentation). 4th International conference on biomolecular engineering, Ft. Lauderdale, Florida, USA. Jan. 16, 2013.

Lan, E.I., Shen, C.R., Dekishima, Y., Liao, J.C, Pathway design and metabolic engineering for the production of 1-butanol using cyanobacteria. (Oral presentation). 243rd ACS National Meeting, San Diego, California, USA. Mar. 28, 2012.

Lan, E.I., Shen, C.R., Dekishima, Y., Liao, J.C, Metabolic Engineering for 1-Butanol Production From Glucose or Carbon Dioxide. (Oral presentation). AIChE Annual Meeting, Minneapolis, Minnesota, USA. Oct. 20, 2011.

Shen, C.R., Lan, E.I., Dekishima, Y, Baez, A, Cho, K.M., and Liao, J.C., High-flux anaerobic 1-butanol synthesis in Escherichia coli enabled by cofactor driving forces. (Poster Presentation). University of California, Los Angeles, Henry Samueli School of Engineering and Applied Science Annual Tech Forum, Los Angeles, California, USA. Mar, 2011.

1. INTRODUCTION

1.1 Background and Significance

Finite supply of fossil fuel cannot meet the rapidly increasing energy demand of the future. To search for a potential solution to replace fossil fuels, biological production of fuels is one of the most promising approaches. The conventional raw material for bio-based production is sugar and starch, from which ethanol and various other fuels and chemicals can be synthesized. Among the non-ethanol products, of particular interest are compounds that can serve as both fuel and chemical feedstock and are compatible with current infrastructure. *n*-Butanol, isobutanol, and other higher alcohols are some examples. *n*-Butanol and isobutanol are regarded as potential surrogates for gasoline. These compounds have a energy density (27 MJ/L) close to that of gasoline (32 MJ/L) and lower hygroscopicity compared to ethanol. *n*-Butanol is naturally produced by selected species of *Clostridia* (1, 2). Indeed, *n*-butanol production from sugar using *Clostridia* has been commercialized almost a century ago. After a long quiescent period, the interest in bio-production of *n*-butanol and related compounds has re-emerged in recent years. Initially, sugar is still the most common raw material, and efforts have focused on developing more efficient pathways for synthesizing these specific products from glucose. As the bioproduction technology matures, alternative resources such as lignocellulose, macroalgae biomass, waste proteins, syngas, and CO_2, have been explored as renewable raw material to produce these compounds.

To utilize these non-conventional resources for fuel production, the production organism must first convert the raw materials to central metabolites such as pyruvate and acetyl coenzyme A (CoA), which are then diverted to fuel synthesis through engineered pathways. Thus, strain engineering efforts must address problems in both resource utilization and fuel synthesis. To do

so, one can construct the resource utilization pathways into an organism that already produces the desired product, or construct the biofuel production pathways into a host organism capable of metabolizing the desired resource. The choice of the strategies depends on the complexity of the two types of pathways and difficulties in expressing the proteins involved. The lack of well-developed genetic tools and complex physiology in non-traditional host organisms often limit the speed of strain development. Nevertheless, both approaches have demonstrated successful production of biofuel from non-conventional feedstock, lignocellulosic materials, syngas, waste protein, macroalgae biomass, and CO_2.

1.2. Pathways for carbon and energy intake.

To tap into various raw materials, it is important to understand how microorganisms utilize them. Different microorganisms have different requirements to obtain carbon and energy, thus defining their primary nutritional group. Typically, organisms can be classified as autotrophs or heterotrophs. Autotrophs are organisms capable of growth and producing organic compounds from carbon dioxide, whereas heterotrophs require organic carbon as their carbon source as well as energy sources. Resources for heterotrophs include sugar, glycerol, soluble and insoluble polysaccharides, alginates, proteins, and other organic carbons. These organic compounds serve as both carbon and energy source for the heterotrophs, which partially oxidize these organic compounds and to various metabolites and generate reducing equivalents (NAD(P)H) and energy (ATP) in the process. Alternatively, the organic compounds can be completely oxidized to CO_2 for generation of even larger amounts of energy (e.g. via TCA cycle and respiration) and reducing equivalents. A comprehensive diagram connecting various pathways is shown in Fig. 1.1 to demonstrate the interconnection between different
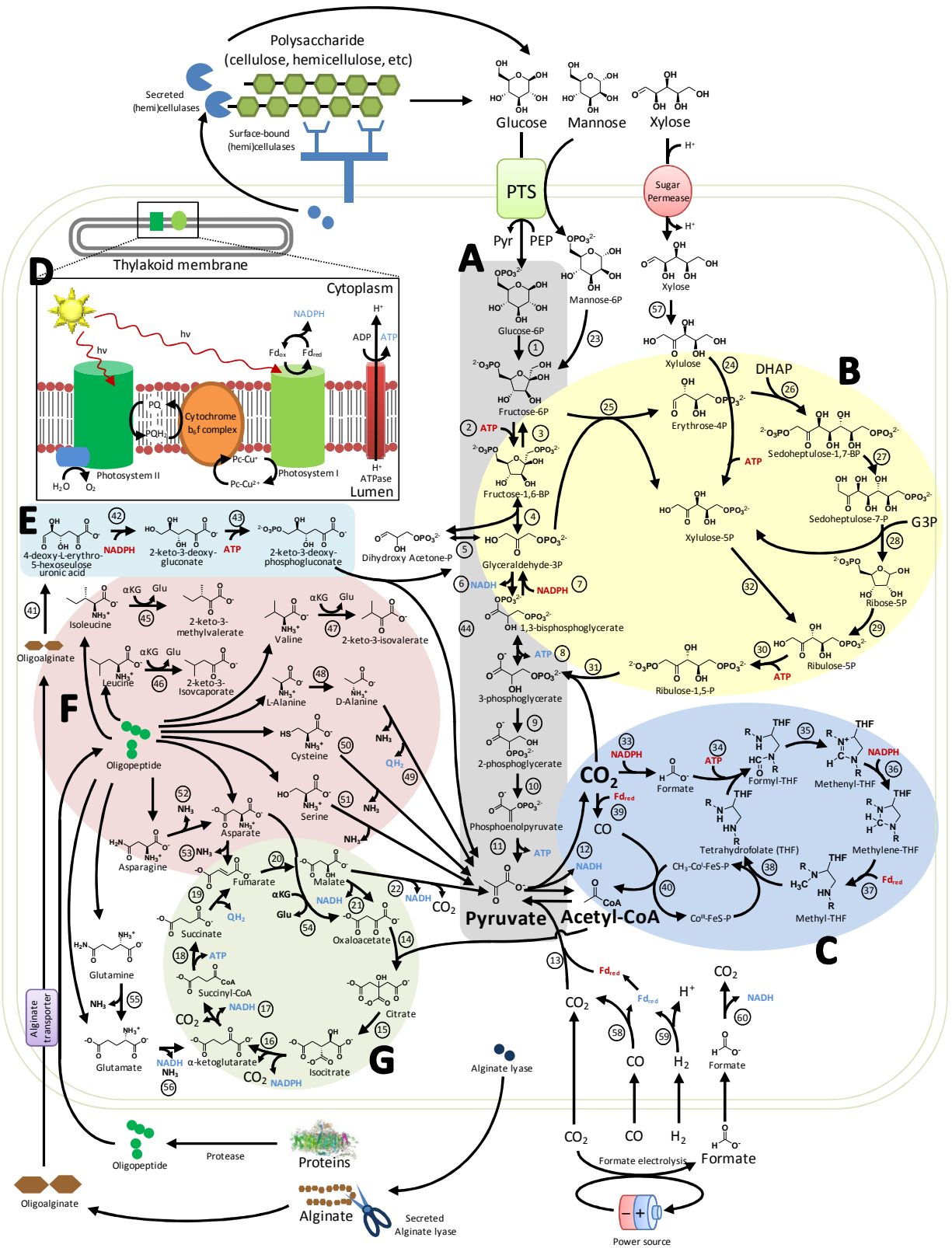
Figure 1.1. Schematic of carbon and energy intake by microorganisms. Energy and reduced electron carrier generation is in blue fonts; consumption is in red fonts. A) glycolysis; B) Calvin cycle; C) reductive acetyl-CoA cycle; D) Photosynthesis; E) alginate degradation and ED

pathway; F) Polypeptide degradation; G) TCA cycle; 1. phosphoglucose isomerase; 2. 6-phosphofructokinase; 3. fructose-1,6-bisphosphatase; 4. fructose bisphophate aldolase; 5. triose phosphate isomerase; 6. glyceraldehyde-3-phosphate dehydrogenase; 7. glyceraldehyde 3-phosphate dehydrogenase; 8. phosphoglycerate kinase; 9. phosphoglycerate mutase;10. enolase; 11. Pyruvate kinase; 12. Pyruvate dehydrogenase; 13. Pyruvate:ferredoxin oxidoreductase; 14. Citrate synthase; 15. Aconitase; 16. isocitrate dehydrogenase; 17. 2-ketoglutarate dehydrogenase; 18. succinyl-CoA synthetase; 19. succinate dehydrogenase; 20. fumarase; 21. malate dehydrogenase; 22. malic enzyme; 23. mannose-6-phosphate isomerase; 24. xylulokinase; 25. transketolase; 26. aldolase; 27. sedoheptulose 1,7-bisphosphatase; 28. transketolase; 29. ribose 5-phosphate isomerase; 30. phosphoribulokinase; 31. ribulose bisphosphate carboxylase; 32. pentose-5-phosphate 3-epimerase; 33. NADP dependent formate dehydrogenase; 34. Formyltetrahydrofolate synthetase; 35. methenyltetrahydrofolate cyclohydrolase; 36. methenyltetrahydrofolate cyclohydrolase; 37. Methylenetetrahydrofolate reductase; 38. methyltetrahydrofolate:corrinoid/iron-sulfur protein methyltransferase; 39. carbon monoxide dehydrogenase; 40. acetyl-CoA synthase; 41. Oligoalginate lyase; 42. DEH reductase; 43. 2-keto-3-deoxy-gluconate kinase; 44. 2-keto-3-deoxy-6-phosphogluconate aldolase; 45. branched-chain amino-acid aminotransferase; 46. branched-chain amino-acid aminotransferase; 47. branched-chain amino-acid aminotransferase; 48. alanine racemase; 49. D-amino acid dehydrogenase; 50. L-cysteine desulfhydrase; 51. L-serine deaminase; 52. asparaginase; 53. aspartate ammonia-lyase; 54. aspartate aminotransferase; 55. glutaminase; 56. glutamate dehydrogenase; 57. xylose isomerase; 58. CO dehydrogenase; 59. Hydrogenase; 60. Formate dehydrogenase; Abbreviations: Pyr, pyruvate; PEP, phosphoenolpyruvate; DHAP, dihydroxy acetone phosphate; G3P, glyeraldehyde-3-phosphate; Fd_{red}, reduced ferredoxin; Fd_{ox}, oxidized ferredoxin.

pathways and metabolites. This diagram shows how external resources (CO_2, syngas, proteins, cellulose, hemicellulose, and alginates) are converted to pyruvate and acetyl-CoA, which are then used for biofuel synthesis. Details of these resource utilization pathways can be found elsewhere (3, 4).

1.3. Pathways for higher chain alcohol synthesis

Biosynthetic pathways for higher alchols elongate and reduce central metabolites such as acetyl-CoA and pyruvate into more electron-rich compounds, higher carbon acyl-CoA and 2-keto acids. These reduced metabolites are then further reduced into higher alcohols and secreted from the microorganism into the solution.

1.3.1 Isobutanol and other 2-keto acid-based higher alcohols

2-Keto acids are common intermediates for amino acid biosynthesis as they are the immediate precursors of amino acids. In particular, the precursor 2-keto acids of the aliphatic amino acids such as valine, isoleucine, and leucine can be diverted to synthesize higher alcohols (Fig. 1.2). The synthetic pathway for isobutanol production (Fig. 1.2 following steps E1 – E2 – E3 – E4 – E5) diverts the carbon fluxes from valine biosynthetic pathway into synthesis of isobutanol (5) by overexpression of 2-ketoisovalerate decarboxylase (KivD) and alcohol dehydrogenase (AdhA). With further overexpression of valine biosynthetic pathway, *E. coli* was engineered to produce 22 g/L of isobutanol, a value exceeding the *n*-butanol produced by most of its native producers, and comparable to the best result (6). Further optimization of isobutanol production in lab scale fermentors with in situ product removal was able to increase the effective production titer of isobutanol to 50 g/L (7). Using valine analog norvaline, a mutant strain of *E. coli* was selected for improved isobutanol productivity (8). Furthermore, to increase isobutanol yield under anaerobic condition, typically NADPH-dependent ketol-acid reductoisomerase (IlvC), second step of the pathway, was engineered to utilize NADH and enabled production of isobutanol at 100% theoretical yield anaerobically (9). Table 1.1 summarizes the strain development for the heterologous production of isobutanol and *n*-butanol using diverse resources. Isobutanol production has also been implemented in other heterotrophs (Table 1.1) such as *Saccharomyces cerevisiae* (0.14 to 0.18 g/L; (10-12)), *Corynebacterium glutamicum* (4.9 to 12.6 g/L; (13, 14)), *and Bascillus subtilis* (2.62 g/L; (15)) using glucose as the substrate.

In addition to isobutanol, 2-methyl-1-butanol (16) and 3-methyl-1-butanol (17) are also produced from naturally occurring 2-keto acids, 2-Keto-3-methylvalerate and 2-keto-4-

Table 1.1. Summary of *n*-butanol and isobutanol production by recombinant organisms

Organism	Target	Carbon source	electron source	energy source	Pathway	Genes overexpressed	Host engineering	Titer	Production Vessel	Reference
Escherichia coli	*n*-Butanol	Glucose	Glucose	Glucose	*Clostridium* CoA pathway	*atoB, hbd, crt, bcd, etfAB, AdhE2*	Δ*adhE*, Δ*ldhA*, Δ*frdBC*, Δ*fnr*, Δ*pta*	0.552 g/L	Flask	(Atsumi, et al., 2008a)
	n-Butanol	Glucose	Glucose	Glucose	Modified CoA pathway	*atoB, hbd, crt, ter, AdhE2, fdh*	Δ*adhE*, Δ*ldhA*, Δ*frdBC*, Δ*pta*	15 g/L, 30 g/L	Test tube and lab scale fermentor	(Shen, et al., 2011)
	n-Butanol	Glucose	Glucose	Glucose	Threonine pathway	*thrA^fbr^BC, ilvA, leuABCD, kivD, ADH2*	Δ*metA*, Δ*tdh*, Δ*ilvB*, Δ*ilvI*, Δ*adhE*	1 g/L	Flask	(Shen and Liao, 2008)
	n-Butanol	Glucose	Glucose	Glucose	Citramalate pathway	*cimA*3.7, leuABCD, kivd, ADH2*	Δ*ilvI*, Δ*ilvB*	524 mg/L	Flask	(Atsumi and Liao, 2008)
	n-Butanol	Glucose	Glucose	Glucose	Reversed β-oxidation	*yqeF, fadB, ydiO, mhpF, fucO*	Δ*yqhD*, Δ*eutE, fadR*, atoC*(c), *crp**	2.2 g/L, 14 g/L	Flask and lab scale fermentor	(Dellomonaco, et al., 2011)
	n-Butanol	Glucose	Glucose	Glucose	Reversed β-oxidation	*atoB, fadB, fadE, adhE*		0.001 g/L	Flask	(Gulevich, et al., 2012)
	n-Butanol	IL-switch grass	IL-switch grass	IL-switch grass	*Clostridium* CoA pathway	*atoB, hbd, crt, bcd, etfAB, AdhE2, osmY-cel, cel3A*	Δ*adhE*	0.028 g/L	Test tube	(Bokinsky, et al., 2011)
Clostridium tyrobutyricum	*n*-Butanol	Mannitol	Mannitol	Mannitol	*Clostridium* CoA pathway	*adhE2*	Δ*ack*	16 g/L	Bottle	(Yu, et al., 2011)
Saccharomyces cerevisiae	*n*-Butanol	Galactose	Galactose	Galactose	*Clostridium* CoA pathway	*thl, hbd, crt, bcd, etfAB, adhE2*		0.0025 g/L	Vials	(Steen, et al., 2008)
Bacillus subtilis	*n*-Butanol	Glycerol	Glycerol	Glycerol	*Clostridium* CoA pathway	*thl, hbd, crt, bcd, etfAB, adhE2*		0.024 g/L	Flask	(Nielsen, et al., 2009)
Pseudomonas putida	*n*-Butanol	Glycerol	Glycerol	Glycerol	*Clostridium* CoA pathway	*thl, hbd, crt, bcd, etfAB, adhE1*		0.122 g/L	Flask	(Nielsen, et al., 2009)
Lactobacillus brevis	*n*-Butanol	Glucose	Glucose	Glucose	*Clostridium* CoA pathway	*thl, hbd, crt, bcd, etfAB*		0.300 g/L	Vials	(Berezina, et al., 2010)
Clostridium ljungdahlii	*n*-Butanol	CO₂/CO	H₂/CO	H₂/CO	*Clostridium* CoA pathway	*thlA, hbd, crt, bcd, adhE, and bdhA*		0.148 g/L	Flask	(Kopke, et al., 2010)
Synechococcus elongatus PCC 7942	*n*-Butanol	CO₂	H₂O	Light	Redesigned CoA pathway	*atoB, hbd, crt, ter, AdhE2*		0.015 g/L	Test tube	(Lan and Liao, 2011)
	n-Butanol	CO₂	H₂O	Light	Malonyl-CoA dependent modified CoA pathway	*nphT7, phaB, phaJ, ter, bldh, yqhD*		0.030 g/L	Flask	(Lan and Liao, 2012)
Escherichia coli	Isobutanol	Glucose	Glucose	Glucose	Valine pathway	*alsS, ilvCD, kivd, adhA*	Δ*adhE*, Δ*frdBC*, Δ*fnr*, Δ*ldhA*, Δ*pta*, Δ*pflB*	22 g/L, 50 g/L	Flask and lab scale fermentor	(Atsumi, et al., 2008b, Baez, et al., 2011)
	Isobutanol	Amino acids	Amino acids	Amino acids	Valine pathway	*alsS, ilvCD, kivd, yqhD, LeuDH, AvtA ilvE, ilvA, sdaB*	High Amino acid consumer; Δ*glnA*, Δ*gdhA*, Δ*lsrA*	4.04 g/L	Flask	(Huo, et al., 2011)
Clostridium cellulolyticum	Isobutanol	Cellulose	Cellulose	Cellulose	Valine pathway	*alsS, ilvCD, kivd, yqhD*		0.660 g/L	Bottle	(Higashide, et al., 2011)
Ralstonia Eutropha	Isobutanol	CO₂	H₂O	electricity	Valine pathway	*alsS, ilvCD, kivd, yqhD*	Δ*phaC1AB1*	0.100 g/L	Bottle	(Li, et al., 2012)
	Isobutanol	CO₂	Formate	Formate	Valine pathway	*alsS, ilvCD, kivd, yqhD*	Δ*phaC1AB1*	0.846 g/L	Lab scale fermentor	(Li, et al., 2012)
Saccharomyces cerevisiae	Isobutanol	Glucose	Glucose	Glucose	Valine pathway	*ILV2, ILV3, ILV5, KDC, ADH*	Δ*PDC1*	0.143 g/L	Flask	(Kondo, et al., 2012)
Corynebacterium glutamicum	Isobutanol	Glucose	Glucose	Glucose	Valine pathway	*ilvBNCD, kivd, adhA, pntAB*	Δ*aceE*, Δ*pqo*, Δ*ilvE*, Δ*ldhA*, Δ*mdh*	12.6 g/L	Flask	(Blombach, et al., 2011)
Synechococcus elongatus PCC 7942	Isobutanol	CO₂	H₂O	Light	Valine pathway	*alsS, ilvCD, kivd, yqhD*		0.450 g/L	Bottle	(Atsumi, et al., 2009)
Bascillus subtilis	Isobutanol	Glucose	Glucose	Glucose	Valine pathway	*alsS, ilvCD, kivd, adh2*		2.62 g/L	Flask	(Li, et al., 2011)
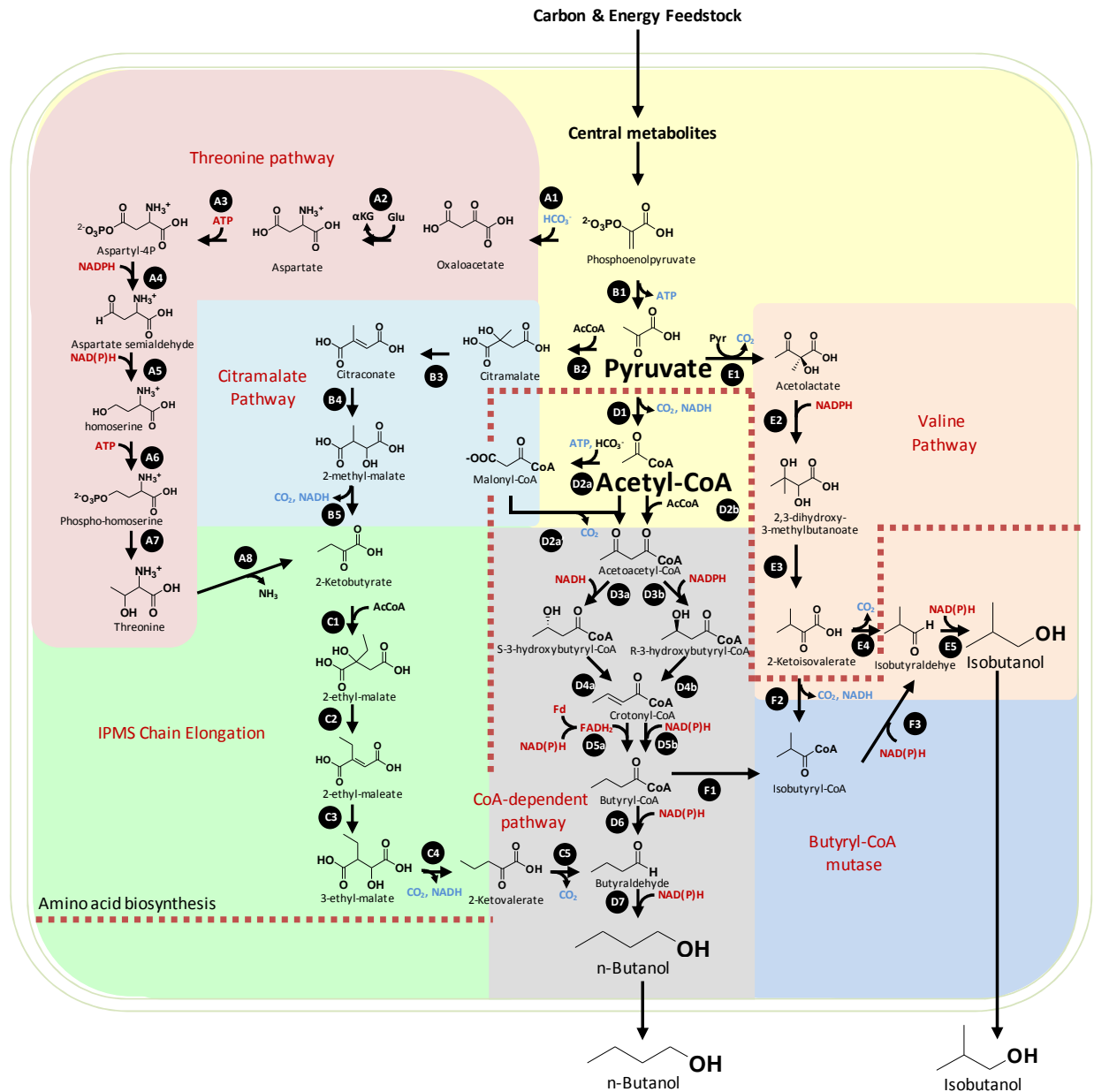
Figure 1.2. Schematic of biosynthetic pathways for *n*-butanol and isobutanol production. Above the red dashed line represents reactions naturally occur in amino acid biosynthesis. A1. phosphoenolpyruvate carboxylase; A2. aspartate transaminase; A3. aspartate kinase; A4. aspartate semialdehyde dehydrogenase; A5. homoserine dehydrogenase; A6. homoserine kinase; A7. threonine synthase; A8. threonine deaminase; B1. pyruvate kinase; B2. citramalate synthase; B3. 2-isopropylmalate hydro-lyase; B4. 2-isopropylmalate hydro-lyase; B5. 3-isopropylmalate dehydrogenase; C1. 2-isoproylmalate synthase; C2. 2-isopropylmalate hydro-lyase; C3. 2-isopropylmalate hydro-lyase; C4. 3-isopropylmalate dehydrogenase; C5. 2-keto acid decarboxylase; D1. pyruvate dehydrogenase; D2a. acetyl-CoA carboxylase; D2a'. acetoacetyl-CoA synthase; D2b. Thiolase; D3a. 3-hydroxybutyryl-CoA dehydrogenase (NADH dependent); D3b. acetoacetyl-CoA reductase (NADPH dependent); D4a. Crotonase; D4b. R-specific enoyl-CoA hydratase; D5a. Butyryl-CoA dehydeogrnase/Electron transferring flavoprotein complex;

7

D5b. trans-2-enoyl-CoA reductase; D6. CoA-acylating aldehyde dehydrogenase; D7. alcohol dehydrogenase; E1. acetolactate synthase; E2. 2,3-dihydroxy-isovalerate: NADP+ oxidoreductase; E3. 2,3-dihydroxy-isovalerate dehydratase; E4. 2-keto acid decarboxylase; E5. alcohol dehydrogenase; F1. butyryl-CoA mutase; F2. branched-chain alpha-keto acid dehydrogenase; F3. CoA-acylating aldehyde dehydrogenase.

methylvalerate, respectively. Synthesis of alcohols longer than 2-methyl-butanol and 3-methyl-buanol requires longer 2-keto acid precursors (Fig. 1.3; for review on carbon chain elongation see (18, 19)). To do so, 2-isopropylmalate synthase (IPMS; LeuA), which is the key enzyme responsible for carbon elongation of 2-keto acid with acetyl-CoA, and KivD were engineered to accept larger substrates (20, 21). As a result, longer chain alcohol such as heptanol and octanol were produced. Figure 1.3 illustrates the diversity of aliphatic higher alcohols that are produced via 2-keto acid-based pathways.

The 2-keto acid based pathway can also produce *n*-butanol by decarboxylating and reducing 2-ketovalerate, which is a precursor to an unnatural amino acid norvaline. 2-Ketovalerate is naturally produced by IPMS chain elongation (Fig. 1.2 following steps C1 – C2 – C3 – C4) of 2-ketobutyrate. 2-ketobutyrate, on the other hand, can be synthesized via two mechanisms. The first mechanism is by deamination of threonine (threonine pathway; Fig. 1.2 following steps A1 – A2 – A3 – A4 – A5 – A6 – A7) and the other mechanism (citramalate pathway; Fig. 1.2 following steps B2 – B3 – B4 – B5), found in *Methanococcus jannaschii*, extend pyruvate to 2-ketobutyrate by IPMS chain elongation. Both the threonine and citramalate pathway were used to produce 0.5 – 1 g/L of *n*-butanol in *E. coli* using glucose (22, 23).
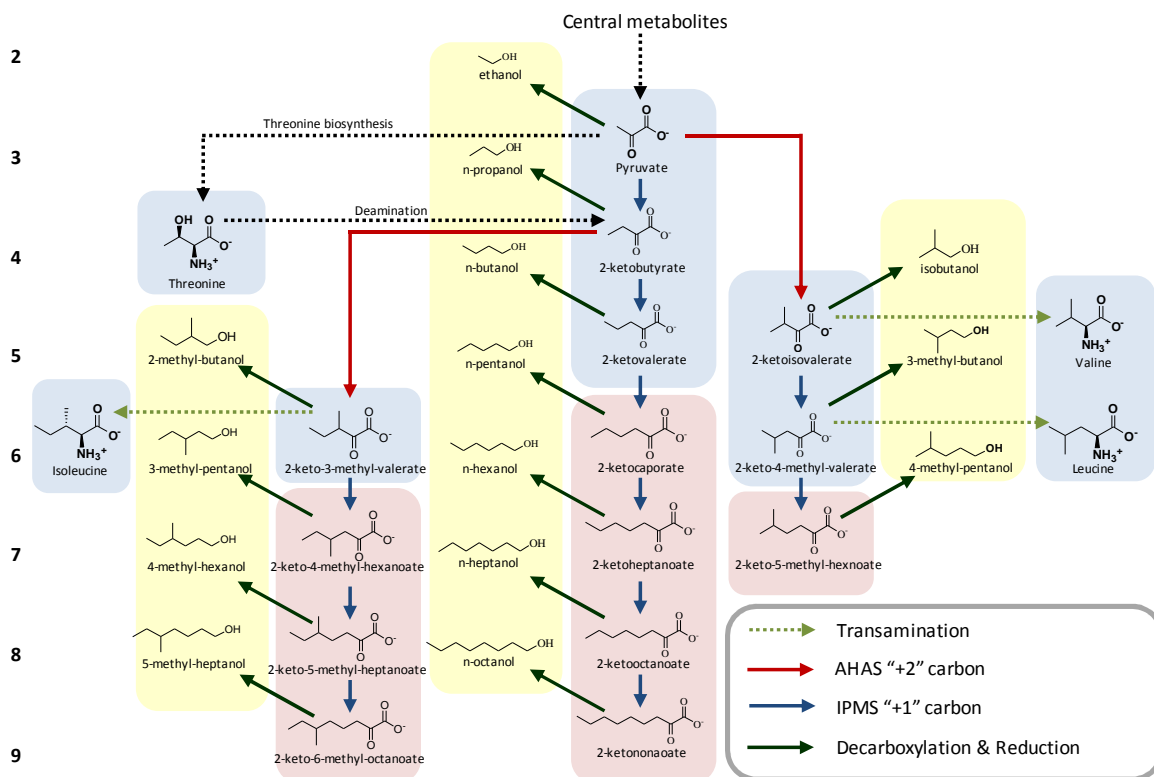
Figure 1.3. 2-Keto acid based production of alcohols. AHAS (Acetohydroxy acid synthase) pathway is catalyzed by IlvIHCD with pyruvate as carbon addition unit. IPMS pathway is catalyzed by LeuABCD with acetyl-CoA as carbon addition unit. Compounds highlighted in blue are natural metabolites; in red are non-natural 2-keto acids; in yellow are alcohols produced from 2-keto acid.

1.3.2. *n*-Butanol and the Coenzyme A -dependent pathway

The natural *n*-butanol biosynthetic pathway from *Clostridia* is mediated by Coenzyme A (CoA). As illustrated in Fig. 1.2, *Clostridium* pathway (Fig 1.2 following steps D2b – D3a – D4a – D5a – D6 – D7) proceeds first by condensation of two acetyl-CoA, followed by reduction and dehydration into *n*-butanol. As an alternative to using *Clostridia* for *n*-butanol production, the *Clostridium n*-butanol production pathway was transferred to other heterotrophs (Table 1.1). These heterotrophs including *Escherichia coli* (24, 25), *Saccharomyces cerevisiae* (26), *Lactobacillus brevis* (27)*, Pseudomonas putida* (28) *and Bacillus subtilis* (28) were able to

produce *n*-butanol from sugars or glycerol. However, the *n*-butanol titers produced from these recombinant heterotrophs are much lower than that of the native *Clostridium* producers by one to two orders of magnitude. One hypothesis that explain this deficiency was that butyryl-CoA dehydrogenase electron transferring flavoprotein (Bcd/Etf) complex (Fig 1.2; step D5a) was poorly expressed in recombinant organisms due to its potential oxygen sensitivity and requirement of ferredoxin as an additional redox partner (29).

The difficulty of functionally expressing Bcd/Etf complex was overcome by recruiting trans-2-enyol-CoA reductase (Ter) for the reduction of crotonyl-CoA (30, 31). Ter is readily expressed in *Escherichia coli* and directly reduces crotonyl-CoA using NADH without requirement of additional ferredoxin partners. This strategy efficiently avoids expression of foreign ferredoxins and couples the production of *n*-butanol to the consumption of glucose as glycolysis generates NADH. Further characterization reveals that reduction of crotonyl-CoA with NADH is an irreversible reaction as opposed to the potentially reversible reaction catalyzed by the FAD mediated Bcd/Etf complex (31). This strategy effectively increased productivity of *n*-butanol in *E. coli* to 800 ~ 1,600 mg/L/d, exceeding the productivity (150 mg/L/d) of the pathway utilizing Bcd/Etf.

While the use of Ter in the CoA-dependent pathway in *E. coli* outperformed the original *Clostridium* pathway, the production titer remains inferior to the native *n*-butanol producers. To increase the productivity of *n*-butanol in heterologous hosts, additional host engineering was required. The successful productions of other alcohols such as ethanol , isopropanol (32, 33), and isobutanol (5, 7) have decarboxylation towards the end of the pathway as a common feature. Decarboxylation effectively drives the reaction equilibrium towards the product as gaseous CO_2

leaves the solution. The lack of a natural driving force possibly explains the low production of *n*-butanol in *E. coli*.

Therefore, to engineer driving forces for *n*-butanol production, synthetic accumulation of the precursor acetyl-CoA and cofactor NADH was achieved by knocking out mixed acid fermentation (Δ*ldh*, Δ*adhE*, and Δ*frd*) and acetate formation (Δ*pta*) (30). Furthermore, formate dehydrogenase (Fdh) was overexpressed to convert formate, product of anaerobic synthesis of acetyl-CoA, into NADH. Together, the accumulation of acetyl-CoA and NADH drives the reaction towards product formation, enabling production up to 15 g/L in titer of fed batch fermentation under anaerobic condition (30). This engineered strain of *E. coli* produced *n*-butanol to a titer comparable to that demonstrated by *Clostridium* producers. To further strengthen the driving force of *n*-butanol production and minimize product toxicity, this engineered strain was tested for a scale up experiment using 1 L chemostat with continuous product removal by gas stripping. The effective titer reached 30 g/L in 7 days with a yield of 70% maximum theoretical (30). This work demonstrates the importance of driving forces in metabolite production.

Utilizing the acetyl-CoA and NADH accumulation driving force constructed in *E. coli*, the CoA-dependent pathway was constructed to increase carbon chain length of butyryl-CoA by condensation with another acetyl-CoA (34). This condensation is catalyzed by 3-keto-thiolase (BktB) from *Ralstonia eutropha*. Upon expression of BktB with the CoA-dependent pathway for *n*-butanol synthesis, n-hexanol production was observed, demonstrating the feasibility of higher chain alcohol production by extension of the CoA-dependent pathway. By designing a selection platform (35) to enhance higher alcohol production using the CoA-dependent pathway, 469 mg/L of n-hexanol and 65 mg/L of n-octanol was produced from *E. coli*.

11

1.3.3 Higher alcohols via reversed β-oxidation pathway

The CoA-dependent pathway resembles the sequence of reactions in β-oxidation in reverse (Fig. 1.4). This reversed β-oxidation is naturally used by *Clostridium kluyveri* to produce hexanoic acid from ethanol. However, the enzymes responsible for the recursive chain elongation are not clearly defined. Reversed β-oxidation (Fig. 1.4) using native enzymes was investigated in *E. coli* (36). To operate the native β-oxidation in reverse, the *fad* and *ato* regulons, encoding the β-oxidation enzymes, must be active without requiring the presence of their natural fatty acid inducers. This phenotype was achieved by creating mutations in transcriptional regulators *fadR*, *atoC*, *crp* and knock out of *arcA*. Upon further knock out of its fermentation pathways (ΔadhE, ΔfrdA, Δpta) (36) and overexpression of native thiolase (YqeF) and alcohol dehydrogenase (FucO), production of *n*-butanol at 1.9 g/L was achieved. Further scale up of *n*-butanol production in lab scale fermentor resulted in a titer of 14 g/L (36). Instead of using acyl-CoA dehydrogenase (FadE) of the native β-oxidation pathway, this reversed β-oxidation sequence requires an uncharacterized enzyme YdiO, a predicted acyl-CoA dehydrogenase, and its associated proteins YdiQRST for the reduction of crotonyl-CoA to butyryl-CoA. YdiQRS are putative flavoproteins, and YdiT is a ferredoxin-like protein, suggesting that the reduction of crotonyl-CoA may be associated with ferredoxin similar to that of the *Clostridium* Bcd/Etf complex. Further overexpression of alcohol dehydrogenase favoring long chain acyl-CoA reduction resulted in the production of long chain alcohols such as octanol (100 mg/L) and decanol (170 mg/L), within the same order of magnitude of fatty alcohol (598.6 mg/L) produced via fatty acid synthesis (37).
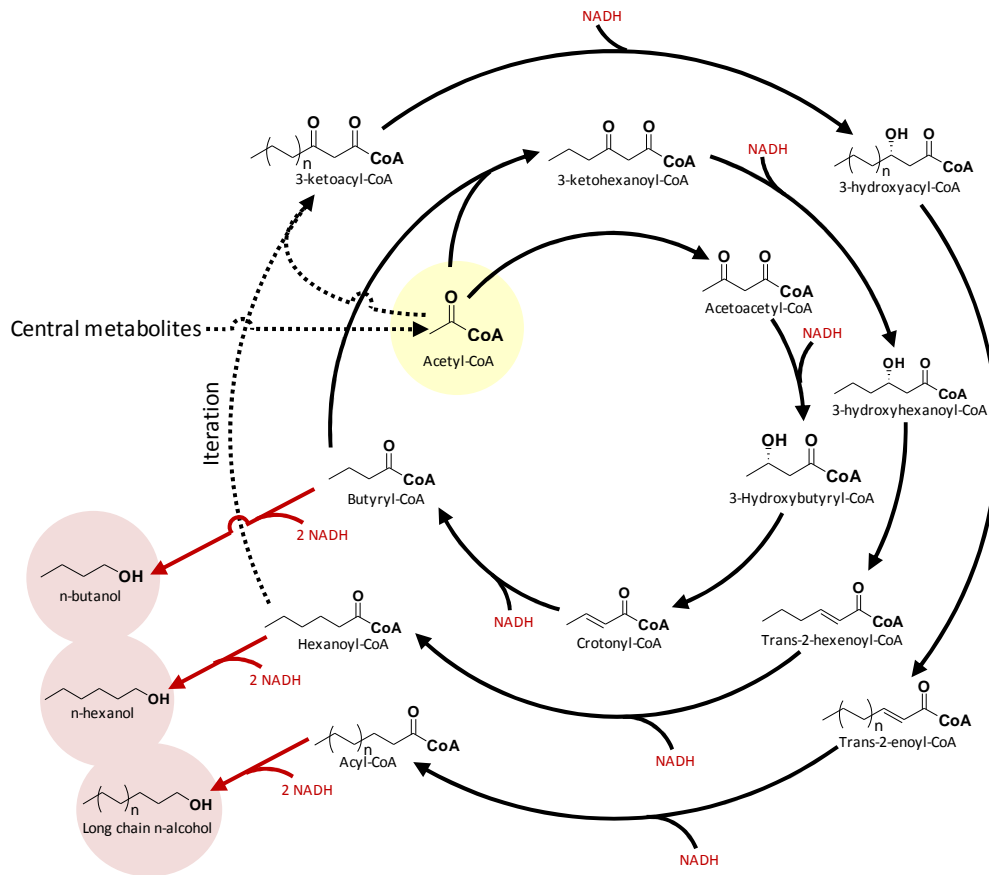
Figure 1.4. Schematics of CoA-dependent reversed β-oxidation. Acetyl-CoA from central metabolism is used as carbon extension unit to elongate carbon chain with 2 carbons at a time. Acyl-CoAs such as butyryl-CoA and hexanoyl-CoA can be reduced into alcohols.

Another study utilizing reversed β-oxidation for *n*-butanol production in *E. coli* resulted in minimal titer of 1 mg/L *n*-butanol produced (38). In this study, FadE was used for the reduction of crotonyl-CoA instead of YdiO, and native bifunctional aldehyde alcohol dehydrogenase (AdhE) was used instead of FucO. Furthermore, mixed acid fermentation pathways were not deleted.

1.4. Butanol production from diverse resources

As the design for efficient higher alcohol production pathways mature, alternative resources such as lignocellulose, waste proteins, syngas, and CO_2, have been assessed as renewable raw material to produce these compounds. In this section, we review the current status of strain engineering for utilization of alternative resources for the production of higher alcohols.

1.4.1. Photosynthesis-based isobutanol production from CO_2

Production of biofuel directly from CO_2 using autotrophs is attractive because it bypasses the difficulty of feedstock recalcitrance. To meet this goal, recombinant cyanobacterium *Synechococcus elongatus* PCC 7942 has been engineered to synthesize isobutanol (39) by using the valine biosynthetic pathway coupled with KivD and an alcohol dehydrogenase YqhD. The *Bacillus subtilis* acetolactate synthase (AlsS) and *E. coli* valine biosynthetic enzymes IlvC and IlvD were overexpressed in *S. elongatus* PCC 7942 to direct carbon flux towards isobutanol production. This engineered strain of *S. elongatus* produced 450 mg/L of isobutanol in 6 days, representing a productivity of higher than 3,000 µg/L/h (39), exceeding current the productivity of hydrogen and ethanol from cyanobacteria and comparable to that of algal diesel productivity (40). It was also demonstrated in the same study that overexpression of RuBisCo was able to increase the isobutyraldehyde, intermediate one step before isobutanol, production up to two fold reaching a final titer of 1.1 g/L of isobutyraldehyde produced at a productivity of 6,230 µg/L/h, demonstrating improvement of photosynthetic rate. Numerous efforts have also been made to construct recombinant cyanobacteria for the production of other fuel and chemical targets (41).

1.4.2 Photosynthesis-based *n*-butanol production from CO_2

n-Butanol production in cyanobacteria using the CoA-dependent pathway is a more challenging task as this pathway comes from strict anaerobes. This section is an overview of what this work as accomplished. To produce *n*-butanol in cyanobacteria, the modified CoA-dependent pathway consisting of AtoB (thiolase), Hbd (3-hydroxybutyryl-CoA dehydrogenase), Crt (crotonase), Ter, and AdhE2 (aldehyde/alcohol dehydrogenase) was recombined into *S. elongatus* PCC 7942 (42). The activities of these enzymes were verified by in vitro assay using crude extract. However, even with functional expression of all enzymes in the pathway, *n*-butanol production was barely detected (42). Only upon anoxic incubation of grown culture, 14.5 mg/L of *n*-butanol was observed in culture broth after 7 days.

To overcome the challenge of producing *n*-butanol in cyanobacteria under photosynthetic condition, additional driving force is needed. Thiolase mediated synthesis of acetoacetyl-CoA is thermodynamically unfavorable with a calculated ΔG' of 27.4 kJ/mol (calculated using eQuilibrator (43) with substrate concentrations of 1 mM, pH 7, and ionic strength of 0.1 M). To overcome this large energy barrier, acetyl-CoA concentration must be much greater than the concentration of acetoacetyl-CoA. This issue was overcome in *E. coli* (30) by constructing the accumulation of intracellular acetyl-CoA and NADH. Accumulation of NADH drives the downstream reactions to synthesis of *n*-butanol, therefore lowering the concentration of acetoacetyl-CoA. The net effect of this engineering is the increased concentration ratio of acetyl-CoA to acetoacetyl-CoA, which effectively drives the synthesis of *n*-butanol. However, this scenario is difficult to recreate in cyanobacteria because accumulation of acetyl-CoA and NADH is challenging.

To circumvent the difficulty of accumulating acetyl-CoA and NADH as a driving force for *n*-butanol synthesis, energy from ATP was used to drive the thermodynamically unfavorable condensation of two acetyl-CoA (44). Acetyl-CoA is activated by ATP and bicarbonate to form malonyl-CoA, which can undergo a decarboxylative condensation with acetyl-CoA to synthesize acetoacetyl-CoA. This ATP mediated condensation of two acetyl-CoA has an overall ΔG' of -13.8 kJ/mol with -9.2 kJ/mol from activation of acetyl-CoA to malonyl-CoA by ATP and -4.6 kJ/mol from decarboxylative condensation of malonyl-CoA and acetyl-CoA. Malonyl-CoA synthesis is catalyzed by acetyl-CoA carboxylase (Acc), which is present in cyanobacteria. However, there is no native enzyme for condensation of malonyl-CoA and acetyl-CoA. Therefore, acetoacetyl-CoA synthase was expressed with the enzymes of the modified CoA-dependent pathway (Fig. 1.2 following steps D2a – D2a' – D3b – D4b – D5b – D6 – D7). As a result, 30 mg/L of *n*-butanol was produced under photosynthetic condition.

1.4.3 Electricity-based isobutanol production from CO_2

Although photosynthetic CO_2 fixation is a natural process, the energy conversion efficiency is limited by the natural photosynthetic apparatus (45). In addition, biofuel production by photoautotrophs requires photobioreactors. The 2-dimensional light-exposing surface is much more costly than the 3-dimensional fermentors that are used to cultivate microbes in the bulk. As an alternative, the light reactions can be separated from the dark reactions (CO_2 fixation and biofuel production). The light reactions can be realized by using man-made photovoltaic cells that are reasonably efficient in converting sunlight into electricity, which can then be used to drive CO_2 fixation in the dark either directly (46) or via an electron mediator (47). Using such a strategy, CO_2 can be reduced to fuels and chemicals without direct photosynthesis. This strategy

also serves as an effective way to store electricity as liquid fuel (47, 48). In this case, electric energy is converted to chemical energy in the form of biofuel.

The use of a diffusible electron mediator is scalable using conventional technologies. To do so, electrical energy first has to be converted into simple electron carrier such as H_2. Chemoautotroph can then utilize the energy stored in H_2 and fix CO_2 and produce biofuel. However, H_2 is not an ideal electron source for microbes because of its low solubility in H_2O and safety concerns. Formate on the other hand is highly soluble in water and can be produced by electrolysis of CO_2 and H_2O (49). Furthermore, formate can also be metabolized by some microorganism to produce NADH and CO_2 by formate dehydrogenase.

To convert electricity into biofuel, *R. eutropha*, a chemoautotroph capable of CO_2 fixation with formate as an energy source, has been engineered to produce isobutanol and 3-methylbutanol in an integrated process of electricity driven biofuel production (47). Isobutanol production genes (*alsS*, *ilvCD*, *kivD*, and *yqhD*) were introduced into *R. eutropha*. The polyhydroxybutyrate, natural carbon storage of *R. eutropha*, biosynthesis pathway was knocked out to redirect the carbon flux to isobutanol. As a result, the isobutanol production pathway served as the new metabolic sink for carbon and reducing equivalent. In order to construct an integrated system with electricity as the energy input, bioreactor design was necessary to remove reactive oxygen species O_2^- and NO, which were identified as by-products of formate electrolysis in that particular medium and inhibit cell growth. As a result, this integrated process was able to produce about 100 mg/L of isobutanol and 50 mg/L of 3-methylbutanol directly from electricity and CO_2 (47). By directly feeding formate, this engineered strain of *R. eutropha* produced 846 mg/L of isobutanol and 570 mg/L of 3-methylbutanol in 130 hours using pH-coupled formic acid feeding fermentor (47).

1.4.4 Syngas-based *n*-butanol production

Syngas is a mixture of CO and H_2 and is used as an energy source for CO_2 fixation by acetogens such as *Clostridium ljungdahlii* (50) and *Clostridium carboxidivorans* (51). Syngas can be produced from renewable resources such as biomass and municipal waste (52). Syngas production and utilization by microorganisms have been previously reviewed (53) and will not be discussed extensively here. *C. carboxidivorans* naturally produces *n*-butanol, ethanol, butyrate and acetate from syngas (51). However, the major product produced by wild type *C. carboxidivorans* is acetate (56 mmol per mol of CO consumed), and *n*-butanol is a minor product (8.9 mmol per mol of CO consumed; (51)). On the other hand, *C. ljungdahlii*, first isolated for its ability to produce ethanol from syngas (54), does not naturally produce *n*-butanol. Upon engineering the CoA-dependent *n*-butanol synthesis pathway from C. acetobutylicum into *C. ljungdahlii*, the resulting strain produced about 0.5 mM of *n*-butanol (50) from syngas. However, it was observed that *n*-butanol was metabolized into butyrate.

1.4.5 Cellulose-based butanol production

Lignocellulose has long been considered to be an attractive source of biological feedstock (55). It commonly exists in plants as cell wall and structural support. Lignocellulosic materials are composed of cellulose, hemicelluloses, and lignin. In particular, cellulose and hemicellulose represent the majority of fermentable carbon composite in these materials (56). Therefore, enzymes and microorganisms capable of degrading cellulose and hemicellulose are of particular interest for biofuel applications. However, the major problem of lignocellulose utilization is the deconstruction of this complex or recalcitrant material. The breakdown of lignocellulose and the strain development for production of chemical and fuel have been reviewed extensively (57-59)

and are not covered here. More cost-efficient methods for the preparation (60) and the fermentation (61) of inexpensive cellulosic substrates have been developed to enhanced the efficiency of the overall process. Furthermore, recent Improvements in the fermentation process such as reduction of operation energy (62) and reuse of wastewater (63) increase the overall efficiency of fermentative butanol production.

To utilize cellulose and hemicellulose, cellulase, xylanase, β-glucosidase, and xylobiosidase were expressed in *E. coli* for utilization and degradation of cellulose and xylan, components of plant biomass (64). In order for *E. coli* to excrete cellulose and xylanase, these enzymes were expressed as protein fusions with OsmY, a protein induced by hyperosmotic stress. The resulting strain cleaves cellulose and xylan into their shorter oligosaccharides cellodextrin and xylodextrins, respectively. To further hydrolyze these oligosaccharides, β-glucosidase, and xylobiosidase were overexpressed. As a result, engineered *E. coli* expressing cellulase (Cel) from *Bacillus* sp. D04 and β-glucosidase (cel3A) from *Cellvibrio japonicus* was able to grow on phosphoric acid swollen cellulose (64). Engineered *E. coli* expressing xylanase (Xyn10B) and xylobiosidase (Gly43F) from *Clostridium stercorarium* was able to grow beechwood xylan, a model substrate for hemicellulose. Upon further expression of *Clostridium* CoA-dependent *n*-butanol synthetic operon, *n*-butanol (28 mg/L) was produced from Ionic liquid treated switch grass (64). In the same study, fatty acid ethyl ester and pinene were also produced.

Alternatively, *Clostridium cellulolyticum*, a mesophilic *Clostridium* with natural cellulose and hemicellulose utilization ability, was engineered to produce isobutanol from crystalline cellulose (55). Isobutanol production pathway (Fig 1.2; (5)) was introduced into *C. cellulolyticum* via borad-host-range plasmid transformation. The resulting strain produced 364 mg/L in 4 days and 660 mg/L in 7 days of isobutanol from cellobiose and cellulose, respectively.

19

1.4.6 Protein-based higher alcohol production

Protein from animal waste such as cattle and poultry litter and manure is often an overlooked resource for potential biofuel production. Amount of animal litter and manure are increasing as the world human population increases. Animal litter and manure are commonly used as fertilizer for crop land because of their richness in nitrogen, phosphorus, and potassium. However, due to accumulation of phosphorus and potassium in crop land (65), there is a limit as to how much animal litter and manure can be used as fertilizer. Excess of animal litter and manure accumulates, and disposal becomes a challenge. Recycling these wastes into biofuel is an attractive solution to this environmental problem.

Utilization of protein as a resource for biofuel production also increases the efficiency of biofuel production because it recycles reduced nitrogen (66). Reduced nitrogen is necessary for the successful development of biofuel as both plant-based and algae-based biofuel productions require reduced nitrogen as fertilizer. Industrially, ammonia is chemically produced via the Haber-Bosch process, an energy intensive process, representing a large energy debt for biofuel production. Furthermore, high-protein containing residuals are commonly used as animal feeds, resulting in increased production of N_2O, a green house gas 300 times worse than CO_2 (67). Therefore the incentive for protein-based biofuel production is potentially substantial.

To utilize protein as the carbon source for biofuel production, an efficient microbe capable of metabolizing protein and its amino acid residues is required. To generate such microbe, an *E. coli* strain was engineered by directed evolution to more efficiently utilize amino acids (68). The resulting strain was able to grow on 13 individual amino acids, as opposed to only 4 amino acids utilized by the wild type, as the sole carbon source. This engineered strain produced 4.06 g/L of higher alcohols including isobutanol, 2-methyl butanol, and 3-methyl

butanol from yeast extract. Furthermore, the cell's ammonia assimilation pathways (*gdhA* and *glnA*) were knocked out and genes responsible for transamination (*leuDH, avtA, ilvE, ilvA*, and *sdaB*) were overexpressed. The net effect of this engineering is the evolution of NH_3, which is excreted from the cell, providing a driving force for amino acid consumption. With further knockouts of quorum-sensing genes, the final engineered strain produced 4 g/L of higher alcohols from amino acids, representing a yield of 55.7% maximum theoretical (68). Huo et al. also demonstrated that up to 3 g/L of higher alcohol were produced from pretreated algal and bacterial biomass as feedstocks.

1.5. Systematic approach for strain development

Strain development for the production of chemicals from engineered organisms can be organized into different levels (Fig. 1.5). The First level focuses on the expression of necessary enzymes. Recombinant protein expression techniques such as modification of gene copy number, codon optimization, and choice of proper strength for promoter and ribosomal bind site (RBS) are some important considerations for functional expression of heterologous pathway. Computational tools such as RBS calculator (69) are useful for designing and controlling expression strength.

Next, pathway optimization is achieved by reducing pathway toxicity (70), knocking out obvious competing pathways, enhancing substrate and cofactor availability (30). In Addition, to enhance the performance of heterologous pathways, a driving force is usually necessary. Driving force such as decarboxylation, product phase separation, and reaction irreversibility effectively favors the formation of the product. These rational design strategies require careful biochemical

Individual gene level

Expression of necessary enzymes
• Gene copy number
• Codon usage
• Promoter strength
• RBS strength
• Enzyme activity

0.1 ~ 1 g/L

Pathway level

Pathway balance
• Cofactor usage
• Pathway toxicity
• Substrate availability
• knock out of obvious competing pathways
• Pathway expression balance and optimization

1 ~ 5 g/L

Driving force
• Substrate and cofactor build up
• Decarboxylation
• Irreversible reactions

15 ~ 30 g/L

Systems level

≥50 ~ 100 g/L

Systems optimization
• muti-omics analysis
• *in silico* models
• knock out of non-obvious pathways
• overexpression of non-obvious enzymes
• High throughput screening
• Directed evolution

Approximate production range

Figure 1.5. Systematic approach of strain development for the production of chemicals from engineered organisms. Production range is shown as approximate values.

consideration and detailed knowledge for the specific pathway and organism in study, and would give sufficient results for proof of principle.

Further optimization of pathway expression requires high-throughput technologies with systems analysis. The "omics" technology and *in silico* models are useful to identify non-obvious competing pathways and additional beneficial enzymes for overexpression. These systematic approaches have been reviewed previously (71, 72) and will not be discussed in detail here. Genomic reconstruction models have been developed for many industrially relevant microorganisms such as butanol-producing *Clostridium beijerinckii* NCIMB 8052 (73) and cyanobacterium *Synechocystis* PCC 6803 (74). The systems level of optimization is a fast growing area of research and can offer opportunities that previous design strategies cannot.

1.6. Summary

Enhanced utilization of non-food-based resources for biofuel production will to continue as a main focus of biofuel research. Utilization of resources including CO_2, waste protein, lignocellulosic material, and syngas, addresses energy and environmental problems, and waste management. Except for lignocellulose, utilization of other resources has not been investigated

extensively. The development of advanced biofuel production from these alternative resources is still a young field. While microbes designed to utilize such alternative resources for producing higher alcohols have shown success, further strain optimizations, especially at the systems level, are needed to improve yield and productivity.

1.7. Reference

1.   Tracy BP, Jones SW, Fast AG, Indurthi DC, & Papoutsakis ET (2012) Clostridia: the importance of their exceptional substrate and metabolite diversity for biofuel and biorefinery applications. Curr Opin Biotechnol 23(3):364-381.

2.   Jang YS, Malaviya A, Cho C, Lee J, & Lee SY (2012) Butanol production from renewable biomass by clostridia. Bioresour Technol.

3.   Caspi R, et al. (2012) The MetaCyc database of metabolic pathways and enzymes and the BioCyc collection of pathway/genome databases. Nucleic Acids Res 40(Database issue):D742-753.

4.   Wargacki AJ, et al. (2012) An engineered microbial platform for direct biofuel production from brown macroalgae. Science 335(6066):308-313.

5.   Atsumi S, Hanai T, & Liao JC (2008) Non-fermentative pathways for synthesis of branched-chain higher alcohols as biofuels. Nature 451(7174):86-89.

6.   Qureshi N & Blaschek HP (2001) Recent advances in ABE fermentation: hyper-butanol producing Clostridium beijerinckii BA101. J Ind Microbiol Biotechnol 27(5):287-291.

7.   Baez A, Cho KM, & Liao JC (2011) High-flux isobutanol production using engineered Escherichia coli: a bioreactor study with in situ product removal. Appl Microbiol Biotechnol 90(5):1681-1690.

8.   Smith KM & Liao JC (2011) An evolutionary strategy for isobutanol production strain development in Escherichia coli. Metab Eng 13(6):674-681.

9.   Bastian S, et al. (2011) Engineered ketol-acid reductoisomerase and alcohol dehydrogenase enable anaerobic 2-methylpropan-1-ol production at theoretical yield in Escherichia coli. Metab Eng 13(3):345-352.

10.   Kondo T, et al. (2012) Genetic engineering to enhance the Ehrlich pathway and alter carbon flux for increased isobutanol production from glucose by Saccharomyces cerevisiae. J Biotechnol 159(1-2):32-37.

11.   Chen X, Nielsen KF, Borodina I, Kielland-Brandt MC, & Karhumaa K (2011) Increased isobutanol production in Saccharomyces cerevisiae by overexpression of genes in valine metabolism. Biotechnology for biofuels 4:21.

12.   Lee WH, et al. (2012) Isobutanol production in engineered Saccharomyces cerevisiae by overexpression of 2-ketoisovalerate decarboxylase and valine biosynthetic enzymes. Bioprocess Biosyst Eng.

13.   Smith KM, Cho KM, & Liao JC (2010) Engineering Corynebacterium glutamicum for isobutanol production. Appl Microbiol Biotechnol 87(3):1045-1055.

14. Blombach B, et al. (2011) Corynebacterium glutamicum tailored for efficient isobutanol production. Appl Environ Microbiol 77(10):3300-3310.

15. Li S, Wen J, & Jia X (2011) Engineering Bacillus subtilis for isobutanol production by heterologous Ehrlich pathway construction and the biosynthetic 2-ketoisovalerate precursor pathway overexpression. Appl Microbiol Biotechnol 91(3):577-589.

16. Cann AF & Liao JC (2008) Production of 2-methyl-1-butanol in engineered Escherichia coli. Appl Microbiol Biotechnol 81(1):89-98.

17. Connor MR & Liao JC (2008) Engineering of an Escherichia coli strain for the production of 3-methyl-1-butanol. Appl Environ Microbiol 74(18):5769-5775.

18. Shen CR & Liao JC (2011) A Synthetic Iterative Pathway for Ketoacid Elongation. Method Enzymol 497:469-481.

19. Felnagle EA, Chaubey A, Noey EL, Houk KN, & Liao JC (2012) Engineering synthetic recursive pathways to generate non-natural small molecules. Nat Chem Biol 8(6):518-526.

20. Zhang K, Sawaya MR, Eisenberg DS, & Liao JC (2008) Expanding metabolism for biosynthesis of nonnatural alcohols. Proc Natl Acad Sci USA 105(52):20653-20658.

21. Marcheschi RJ, et al. (2012) A synthetic recursive "+1" pathway for carbon chain elongation. ACS chemical biology 7(4):689-697.

22. Shen CR & Liao JC (2008) Metabolic engineering of Escherichia coli for 1-butanol and 1-propanol production via the keto-acid pathways. Metab Eng 10(6):312-320.

23. Atsumi S & Liao JC (2008) Directed Evolution of Methanococcus jannaschii Citramalate Synthase for Biosynthesis of 1-Propanol and 1-Butanol by Escherichia coli. Appl Environ Microbiol 74(24):7802-7808.

24. Atsumi S, et al. (2008) Metabolic engineering of Escherichia coli for 1-butanol production. Metab Eng 10(6):305-311.

25. Inui M, et al. (2008) Expression of Clostridium acetobutylicum butanol synthetic genes in Escherichia coli. Appl Microbiol Biotechnol 77(6):1305-1316.

26. Steen EJ, et al. (2008) Metabolic engineering of Saccharomyces cerevisiae for the production of n-butanol. Microb Cell Fact 7(36).

27. Berezina OV, et al. (2010) Reconstructing the clostridial n-butanol metabolic pathway in Lactobacillus brevis. Appl Microbiol Biotechnol 87(2):635-646.

28. Nielsen DR, et al. (2009) Engineering alternative butanol production platforms in heterologous bacteria. Metab Eng 11(4-5):262-273.

29. Li F, et al. (2008) Coupled ferredoxin and crotonyl coenzyme a (CoA) reduction with NADH catalyzed by the butyryl-CoA dehydrogenase/Etf complex from Clostridium kluyveri. J Bacteriol 190(3):843-850.

30. Shen CR, et al. (2011) Driving forces enable high-titer anaerobic 1-butanol synthesis in Escherichia coli. Appl Environ Microbiol 77(9):2905-2915.

31. Bond-Watts BB, Bellerose RJ, & Chang MCY (2011) Enzyme mechanism as a kinetic control element for designing synthetic biofuel pathways. Nat Chem Biol 7(4):222-227.

32. Soma Y, et al. (2012) Direct isopropanol production from cellobiose by engineered Escherichia coli using a synthetic pathway and a cell surface display system. J Biosci Bioeng.

33. Hanai T, Atsumi S, & Liao JC (2007) Engineered synthetic pathway for isopropanol production in Escherichia coli. Appl Environ Microbiol 73(24):7814-7818.

34. Dekishima Y, Lan EI, Shen CR, Cho KM, & Liao JC (2011) Extending Carbon Chain Length of 1-Butanol Pathway for 1-Hexanol Synthesis from Glucose by Engineered Escherichia coli. J Am Chem Soc 133(30):11399-11401.

35. Machado HB, Dekishima Y, Luo H, Lan EI, & Liao JC (2012) A selection platform for carbon chain elongation using the CoA-dependent pathway to produce linear higher alcohols. Metab Eng.

36. Dellomonaco C, Clomburg JM, Miller EN, & Gonzalez R (2011) Engineered reversal of the beta-oxidation cycle for the synthesis of fuels and chemicals. Nature 476(7360):355-359.

37. Zheng YN, et al. (2012) Optimization of fatty alcohol biosynthesis pathway for selectively enhanced production of C12/14 and C16/18 fatty alcohols in engineered Escherichia coli. Microb Cell Fact 11:65.

38. Gulevich AY, Skorokhodova AY, Sukhozhenko AV, Shakulov RS, & Debabov VG (2012) Metabolic engineering of Escherichia coli for 1-butanol biosynthesis through the inverted aerobic fatty acid beta-oxidation pathway. Biotechnol Lett 34(3):463-469.

39. Atsumi S, Higashide W, & Liao JC (2009) Direct photosynthetic recycling of carbon dioxide to isobutyraldehyde. Nat Biotechnol 27(12):1177-1180.

40. Sheehan J (2009) Engineering direct conversion of CO2 to biofuel. Nat Biotechnol 27(12):1128-1129.

41. Machado IM & Atsumi S (2012) Cyanobacterial biofuel production. J Biotechnol.

42. Lan EI & Liao JC (2011) Metabolic engineering of cyanobacteria for 1-butanol production from carbon dioxide. Metab Eng 13(4):353-363.

43. Flamholz A, Noor E, Bar-Even A, & Milo R (2012) eQuilibrator--the biochemical thermodynamics calculator. Nucleic Acids Res 40(Database issue):D770-775.

44. Lan EI & Liao JC (2012) ATP drives direct photosynthetic production of 1-butanol in cyanobacteria. Proc Natl Acad Sci USA 109(16):6018-6023.

45. Zhu XG, Long SP, & Ort DR (2008) What is the maximum efficiency with which photosynthesis can convert solar energy into biomass? Curr Opin Biotechnol 19(2):153-159.

46. Nevin KP, et al. (2011) Electrosynthesis of Organic Compounds from Carbon Dioxide Is Catalyzed by a Diversity of Acetogenic Microorganisms. Appl Environ Microbiol 77(9):2882-2886.

47. Li H, et al. (2012) Integrated electromicrobial conversion of CO2 to higher alcohols. Science 335(6076):1596.

48. Hawkins AS, et al. (2011) Extremely Thermophilic Routes to Microbial Electrofuels. Acs Catal 1(9):1043-1050.

49. Kang P, et al. (2012) Selective Electrocatalytic Reduction of CO2 to Formate by Water-Stable Iridium Dihydride Pincer Complexes. J Am Chem Soc 134(12):5500-5503.

50. Kopke M, et al. (2010) Clostridium ljungdahlii represents a microbial production platform based on syngas. Proc Natl Acad Sci USA 107(29):13087-13092.

51. Bruant G, Levesque MJ, Peter C, Guiot SR, & Masson L (2010) Genomic analysis of carbon monoxide utilization and butanol production by Clostridium carboxidivorans strain P7. PloS one 5(9):e13033.

52. Goransson K, Soderlind U, He J, & Zhang WN (2011) Review of syngas production via biomass DFBGs. Renew Sust Energ Rev 15(1):482-492.

53. Munasinghe PC & Khanal SK (2010) Biomass-derived syngas fermentation into biofuels: Opportunities and challenges. Bioresour Technol 101(13):5013-5022.

54. Tanner RS, Miller LM, & Yang D (1993) Clostridium-Ljungdahlii Sp-Nov, an Acetogenic Species in Clostridial Ribosomal-Rna Homology Group-I. Int J Syst Bacteriol 43(2):232-236.

55. Higashide W, Li Y, Yang Y, & Liao JC (2011) Metabolic engineering of Clostridium cellulolyticum for production of isobutanol from cellulose. Appl Environ Microbiol 77(8):2727-2733.

56. Sun Y & Cheng J (2002) Hydrolysis of lignocellulosic materials for ethanol production: a review. Bioresour Technol 83(1):1-11.

57. Alvira P, Tomas-Pejo E, Ballesteros M, & Negro MJ (2010) Pretreatment technologies for an efficient bioethanol production process based on enzymatic hydrolysis: A review. Bioresour Technol 101(13):4851-4861.

58. Chundawat SPS, Beckham GT, Himmel ME, & Dale BE (2011) Deconstruction of Lignocellulosic Biomass to Fuels and Chemicals. Annu Rev Chem Biomol 2:121-145.

59. Adsul MG, Singhvi MS, Gaikaiwari SA, & Gokhale DV (2011) Development of biocatalysts for production of commodity chemicals from lignocellulosic biomass. Bioresour Technol 102(6):4304-4312.

60. Survase SA, Sklavounos E, Jurgens G, van Heiningen A, & Granstrom T (2011) Continuous acetone-butanol-ethanol fermentation using SO2-ethanol-water spent liquor from spruce. Bioresour Technol 102(23):10996-11002.

61. Lu C, Zhao J, Yang ST, & Wei D (2012) Fed-batch fermentation for n-butanol production from cassava bagasse hydrolysate in a fibrous bed bioreactor with continuous gas stripping. Bioresour Technol 104:380-387.

62. Mariano AP, Maciel R, & Ezeji TC (2012) Energy requirements during butanol production and in situ recovery by cyclic vacuum. Renew Energ 47:183-187.

63. Chen XF, et al. (2012) Oil production on wastewaters after butanol fermentation by oleaginous yeast Trichosporon coremiiforme. Bioresour Technol 118:594-597.

64. Bokinsky G, et al. (2011) Synthesis of three advanced biofuels from ionic liquid-pretreated switchgrass using engineered Escherichia coli. Proc Natl Acad Sci USA 108(50):19949-19954.

65. Edwards DR & Daniel TC (1992) Environmental Impacts of on-Farm Poultry Waste-Disposal - a Review. Bioresour Technol 41(1):9-33.

66. Huo YX, Wernick DG, & Liao JC (2012) Toward nitrogen neutral biofuel production. Curr Opin Biotechnol 23(3):406-413.

67. Crutzen PJ, Mosier AR, Smith KA, & Winiwarter W (2008) N2O release from agro-biofuel production negates global warming reduction by replacing fossil fuels. Atmos Chem Phys 8(2):389-395.

68. Huo YX, et al. (2011) Conversion of proteins into biofuels by engineering nitrogen flux. Nat Biotechnol 29(4):346-351.

69. Salis HM, Mirsky EA, & Voigt CA (2009) Automated design of synthetic ribosome binding sites to control protein expression. Nat Biotechnol 27(10):946-950.

70. Dueber JE, et al. (2009) Synthetic protein scaffolds provide modular control over metabolic flux. Nat Biotechnol 27(8):753-759.

71. Zhang WW, Li F, & Nie L (2010) Integrating multiple 'omics' analysis for microbial biology: application and methodologies. Microbiol-Sgm 156:287-301.

72. Feist AM, Herrgard MJ, Thiele I, Reed JL, & Palsson BO (2009) Reconstruction of biochemical networks in microorganisms. Nat Rev Microbiol 7(2):129-143.

73. Milne CB, et al. (2011) Metabolic network reconstruction and genome-scale model of butanol-producing strain Clostridium beijerinckii NCIMB 8052. BMC systems biology 5:130.

74. Yoshikawa K, et al. (2011) Reconstruction and verification of a genome-scale metabolic model for Synechocystis sp. PCC6803. Appl Microbiol Biotechnol 92(2):347-358.

75. Yu M, Zhang Y, Tang IC, & Yang ST (2011) Metabolic engineering of Clostridium tyrobutyricum for n-butanol production. Metab Eng 13(4):373-382.

2. METABOLIC ENGINEERING OF CYANOBACTERIA FOR N-BUTANOL PRODUCTION FROM CARBON DIOXIDE

2.1. Introduction

While lignocellulose and sugars have been the major source of carbon for microbial production of biofuels (1-3), direct conversion of CO_2 to fuel using photoautotrophic organisms, such as cyanobacteria, has received increasing attention. The readily available genetic tools and genome sequences make cyanobacteria a favored target of metabolic engineering for producing desired products (Fig. 2.1A). For example, cyanobacteria have been demonstrated to produce Isobutyraldehyde (1,100 mg/L), isobutanol (450 mg/L) (4), ethanol (0.021 – 550 mg/L) (5, 6), ethylene (~37 mg/L) (7), isoprene (0.05 mg/g dry cell/day) (8), sugars (~36 mg/L) and lactic acid (~56 mg/L) (9). The relatively high-flux production of isobutanol and isobutyraldehyde (4, 10) demonstrates the feasibility for commercial scale synthesis from CO_2.

n-Butanol is considered as a potential fuel substitute to displace gasoline. The energy density of n-butanol (27 MJ/L) is higher than that of ethanol (21 MJ/L) and closer to that of gasoline (32 MJ/L). In addition, its low hygroscopicity and compatibility with current infrastructure make n-butanol an attractive fuel substitute. n-Butanol is also an important feedstock used to produce various chemicals. To produce one molecule of n-butanol using photosynthesis and the Calvin-Benson cycle, 48 photons are required (See Box 2.1). This photon yield is the same as glucose and isobutanol, and compares favorably to other chemicals such as isoprene and ethylene (Table 2.1). Therefore, it is desirable to produce n-butanol directly from CO_2 and light.

n-Butanol can be produced via two distinct pathways. The synthetic 2-ketoacid pathway utilizes intermediates from amino acid biosynthesis routes (11, 12). 2-ketovalerate, a non-natural intermediate produced by the enzymes LeuABCD of leucine biosynthesis, is decarboxylated and

---

Box 2.1.

Maximum theoretical yield of n-butanol

On average, **200 W/m^2** of solar energy is available on earth. (Brenner, 2008). This equals to **6.32×10^6 kJ/m^2/yr**. However, only a fraction of the total solar energy can be utilized by photosynthetic organisms. The energy used for carbon fixation is limited by photosynthetically inactive spectrum (Zhu, et al., 2008) (51.3% loss of total energy), light reflected and transmitted (green is reflected, 4.9%), and photochemical inefficiency (as a result of energy lost by relaxation of higher excitation state of chlorophyll, 6.6%), photorespiration (6.1%), respiration (1.9%). Therefore, only **29.2%**, corresponding to **1.85×10^6 kJ/m^2/yr**, of the solar irradiation can be used by photosynthetic machinery to produce biological compounds.

48 moles of photons (of energy 173.5 kJ/mol, representing the average energy of 680 nm and 700 nm photons) are required to make one mole of n-butanol **(Fig. 1A)**. This photon yield is calculated by the number of photons needed to fix CO_2 into glyceraldehyde-3-phosphate (G3P) and then the number of G3P and NAD(P)H required to produce n-butanol. 2 photons (one from each photosystem) are required to transfer 1 electron from H_2O to NADP$^+$. Production of NADPH from NADP$^+$ requires two electrons. Therefore 4 photons are required to produce 1 NADPH. 6 NADPH are required to produce 1 G3P from 3 CO_2. Thus 24 photons are required for producing G3P. To produce n-butanol, 2 G3P are required, which is equal to 48 photons.

Therefore,

(48 mol photon/ mol n-butanol) x (173.5 kJ/mol photon) = **8328 kJ/mole n-butanol**

Taking the total energy available for producing compounds (**1.85×10^6 kJ/m^2/yr**), divided by **8328 kJ/mol** yields **221 mol/m^2/yr** , or **16 kg/m^2/yr** , of n-butanol can be produced.
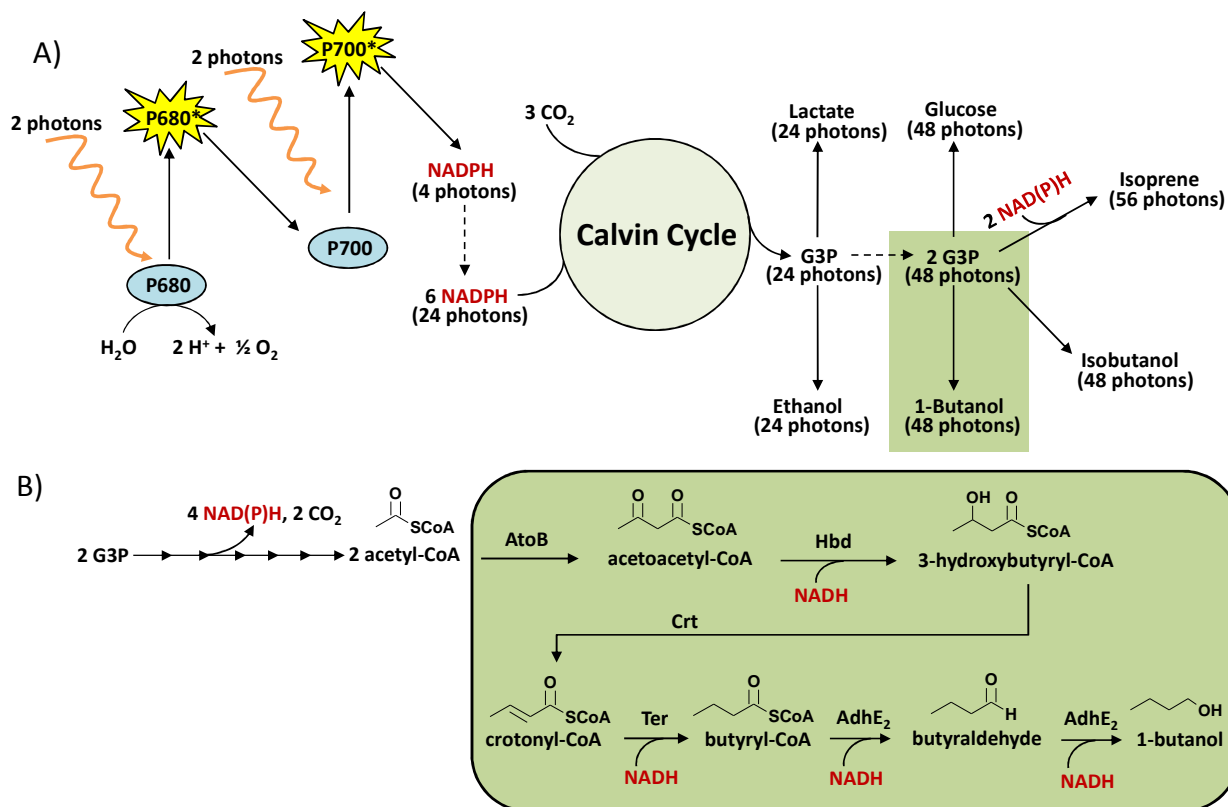
Figure. 2.1. Schematic representation of n-butanol production in engineered *S. elongatus* PCC 7942. A) Light reaction provides NADPH as reductant for carbon fixation into bioproducts. Photons required to produce each product is calculated based on the number of glyceraldehydes-3-phosphate (G3P) and NAD(P)H required. B) The engineered *S. elongatus* 7942 contains heterologous expression of five enzymes for the conversion of acetyl-CoA to n-butanol (boxed in green). AtoB, acetyl-CoA acetyltransferase; Hbd, 3-hydroxybutyryl-CoA dehydrogenase; Crt, crotonase; Ter, trans-2-enoyl-CoA reductase; AdhE2, bifunctional aldehyde/alcohol dehydrogenase.

then reduced to n-butanol. The other pathway synthesizes butyryl-CoA from acetyl-CoA in a pathway similar to fatty acid biosynthesis. Butyryl-CoA is then reduced to n-butanol. This pathway is referred to as the CoA-dependent pathway and is used in nature by various *Clostridium* species to produce n-butanol along with ethanol and acetone.

Among *Clostridium* species, *C. acetobutylicum* and *C. beijerinckii* have been used to ferment carbohydrates into n-butanol (13, 14) with increased butanol tolerance (15) and selectivity over by-products (16, 17). As an alternative, various groups have produced n-butanol

Table 2.1. Photon yields

Compound	Photons required	Maximum yield $(kg/m^2/yr)$
Ethanol	24	20.5
Lactate	24	40.0
Glucose	48	40.0
Ethylene	48	6.2
1-Butanol	**48**	**16.5**
Isobutanol	48	16.5
Isoprene	56	13.0

using the CoA-dependent pathway by non-native hosts, including *Escherichia coli (550 – 1,200 mg/L) (18-20), Saccharomyces cerevisiae (2.5 mg/L) (21), Lactobacillus brevis (300 mg/L) (22), Pseudomonas putida (120 mg/L) and Bacillus subtilis (24 mg/L) (20). The* related pathway for production of isopropanol has also been transferred to *E. coli* (23). The native *Clostridium* n-butanol formation pathway consists of seven enzymes: Thiolase (Thl), 3-hydroxybutyryl-CoA dehydrogenase (Hbd), crotonase (Crt), butyryl-CoA dehydrogenase (Bcd), electron transferring protein A and B (EtfAB), and bifunctional aldehyde alcohol dehydrogenase (AdhE2). In particular, Bcd/EtfAB catalyzes the hydrogenation of crotonyl-CoA to butyryl-CoA and is coupled to ferredoxin reduction (24). This enzyme complex has not been expressed well in heterologous hosts and is oxygen sensitive (18-20, 22, 25). In addition, Bcd/Etf complex may require *Clostridial* ferredoxins to function at its optimum. Recently Shen et al. (2011) obtained high yield (88% of theoretical) and high flux production with an effective titer up to 30 g/L of n-butanol in *E. coli* by streamlining both carbon flux and reducing cofactors using acetyl-CoA and NADH driving forces coupled with the NADH-dependent trans-enoyl-CoA reductase (Ter) (26). The use of Ter effectively avoids the problems of expressing *Clostridium* Bcd/EtfAB complex as well as by-passing the need for expressing *Clostridial* ferredoxins.

No reports thus far have engineered autotrophic organisms to produce n-butanol. Expression of the CoA-dependent pathway is challenging for cyanobacteria in many aspects. Since this pathway is derived from strict anaerobes, expressing such a pathway into cyanobacteria, which

produce oxygen during photosynthesis, is challenging as enzymes involved may be negatively affected by the presence of oxygen. In addition, heterologous protein expression requires careful modulation. Unfortunately, the ability to control gene expression in cyanobacteria is limited. In this article, we successfully express all of the genes in the CoA-dependent n-butanol pathway in *S. elongatus 7942* and achieved n-butanol production from CO_2 and light. We introduce (Fig. 2.1B) *hbd*, *crt*, and *adhE2* genes from *C. acetobutylicum*, the *ter* gene from *T. denticola*, and the *atoB* gene from *E. coli* into wild-type *S. elongatus* 7942. AtoB is selected for this work because it has been demonstrated to outperform Thl in previous *E. coli* results (18, 27) . In addition, AtoB (28) has been shown with higher specific activity (1078 U/mg) when compared to Thl (216 U/mg) (29). Interestingly, polyhistidine-tag increases the expression of T.d-Ter, which enhances n-butanol production. By inhibiting the cyanobacteria's oxygen evolving capability after growth, we demonstrate the first production of n-butanol in cyanobacteria.
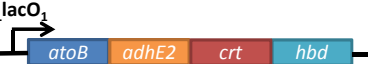
2.2. Results

2.2.1. Expression of n-butanol pathway genes.

The five genes required for n-butanol production, *atoB*, *hbd*, *crt*, T.d-*ter*, and *adhE2*, were cloned into two separate plasmids, pEL5 and pEL14, designed for recombination at NSI (31) and NSII (32) of the *S. elongatus* 7942 genome (Table 2.2). Plasmid pEL5 targeted NSI and harbored *atoB* and *adhE2* under an IPTG inducible promoter, Ptrc, with spectinomycin as the antibiotic selection marker. Plasmid pEL14 targeted NSII and harbored *T.d-ter*, *crt*, *hbd* under another IPTG inducible promoter, $P_L$lacO$_1$, with kanamycin as the selection marker. The gene insertions (Fig. 2.2A) were then verified by whole cell colony PCR (Fig. 2.2B) of transformants obtained

on antibiotic selection plates. The resulting recombinant strain EL1 (Fig 2.2A) was cultured in

liquid BG-11 medium for enzyme assay.

A

Strain	Modification on Ter	NSI	NSII	Ter activity (U/mg)	Butanol production (mg/L)
EL1	Original	Ptrc — *atoB* *adhE2*	$P_L lacO_1$ — *T.d-ter* *crt* *hbd*	0.0021	3.04 ± 0.41
EL7	Codon optimized for *S. elongatus* 7942	Ptrc — *atoB* *adhE2*	$P_L lacO_1$ — *T.d-ter$_{op}$* *crt* *hbd*	0.019	3.67 ± 0.33
EL13	Gene rearrangement	Ptrc — *T.d-ter* *hbd* *crt*	$P_L lacO_1$ — *atoB* *adhE2*	0.057	11.58 ± 0.58
EL14	Gene rearrangement + His-tag	Ptrc — His-*T.d-ter*	$P_L lacO_1$ — *atoB* *adhE2* *crt* *hbd*	0.41	13.16 ± 0.40

B
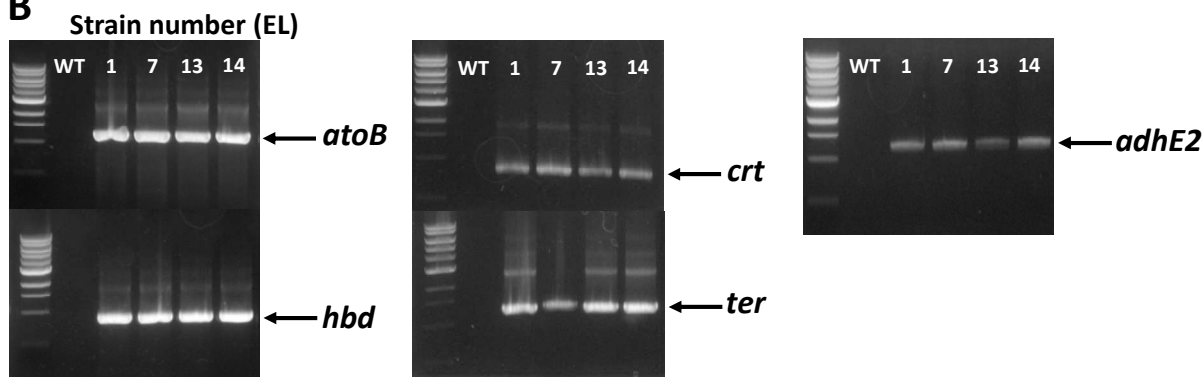
Figure. 2.2. Recombinant S. elongatus strain design. A) Schematics of gene arrangements in different strains that contain all of the n-butanol production genes. Thiolase (*atoB*), aldehyde/alcohol dehydrogenase (*adhE2*), crotonase (*crt*), hydroxybutyryl-CoA dehydrogenase (*hbd*), trans-enoyl-CoA reductase (T.d-*ter*), codon optimized Ter (T.d-*ter$_{op}$*), His-tagged Ter (His-*T.d-ter*). Error for Ter specific activity is listed in Table 4. One unit (U) is defined as μmol/min. B) Whole cell PCR with gene-specific primers demonstrated the integration of each gene into the recombinant *S. elongatus* 7942 strains.

Crude extract of strain EL1 was assayed for each enzymatic reaction in the pathway. All

enzyme activities were detected (Table 2.2). Specific activities of AdhE2 and Ter (Table 2.2)

were two orders of magnitude lower than that of other enzymes in the pathway. The enzyme assay associated with AdhE2 has been previously conducted under anoxic condition (36, 37), indicating its potential oxygen sensitivity. However *S. elongatus* 7942 generates oxygen during photosynthesis. Thus AdhE2 within *S. elongatus* 7942 were expected to receive exposure of oxygen, which may have led to its reduction of activity. Therefore, we sought to investigate the potential oxygen sensitivity of AdhE2 by comparing its activities under oxic and anoxic conditions. The result (Table 2.3) of anoxic AdhE2 enzyme assay was consistent with the result obtained from the oxic assay, indicating that low AdhE2 activities were not completely due to oxygen sensitivity. Nevertheless, relative specific activities of AdhE2, to other enzymes, were

Table 2.2. Enzymatic activities of different strains cultured oxygenically

Enzyme	Strains					
	Wild-type	EL1	EL7	EL13	EL14	*E. Coli**
AtoB	n.d.	0.41 ± 0.02	0.20 ± 0.02	3.20 ± 1.0	0.18 ± 0.01	17 ± 2
Hbd	n.d.	0.27 ± 0.002	0.27 ± 0.06	0.29 ± 0.10	0.64 ± 0.29	4.6 ± 0.8
Crt	n.d.	7.92 ± 0.04	2.90 ± 1.3	2.90 ± 1.5	8.8 ± 4.6	97.9 ± 13.6
Ter	n.d.	0.0021 ± 0.0015	0.019 ± 0.002	0.057 ± 0.005	0.41 ± 0.25	3.7 ± 0.5
AdhE2 (Bldh)	n.d.	0.0042 ± 0.0010	0.0044 ± 0.0014	0.0034 ± 0.0010	0.0011 ± 0.0010	0.014 ± 0.001
AdhE2 (Bdh)	0.0021	0.0084 ± 0.0010	0.0086 ± 0.0010	0.0079 ± 0.0010	0.0031 ± 0.0010	0.007 ± 0.001

n.d. not detected. Specific activity is given in μmol/min/mg crude extract. AtoB, acetyl-CoA acetyltransferase; Hbd, 3-hydroxybutyryl-CoA dehydrogenase; Crt, crotonase; Ter, trans-2-enoyl-CoA reductase; Bldh, butyraldehyde dehydrogenase; Bdh, butanol dehydrogenase.
*Data from Shen et al. (2011)

comparable to that observed in *E. coli* (Table 2.2) by Shen et al. (2011). On the other hand, T.d-Ter activity, in contrast to the other enzymes, was significantly lower than expected when compared to previous *E. coli* results (27), which demonstrated T.d-Ter activity comparable to

that of AtoB and Hbd in the high n-butanol producing *E. coli* strain. Therefore these data suggested that T.d-Ter could be potential limiting steps for producing n-butanol.

2.2.2. Improvement of Ter activity.

To investigate the cause of low Ter activity, several approaches were taken. Ter homologues from *Treponema vincentii, Fibrobacter succinogenes, Flavobacterium johnsoniae, and E. gracilis* (38) have been identified based on sequence similarity with T.d-Ter. In particular, *E. gracilis* Ter (E.g-Ter) has been expressed in recombinant *E. coli* (38), indicating its potential for expression in other heterologous hosts. The two Ter homologues (from *T. denticola* and *E. gracilis*) were polyhistidine-tagged and expressed in *S. elongatus* 7942. His-*T.d-ter* and His-*E.g-ter* were separately cloned into two plasmids, pEL30 and pEL31, respectively. The two plasmids were then used to recombine the respective *ter* into wild-type *S. elongatus* 7942 at the NSI site. The resulting strains, EL9 with His-T.d-Ter and EL10 with His-E.g-Ter, were analyzed for their Ter expression by both Western blot and enzyme assay. Western blot (Fig. 2.3A) with His-tag specific probe showed expression of both His-T.d-Ter and His-E.g-Ter. The expression of His-T.d-Ter was higher than that of His-E.g-Ter as indicated by the thicker band in Western blot analysis (Fig. 2.3A). Furthermore, the expression of both His-T.d-Ter and His-E.g-Ter was analyzed by their *in vitro* activity (Fig. 2.3B). Interestingly, strain EL9, expressing His-T.d-Ter, showed Ter specific activity (0.444 µmol/min/mg) comparable to the activities of the other enzymes (Table 2.2) initially observed in strain EL1. This activity exceeded the Ter activity observed from EL1 by more than 100-fold. The His-E.g-Ter, on the other hand, demonstrated lower specific activity (0.065 µmol/min/mg) most likely due to less expression. The other genes of the pathway were then integrated into EL9 at NSII, resulting in Strain EL14.
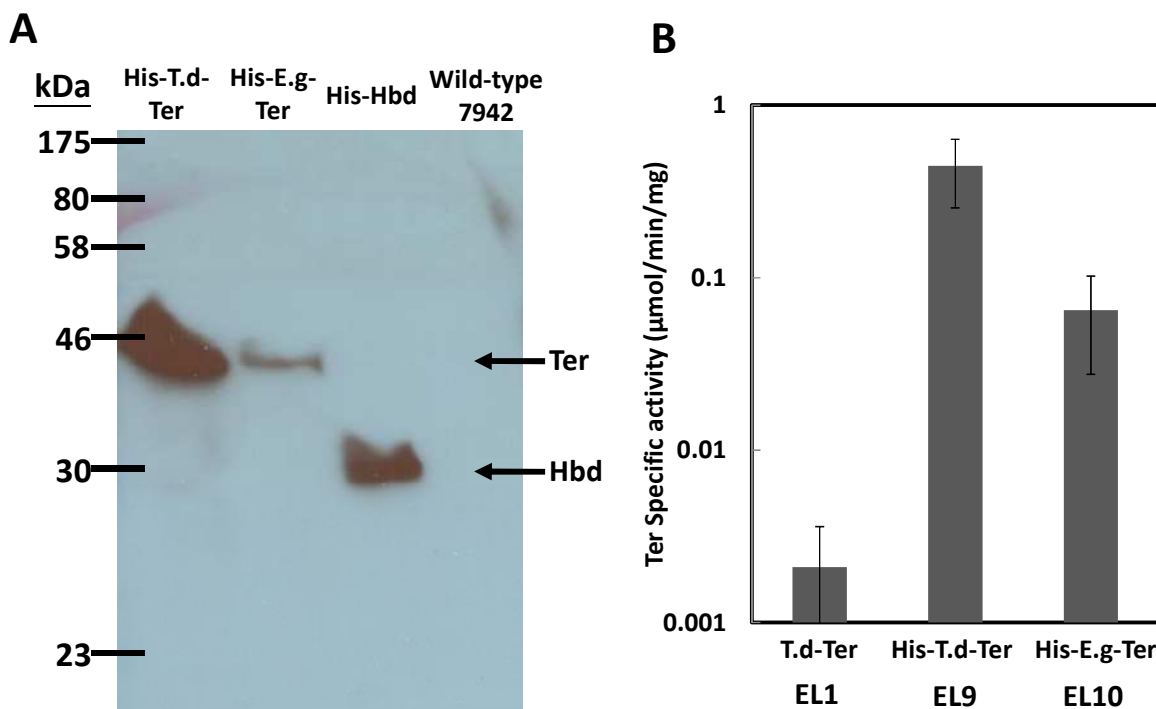
Figure 2.3. Expression of His-tagged *T. denticola* and *E. gracilis* Ter demonstrated by enzymatic activity and western blot. A) Analyzed protein samples were soluble fraction of crude extract from recombinant *S. elongatus 7942* strains expressing individual enzymes. Lane 1, from the left, EL9 expressed His-tagged *T. denticola* Ter. Lane 2, EL10 expressed His-tagged *E. gracilis* Ter. Lane 3, EL11 expressed His-tagged *C. acetobutylicum Hbd*. Lane 4, crude extract from wild-type *S. elongatus 7942*, showing the absence of non-specific binding of the His-specific probe. B) Ter specific activity of three different strains. In particular, Strain EL9, expressing His-T.d-Ter, demonstrated highest activity which is more than 100-fold higher than that of Strain EL1 which expressed T.d-Ter.

Simultaneously, we varied gene arrangement and optimized codon usage of T.d-*ter* for *S. elongatus 7942*, attempting to improve its activity or expression. Strain EL13 (Fig. 2.2A) contained every gene in the pathway at NSI under promoters Ptrc and $P_L$lacO$_1$. Strain EL7 (Fig. 2.2A) was constructed with the same gene configuration as strain EL1 with the substitution of *T.d-ter* with its codon-optimized version (T.d-ter$_{op}$). These strains were assayed for their enzyme activities from both oxic and anoxic incubated cultures (Table 2.2 and Table 2.3). Ter activity was highest in strain EL14 (Fig. 2.2A), which expressed His-T.d-Ter. Therefore strain EL14 was used as the potential production strain.

Table 2.3. Enzymatic activities of different strains after anoxic incubation

Enzyme	Strain s				
	Wild-type	EL1	EL7	EL13	EL14
AtoB	n.d.	0.46 ± 0.13	0.44 ± 0.18	4.71 ± 1.34	0.68 ± 0.19
Hbd	0.012 ± 0.005	0.31 ± 0.10	0.91 ± 0.22	1.08 ± 0.22	0.91 ± 0.16
Crt	n.d.	9.79 ± 3.49	26.56 ± 9.76	35.71 ± 9.63	17.06 ± 4.43
Ter	n.d.	0.017 ± 0.005	0.023 ± 0.006	0.18 ± 0.06	1.12 ± 0.22
AdhE$_2$ (Bldh)	n.d.	0.0054 ± 0.0050	0.0048 ± 0.0040	0.0027 ± 0.0033	0.0010 ± 0.0016
AdhE$_2$ (Bdh)	n.d.	0.0022 ± 0.0007	0.0023 ± 0.0004	0.0011 ± 0.0001	0.0003 ± 0.0001

n.d. not detected. Specific activity is given in µmol/min/mg crude extract. AtoB, acetyl-CoA acetyltransferase; Hbd, 3-hydroxybutyryl-CoA dehydrogenase; Crt, crotonase; Ter, trans-2-enoyl-CoA reductase; Bldh, butyraldehyde dehydrogenase; Bdh, butanol dehydrogenase.

2.2.3. Dark anoxic incubation led to production of n-butanol.

Strain EL14 was tested for n-butanol production under standard oxygenic incubation in constant light exposure. However, no n-butanol production was observed both in screw-capped flasks and air-bubbling cultures. To test the effect of oxygen on the production of n-butanol, we investigated in different culturing conditions. Strain EL14 was grown under light with continuous bubbling of 5% CO_2 with 95% N_2 intended to remove oxygen from the culturing system. However, the effect seemed small as the culture accumulated only 2.2 mg/L (data not shown) of n-butanol at the end of two weeks of growth. This result suggested that anoxic condition may aid butanol production in *S. elongatus* 7942. We then raised the question of perhaps bubbling CO_2/N_2 mixed gas was insufficient to remove oxygen generated from photosynthesis. Therefore, to further reduce oxygen exposure, a grown culture (OD_{730} of 4.3) of EL14 was incubated in dark anoxic condition (Fig. 2.4). n-Butanol accumulation reached 14.5
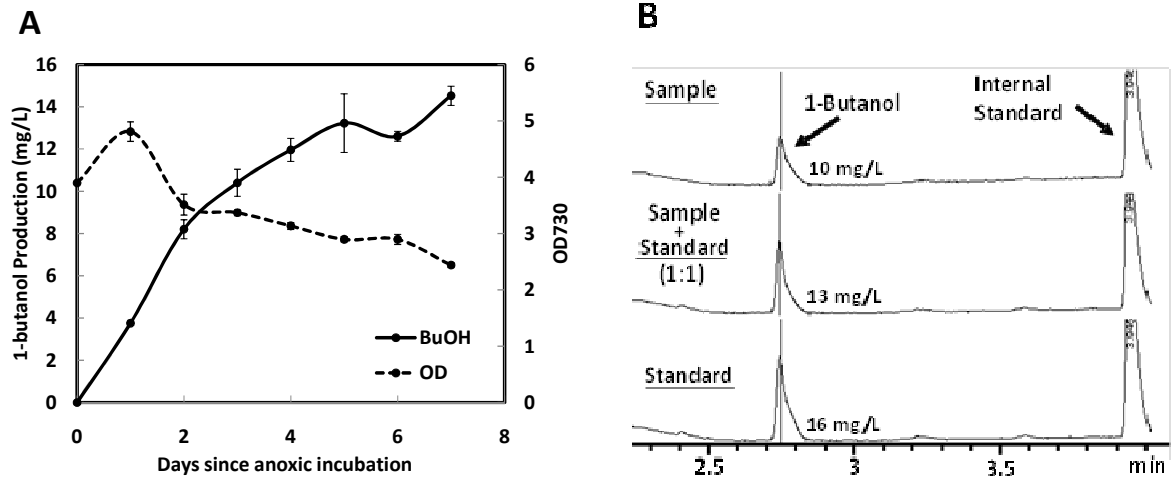
Figure 2.4. n-Butanol production from anoxically incubated strain EL14 in Dark. n-Butanol accumulated in culture medium to 14.5 mg/L with continuous decrease of cell density from OD_{730} of 3.9 to OD_{730} of 2.4. Solid line represents n-butanol accumulation. Dashed line represents cell density measured by OD_{730}. Error bars represent standard deviation of triplicate experiments. B) GC measurement of n-butanol accumulation in culture medium. Spiking the sample with 0.002% v/v butanol (1:1 volume ratio) showed complete overlap and consistent increment of n-butanol peak. Internal standard used was 0.1% 2-methyl-pentanol.

mg/L in seven days while the cell density declined from OD_{730} of 3.9 to 2.4. This result suggested that the production of n-butanol in *S. elongatus* 7942 is oxygen sensitive.

To test the effect of Ter activity on n-butanol production, strains EL1, EL7, EL13, and EL14 (Fig. 2.2A) were incubated in the dark anoxic condition. Results (Fig. 2.2A) showed that EL14 and EL13 produced much better than EL1 and EL7. The production from these different recombinant strains positively correlated with their Ter activities (Table 2.3), indicating that this enzymatic step is important in the pathway. However, EL13 and EL14 produced comparable amount of n-butanol while Ter activity of EL13 was about 10-fold lower than that of EL14. This result indicated that some other bottleneck exists in the pathway. Nevertheless, we demonstrated here that sufficient Ter activity more efficiently directs carbon flux to n-butanol.

40
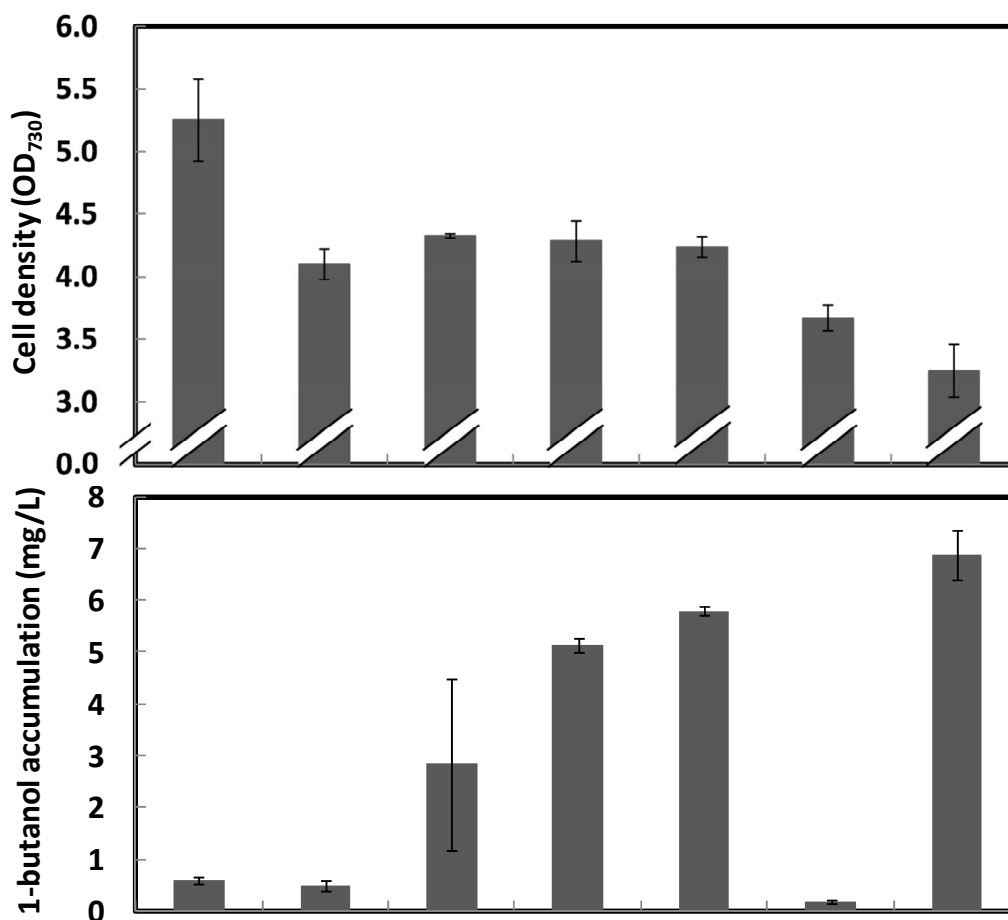
Light Condition	Light					Dark	
Aerobicity	Oxic		Anoxic			Oxic	Anoxic
DCMU		20 µM	5 µM	20 µM	40 µM		

Figure 2.5. Condition comparison for n-butanol accumulation in recombinant cyanobacteria strain EL14. n-Butanol accumulation was higher under anoxic condition. Amount of DCMU added had positive correlation with amount of n-butanol produced. Culture was incubated under various conditions after 2 weeks of growth in light with continuous bubbling of 5% CO_2 and 95% N_2 until OD_{730} of 4.3. Error bars represent standard deviation of triplicate experiments. Initial culture cell density was OD_{730} of 4.3

2.2.4. Oxygen inhibits n-butanol production

To further test the effect of oxygen, 3-(3,4-dichlorophenyl)-1,1-dimethylurea (DCMU) was used to inhibit photosystem II (PSII). DCMU blocks the plastoquinone binding site of PSII,

efficiently inhibiting PSII's function and ability to generate oxygen under light. DCMU was added to both oxic and anoxic culture of strain EL14 in continuous light to test if oxygen inhibits the n-butanol synthesis. If the lack of production in standard light oxygenic condition was due to light-induced regulation, rather than oxygen, then both light oxic and light anoxic culture with DCMU would not produce n-butanol. However, n-butanol accumulated in the light anoxic culture with DCMU (Fig. 2.5), suggesting that oxygen, rather than light, inhibited the production. The amount of n-butanol accumulated in the culture medium positively correlated with the amount of DCMU added (Fig. 2.5). This correlation indicated that 5 μM of DCMU only partially inhibited photosystem II, allowing the ability of the cells to produce small amounts of oxygen. The cell densities of these cultures remained constant for the 5 days period, maintaining at around OD_{730} of 4.3 (Fig. 2.5), indicating the ability of the cell to use photosystem I to maintain cellular functions. These results suggested that oxygen plays an important role in the production of n-butanol in cyanobacteria. Elimination of oxygen was required for n-butanol production.

2.3. Discussion

Production of chemicals and fuels from CO_2 is advantageous for reducing carbon emission as well as reducing reliance on petroleum. In this work, we achieved production of n-butanol from CO_2 and light. Theoretically, at least 48 photons (Box 2.1) are required for producing one n-butanol. This photon requirement is identical to that of glucose (Table 2.4). Thus, it is advantageous to produce n-butanol directly from light rather than harvesting glucose and converting glucose to n-butanol. The per photon value of n-butanol (Table 2.4) is higher than that of sugar and octane (39).

Among the CoA-dependent n-butanol biosynthesis reactions, the crotonyl-CoA reduction has been previously (18) identified as the limiting step in this pathway. Ter (27, 40) has been

Table 2.4. Photons required for producing desirable products

Molecule	Molecular Weight (g/mol)	Photon required	Cost/kg	Relative value /photon
Octane	114	100	0.94	1
Sugar	180	48	0.5	1.75
Lactate	90	24	1	3.50
1-Butanol	72	48	1.4	1.96
Isobutanol	72	48	1.4	1.96

demonstrated to outperform *Clostridium* Bcd-EtfAB complex by utilizing NADH as the direct reducing cofactor in effect forcing the reduction irreversible. In this work, we also observed that this step was a potential bottleneck, as insufficient Ter activity led to lower n-butanol production. Interestingly, the overall activity of this enzyme was increased 100-fold by attaching a polyhistidine-tag to *T. d*-Ter, and the n-butanol production increased about 5-fold. N-terminus His-tag has been previously (41) shown to increase expression of enzymes. We attributed the Ter activity increase to similar phenomenon. This result highlights the possibility of using protein fusion as a way to improve expression in metabolic engineering work. In *E. coli*, Shen et al. (2011) further increase the metabolic driving force by artificially building up NADH and acetyl-coA availability. Such efforts are expected to improve n-butanol production in cyanobacteria as well.

Absence of oxygen is an important factor in the production of n-butanol in cyanobacteria. While AdhE2 has been purified and assayed only in anoxic atmosphere (36), suggesting its oxygen sensitivity, we were able to detect comparable AdhE2 activities both under oxic and anoxic conditions. Therefore, it is unclear whether the potential oxygen-sensitivity of AdhE2 is

the limitation for oxygenic production of n-butanol. Other factors such as cofactor availability may contribute to the anoxic requirement of n-butanol production.

In this study, the internal storage of reduced carbon compounds in cyanobacteria is directed to n-butanol pathway under anoxic condition. This production system could be suitable and even advantageous for natural light cycles. In day time, cyanobacteria accumulate internal storage reduced carbon. At night, when light energy is not available, cyanobacteria produce n-butanol after removal of oxygen in the system. This system could be optimized by increasing storage of reduced carbon. The production described here is similar to that of hydrogen production in cyanobacteria and algae (42, 43), which also involves inhibition of photosystem II once entering production phase due to the oxygen sensitivity nature of hydrogenases.

The high flux production of isobutyraldehyde and isobutanol (4) demonstrates that high efficiency conversion of solar energy into desirable compounds is feasible. Having the same 48 photon requirement as isobutanol, n-butanol production has potential for improvement. For example, expression of a NAD(P) transhydrogenase, such as *E. coli* UdhA or PntAB, will interconvert NADH and NADPH. This approach is beneficial for production because NADH is the cofactor required by this pathway. In addition, changing the enzyme cofactor dependence from NADH to NADPH either by bio-prospecting for enzymes that naturally use NADPH or by protein engineering methods (44) would also compensate the cofactor discrepancy. For example, enzymes such as acetoacetyl-CoA reductase (PhaB) (45) from *Ralstonia eutropha* and crotonyl-CoA reductase (Ccr) (46) from *Streptomyces collinus* use NADPH as the reducing agent to catalyze similar reactions as Hbd and Ter, respectively.

As an alternative, purple or green sulfur bacteria may be engineered with this pathway to avoid oxygen sensitivity. Purple and green sulfur bacteria are anaerobes or microaerobes that

perform anoxygenic photosynthesis by utilizing hydrogen sulfide as electron donor. In these organisms, production of n-butanol would not depend on internal storage of reduced carbon. Instead, they may directly convert CO_2 into n-butanol.

2.4 Materials and methods

2.4.1. Chemicals and reagents

All chemicals were purchased from Sigma-Aldrich (St. Louis, MO) or Fisher Scientifics (Pittsburgh, PA) unless otherwise specified. B-PERII protein extraction reagent was purchased from Thermo Scientific (Rockford, IL). iProof high-fidelity polymerase, SDS-Page gel, and Bradford reagent were purchased from Bio-Rad (Hercules, CA). Restriction enzymes, Phusion DNA polymerase, and ligases were purchased from New England Biolabs (Ipswich, MA). T5-Exonuclease was purchased from Epicentre Biotechnologies (Madison, WI). Lysonase™ was purchased from EMD Biosciences (San Diego, CA).

2.4.2. Culture medium and condition

All *S. elongatus* 7942 strains were grown on modified BG-11 (1.5 g/L $NaNO_3$, 0.0272 g/L $CaCl_2$, 0.012 g/L ferric ammonium citrate, 0.001 g/L Na_2EDTA, 0.040 g/L K_2HPO_4, 0.0361 g/L $MgSO_4$, 0.020 g/L Na_2CO_3, 1000x trace mineral (1.43 g H_3BO_3, 0.905 g/L $MnCl_2 \cdot 4H_2O$, 0.111 g/L $ZnSO_4 \cdot 7H_2O$, 0.195 g/L $Na_2MoO_4 \cdot 2H_2O$, 0.0395 g $CuSO_4 \cdot 5H_2O$, 0.0245 g $Co(NO_3)2 \cdot 6H_2O$), 0.00882 g/L sodium citrate (30)) agar (1.5% w/v) plates. All S. elongatus 7942 strains were cultured in BG-11 medium (Sigma-Aldrich) containing 50 mM $NaHCO_3$ either in shake flasks, screw-capped flasks, or Roux culture bottles. Cultures were grown under 150

μE/s/m^2 light condition at 30°C. Cell growth was monitored by measuring OD$_{730}$ with Beckman Coulter DU800 spectrophotometer.

2.4.3. DNA manipulations

All chromosomal manipulations were carried out by recombination of plasmid DNA into *S. elongatus 7942* genome at neutral sit.e I (NSI)(31) and II (NSII) (32). Unless specified otherwise, all plasmid were constructed using the isothermal DNA assembly method (33). Plasmids were constructed in *E. coli* XL-1 strain for propagation and storage (Table 2.5). Genes *atoB, adhE2* were cloned from pJCL17 (18). Genes *crt and hbd* were cloned from pEL11 (27), and *Treponema denticola ter* (here forth referred to as *T.d-ter.*) was cloned from pIM8 (27). Poly-His-tagged *T.*d-*ter* (His-*T.d-ter*) was cloned from an expression vector containing this gene that was cloned previously by inserting the T.d-*ter* gene from pIM8 into pCDF-duet plasmid (Novagene) between the BamHI and SalI sites. His-tagged *Euglena gracilis ter* (here forth referred to as His-*E.g-ter*) and His-tagged *C. acetobutylicum hbd* (His-*hbd*) were cloned in a similar fashion. Codon optimized *T. denticola ter* (*T.d-ter*$_{op}$) for *S. elongatus* 7942 was synthesized by Genewiz Inc.

2.4.4. Plasmid constructions

The plasmids used and constructed in this work are listed in Table 2.5 and briefly described below. Plasmid pEL5 was constructed by insertion of *atoB* and *adhE2* into pAM2991, between the BamHI and NotI sites, under an IPTG-inducible promoter Ptrc. The *atoB-adhE2* fragment was amplified by PCR using primers rEL-56 and rEL-57 with pJCL17 as the template. Primer sequences are listed in Table 2.6.

46

Plasmid pEL14 was constructed by inserting a *T.d-ter-crt-hbd* fragment between BamHI and MluI site of a digested plasmid pYX35. The *T.d-ter-crt-hbd* fragment was amplified via splicing by overlap extension (SOE) of *T.d-ter* and *crt-hbd* fragment using primers rEL-58 and rEL-61. The *T.d-ter* fragment was amplified by using primers rEL-58 and rEL-59 with pIM8 as template. The *crt-hbd* fragment was amplified with primers rEL-60 and rEL-61 using pEL11 as the template.

Plasmid pEL17 was constructed by DNA assembly of two pAM2991 (30) fragments, a *T.d-ter-hbd-crt* fragment, and a $P_L lacO_1$-*atoB-adhE2* fragment. The two pAM2991 fragments were separately amplified with primers rEL-202 and rEL-220 for one fragment and rEL-219 and rEL226 for the other with pAM2991 as the template. The *T.d-ter-hbd-crt* fragment was amplified by SOE of a *T.d-ter* fragment and *hbd-crt* fragment using primers rEL-176 and rEL-181. The *T.d-ter* fragment was amplified by using primers rEL-176 and rEL-177 with pIM8 as the template. The *hbd-crt* fragment was amplified by another SOE using primers rEL-178 and rEL-181. The *hbd* fragment was amplified using primers rEL-178 and rEL-179 with pEL11 as template as well. The *crt* fragment was amplified with primers rEL-180 and rEL-181 and pEL11 as template.

Plasmid pEL19 was constructed by DNA assembly of a pEL14 fragment without *T.d-ter* and a codon optimized *T.d-ter* (*T.d*-ter$_{op}$) fragment. The pEL14 fragment without wild-type *T.d-ter* was amplified by using primers rEL-195 and rEL-217 with pEL14 as the template. The *T.d-ter$_{op}$* fragment was amplified with primers rEL-209 and rEL-218 and the plasmid synthesized by Genewiz Inc. as the template.

Plasmid pEL30 was constructed by DNA assembly of two pAM2991 fragments and a His-*T.d-ter* fragment. The pAM2991 fragments were amplified in the same manner as in the

47

construction for plasmid pEL17. The His-*T.d-ter* fragment was amplified by using primers rEL-192 and rEL-204 with a previously cloned pCDFduet (Novagen) plasmid containing His-*T.d-ter* as the template.

Plasmid pEL31 was constructed in a similar fashion as plasmid pEL30. It was constructed by DNA assembly of 2 pAM2991 fragments and a His-*E.g-ter* fragment. Primers rEL-192 and rEL-203 and a pCDFduet plasmid containing His-*E.g-ter* were used for the amplification of the His-*E.g-ter* fragment.

Plasmid pEL32 was also constructed in a similar fashion as pEL30 by DNA assembly of 2 pAM2991 fragments and a His-*hbd* fragment. The His-*hbd* fragment was amplified by primers rEL-192 and rEL-205 and a pCDFduet plasmid containing His-*hbd* as the template.

Plasmid pEL37 was constructed by DNA assembly of a pEL14 backbone fragment without the *T.d-ter-crt-hbd genes* and a *atoB-adhE2-crt-hbd* fragment. The pEL14 backbone fragment was amplified by using primers rEL-217 and rEL-253 and pEL14 as the template. The *atoB-adhE2-crt-hbd* fragment was amplified with primers rEL-254 and rEL-255 and pEL11 as the template.

2.4.5. Strain construction

The strains used and constructed are listed in Table 2. Briefly, strain EL1 was constructed by recombination of plasmids pEL5 and pEL14 at NSI and NSII of wild-type *S. elongatus* 7942, respectively (Table 2.5 for relevant genotypes). Strain EL7 was constructed by recombination of plasmids pEL5 and pEL19 into wild-type *S. elongatus* 7942. Strain EL9 was constructed by recombination of plasmid pEL30 into NSI of wild-type *S. elongatus* 7942. Strain EL10 was constructed by recombination of plasmid pEL31 into NSI of wild-type *S. elongatus* 7942. Strain

EL11 was constructed by recombination of plasmid pEL32 into NSI of wild-type *S. elongatus* 7942. Strain EL13 was constructed with plasmid pEL17 recombination into NSI site of wild-type *S. elongatus* 7942 genome. Strain EL14 was constructed by pEL37 recombination into a strain EL9 at NSII.

2.4.6. Plasmid Transformation

S. elongatus 7942 strains were transformed by incubating cells at mid-log phase (OD$_{730}$ of 0.4 to 0.6) with 2 µg of plasmid DNA overnight in dark. The culture was then spread on BG-11 plates with appropriate antibiotics for selection of successful recombination. For selection and culture maintenance, 20 µg/ml spectinomycin and 10 µg/ml kanamycin were added into BG-11 agar plates and BG-11 medium where appropriate. Colonies grown on BG-11 agar plates were analyzed by PCR using gene-specific primers (Table 2.6) to verify integration of inserted genes into the recombinant strain. In all cases, four individual colonies were analyzed by PCR for verification. One positive colony was then propagated and tested for downstream experiments.

2.4.7. Western blot analysis

Western blot was performed using standard procedure. 20 µg of soluble protein was separated by SDS-PAGE. Commercially available His-probe-HRP kit (Thermo Scientific) was used to detect protein expression of His-tagged *T. denticola* Ter, *E. gracilis* Ter, and *C. acetobutylicum* Hbd. Film exposure time was 5 seconds.

2.4.8. Production of n-butanol

Seed culture was grown in 250 mL screw-cap bottle until OD_{730} reaches 1.5. The seed culture was then used to inoculate a new culture which was grown under continuous light and constant bubbling of 5% CO_2/ 95% N_2 in Roux culture bottle placed vertically. 1 mM IPTG was added to the culture (OD_{730} of 0.6) for gene induction. The culture was grown to OD_{730} of 3.5-4.0 at which the culture was used to test n-butanol accumulation in various conditions and separated into different test tubes. Dark condition was accomplished by wrapping the test tubes with aluminum foil, whereas light condition was done without wrapping. Anoxic condition was introduced by purging the head-space of the test tube with 5%H_2/95% N_2 mixed gas several times using the anaerobic chamber (Coy Laboratory Products, Inc). Oxic condition was performed by not purging the head space, leaving the space with atmospheric oxygen.

2.4.9. n-Butanol quantification

Culture samples (1 ml) were centrifuged for 5 minutes at 21,130 x g. The supernatant (95 µL) was then mixed with 0.1% v/v 2-methyl-pentanol (5 µL) as internal standard. The mixture was then vortexed and directly analyzed on Agilent GC 6850 system with flame ionization detector and DB-FFAP capillary column (30m, 0.32mm i.d., 0.25 film thickness) from Agilent Technologies (Santa Clara, CA). n-Butanol in the sample was identified and quantified by comparing to 0.001% v/v n-butanol standard. n-Butanol standard of 0.001% v/v was prepared by 100-fold dilution of a 0.1% v/v solution. The GC result was analyzed by Agilent software Chem Station (Rev.B.04.01 SP1). Amount of n-butanol in the sample was then calculated based on the ratio of its integrated area and that of the 0.001% n-butanol standard. n-butanol was verified by addition of 0.002% v/v butanol standard to the sample, showing complete overlap between butanol peak in the sample and standard.

Helium gas was used as the carrier gas with 9.52 psi inlet pressure. The injector and detector temperatures were maintained at 225°C. Injection volume was 1 μL. The GC oven temperature was initially held at 85°C for 3 minutes and then raised to 235°C with a temperature ramp of 45°C/min. The GC oven was then maintained at 235°C for 1 minute before completion of analysis. Column flow rate was 1.7 ml/min. n-Butanol typically had a retention time of 2.745 minutes. The internal standard 2-methyl-pentanol typically had a retention time of 3.945. The integrated area for the standard 0.001% v/v n-butanol was usually about 3.36.

2.4.10. Preparation of cell extract for enzyme assays

For aerobic enzyme assays, the crude extract was obtained by pelleting 10 mL of cyanobacteria culture at OD_{730} of 1.5. The harvested cells were then resuspended in 3 mL of B-PERII (Thermo Scientific) solution mixed with lysonase[TM]. After 10 minutes incubation, the solution was centrifuged. The supernatant was collected to use for enzyme assay. For the anoxic enzyme assays, similar procedure was followed with the exception of keeping samples in anoxic environment. Crude cell extract was prepared by centrifuging 5 mL of culture from anoxic production experiment in 4°C for 20 minutes and resuspended the pellet in 1.5 mL of B-PERII with Lysonase[TM] and 5 mM DTT and incubated in room-temperature for 10 minutes in which the culture turned clear. The lysed cell extract was then centrifuged in 4°C for 20 minutes to remove cell debris. The supernatant, containing soluble proteins, was used for enzyme assay. The protein concentration was determined by Bradford reagent using BSA as standards.

2.4.11. Thiolase (AtoB) assay

Thiolase activity was measured via the thiolysis direction. The enzymatic reaction was monitored by the decrease of absorbance at 303 nm which corresponded to the result of acetoacetyl-CoA cleavage (34). The enzymatic reaction was initiated by the addition of the crude extract. The reaction mixture contained 100 mM Tris-HCl (pH 8.0), 10 mM MgCl$_2$, 200 μM acetoacetyl-CoA and 200 μM CoA. Reaction temperature was at 30°C

2.4.12. 3-hydroxybutyryl-CoA dehydrogenase (Hbd) assay

Hbd activity was measured by monitoring the decrease of absorbance at 340 nm which corresponded to consumption of NADH. The assay was conducted similar to previous reports (25). The reaction mixture contained 100 mM MOPS (pH 7.0), 200 μM acetoacetyl-CoA, 400 μM NADH. The reaction was initiated at the addition of crude extract.

2.4.13. Trans-2-enoyl-CoA reductase (Ter) assay

Ter activity was also measured by monitoring the decrease of absorbance at 340nm similar to the Hbd assay. The assay was conducted similar to previous reports (26) with slight modification. The mixture contained 100 mM potassium phosphate buffer (pH 6.2), 200 μM Crotonyl-CoA, 400 μM NADH.

2.4.14. Crotonase (Crt) assay

The Crt assay was conducted as described previously (35) with minor modification. The assay reaction was monitored by a decrease of absorbance in 263 nm, corresponding to the disruption of the alpha-beta unsaturation of crotonyl-CoA. The assay mixture contained 100 mM Tris-HCl pH 7.6, 200 μM Crotonyl-CoA. The reaction was initiated by addition of the enzyme.

52

The standard curves of crotonyl-CoA and 3-hydroxybutyryl-CoA were constructed by measuring the absorbance of the two compounds at 263 nm with different concentrations. The difference in the molar absorptivity of the two compounds was used to calculate concentration of crotonyl-CoA.

2.4.15. Aldehyde/alcohol dehydrogenase assay.

The aldehyde and alcohol dehydrogenase assay of AdhE2 was performed by monitoring the decrease of absorbance in 340 nm, corresponding to the consumption of NADH. The absorbance was monitored by using Beckman-Coulter spectrophotometer DU-800. The reaction mixture contained 100 mM Tris-HCl pH 7.6, 5 mM DTT, 200 μM NADH, and 200 μM butyryl-CoA for the butyraldehyde dehydrogenase (Bldh) reaction and 10 mM butyraldehyde for the butanol dehydrogenase (Bdh) reaction. The total crude cell extract was used instead of only the soluble fraction. The reaction was initiated by the addition of the substrate (either butyryl-CoA or butyraldehyde). To determine the AdhE2 activity in anoxic condition, all procedure was performed in an anaerobic chamber with the exception of spectrophotometric measurement. The reaction was initiated in the anaerobic chamber. After thorough mixing, plastic cap was added onto the cuvette to prevent and reduce introduction of oxygen. The cuvette was then taken out of the anaerobic chamber and rapidly placed into spectrophotometer for kinetic measurement.

Table 2.5. Strains and plasmids used

Strain	Relevant genotypes	Reference
PCC 7942	Wild-type	S.S.Golden
EL1	*atoB-adhE2* integrated at NSI and *T.d-ter-crt-hbd* integrated at NSII in PCC7942 genome	This work
EL7	*atoB-adhE2* integrated at NSI and *ter_op* (optimized for *S.elongatus* 7942)-*crt-hbd* integrated at NSII in PCC7942 genome	This work
EL9	His-tagged *T. denticola ter* (His-*T.d-ter*) integrated at NSI in PCC7942 genome	This work
EL10	His-tagged *E. gracilis ter* (His-*E.g-ter*) integrated at NSI in PCC7943 genome	This work
EL11	His-tagged *C. acetobutylicum hbd* (His-*hbd*) integrated at NSI in PCC7944 genome	This work
EL13	*atoB-adhE2-T.d-ter-hbd-crt* integrated at NSI in PCC7942 genome	This work
EL14	His-*T.d-ter* integrated at NSI and *atoB-adhE2-crrt-hbd* integrated at NSII in PCC7942 genome	This work

Plasmid	Genotypes	
pCDF-duet	SpecR; plasmid containing poly-His tag	Novagen
pAM2991	Spec^R; NSI targeting vector; Ptrc	Busto and Golden (1991)
pYX35	Kan^R; NSII targeting vector; PLlacO1::*rbcL, rbcS*	Yixin Huo (unpublished)
pJCL17	Amp^R; ColE1 ori; P$_L$lacO$_1$::*atoB, adhE2*	Atsumi et al. (2008)
pEL11	Amp^R; ColE1 ori; P$_L$lacO$_1$::*atoB, adhE2, crt, hbd*	Shen et al. (2011)
pIM8	Kan^R; ColA ori; P$_L$lacO$_1$::T.d-*ter*	Shen et al. (2011)
pEL5	Spec^R; NSI targeting; Ptrc::*atoB, adhE2*	This work
pEL14	Kan^R; NSII targeting; P$_L$lacO$_1$::T.d-*ter, crt, hbd*	This work
pEL17	Spec^R; NSI targeting; Ptrc::*atoB, adhE2, PLlacO1::T.d-ter, hbd, crt*	This work
pEL19	Kan^R; NSII targeting; P$_L$lacO$_1$::T.d-*ter_op, crt, hbd*	This work
pEL30	Spec^R; NSI targeting; Ptrc::His-T.d-*ter*	This work
pEL31	Spec^R; NSI targeting; Ptrc::His-E.g-*ter*	This work
pEL32	Spec^R; NSI targeting; Ptrc::His-*hbd*	This work
pEL37	Kan^R; NSII targeting; P$_L$lacO$_1$::*atoB, adhE2, crt, hbd*	This work

Kan^R, kanamycin resistance; Spec^R, spectinomycin resistance; Amp^R, ampicillin resistance.

Table 2.6. Primers sequences

Primers	Sequence (5' -> 3')	Used for plasmid
rEL-56	GGGAAAGGATCCATGAAAAATTGTGTCATCGTCAGTGCGG	pEL5
rEL-57	GGGAAAGCGGCCGCTTAAAATGATTTTATATAGATATCCTTAAGTTCACTTATA	pEL5
rEL-58	GGGAAAGGATCCATGATTGTAAAACCAATGGTTAGGAACAAT	pEL14
rEL-59	AGTTCCATGGTATATCTCCTCTAAATCCTGTCGAACCTTTCTACCTCG	pEL14
rEL-60	AAAGGTTCGACAGGATTTAGAGGAGATATACCATGGAACTAAACAATGTCATCC	pEL14
rEL-61	GGGAAAACGCGTTTATTTTGAATAATCGTAGAAACCTTTTCCTGATT	pEL14
rEL-176	ACAGAAGGAGACTTAAGGATCACTAGTATGATTGTAAAACCAATGGTTAGGAACAATATT	pEL17
rEL-177	CATACCTTTTTCATGGTATATCTCCTACTAGTTTAAATCCTGTCGAACCTTTCTACCTCG	pEL17
rEL-178	CAGGATTTAAACTAGTAGGAGATATACCATGAAAAAGGTATGTGTTATAGGTGCAGGTAC	pEL17
rEL-179	GGTATATCTCCTCTCGAGTTATTTTGAATAATCGTAGAAACCTTTTCCTG	pEL17
rEL-180	ATTCAAAATAACTCGAGAGGAGATATACCATGGAACTAAACAATGTCATCCTTGAAAGG	pEL17
rEL-181	CTAAATACATTCAAATATGTCTATCTATTTTTGAAGCCTTCAATTTTTCTTTTC	pEL17
rEL-182	TTGAAGGCTTCAAAAATAGATAGACATATTTGAATGTATTTAGAAAAATAAACAAATAGG	pEL17
rEL-187	AGCATACTAGAGGATCGGCGGCCGCTTAAAATGATTTTATATAGATATCCTTAAGTTCAC	pEL17
rEL-202	CGATCCTCTAGTATGCTTGTAAACCGTTTT	pEL17, pEL30, pEL31, pEL32
rEL-219	CGGTAATACGGTTATCCACAGAATCA	pEL17, pEL30, pEL31, pEL32
rEL-220	TGATTCTGTGGATAACCGTATTACCG	pEL17, pEL30, pEL31, pEL32
rEL-226	GTGTGAAATTGTTATCCGCTCACAATTC	pEL17, pEL30, pEL31, pEL32
rEL-209	TGTTTAGTTCCATGGTATATCTCCTTTAGATGCGGTCAAAACGCTCAACC	pEL19
rEL-218	CTGACCGAATTCATTAAAG AGGAGATATACC ATGATCGTAAAACCTATGGTTCGTAACAA	pEL19
rEL-195	AGGAGATATACCATGGAACTAAACAATGTCATC	pEL19
rEL-217	CTTTAATGAATTCGGTCAGTGCGTCCT	pEL19, pEL37
rEL-192	AACAATTTCACACAGGAGATATACCATGGGCAGCAGCCATCACCATCATC	pEL30, pEL31, pEL32
rEL-204	GTTTACAAGCATACTAGAGGATCGTTAAATCCTGTCGAACCTTTCTACCTCG	pEL30, pEL31, pEL32
rEL-203	GTTTACAAGCATACTAGAGGATCGTTATTGTTGAGCGGCAGAAGGCAGATCC	pEL31
rEL-205	GTTTACAAGCATACTAGAGGATCGTTATTTTGAATAATCGTAGAAACCTTTTCCTGATT	pEL32
rEL-254	AGGACGCACTGACCGAATTCATTAAAG	pEL37
rEL-255	TTTATTTGATGCCTCTAGCACGCGTTTATTTTGAATAATCGTAGAAACCTTTTCCTG	pEL37
rEL-253	ACGCGTGCTAGAGGCATCAAATAAA	pEL37
rEL-148	GGGAAAGGATCCATGAAAAATTGTGTCATCGTCAGTGCGG	N/A; *atoB* gene specific
rEL-149	GGGAAAGCGGCCGCATTAATTCAACCGTTCAATCACCATCGC	N/A; *atoB* gene specific
rEL-156	GGGAAAGGATCCATGAAAAAGGTATGTGTTATAGGTGCAGGTACTATG	N/A; *hbd* gene specific
rEL-157	GGGAAAGCGGCCGCATTATTTTGAATAATCGTAGAAACCTTTTCCTG	N/A; *hbd* gene specific
rEL-158	GGGAAAGGATCCATGGAACTAAACAATGTCATCCTTGAAAGGA	N/A; *crt* gene specific
rEL-159	GGGAAAGCGGCCGCACTATCTATTTTTGAAGCCTTCAATTTTTCTTTTC	N/A; *crt* gene specific
rEL-160	GGGAAAGGATCCATGATTGTAAAACCAATGGTTAGGAACAAT	N/A; T.d-*ter* gene specific
rEL-161	GGGAAAGCGGCCGCATTAAATCCTGTCGAACCTTTCTACCTCG	N/A; T.d-*ter* gene specific
rEL-209	TGTTTAGTTCCATGGTATATCTCCTTTAGATGCGGTCAAAACGCTCAACC	N/A; T.d-*ter*$_{op}$ gene specific
rEL-218	CTGACCGAATTCATTAAAG AGGAGATATACC ATGATCGTAAAACCTATGGTTCGTAACAA	N/A; T.d-*ter*$_{op}$ gene specific

rEL-163 GGGAAAGCGGCCGCATTAAAATGATTTTATATAGATATCCTTAAGTTCAC N/A; *adhE2* gene specific

rEL-adhE2-f3 TCTTAGATTTGCATTAAAAG N/A; *adhE2* gene specific

2.5. References

1. Fischer CR, Klein-Marcuschamer D, & Stephanopoulos G (2008) Selection and optimization of microbial hosts for biofuels production. Metab Eng 10(6):295-304.

2. Zhang K, Sawaya MR, Eisenberg DS, & Liao JC (2008) Expanding metabolism for biosynthesis of nonnatural alcohols. Proc Natl Acad Sci USA 105(52):20653-20658.

3. Atsumi S & Liao JC (2008) Metabolic engineering for advanced biofuels production from Escherichia coli. Curr Opin Biotechnol 19(5):414-419.

4. Atsumi S, Higashide W, & Liao JC (2009) Direct photosynthetic recycling of carbon dioxide to isobutyraldehyde. Nat Biotechnol 27(12):1177-1180.

5. Deng MD & Coleman JR (1999) Ethanol synthesis by genetic engineering in cyanobacteria. Appl Environ Microbiol 65(2):523-528.

6. Dexter J & Fu PC (2009) Metabolic engineering of cyanobacteria for ethanol production. Energy Environ Sci 2(8):857-864.

7. Takahama K, Matsuoka M, Nagahama K, & Ogawa T (2003) Construction and analysis of a recombinant cyanobacterium expressing a chromosomally inserted gene for an ethylene-forming enzyme at the psbAI locus. J Biosci Bioeng 95(3):302-305.

8. Lindberg P, Park S, & Melis A (2010) Engineering a platform for photosynthetic isoprene production in cyanobacteria, using Synechocystis as the model organism. Metab Eng 12(1):70-79.

9. Niederholtmeyer H, Wolfstadter BT, Savage DF, Silver PA, & Way JC (2010) Engineering Cyanobacteria To Synthesize and Export Hydrophilic Products. Appl Environ Microbiol 76(11):3462-3466.

10. Sheehan J (2009) Engineering direct conversion of CO2 to biofuel. Nat Biotech 27(12):1128-1129.

11. Atsumi S, Hanai T, & Liao JC (2008) Non-fermentative pathways for synthesis of branched-chain higher alcohols as biofuels. Nature 451(7174):86-89.

12. Shen CR & Liao JC (2008) Metabolic engineering of Escherichia coli for 1-butanol and 1-propanol production via the keto-acid pathways. Metab Eng 10(6):312-320.

13. Lin YL & Blaschek HP (1983) Butanol Production by a Butanol-Tolerant Strain of Clostridium-Acetobutylicum in Extruded Corn Broth. Appl Environ Microbiol 45(3):966-973.

14. Ezeji TC, Qureshi N, & Blaschek HP (2004) Butanol fermentation research: Upstream and downstream manipulations. Chemical Record 4(5):305-314.

15. Nicolaou SA, Gaida SM, & Papoutsakis ET (2010) A comparative view of metabolite and substrate stress and tolerance in microbial bioprocessing: From biofuels and chemicals, to biocatalysis and bioremediation. Metab Eng 12(4):307-331.

16. Jiang Y, et al. (2009) Disruption of the acetoacetate decarboxylase gene in solvent-producing Clostridium acetobutylicum increases the butanol ratio. Metab Eng 11(4-5):284-291.

17. Sillers R, Chow A, Tracy B, & Papoutsakis ET (2008) Metabolic engineering of the non-sporulating, non-solventogenic Clostridium acetobutylicum strain M5 to produce butanol without acetone demonstrate the robustness of the acid-formation pathways and the importance of the electron balance. Metab Eng 10(6):321-332.

18. Atsumi S, et al. (2008) Metabolic engineering of Escherichia coli for 1-butanol production. Metab Eng 10(6):305-311.

19. Inui M, et al. (2008) Expression of Clostridium acetobutylicum butanol synthetic genes in Escherichia coli. Appl Microbiol Biotechnol 77(6):1305-1316.

20. Nielsen DR, et al. (2009) Engineering alternative butanol production platforms in heterologous bacteria. Metab Eng 11(4-5):262-273.

21. Steen EJ, et al. (2008) Metabolic engineering of Saccharomyces cerevisiae for the production of n-butanol. Microb Cell Fact 7(36).

22. Berezina OV, et al. (2010) Reconstructing the clostridial n-butanol metabolic pathway in Lactobacillus brevis. Appl Microbiol Biotechnol 87(2):635-646.

23. Hanai T, Atsumi S, & Liao JC (2007) Engineered synthetic pathway for isopropanol production in Escherichia coli. Appl Environ Microbiol 73(24):7814-7818.

24. Li F, et al. (2008) Coupled ferredoxin and crotonyl coenzyme a (CoA) reduction with NADH catalyzed by the butyryl-CoA dehydrogenase/Etf complex from Clostridium kluyveri. J Bacteriol 190(3):843-850.

25. Boynton ZL, Bennett GN, & Rudolph FB (1996) Cloning, sequencing, and expression of clustered genes encoding beta-hydroxybutyryl-coenzyme A (CoA) dehydrogenase, crotonase, and butyryl-CoA dehydrogenase from Clostridium acetobutylicum ATCC 824. J Bacteriol 178(11):3015-3024.

26. Tucci S & Martin W (2007) A novel prokaryotic trans-2-enoyl-CoA reductase from the spirochete Treponema denticola. FEBS Lett 581(8):1561-1566.

27. Shen CR, et al. (2011) High titer anaerobic 1-butanol synthesis in Escherichia coli enabled by driving forces. Appl Environ Microbiol.

28. Duncombe GR & Frerman FE (1976) Molecular and Catalytic Properties of Acetoacetyl-Coenzyme-a Thiolase of Escherichia-Coli. Arch Biochem Biophys 176(1):159-170.

29. Wiesenborn DP, Rudolph FB, & Papoutsakis ET (1988) Thiolase from Clostridium-Acetobutylicum Atcc-824 and Its Role in the Synthesis of Acids and Solvents. Appl Environ Microbiol 54(11):2717-2722.

30. Bustos SA & Golden SS (1991) Expression of the Psbdii Gene in Synechococcus Sp Strain-Pcc-7942 Requires Sequences Downstream of the Transcription Start Site. J Bacteriol 173(23):7525-7533.

31. Bustos SA & Golden SS (1992) Light-Regulated Expression of the Psbd Gene Family in Synechococcus-Sp Strain Pcc-7942 - Evidence for the Role of Duplicated Psbd Genes in Cyanobacteria. Mol Gen Genet 232(2):221-230.

32. Andersson CR, et al. (2000) Application of bioluminescence to the study of circadian rhythms in cyanobacteria. Bioluminescence and Chemiluminescence, Pt C 305:527-542.

33. Gibson DG, et al. (2009) Enzymatic assembly of DNA molecules up to several hundred kilobases. Nat Methods 6(5):343-345.

34. Nishimura T, Saito T, & Tomita K (1978) Purification and properties of beta-ketothiolase from Zoogloea ramigera. Arch Microbiol 116(1):21-27.

35. Hartmanis MGN & Gatenbeck S (1984) Intermediary Metabolism in Clostridium-Acetobutylicum - Levels of Enzymes Involved in the Formation of Acetate and Butyrate. Appl Environ Microbiol 47(6):1277-1283.

36. Fontaine L, et al. (2002) Molecular characterization and transcriptional analysis of adhE2, the gene encoding the NADH-dependent aldehyde/alcohol dehydrogenase responsible for butanol production in alcohologenic cultures of Clostridium acetobutylicum ATCC 824. J Bacteriol 184(3):821-830.

37. Vasconcelos I, Girbal L, & Soucaille P (1994) Regulation of Carbon and Electron Flow in Clostridium-Acetobutylicum Grown in Chemostat Culture at Neutral Ph on Mixtures of Glucose and Glycerol. J Bacteriol 176(5):1443-1450.

38. Hoffmeister M, Piotrowski M, Nowitzki U, & Martin W (2005) Mitochondrial trans-2-enoyl-CoA reductase of wax ester fermentation from Euglena gracilis defines a new family of enzymes involved in lipid synthesis. J Biol Chem 280(6):4329-4338.

39. Ducat DC, Way JC, & Silver PA (2011) Engineering cyanobacteria to generate high-value products. Trends Biotechnol.

40. Bond-Watts BB, Bellerose RJ, & Chang MCY (2011) Enzyme mechanism as a kinetic control element for designing synthetic biofuel pathways. Nat Chem Biol 7(4):222-227.

41. Doray B, Chen CD, & Kemper B (2001) N-terminal deletions and His-tag fusions dramatically affect expression of cytochrome p450 2C2 in bacteria. Arch Biochem Biophys 393(1):143-153.

42.   Antal TK, et al. (2003) The dependence of algal H2 production on Photosystem II and O2 consumption activities in sulfur-deprived Chlamydomonas reinhardtii cells. Biochim Biophys Acta 1607(2-3):153-160.

43.   Melis A, Zhang LP, Forestier M, Ghirardi ML, & Seibert M (2000) Sustained photobiological hydrogen gas production upon reversible inactivation of oxygen evolution in the green alga Chlamydomonas reinhardtii. Plant Physiol 122(1):127-135.

44.   Scrutton NS, Berry A, & Perham RN (1990) Redesign of the coenzyme specificity of a dehydrogenase by protein engineering. Nature 343(6253):38-43.

45.   Peoples OP & Sinskey AJ (1989) Poly-Beta-Hydroxybutyrate (Phb) Biosynthesis in Alcaligenes-Eutrophus H16 - Identification and Characterization of the Phb Polymerase Gene (Phbc). J Biol Chem 264(26):15298-15303.

46.   Wallace KK, et al. (1995) Purification of crotonyl-CoA reductase from Streptomyces collinus and cloning, sequencing and expression of the corresponding gene in Escherichia coli. Eur J Biochem 233(3):954-962.

47.   Brenner MP, et al. (2008) Engineering Microorganisms for Energy Production. (U.S. Department of Energy, Washington, DC).

48.   Zhu XG, Long SP, & Ort DR (2008) What is the maximum efficiency with which photosynthesis can convert solar energy into biomass? Curr Opin Biotechnol 19(2):153-159.

3. ATP DRIVES DIRECT PHOTOSYNTHETIC PRODUCTION OF N-BUTANOL IN CYANOBACTERIA

3.1. Introduction

Anoxic incubation in the dark or in light with photosystem II inhibition switches cyanobacteria into fermentative condition which enables accumulation of acetyl-CoA and NADH as driving forces for downstream n-butanol production. In this Chapter we engineered a synthetic pathway which alleviates the need of high acetyl-CoA pool by engineering a malonyl-CoA dependent pathway using ATP as a driving force for n-butanol production.

n-Butanol can be produced by two distinct routes: the coenzyme A (CoA)-dependent pathway (1, 2) and the keto acid pathway (3-5). The CoA-dependent pathway follows the chemistry of β-oxidation in the reverse direction, in which acetyl-CoA is condensed to form acetoacetyl-CoA and then reduced to n-butanol. The keto acid pathway utilizes 2-ketobutyrate as an intermediate, which is elongated to 2-ketovalarate using the leucine biosynthesis enzymes. 2-Ketovalarate is then decarboxylated and reduced into n-butanol. In each case, the pathway can be extended to produce 1-hexanol and other higher alcohols (6-8).

The CoA-dependent reverse β-oxidation is a natural fermentation pathway used by *Clostridium* species (9-11) and has been transferred to various recombinant heterotrophs, resulting in n-butanol titers ranging from 2.5 mg/L to 1.2 g/L with glucose as the substrate (12-16). One of the challenges in transferring this pathway to other organisms lies in the hydrogenation of crotonyl-CoA to butyryl-CoA catalyzed by the butyryl-CoA dehydrogenase/electron transferring flavoprotein (Bcd/EtfAB) complex. Bcd/EtfAB complex is difficult to express in recombinant systems, is presumably oxygen sensitive (12, 17), and requires ferredoxin (18). This difficulty was overcome by expressing trans-2-enoyl-CoA
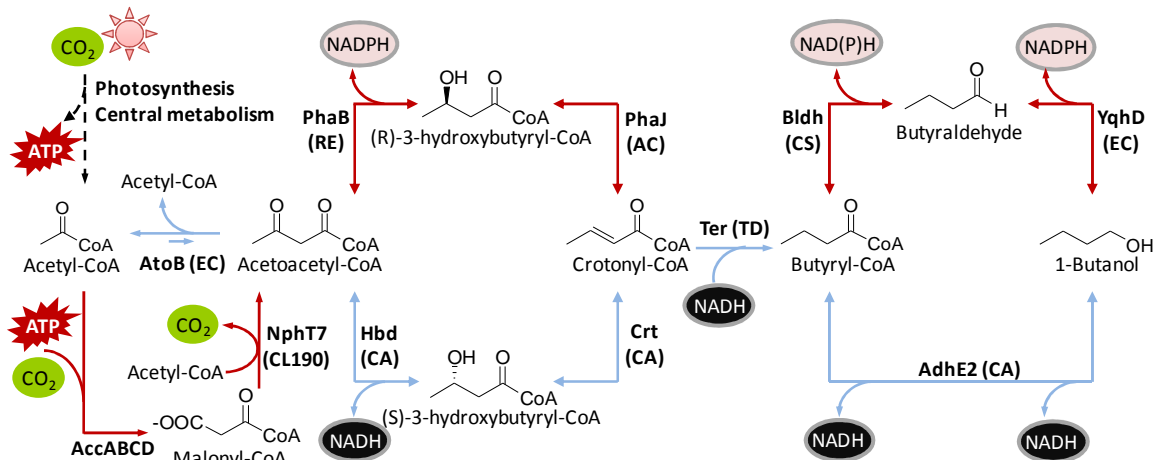
Figure 3.1. Redesigning the Clostridium CoA-dependent n-butanol pathway. The fermentative CoA n-butanol pathway is in blue. Alternative routes are in red. EC, *E. coli*; RE, *R. eutropha*; CA, *C. acetobutylicum*; AC, *A. caviae*; TD, *T. denticola*; CS, *C. saccharoperbutylacetonicum; CL190, Streptomyces* sp. strain CL190. *atoB*, thiolase; *nphT7*, acetoacetyl-CoA synthase; *phaB*, acetoacetyl-CoA reductase; *phaJ*, (R)-specific enoyl-CoA hydratase; *hbd*, 3-hydroxybutyryl-CoA dehydrogenase; *crt*, crotonase; *ter*, Trans-2-enoyl-CoA reductase; *bldh*, butyraldehyde dehydrogenase; *paaH1*, 3-hydroxybutyryl-CoA dehydrogenase; *yqhD*, NADP-dependent alcohol dehydrogenase; *adhE2*, bifunctional alcohol/aldehyde dehydrogenase.

reductase (Ter) (19, 20), which is readily expressed in *Escherichia coli* and directly reduces crotonyl-CoA using NADH. This modified n-butanol pathway (Fig. 3.1; outlined in blue) is catalyzed by five enzymes: thiolase (AtoB), 3-hydroxybutyryl-CoA dehydrogenase (Hbd), crotonase (Crt), Ter, and bifunctional aldehyde/alcohol dehydrogenase (AdhE2). Simultaneously expressing these enzymes and engineering NADH and acetyl-CoA accumulation as driving forces, n-butanol production with a high titer of 15 g/L and 88% of theoretical yield has been achieved using *E. coli* in flasks without product removal (19). This result demonstrates the feasibility of transferring the CoA-dependent pathway to non-native organisms for high-titer n-butanol fermentation from glucose.

However, the success of the CoA-dependent pathway in *E. coli* is not directly transferrable to photoautotrophs. By expressing the same enzymes in cyanobacteria *Synechococcus elongatus* PCC 7942, photosynthetic n-butanol production from CO_2 was barely detectable (21). n-Butanol

production was achieved by this strain only when internal carbon storage made by CO_2 fixation in light conditions was fermented under anoxic conditions (21). We hypothesized that both the acetyl-CoA and NADH pools in this organism under photosynthetic conditions may be insufficient to drive n-butanol formation. Acetyl-CoA is the precursor for fermentation pathway and the TCA cycle, both of which are not active in light conditions. Furthermore, photosynthesis generates NADPH, but not NADH, and the inter-conversion between the two may not be efficient enough. Without a significant driving force against the unfavorable thermodynamic gradient, n-butanol production cannot be achieved. The difficulty of direct photosynthetic production of n-butanol is in sharp contrast to the production of isobutanol (450 mg/L) and isobutyraldehyde (1,100 mg/L) by *S. elongatus* PCC 7942 (22), which has an irreversible decarboxylation step as the first committed reaction to drive the flux towards the products. This difference suggests the importance of driving forces in altering the direction of metabolic flux.

We reason that instead of the acetyl-CoA pool, ATP may be used to drive the thermodynamically unfavorable condensation of two acetyl-coA molecules under photosynthetic conditions. Thus, we engineered the ATP-driven malonyl-CoA synthesis and decarboxylative carbon chain elongation used in fatty acid synthesis to drive the carbon flux into the formation of acetoacetyl-CoA, which then undergoes the reverse β-oxidation to synthesize n-butanol. We further replaced the subsequent NADH-dependent enzymes with NADPH-dependent ones, and successfully achieved n-butanol synthesis under photosynthetic conditions. In theory, excess ATP consumption in the cell might cause a decrease in biomass. Thus, with notable exceptions (23-26), most metabolic engineering design do not choose to increase ATP consumption. Although many natural examples of microbes using ATP to drive reactions, most of them are

highly regulated. Therefore, it is unpredictable whether it is feasible to use ATP consumption to push flux in a non-native pathway, for which no regulation exists.

3.2. Results

3.2.1. Incorporating an ATP driving force in n-butanol pathway design

The thiolase-mediated condensation of two acetyl-CoA molecules is reversible but strongly favors the thiolysis of acetoacetyl-CoA. To examine the thermodynamic property of this reaction, we overexpressed and purified *E. coli* thiolase (AtoB) and used an in vitro assay to determine its equilibrium constant and $\Delta G^{o'}$. The result showed that the condensation reaction is unfavorable (Fig. 3.2) with equilibrium constant (K_{eq}) of $(1.1 \pm 0.2) \times 10^{-5}$ at pH 8.0, within the optimum pH range for cyanobacteria (27). This experimentally determined K_{eq} approximately corresponds to a $\Delta G^{o'}$ of 6.8 kcal/mol, consistent with the literature reported K_{eq} using partially purified thiolase from pig heart protein homogenate (28). Therefore, without a sufficiently large acetyl-CoA pool or an efficient product trap, there is no driving force for the formation of acetoacetyl-CoA. Although the irreversible hydrogenation of crotonyl-CoA catalyzed by Ter provides a driving force, it is insufficient to drive the reaction forward without large pools of acetyl-CoA and reducing equivalent (19).

Instead of using the direct condensation of acetyl-CoA, we contemplated an alternative route through the ATP-driven malonyl-CoA synthesis. Malonyl-CoA is synthesized from acetyl-CoA, HCO_3^-, and ATP by acetyl-CoA carboxylase (Acc). The formation of malonyl-CoA is effectively irreversible due to ATP hydrolysis. In fatty acid synthesis, malonyl-CoA is then converted into malonyl-acyl carrier protein (ACP) and acts as the carbon addition unit for fatty acid synthesis. For n-butanol synthesis, malonyl-CoA can react with acetyl-coA in a decarboxylative condensation to form acetoacetyl-CoA, in a reaction analogous to ketoacyl-ACP
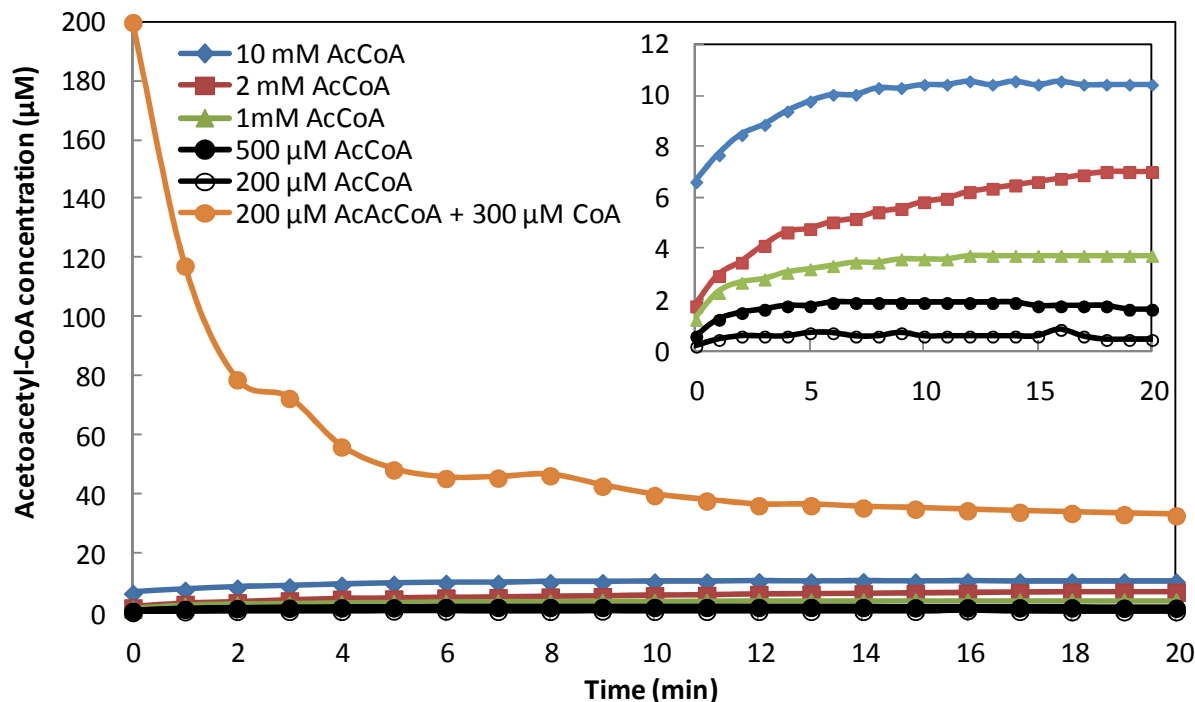
Figure 3.2. Determination of equilibrium concentrations for the thiolase (AtoB) mediated reaction. The equilibrium constant (K_{eq}) was determined from the equilibrium concentrations. *E. coli* AtoB was cloned, purified, and used in an in vitro assay. Detailed conditions and methods are listed.

synthase III (KAS III) that catalyzes the irreversible condensation of malonyl-ACP and acetyl-CoA to synthesize the four carbon intermediate 3-ketobutyryl-ACP.

We note that the energy release from ATP hydrolysis ($\Delta G^{o'}$ of -7.3 kcal/mol) would compensate for the energy required for condensation of acetyl-CoA into acetoacetyl-CoA. By combining the reaction catalyzed by thiolase with ATP hydrolysis (Fig. 3.S1), the net reaction is thermodynamically favorable ($\Delta G^{o'} < 0$), which would reduce the need for high concentration of acetyl-CoA required to push the reaction forward. More importantly, CO_2 released from the second step, decarboxylative chain elongation, shifts the reaction towards the formation of acetoacetyl-CoA. Fatty acid and polyketide syntheses have naturally evolved this mechanism to enable the thermodynamically unfavorable formation of 3-ketoacyl-ACP. By taking advantage of
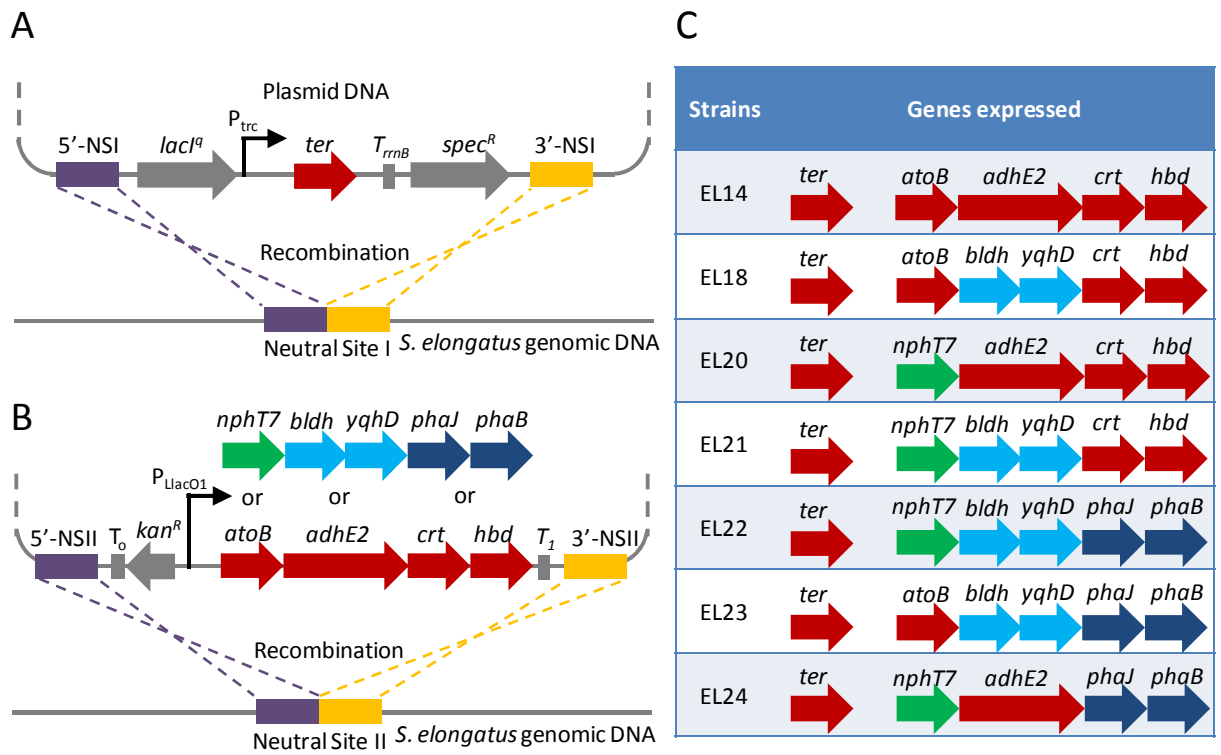
Figure 3.3. Schematic representation of recombination to integrate A) *ter* at NSI, B) *atoB*, *adhE2*, *crt*, and *hbd* at NSII in the genome of *S. elongatus*. Different combinations of alternative genes *nphT7*, *bldh*, *yqhD*, *phaJ*, and *phaB* can replace their counterpart enzymes to recombine into NSII. C) List of strains with different combinations of overexpressed genes used in this study.

this mechanism, it is possible to push the carbon flux to the n-butanol pathway without the acetyl-CoA driving force artificially constructed in *E. coli* (19).

3.2.2. Expression of acetoacetyl-CoA synthase enables photosynthetic production of n-butanol.

Therefore, we bioprospected for a KAS III that utilizes malonyl-CoA rather than malonyl-ACP for condensation with acetyl-CoA. Since both ACP and CoA carry phosphopantetheine which forms thioester bond with the malonyl moiety, KAS III and KAS III-like enzymes may

Table 3.1. Specific activities of acetoacetyl-coa synthases (μmol/min/mg)

Enzyme	Specific activity	Enzyme	Specific activity
Burkholderia ambifaria BAMB6244	0.0116 ± 0.0002	*Pseudomonas aeruginosa* PAE-FabH2	0.0140 ± 0.0010
Gluconobacter oxydans GOX0115	0.0099 ± 0.0011	*Streptomyces avermitilis* SAV-FabH4	n.d
Helicobacter pylori HP0202	n.d	*Streptomyces coelicolor* SCO5858	n.d
Listeria monocytogenes LMO2202	n.d	*Streptomyces* sp. strain CL190 NphT7	6.02 ± 0.25

also react with malonyl-CoA. We cloned a variety of KAS III and KAS III-like enzymes from different organisms, and examined their expression in *E. coli* (Fig. 3.S2). After His-tag purification, we assayed their activity for condensing malonyl-CoA with acetyl-CoA (Table 3.1). Among the enzymes tested, NphT7 (29) was the most active. Other enzymes such as Bamb6244, GOX0115, and PAE-FabH2 were also active while the rest showed no detectable activity. The condensation reaction (Fig. 3.S3) catalyzed by NphT7 using malonyl-CoA and acetyl-CoA is irreversible and accumulates acetoacetyl-CoA as the product. At low starting concentrations of malonyl-CoA, conversion yield to acetoacetyl-CoA is higher than high starting substrate concentrations. This result is likely due to the fact that NphT7 also catalyzes malonyl-CoA self condensation, and is particularly useful for n-butanol synthesis, since both malonyl-CoA and acetyl-CoA pools are expected to be low in *S. elongatus* PCC 7942.

Next, we constructed a plasmid harboring genes *nphT7*, *hbd*, *crt*, and *adhE2* under an IPTG inducible promoter P_{LlacO1} with Neutral Site II (NSII) recombination sequences flanking the genes and kanamycin resistance marker (Fig. 3.3). By DNA homologous recombination, we integrated these genes into the genome of *S. elongatus* strain EL9 (expressing *ter* at Neutral Site I (NSI) under the control of another IPTG inducible promoter P_{trc}) at NSII and selected for
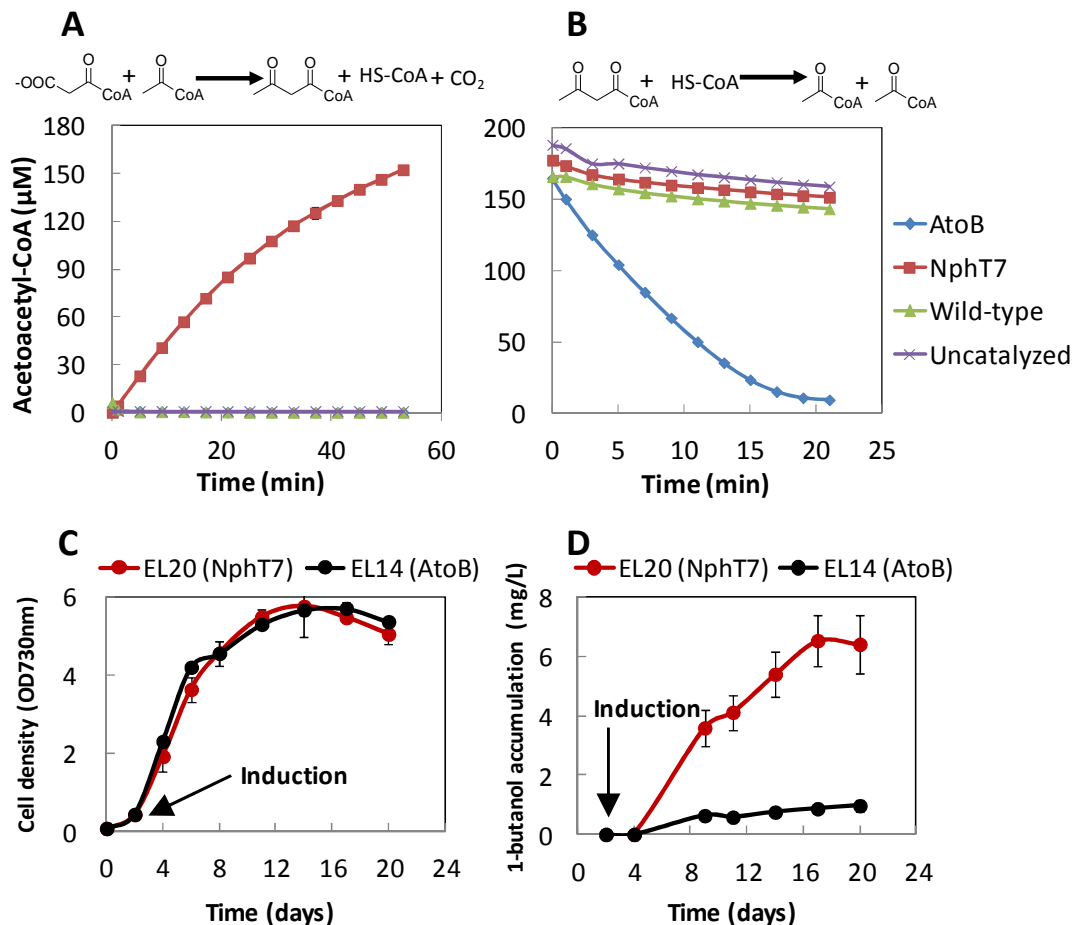
Figure 3.4. ATP aided n-butanol production in cyanobacteria. A) In vitro assay for the synthesis of acetoacetyl-CoA using crude extracts of Wild-type *S. elongatus* PCC 7942, strain EL14 and EL20. B) In vitro assay for the thiolysis of acetoacetyl-CoA using crude extracts of wild-type *S. elongatus PCC* 7942, strain EL14 and EL20. C) Cell density and D) n-butanol accumulation as a function of time of strain EL14 and EL20. n-Butanol production by strain EL14 was near detection limit of about 1 mg/L.

successful transformant on kanamycin containing BG-11 plates. The successful transformant

strain EL20 was then analyzed for in-vitro enzyme activity and n-butanol production. As shown

in (Fig. 3.4A), crude extract from strain EL20 catalyzed the formation of acetoacetyl-CoA by

condensation of malonyl-CoA and acetyl-CoA and did not catalyze the thiolysis of acetoacetyl-

CoA (Fig. 3.4B). On the other hand, crude extract from strain EL14 expressing *atoB* along with

hbd, *crt*, *ter*, and *adhE2* catalyzed thiolysis (Fig. 3.4B) much more efficiently than the condensation reaction (Fig. 3.4A). The two strains EL20 and EL14 exhibited nearly identical growth rate (Fig. 3.4C). However, Strain EL20 produced 6.5 mg/L (Fig. 3.4D) of n-butanol while Strain EL14 produced only barely detectable amounts (detection limit of about 1 mg/L) of n-butanol (Fig. 3.4D). This result indicated that ATP driven acetoacetyl-CoA formation is required for photosynthetic production of n-butanol using the CoA-dependent pathway.

3.2.3. Substitution of NADPH utilizing enzymes aids n-butanol production

Another useful driving force in n-butanol synthesis is the reducing equivalent (19). Cyanobacteria produce NADPH as the direct result of photosynthesis. Intracellular NAD^+ and $NADP^+$ levels exist in a ratio of about 1:10 (30) in *S. elongatus* PCC 7942. Thus NADH utilizing pathway may be unfavorable in cyanobacteria. To synthesize one mole of n-butanol from acetoacetyl-CoA requires four moles of NADH. Therefore, changing the cofactor preference to NADPH may aid the production of n-butanol.

As depicted in Fig. 3.1 (outlined in red), we identified enzymes that utilize NADPH or both NADPH and NADH by bioprospecting. Acetoacetyl-CoA reductase (PhaB) (31) was used to replace Hbd. PhaB from *Ralstonia eutropha* is an enzyme found in the poly-hydroxyalkanoate biosynthetic pathway for reducing 3-ketobutyryl-CoA to 3-hydroxybutyryl-CoA using NADPH. However, PhaB produces the (R)-stereoisomer of 3-hydroxybutyryl-CoA instead of the (S)-stereoisomer produced by Hbd. As a result, Crt cannot be used for the subsequent dehydration to produce crotonyl-CoA. Therefore, a different crotonase is necessary for dehydration of (R)-3-hydroxybutyryl-CoA. (R)-specific enoyl-CoA hydratase (PhaJ) (32) is found in *Aeromonas caviae* and dehydrates (R)-3-hydroxybutyryl-CoA into crotonyl-CoA. Together, PhaB and PhaJ
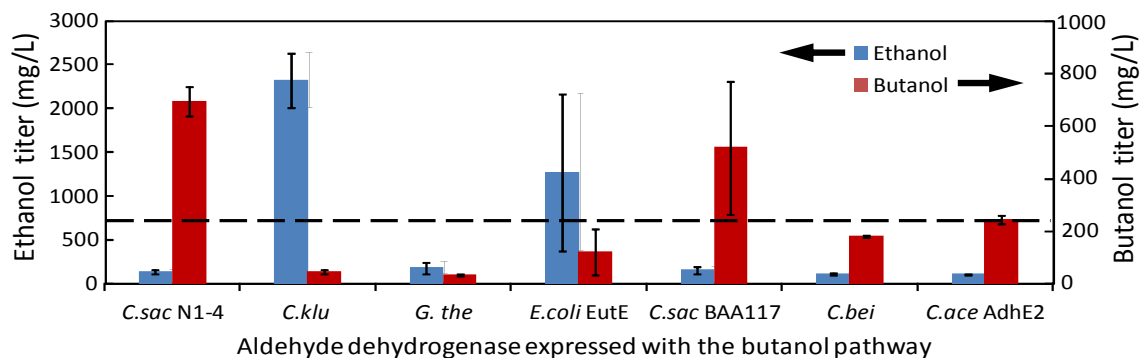
Figure 3.5. Production of n-butanol and ethanol by recombinant *E. coli* strains JCL299 expressing CoA-dependent n-butanol pathway with YqhD from *E. coli* and Bldh from different organisms. Dashed line represents the baseline production by using AdhE2. Detailed production procedure is listed in the methods.

can replace Hbd and Crt, respectively, to change the cofactor preference of 3-ketobutyryl-CoA reduction to NADPH.

To replace AdhE2, NADP-dependent alcohol dehydrogenase (YqhD) (33) from *E. coli* has been demonstrated to aid the production of higher chain alcohols (22). In addition, we needed a CoA-acylating butyraldehyde dehydrogenase (Bldh) to replace the aldehyde dehydrogenase function of AdhE2. We thus bioprospected for enzymes catalyzing reduction of butyryl-CoA to butyraldehyde. Bldh was found in high butanol producing *Clostridium* species including C. *beijerinckii* NCIMB 8052 (34), *C. saccharobutylicum* ATCC BAA-117, and C. *saccharoperbutylacetonicum* NI-4 (35). In particular, Bldh from *C. beijerinckii* has been purified and demonstrated activity *in vitro* with both NADH and NADPH as a reducing cofactor.

Using the sequence of *C. beijerinckii* Bldh, we searched by homology and cloned additional Bldh-like enzymes from various organisms including C. *saccharoperbutylacetonicum* NI-4, C. *saccharobutylicum* ATCC BAA-117, *Geobacillus thermoglucosidasius*, *Clostridium kluyveri*, and *E. coli*. We assessed the performance of these Bldh's by n-butanol production in recombinant *E. coli*. As shown in Fig. 3.5, the *E. coli* strain expressing C.

70

Strain	EL14	EL20	EL18	EL21	EL24	EL23	EL22
Enzyme Specific activity (µmol/min/mg)							
AtoB	0.73±0.01	N/A	0.62±0.04	N/A	N/A	0.69±0.01	N/A
NphT7	N/A	0.019±0.001	N/A	0.022±0.001	0.024±0.001	N/A	0.021±0.001
Hbd (NADH)	0.31±0.01	0.22±0.01	0.16±0.01	0.21±0.01	N/A	N/A	N/A
PhaB (NADPH)	N/A	N/A	N/A	N/A	0.030±0.005	0.007±0.003	0.014±0.005
Crt (PhaJ)	41.2±0.7	41.3±0.3	23.6±2.7	39.8±3.3	30.7±5.1	13.7±0.8	25.0±1.8
Ter	0.71±0.14	1.12±0.31	1.25±0.51	1.25±0.043	1.10±0.20	0.91±0.70	1.18±0.56

Figure 3.6. n-butanol production and enzyme activity of strains expressing different enzymes. Strain genotype is listed in Fig. 3.3C. Expression of *nphT7* enables direct photosynthetic production of n-butanol under oxygenic condition. Strains EL21 and EL22 expressing *bldh* and *yqhD* achieved the highest production.

saccharoperbutylacetonicum NI-4 Bldh along with rest of the CoA n-butanol pathway produced the highest titer of n-butanol, exceeding the n-butanol produced by *E. coli* strain expressing AdhE2 by nearly 3-fold.

To test the effect of cofactor utilization, we constructed various combinations of different routes by overexpressing different genes in *S. elongatus* (Fig. 3.3C). We constructed plasmids

containing different genes and recombined them into the genome of *S. elongatus* strain EL9. We then assayed the activity of overexpressed enzymes to confirm expression (Fig. 3.6). Of the strains tested, strain EL22 expressing the NADPH utilizing enzymes produced the highest amount of n-butanol (29.9 mg/L) exceeding that of EL20 (6.4 mg/L) by more than 4-fold. This result reinforced the importance of cofactor as driving force.

3.3. Discussion

In a metabolic system involving multiple pathways, the direction and rate of each reaction are determined by kinetics, regulated by the enzyme expression levels and metabolite pool sizes. Typically, a reaction with a large positive $\Delta G^{o'}$ is considered practically unfeasible in the forward direction because it requires high concentrations of the substrate pool to drive the reaction forward. The condensation of two molecules of acetyl-CoA to acetoacetyl-CoA is such an example. On the other hand, the reverse direction, thiolysis of acetoacetyl-CoA, is readily achievable and used as the last step in the β-oxidation. However, some fermentative organisms, such as *Clostridium* species, use direct acetyl-CoA condensation for n-butanol synthesis. These organisms accomplish this thermodynamically unfavorable reaction presumably through a large pool of acetyl-CoA and high reducing equivalents that drive the subsequent reactions. This situation was re-created in *E. coli* expressing the enzymes for n-butanol synthesis (19). Unfortunately, this strategy cannot be readily implemented in photosynthetic organisms for multiple reasons: Acetyl-CoA is a precursor for fermentative pathways and the oxidative TCA cycle, which are not active under photosynthetic conditions. Thus, the acetyl-CoA pool size is not expected to be high and is difficult to modulate. Instead of using high acetyl-CoA pool as a driving force, here ATP and the evolution of CO_2 effectively drive the reactions towards n-

butanol synthesis. This strategy is used in fatty acid synthesis in nature, and is used to couple the fatty acid synthesis to the energy status in the cell.

ATP consumption has been used by cells to drive various thermodynamically unfavorable reactions. In engineered *E. coli*, ATP consumption has been used to stimulate glycolysis by futile cycling (23, 24) or by deletion of membrane-coupling subunits in (F_1F_0)-ATP synthase (25). Increased ATP consumption by overexpressing enzymes that promote malonyl-CoA biosynthesis also increased production yield of compounds downstream of malonyl-CoA (26). However, additional ATP consumption in heterologous pathways may cause adverse effects in the cell, and may result in reduced biomass formation. As such, most metabolic engineering design models have primarily focused on maximizing carbon yield and minimizing ATP expenditure. Here we provide a distinct example using ATP to alter the thermodynamics of the CoA-dependent n-butanol pathway, which naturally does not require additional ATP consumption. By incorporating an ATP-dependent step into the CoA-dependent n-butanol synthesis pathway, we demonstrated for the first time the direct photosynthetic production of n-butanol from CO_2.

Direct photosynthetic n-butanol production from CO_2 is desirable because it reduces the number of processing steps. *S. elongatus* PCC 7942 is naturally competent and therefore is an attractive model organism for engineering. The DNA recombination method used in this study has also been broadly practiced for engineering cyanobacteria for the production of various chemicals. By metabolic engineering, cyanobacteria has also enabled the production of Isobutyraldehyde (1,100 mg/L) (22), isobutanol (450 mg/L) (22), ethanol (550 mg/L) (36), ethylene (37 mg/L) (37), isoprene (0.05 mg/g dry cell weight) (38), sugars (45 mg/L) (39), lactic acid (56 mg/L) (39), fatty alcohols (0.2 mg/L) (40), and fatty acids (194 mg/L) (41) from CO_2.

73

The pathways for the relatively high production of isobutyraldehyde, isobutanol and ethanol naturally involve a decarboxylation step as the first committed reaction. The loss of CO_2 is considered irreversible and serves as a driving force to the product formation. Our result is also consistent with this phenomenon that decarboxylation aids in directing the carbon flux.

Reducing cofactor preference is another important aspect of pathway design. Depending on the production condition and organisms' natural physiology, changing cofactor preference is necessary to achieve high flux production. For example, changing NADPH-dependent enzymes into NADH-dependent increases the isobutanol productivity and yield under anaerobic condition in recombinant *E. coli (42)*. Replacing the Bcd-EtfAB complex that requires an unknown electron donor with an NADH-dependent Ter is helpful in n-butanol production (19, 20). In contrast, pathways utilizing NADPH are preferred in cyanobacteria because NADPH is more abundant. By utilizing NADPH dependent enzymes, our n-butanol production enhanced from 6.5 mg/L to 29.9 mg/L (Fig. 3.6).

Current limitation of our n-butanol production using cyanobacteria may be the synthesis of malonyl-CoA. Compared to the high flux production of isobutanol and isobutyraldehyde in cyanobacteria, the carbon flux through our n-butanol pathway is suboptimal. Malonyl-CoA biosynthesis is considered as the limiting step in fatty acid synthesis (43). Therefore, increasing carbon flux towards the synthesis of acetyl-CoA and malonyl-CoA may be necessary to increase n-butanol production. Intracellular acetyl-CoA and malonyl-CoA supply may be increased by increasing CoA biosynthesis (44), overexpression of Acc (45-48), glycolytic enzymes such as phosphoglycerate kinase and glyceraldehyde-3-phosphate dehydrogenase (26), and inhibition of fatty acid biosynthesis (49). With these approaches, the n-butanol production in cyanobacteria may be further improved.

74

3.4. Materials and methods

3.4.1. Culture medium and condition

All *S. elongatus* PCC 7942 strains were grown on modified BG-11 (1.5 g/L NaNO$_3$, 0.0272 g/L CaCl$_2$·2H$_2$O, 0.012 g/L ferric ammonium citrate, 0.001 g/L Na$_2$EDTA, 0.040 g/L K$_2$HPO$_4$, 0.0361 g/L MgSO$_4$·7H$_2$O, 0.020 g/L Na$_2$CO$_3$, 1000x trace mineral (1.43 g H$_3$BO$_3$, 0.905 g/L MnCl$_2$·4H$_2$O, 0.111 g/L ZnSO$_4$·7H$_2$O, 0.195 g/L Na$_2$MoO$_4$·2H$_2$O, 0.0395 g CuSO$_4$·5H$_2$O, 0.0245 g Co(NO$_3$)2·6H$_2$O), 0.00882 g/L sodium citrate dihydrate (50)) agar (1.5% w/v) plates. All *S. elongatus* PCC 7942 strains were cultured in BG-11 medium containing 50 mM NaHCO$_3$ in 250 mL screw cap flasks. Cultures were grown under 100 μE/s/m^2 light, supplied by 4 Lumichrome F30W-1XX 6500K 98CRI light tubes, at 30 °C. Cell growth was monitored by measuring OD$_{730}$ with Beckman Coulter DU800 spectrophotometer.

3.4.2. Production of n-butanol

A loopful of *S. elongatus* PCC 7942 was used to inoculate fresh 50 mL BG-11. 500 mM IPTG was used to induce the growing culture at cell density OD$_{730nm}$ of 0.4 to 0.6 with 1 mM IPTG as final concentration. 5 mL of growing culture was sampled for cell density and n-butanol production measurements every two days for up to day 8 after which sampling time was switched to every 3 days. After sampling, 5 mL of fresh BG-11 with 500 mM NaHCO$_3$, appropriate antibiotics, and IPTG were added back to the culture. Method for n-butanol quantification is listed in SI Text.

3.4.3. Alcohol production by *E. coli* expressing butyraldehyde dehydrogenase

E. coli wild type is based on strain BW25113 (55). Transformed *E. coli* strain JCL299 ($\Delta adhE$, $\Delta ldhA$, Δfrd, Δpta) was selected on LB plate supplemented with ampicillin (100 μg/mL) and kanamycin (50 μg/mL). Three colonies were picked from the plate to make overnight pre-culture. The pre-cultures were then used to inoculate 5 mL of Terrific broth (TB; 12g tryptone, 24g yeast extract, 2.31g KH_2PO_4, 12.54g K_2HPO_4, 4 mL glycerol per liter of water) supplemented with 20 g/L glucose. Growing culture was then induced with IPTG at OD_{600nm} of 0.6 with 0.1 mM final IPTG concentration. After allowing 1 hour of protein expression, the cultures were then switched to anaerobic condition by purging with N_2 gas using anaerobic chamber. After two days of fermentation, culture sample (2 mL) was centrifuged for 5 minutes at 21,130 x g. The supernatant was analyzed by GC following the same method as that described above in n-butanol quantification.

3.4.4. Chemicals and reagents

All chemicals were purchased from Sigma-Aldrich (St. Louis, MO) or Fisher Scientifics (Pittsburgh, PA) unless otherwise specified. iProof high-fidelity DNA polymerase was purchased from Bio-Rad (Hercules, CA). Restriction enzymes, Phusion DNA polymerase, and ligases were purchased from New England Biolabs (Ipswich, MA). T5-Exonuclease was purchased from Epicentre Biotechnologies (Madison, WI). KOD and KOD xtreme DNA polymerases were purchased from EMD biosciences (Gibbstown, NJ).

3.4.5. DNA manipulations

All chromosomal manipulations were carried out by homologous recombination of plasmid DNA into *S. elongatus* PCC 7942 genome at neutral site I (NSI) (51) and II (NSII) (52). All plasmid were constructed using the isothermal DNA assembly method (53). Plasmids were constructed in *E. coli* XL-1 strain for propagation and storage (Table 3.S1).

3.4.6. Plasmid constructions

The plasmids used and constructed in this work are listed in Table 3.S1 and briefly described below. The sequences of primers used are listed in Table 3.S2. Plasmid pEL29 was synthesized by Genewiz Inc. Plasmid pEL52 was synthesized by DNA 2.0.

Plasmid pEL53 was constructed by assembling a nphT7 fragment and a pEL11 without atoB fragment. nphT7 fragment was amplified by PCR with primers rEL-335 and rEL-336 with pEL52 as template. pEL11 without atoB fragment was amplified by PCR with primers rEL-333 and rEL-334 with pEL11 as template.

Plasmid pEL54 was constructed by assembling a bldh fragment, a yqhD fragment, and a pEL11 without adhE2 fragment. bldh fragment was amplified by PCR with primers rEL-329 and rEL-330 with Clostridium *saccharoperbutylacetonicum* NI-4 genome as template. yqhD fragment was amplified by PCR with primers rEL-331 and rEL-332 with *E. coli* genome as template. pEL11 without adhE2 fragment was amplified by PCR with primers rEL-327 and rEL-328 with pEL11 as template.

Plasmid pEL56 was constructed by assembling a NSII vector fragment and a pEL53 coding sequence fragment. NSII vector fragment was amplified by PCR with primers rEL-217

and rEL-253 with pEL37 as template. pEL53 coding sequence fragment was amplified by PCR with primers rEL-254 and rEL-255 with pEL53 as template.

Plasmid pEL57 was constructed by assembling a NSII vector fragment and a pEL54 coding sequence fragment. NSII vector fragment was amplified by PCR with primers rEL-217 and rEL-253 with pEL37 as template. pEL54 coding sequence fragment was amplified by PCR with primers rEL-254 and rEL-255 with pEL54 as template.

Plasmid pEL59 was constructed by assembling a NSII vector fragment, a pEL54 coding sequence without atoB fragment, and a nphT7 fragment. NSII vector fragment was amplified by PCR with primers rEL-217 and rEL-253 with pEL37 as template. pEL54 coding sequence without atoB fragment was amplified by PCR with primers rEL-352 and rEL-255 with pEL54 as template. nphT7 fragment was amplified by PCR with primers rEL-254 and rEL-351.

Plasmid pEL70 was constructed by assembling a pEL59 without crt.hbd fragment and a phaJ.phaB fragment. pEL59 without crt.hbd fragment was amplified by PCR with primers rEL-390 and rEL-391 with pEL59 as template. phaJ.phaB fragment was amplified by PCR with primers rEL-392 and rEL-393 with pEL29 as template.

Plasmid pEL71 was constructed by assembling a pEL57 without crt.hbd fragment and a phaJ.phaB fragment. pEL57 without crt.hbd fragment was amplified by PCR with primers rEL-390 and rEL-391 with pEL57 as template. phaJ.phaB fragment was amplified by PCR with primers rEL-392 and rEL-393 with pEL29 as template.

Plasmid pEL73 was constructed by assembling a pEL56 without crt.hbd fragment and a phaJ.phaB fragment. pEL56 without crt.hbd fragment was amplified by PCR with primers rEL-390 and rEL-398 with pEL56 as template. phaJ.phaB fragment was amplified by PCR with primers rEL-399 and rEL-393 with pEL70 as template.

Plasmids pEL75, pEL76, pEL77, pEL78, pEL79, and pEL80 were constructed by assembling a pDK26 without *adhE2* fragment and an aldehyde dehydrogenase gene from *Clostridium saccharoperbutylacetonicum* NI-4, *Clostridium Kluyveri*, *Geobacillus thermoglucosidasius, Escherichia coli, Clostridium beijerinckii NCIMB 8052,* and *Clostridium saccharobutylicum ATCC BAA-117*, respectively. pDK26 without *adhE2* fragment was amplified by PCR using primers rEL-403 and rEL-404 with pDK26 as template. C. *saccharoperbutylacetonicum* NI-4 *bldh* fragment was amplified by primers rEL-332 and rEL-394 with C. *saccharoperbutylacetonicum* NI-4 genome as template. *C. Kluyveri bldh* fragment was amplified by primers rEL-405 and rEL-406 with C. kluyveri genome as template. *G. thermoglucosidasius bldh* fragment was amplified by primers rEL-407 and rEL-408 with *G. thermoglucosidasius* genome as template. *E. coli EutE* fragment was amplified by primers rEL-409 and rEL-410 with *E. coli* genome as template. *C. beijerinckii NCIMB 8052 bldh* fragment was amplified by primers rEL-411 and rEL-412 with *C. beijerinckii NCIMB 8052* genome as template. *C. saccharobutylicum ATCC BAA-117 bldh* fragment was amplified by primers rEL-413 and rEL-414 with *C. saccharobutylicum ATCC BAA-117* genome as template.

Plasmids pEL90 to pEL96 were constructed by assembling the KASIII-like genes with a vector fragment. Vector fragment was amplified with primers rEL-455 and rEL-456 with pCS27 as the template. *bamb6224* was amplified with primers rEL-457 and rEL-458 with *Burkholderia ambifaria* gDNA as template. *gox0115* was amplified with primers rEL-459 and rEL-460 with *Gluconobacter oxydans* gDNA as template. *hp0202* was amplified with primers rEL-461 and rEL-462 with *Helicobacter pylori* gDNA as template. *lmo2202* was amplified with primers rEL-463 and rEL-464 with *Listeria monocytogenes* gDNA as template. *pae-fabH2* was amplified with primers rEL-467 and rEL-468 with *Pseudomonas aeruginosa* gDNA as template. *sav-fabH4*

was amplified with primers rEL-469 and rEL-470 with *Streptomyces avermitilis* gDNA as template. *sco5888* was amplified with primers rEL-471 and rEL-472 with *Streptomyces coelicolor* gDNA as template.

3.4.7. Strain construction and transformation

The strains used and constructed are listed in Table 3.S1. Briefly, strain EL18 was constructed by recombination of plasmids pEL57 NSII of Strain EL9 (Table 3.S1 for relevant genotypes). Strain EL20 was constructed by recombination of plasmids pEL56 into NSII of strain EL9. Strain EL21 was constructed by recombination of plasmids pEL59 into NSII of strain EL9. Strain EL22 was constructed by recombination of plasmids pEL70 into NSII of strain EL9. Strain EL23 was constructed by recombination of plasmids pEL71 into NSII of strain EL9. Strain EL24 was constructed by recombination of plasmids pEL73 into NSII of strain EL9.

S. elongatus PCC 7942 *strains* were transformed by incubating cells at mid-log phase (OD$_{730}$ of 0.4 to 0.6) with 2 μg of plasmid DNA overnight in dark. The culture was then spread on BG-11 plates supplemented with appropriate antibiotics for selection of successful recombination. For selection and culture maintenance, 20 μg/ml spectinomycin and 10 μg/ml kanamycin were added into BG-11 agar plates and BG-11 medium where appropriate. Colonies grown on BG-11 agar plates were grown in liquid culture. Genomic DNA was then prepared from the liquid culture and analyzed by PCR using gene-specific primers (Table 3.S2) to verify integration of inserted genes into the recombinant strain. In all cases, four individual colonies were analyzed and propagated for downstream tests

3.4.8. Protein Purification and SDS-PAGE

Protein purification was done by using His-Spin Protein miniprep purification kit from Zymo following manufacturer's manual. Overnight culture of XL-1 blue strains harboring individual plasmid of pEL90 to pEL96, each encodes for a particular KAS III-like enzyme, was used to inoculate fresh 20 ml LB. The newly inoculated culture was incubated at 37°C until OD_{600nm} reaches 0.6 which was then induced with 1 mM IPTG. The induced culture were then incubated in 30°C shaker for 2 hours to allow protein expression. The culture was then harvested by centrifugation at 5,250 x g for 20 min. The pellet was then resuspended with 1mL of 100 mM Tris-HCl pH 7.6 and mixed with 1mL of 0.1 mm glass beads (Biospec). The sample was then homogenated using mini bead beater (biospec). Total protein was then collected. Soluble protein was collected after centrifugation. Purified protein was collected after His-spin column purification. The protein samples were then ran on SDS-PAGE using commercially available precast gels (Biorad) following standard protocol.

3.4.9. Enzyme assays

Enzyme assays were conducted by using Bio-Tek PowerWave XS microplate spectrophotometer. Thiolase activity was measured via both condensation and thiolysis direction. The enzymatic reaction was monitored by the increase or decrease of absorbance at 303 nm which corresponded to the result of Mg^{2+} coordination with the diketo moiety of acetoacetyl-CoA (54). The enzymatic reaction was initiated by the addition of the enzyme. For purified enzyme reaction, the reaction mixture contained 100 mM Tris-HCl (pH 8.0), 20 mM $MgCl_2$, equimolar acetoacetyl-CoA and CoA. For the crude cyanobacteria extract assay, same buffer was used with 200 μM acetoacetyl-CoA and 300 μM CoA. Crude extract of strains EL22 (2.7 μg),

EL14 (5.0 μg), and Wild-type (2.4 μg) were used for assay. Concentration of acetoacetyl-CoA was calculated based on a constructed standard curve.

Acetoacetyl-CoA synthase activity was measured by monitoring the increase of absorbance at 303 nm which corresponds to appearance of acetoacetyl-CoA. The reaction buffer is the same as that used for thiolase assay. Equimolar malonyl-CoA and acetyl-CoA were used for purified enzyme assay, while 400 μM of both malonyl-CoA and acetyl-CoA were used for crude extract assay. Crude extract of strains EL22 (27 μg), EL14 (50 μg), and Wild-type (24 μg) were used for assay.

Enzyme assays for the other enzymes were conducted as previously described (21).

3.4.10. n-Butanol quantification

Culture samples (5 mL) were centrifuged for 20 minutes at 5,250 x g. The supernatant (900 μL) was then mixed with 0.1% v/v 2-methyl-pentanol (100 μL) as internal standard. The mixture was then vortexed and directly analyzed on Agilent GC 6850 system with flame ionization detector and DB-FFAP capillary column (30m, 0.32mm i.d., 0.25 film thickness) from Agilent Technologies (Santa Clara, CA). n-Butanol in the sample was identified and quantified by comparing to 0.001% v/v n-butanol standard. n-Butanol standard of 0.001% v/v was prepared by 100-fold dilution of a 0.1% v/v solution. The GC result was analyzed by Agilent software Chem Station (Rev.B.04.01 SP1). Amount of n-butanol in the sample was then calculated based on the ratio of its integrated area and that of the 0.001% n-butanol standard.

Helium gas was used as the carrier gas with 9.52 psi inlet pressure. The injector and detector temperatures were maintained at 225°C. Injection volume was 1 μL. The GC oven temperature was initially held at 85°C for 3 minutes and then raised to 235°C with a temperature

ramp of 45°C/min. The GC oven was then maintained at 235°C for 1 minute before completion of analysis. Column flow rate was 1.7 ml/min.

3.5. Appendices

Table 3.S1. Strain and plasmid list

Strain	Relevant genotypes	Reference
Cyanobacteria Strains		
PCC 7942	Wild-type *Synechococcus elongatus* PCC 7942	S.S.Golden
EL9	P_{Trc}::His-tagged *T. denticola ter* integrated at NSI in PCC7942 genome	(21)
EL14	P_{Trc}::His-tagged *T. denticola ter* integrated at NSI and P_{LlacO1}::*atoB, adhE2, crt, hbd* integrated at NSII in PCC7942 genome	(21)
EL18	P_{Trc}::His-tagged *T. denticola ter* integrated at NSI and P_{LlacO1}::*atoB, bldh, yqhD, crt, hbd* integrated at NSII in PCC7942 genome	This work
EL20	P_{Trc}::His-tagged *T. denticola ter* integrated at NSI and P_{LlacO1}::*nphT7, adhE2, crt, hbd* integrated at NSII in PCC7942 genome	This work
EL21	P_{Trc}::His-tagged *T. denticola ter* integrated at NSI and P_{LlacO1}::*nphT7, bldh, yqhD, crt, hbd* integrated at NSII in PCC7942 genome	This work
EL22	P_{Trc}::His-tagged *T. denticola ter* integrated at NSI and P_{LlacO1}::*nphT7, bldh, yqhD, phaJ, phaB* integrated at NSII in PCC7942 genome	This work
EL23	P_{Trc}::His-tagged *T. denticola ter* integrated at NSI and P_{LlacO1}::*atoB, bldh, yqhD, phaJ, phaB* integrated at NSII in PCC7942 genome	This work
EL24	P_{Trc}::His-tagged *T. denticola ter* integrated at NSI and P_{LlacO1}::*nphT7, adhE2, phaJ, phaB* integrated at NSII in PCC7942 genome	This work
E. coli strains		
BW25113	$rrnB_{T14}$ $\Delta lacZ_{WJ16}$ $hsdR514$ $\Delta araBAD_{AH33}$ $\Delta rhaBAD_{LD78}$	(58)
XL-1 blue	*recA1 endA1 gyrA96 thi-1 hsdR17 supE44 relA1 lac* [F' *proAB lacI^{q}ZΔM15 Tn10* (Tet^R)]	Stratagene
JCL299	BW25113 Δ*ldhA* Δ*adhE* Δ*frdBC* Δ*pta* / F' [*traD36, proAB+, lacI^q ZΔM15* (Tet^R)]	(19)

Plasmid	genotypes	Reference
pCDFDuet	Spec^R; CDF ori; P_{T7}::MCS	Novagen
pCDF-nphT7	Spec^R; CDF ori; P_{T7}::*nphT7* (his tagged)	This work
pCDF-atoB	Spec^R; CDF ori; P_{T7}::*atoB* (his tagged)	This work
pCS27	Kan^R; P15A ori; P_{LlacO1}::MCS	This work
pCS138	Cm^R; SC101 ori; P_{LlacO1}::*fdh*	(19)
pDK26	Amp^R; ColE1 ori; P_{LlacO1}::*bktB.adhE2.crt.paaH1*	This work
pEL11	Amp^R; ColE1 ori; P_{LlacO1}::*atoB.adhE2.crt.hbd*	(19)
pEL29	Kan^R; pUC ori; *ccr-phaJ-phaB*	This work
pEL37	Kan^R; NSII targeting; P_{LlacO1}::*atoB.adhE2.crt.hbd*	(21)
pEL52	Amp^R; pUC ori; P_{T5}::*nphT7*	This work
pEL53	Amp^R; ColE1 ori; P_{LlacO1}::*nphT7.adhE2.crt.hbd*	This work
pEL54	Amp^R; ColE1 ori; P_{LlacO1}::*atoB.bldh.yqhD.crt.hbd*	This work
pEL56	Kan^R; NSII targeting; P_{LlacO1}::*nphT7.adhE2.crt.hbd*	This work
pEL57	Kan^R; NSII targeting; P_{LlacO1}::*atoB.bldh.yqhD.crt.hbd*	This work
pEL59	Kan^R; NSII targeting; P_{LlacO1}::*nphT7.bldh.yqhD.crt.hbd*	This work
pEL70	Kan^R; NSII targeting; P_{LlacO1}::*nphT7.bldh.yqhD.phaJ.phaB*	This work

pEL71	Kan^R; NSII targeting; P_{LlacO1}::*atoB.bldh.yqhD.phaJ.phaB*	This work
pEL73	Kan^R; NSII targeting; P_{LlacO1}::*nphT7.adhE2.phaJ.phaB*	This work
pEL75	Amp^R; ColE1 ori; P_{LlacO1}::*bktB.bldh.yqhD.crt.paaH1*	This work
pEL76	Amp^R; ColE1 ori; P_{LlacO1}::*bktB.aldh(CK).yqhD.crt.paaH1*	This work
pEL77	Amp^R; ColE1 ori; P_{LlacO1}::*bktB.aldh(GT).yqhD.crt.paaH1*	This work
pEL78	Amp^R; ColE1 ori; P_{LlacO1}::*bktB.eutE.yqhD.crt.paaH1*	This work
pEL79	Amp^R; ColE1 ori; P_{LlacO1}::*bktB.aldh(CB).crt.paaH1*	This work
pEL80	Amp^R; ColE1 ori; P_{LlacO1}::*bktB.aldh(BAA117).yqhD.crt.paaH1*	This work
pEL90	Kan^R; P15A ori; P_{LlacO1}::*bamb6224 (his-tagged)*	This work
pEL91	Kan^R; P15A ori; P_{LlacO1}::*gox0115 (his-tagged)*	This work
pEL92	Kan^R; P15A ori; P_{LlacO1}::*hp0202 (his-tagged)*	This work
pEL93	Kan^R; P15A ori; P_{LlacO1}::*lmo2202 (his-tagged)*	This work
pEL94	Kan^R; P15A ori; P_{LlacO1}::*pae-fabH2 (his-tagged)*	This work
pEL95	Kan^R; P15A ori; P_{LlacO1}::*sav-fabH4 (his-tagged)*	This work
pEL96	Kan^R; P15A ori; P_{LlacO1}::*sco5888 (his-tagged)*	This work

Kan^R, kanamycin resistance; Amp^R, ampicillin resistance.
atoB (*E. coli*), thiolase; *nphT7* (*Streptomyces* sp. strain CL190), acetoacetyl-CoA synthase; *phaB* (*R. Eutropha*), acetoacetyl-CoA reductase; *phaJ* (*A. caviae*), (R)-specific enoyl-CoA hydratase; *hbd* (*C. acetobutylicum*), 3-hydroxybutyryl-CoA dehydrogenase; *crt* (*C. acetobutylicum*), crotonase; *ter* (*T. denticola*), Trans-2-enoyl-CoA reductase; *bldh* (*C. saccharoperbutylacetonicum*), butyraldehyde dehydrogenase; *paaH1* (*R. eutropha*), 3-hydroxybutyryl-CoA dehydrogenase; *yqhD* (*E. coli*), NADP-dependent alcohol dehydrogenase; *adhE2* (*C. acetobutylicum*), bifunctional alcohol/aldehyde dehydrogenase. *bktb* (*R. Eutropha*), thiolase; *aldh* (*C. kluyver*i, C. *beijerinckii*, C. *saccharobutylicum*, or *G. thermoglucosidasius*), aldehyde dehydrogenase; *eutE* (*E. coli*), aldehyde dehydrogenase; KASIII like enzymes: *bamb6224 (Burkholderia ambifaria), gox0115 (Gluconobacter oxydans), hp0202 (Helicobacter pylori), lmo2202 (Listeria monocytogenes), pae-fabH2 (Pseudomonas aeruginosa), sav-fabH4 (Streptomyces avermitilis), sco5888 (Streptomyces coelicolor).*

Table 3.S2. Primer Sequences

Primers	Sequence (5' -> 3')	Used for plasmid
rEL-333	TTGCGCTGATCGAGTGGTAAGCATGCAGGAGAAAGGTACCATGAAAG	pEL53
rEL-334	ATGCGGAAGCGGACGTCGGTCATGGTACCTTTCTCCTCTTTAATGAATTCGGTC	pEL53
rEL-335	CCGAATTCATTAAAGAGGAGAAAGGTACCATGACCGACGTCCGCTTCCGCATCA	pEL53; *nphT7* gene specific
rEL-327	AGGAGATATACCATGGAACTAAACAATGTCATCC	pEL54
rEL-328	TTAATTCAACCGTTCAATCACCATCGC	pEL54
rEL-329	GGTTGAATTAAGCATGCAGGAGAAAGGTACCATGATTAAAGACACGCTAGTTTCTATAAC	pEL54
rEL-330	GTTGTTCATGGTATATCTCCTTTAACCGGCGAGTACACATCTTCTTTGTC	pEL54
rEL-331	GTACTCGCCGGTTAAAGGAGATATACCATGAACAACTTTAATCTGCACACCCC	pEL54; yqhD specific
rEL-332	TTGTTTAGTTCCATGGTATATCTCCTTCTAGATTAGCGGGCGGCTTCGTATATACGGCGG	pEL54; yqhD specific
rEL-217	CTTTAATGAATTCGGTCAGTGCGTCCT	pEL56, pEL57, pEL59
rEL-253	ACGCGTGCTAGAGGCATCAAATAAA	pEL56, pEL57, pEL59
rEL-254	AGGACGCACTGACCGAATTCATTAAAG	pEL56, pEL57, pEL59
rEL-255	TTTATTTGATGCCTCTAGCACGCGTTTATTTTGAATAATCGTAGAAACCTTTTCCTG	pEL56, pEL57, pEL59
rEL-351	CATGGTACCTTTCTCCTGCATGCTTACCACTCGATCAGCGCAAAGCTCGC	pEL59
rEL-352	TAAGCATGCAGGAGAAAGGTACCATGATTAAAGACACGCTAGTTTC	pEL59
rEL-390	TAAACGCGTGCTAGAGGCATCAAATA	pEL70, pEL71, pEL73
rEL-391	GCAGACATGGTATATCTCCTTTAGCGGGCGGCTTCGTATATACGGC	pEL70, pEL71
rEL-392	ACGAAGCCGCCCGCTAAAGGAGATATACCATGTCTGCGCAATC	pEL70, pEL71
rEL-393	TTGATGCCTCTAGCACGCGTTTAACCCATGTGCAGACCACCGTTC	pEL70, pEL71, pEL73
rEL-398	CATGGTATATCTCCTTTAAAATGATTTTATATAGATATCCTTAAGTTCAC	pEL73
rEL-399	ATATCTATATAAAATCATTTTAAAGGAGATATACCATGTCTGCGC	pEL73
rEL-403	TAAAGGAGATATACCATGAACAACTTTAATCTGC	pEL75, pEL76, pEL77, pEL78, pEL79, pEL80
rEL-404	CTTTCTCCTGCATGCTTAGATACGC	pEL75, pEL76, pEL77, pEL78, pEL79, pEL80
rEL-332	TTGTTTAGTTCCATGGTATATCTCCTTCTAGATTAGCGGGCGGCTTCGTATATACGGCGG	pEL75
rEL-394	ATGCAGGAGAAAGGTACCATGATTAAAGACACGCTAGTTTCTATAAC	pEL75
rEL-405	AGCGTATCTAAGCATGCAGGAGAAAGGTACCATGGAGATAATGGATAAGGACTTACAGTC	pEL76
rEL-406	TAAAGTTGTTCATGGTATATCTCCTTTAAAGATTTAATTTAGCCATTATAGCTTTTAC	pEL76
rEL-407	GTATCTAAGCATGCAGGAGAAAGGTACCATGGATGCACAAAAAATTGAGAAACTTG	pEL77
rEL-408	AGTTGTTCATGGTATATCTCCTTTATCTTATCGACAAAGCATCCACTAGG	pEL77
rEL-409	CGTATCTAAGCATGCAGGAGAAAGGTACCATGAATCAACAGGATATTGAACAGGTG	pEL78
rEL-410	TTGTTCATGGTATATCTCCTTTAAACAATGCGAAACGCATCGACTA	pEL78
rEL-411	TCTAAGCATGCAGGAGAAAGGTACCATGAATAAAGACACACTAATACCTACAACTAAAG	pEL79
rEL-412	TAAAGTTGTTCATGGTATATCTCCTTTAGCCGGCAAGTACACATCTTCTTTG	pEL79
rEL-413	GTATCTAAGCATGCAGGAGAAAGGTACCATGAATAATAATTTATTCGTGTCACCAGAAAC	pEL80

86

rEL-414	TAAAGTTGTTCATGGTATATCTCCTTTAGCCTACGAACACACACCTTCTTTGTC	pEL80
rEL-455	GCTGTGGTGATGATGGTGATGGCTGCTGCCCATGGTACCTTTCTCCTCTTTAATGAATTC	pEL90 - 96
rEL-456	CGCGTGCTAGAGGCATCAAATAAAAC	pEL90 - 96
rEL-457	ATCACCATCATCACCACAGCATGGCGGAAATCACCGGCGCGGGGA	pEL90
rEL-458	TTTGATGCCTCTAGCACGCGCTACCAGCGAATCAACGCCGCCCCCCA	pEL90
rEL-459	ATCACCATCATCACCACAGCATGTCCGATCCCATTCGTGTCCGCCT	pEL91
rEL-460	TTTGATGCCTCTAGCACGCGTTACATCCGGATAAGGGCGGATCCCCA	pEL91
rEL-461	ATCACCATCATCACCACAGCATGGAATTTTACGCCTCTCTTAAATCCATT	pEL92
rEL-462	TTTGATGCCTCTAGCACGCGCTAACTTCCTCCAAAATACACCAACGCT	pEL92
rEL-463	ATCACCATCATCACCACAGCATGAACGCAGGAATTTTAGGAGTAGGTAAA	pEL93
rEL-464	TTTGATGCCTCTAGCACGCGTTACTTACCCCAACGAATGATTAGGGC	pEL93
rEL-467	ATCACCATCATCACCACAGCATGCCGCGCGCCGCCGTGGTCT	pEL94
rEL-468	TTTGATGCCTCTAGCACGCGTCAGTCCATTGTCGGAACGATCTTC	pEL94
rEL-469	ATCACCATCATCACCACAGCATGTCCCCTACCGCCGCCGGTTCTT	pEL95
rEL-470	TTTGATGCCTCTAGCACGCGTCATGACGTCGTCCGTTCTCCTTGG	pEL95
rEL-471	ATCACCATCATCACCACAGCATGACCCGGGCGTCCGTGCTGACCG	pEL96
rEL-472	TTTGATGCCTCTAGCACGCGTCAGACCGGATCGACGGCGGGCCAG	pEL96
rEL-148	GGGAAAGGATCCATGAAAAATTGTGTCATCGTCAGTGCGG	N/A; *atoB* gene specific
rEL-149	GGGAAAGCGGCCGCATTAATTCAACCGTTCAATCACCATCGC	N/A; *atoB* gene specific
rEL-157	GGGAAAGCGGCCGCATTATTTTGAATAATCGTAGAAACCTTTTCCTG	N/A; crt.*hbd* fragment specific
rEL-158	GGGAAAGGATCCATGGAACTAAACAATGTCATCCTTGAAAAGGA	N/A; *crt.hbd* fragment specific
rEL-160	GGGAAAGGATCCATGATTGTAAAACCAATGGTTAGGAACAAT	N/A; *ter* gene specific
rEL-161	GGGAAAGCGGCCGCATTAAATCCTGTCGAACCTTTCTACCTCG	N/A; *ter* gene specific
rEL-162	GGGAAAGGATCCATGAAAGTTACAAATCAAAAAGAACTAAAACAAAGC	N/A; *adhE2* gene specific
rEL-163	GGGAAAGCGGCCGCATTAAAATGATTTTATATAGATATCCTTAAGTTCAC	N/A; *adhE2* gene specific
rEL-323	GGGAAAGGATCCGATGTCTGCGCAATCTCTCGAAGTTG	N/A; *phaJ.phaB* fragment specific
rEL-326	GGGAAAAAGCTTTTAACCCATGTGCAGACCACCGTTC	N/A; *phaJ.phaB* fragment specific
rEL-349	GGGAAAGAATTCGATGATTAAAGACACGCTAGTTTCTATAAC	*N/A; bldh* gene specific
rEL-350	GGGAAAAAGCTTTTAACCGGCGAGTACACATCTTCTTTGTC	*N/A; bldh* gene specific
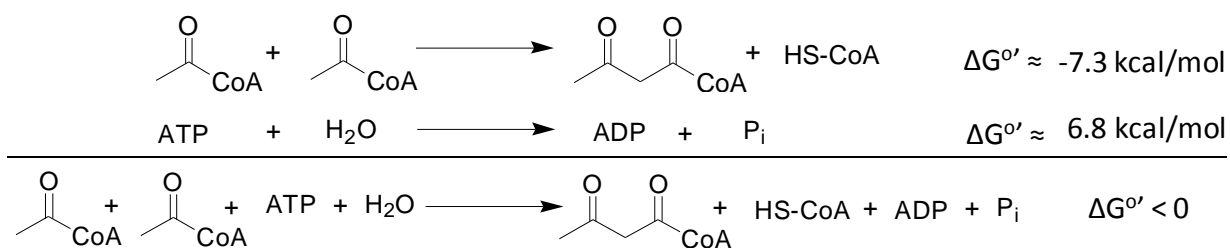
Figure 3.S1. Combining ATP hydrolysis to thiolase reaction yields a favorable net reaction
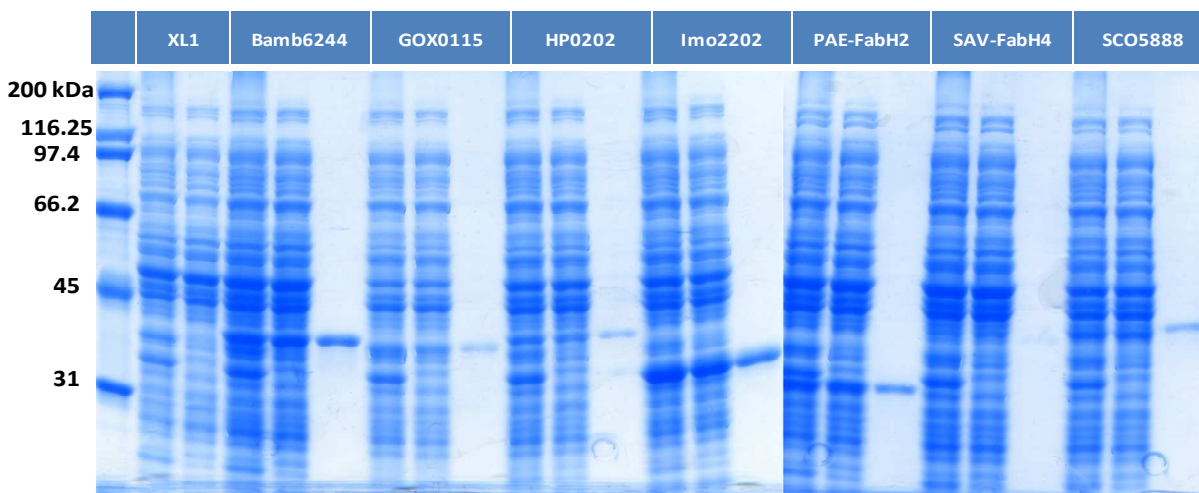
Figure 3.S2. Protein SDS-PAGE of His-tag purified KASIII-like enzymes
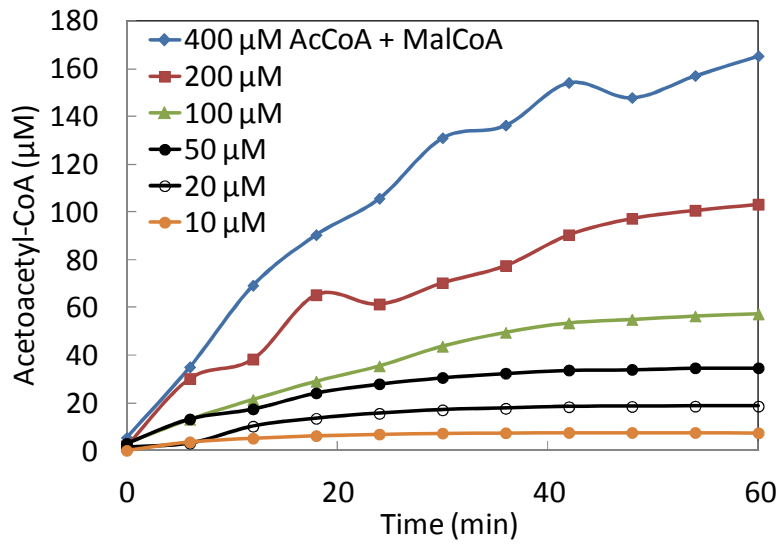
Figure 3.S3. In vitro assay of purified acetoacetyl‑CoA synthase (NphT7). Equimolar acetyl‑CoA and malonyl‑CoA of different concentration were used with 100 mM Tris‑HCl and 20 mM MgCl$_2$. Reaction was conducted at room temperature using spectrophotometer.

3.6. Reference

1.   Papoutsakis ET (2008) Engineering solventogenic clostridia. Curr Opin Biotechnol 19(5):420-429.

2.   Ezeji TC, Qureshi N, & Blaschek HP (2007) Bioproduction of butanol from biomass: from genes to bioreactors. Curr Opin Biotechnol 18(3):220-227.

3.   Atsumi S, Hanai T, & Liao JC (2008) Non-fermentative pathways for synthesis of branched-chain higher alcohols as biofuels. Nature 451(7174):86-89.

4.   Atsumi S & Liao JC (2008) Directed Evolution of Methanococcus jannaschii Citramalate Synthase for Biosynthesis of 1-Propanol and 1-Butanol by Escherichia coli. Appl Environ Microbiol 74(24):7802-7808.

5.   Shen CR & Liao JC (2008) Metabolic engineering of Escherichia coli for 1-butanol and 1-propanol production via the keto-acid pathways. Metab Eng 10(6):312-320.

6.   Dekishima Y, Lan EI, Shen CR, Cho KM, & Liao JC (2011) Extending Carbon Chain Length of 1-Butanol Pathway for 1-Hexanol Synthesis from Glucose by Engineered Escherichia coli. J Am Chem Soc 133(30):11399-11401.

7.   Dellomonaco C, Clomburg JM, Miller EN, & Gonzalez R (2011) Engineered reversal of the beta-oxidation cycle for the synthesis of fuels and chemicals. Nature 476(7360):355-359.

8.   Zhang K, Sawaya MR, Eisenberg DS, & Liao JC (2008) Expanding metabolism for biosynthesis of nonnatural alcohols. Proc Natl Acad Sci USA 105(52):20653-20658.

9.   Nicolaou SA, Gaida SM, & Papoutsakis ET (2010) A comparative view of metabolite and substrate stress and tolerance in microbial bioprocessing: From biofuels and chemicals, to biocatalysis and bioremediation. Metab Eng 12(4):307-331.

10.   Sillers R, Chow A, Tracy B, & Papoutsakis ET (2008) Metabolic engineering of the non-sporulating, non-solventogenic Clostridium acetobutylicum strain M5 to produce butanol without acetone demonstrate the robustness of the acid-formation pathways and the importance of the electron balance. Metab Eng 10(6):321-332.

11.   Yu MR, Zhang YL, Tang IC, & Yang ST (2011) Metabolic engineering of Clostridium tyrobutyricum for n-butanol production. Metab Eng 13(4):373-382.

12.   Atsumi S, et al. (2008) Metabolic engineering of Escherichia coli for 1-butanol production. Metab Eng 10(6):305-311.

13.   Inui M, et al. (2008) Expression of Clostridium acetobutylicum butanol synthetic genes in Escherichia coli. Appl Microbiol Biotechnol 77(6):1305-1316.

14. Nielsen DR, et al. (2009) Engineering alternative butanol production platforms in heterologous bacteria. Metab Eng 11(4-5):262-273.

15. Berezina OV, et al. (2010) Reconstructing the clostridial n-butanol metabolic pathway in Lactobacillus brevis. Appl Microbiol Biotechnol 87(2):635-646.

16. Steen EJ, et al. (2008) Metabolic engineering of Saccharomyces cerevisiae for the production of n-butanol. Microb Cell Fact 7(36).

17. Boynton ZL, Bennett GN, & Rudolph FB (1996) Cloning, sequencing, and expression of clustered genes encoding beta-hydroxybutyryl-coenzyme A (CoA) dehydrogenase, crotonase, and butyryl-CoA dehydrogenase from Clostridium acetobutylicum ATCC 824. J Bacteriol 178(11):3015-3024.

18. Li F, et al. (2008) Coupled ferredoxin and crotonyl coenzyme a (CoA) reduction with NADH catalyzed by the butyryl-CoA dehydrogenase/Etf complex from Clostridium kluyveri. J Bacteriol 190(3):843-850.

19. Shen CR, et al. (2011) Driving forces enable high-titer anaerobic 1-butanol synthesis in Escherichia coli. Appl Environ Microbiol 77(9):2905-2915.

20. Bond-Watts BB, Bellerose RJ, & Chang MCY (2011) Enzyme mechanism as a kinetic control element for designing synthetic biofuel pathways. Nat Chem Biol 7(4):222-227.

21. Lan EI & Liao JC (2011) Metabolic engineering of cyanobacteria for 1-butanol production from carbon dioxide. Metab Eng 13(4):353-363.

22. Atsumi S, Higashide W, & Liao JC (2009) Direct photosynthetic recycling of carbon dioxide to isobutyraldehyde. Nat Biotechnol 27(12):1177-1180.

23. Patnaik R, Roof WD, Young RF, & Liao JC (1992) Stimulation of glucose catabolism in Escherichia coli by a potential futile cycle. J Bacteriol 174(23):7527-7532.

24. Chao YP & Liao JC (1993) Alteration of growth yield by overexpression of phosphoenolpyruvate carboxylase and phosphoenolpyruvate carboxykinase in Escherichia coli. Appl Environ Microbiol 59(12):4261-4265.

25. Causey TB, Zhou S, Shanmugam KT, & Ingram LO (2003) Engineering the metabolism of Escherichia coli W3110 for the conversion of sugar to redox-neutral and oxidized products: Homoacetate production. Proc Natl Acad Sci USA 100(3):825-832.

26. Xu P, Ranganathan S, Fowler ZL, Maranas CD, & Koffas MAG (2011) Genome-scale metabolic network modeling results in minimal interventions that cooperatively force carbon flux towards malonyl-CoA. Metab Eng 13(5):578-587.

27. Rust MJ, Golden SS, & O'Shea EK (2011) Light-driven changes in energy metabolism directly entrain the cyanobacterial circadian oscillator. Science 331(6014):220-223.

28. Stern JR, Coon MJ, & Delcampillo A (1953) Acetoacetyl Coenzyme-a as Intermediate in the Enzymatic Breakdown and Synthesis of Acetoacetate. J Am Chem Soc 75(6):1517-1518.

29. Okamura E, Tomita T, Sawa R, Nishiyama M, & Kuzuyama T (2010) Unprecedented acetoacetyl-coenzyme A synthesizing enzyme of the thiolase superfamily involved in the mevalonate pathway. Proc Natl Acad Sci USA 107(25):11265-11270.

30. Tamoi M, Miyazaki T, Fukamizo T, & Shigeoka S (2005) The Calvin cycle in cyanobacteria is regulated by CP12 via the NAD(H)/NADP(H) ratio under light/dark conditions. Plant J 42(4):504-513.

31. Slater SC, Voige WH, & Dennis DE (1988) Cloning and Expression in Escherichia-Coli of the Alcaligenes-Eutrophus H16 Poly-Beta-Hydroxybutyrate Biosynthetic-Pathway. J Bacteriol 170(10):4431-4436.

32. Fukui T, Shiomi N, & Doi Y (1998) Expression and characterization of (R)-specific enoyl coenzyme A hydratase involved in polyhydroxyalkanoate biosynthesis by Aeromonas caviae. J Bacteriol 180(3):667-673.

33. Perez JM, Arenas FA, Pradenas GA, Sandoval JM, & Vasquez CC (2008) Escherichia coli YqhD exhibits aldehyde reductase activity and protects from the harmful effect of lipid peroxidation-derived aldehydes. J Biol Chem 283(12):7346-7353.

34. Yan RT & Chen JS (1990) Coenzyme a-Acylating Aldehyde Dehydrogenase from Clostridium-Beijerinckii Nrrl-B592. Appl Environ Microbiol 56(9):2591-2599.

35. Kosaka T, Nakayama S, Nakaya K, Yoshino S, & Furukawa K (2007) Characterization of the sol operon in butanol-hyperproducing Clostridium saccharoperbutylacetonicum strain N1-4 and its degeneration mechanism. Biosci, Biotechnol, Biochem 71(1):58-68.

36. Dexter J & Fu PC (2009) Metabolic engineering of cyanobacteria for ethanol production. Energy Environ Sci 2(8):857-864.

37. Takahama K, Matsuoka M, Nagahama K, & Ogawa T (2003) Construction and analysis of a recombinant cyanobacterium expressing a chromosomally inserted gene for an ethylene-forming enzyme at the psbAI locus. J Biosci Bioeng 95(3):302-305.

38. Lindberg P, Park S, & Melis A (2010) Engineering a platform for photosynthetic isoprene production in cyanobacteria, using Synechocystis as the model organism. Metab Eng 12(1):70-79.

39. Niederholtmeyer H, Wolfstadter BT, Savage DF, Silver PA, & Way JC (2010) Engineering Cyanobacteria To Synthesize and Export Hydrophilic Products. Appl Environ Microbiol 76(11):3462-3466.

40. Tan XM, et al. (2011) Photosynthesis driven conversion of carbon dioxide to fatty alcohols and hydrocarbons in cyanobacteria. Metab Eng 13(2):169-176.

41.   Liu XY, Sheng J, & Curtiss R (2011) Fatty acid production in genetically modified cyanobacteria. Proc Natl Acad Sci USA 108(17):6899-6904.

42.   Bastian S, et al. (2011) Engineered ketol-acid reductoisomerase and alcohol dehydrogenase enable anaerobic 2-methylpropan-1-ol production at theoretical yield in Escherichia coli. Metab Eng 13(3):345-352.

43.   Davis MS, Solbiati J, & Cronan JE (2000) Overproduction of acetyl-CoA carboxylase activity increases the rate of fatty acid biosynthesis in Escherichia coli. J Biol Chem 275(37):28593-28598.

44.   Vadali RV, Bennett GN, & San KY (2004) Cofactor engineering of intracellular CoA/acetyl-CoA and its effect on metabolic flux redistribution in Escherichia coli. Metab Eng 6(2):133-139.

45.   Leonard E, Lim KH, Saw PN, & Koffas MAG (2007) Engineering central metabolic pathways for high-level flavonoid production in Escherichia coli. Appl Environ Microbiol 73(12):3877-3886.

46.   Zha WJ, Rubin-Pitel SB, Shao ZY, & Zhao HM (2009) Improving cellular malonyl-CoA level in Escherichia coli via metabolic engineering. Metab Eng 11(3):192-198.

47.   Miyahisa I, et al. (2005) Efficient production of (2S)-flavanones by Escherichia coli containing an artificial biosynthetic gene cluster. Appl Microbiol Biotechnol 68(4):498-504.

48.   Lu XF, Vora H, & Khosla C (2008) Overproduction of free fatty acids in E. coli: Implications for biodiesel production. Metab Eng 10(6):333-339.

49.   Santos CNS, Koffas M, & Stephanopoulos G (2011) Optimization of a heterologous pathway for the production of flavonoids from glucose. Metab Eng 13(4):392-400.

50.   Bustos SA & Golden SS (1991) Expression of the Psbdii Gene in Synechococcus Sp Strain-Pcc-7942 Requires Sequences Downstream of the Transcription Start Site. J Bacteriol 173(23):7525-7533.

51.   Bustos SA & Golden SS (1992) Light-Regulated Expression of the Psbd Gene Family in Synechococcus-Sp Strain Pcc-7942 - Evidence for the Role of Duplicated Psbd Genes in Cyanobacteria. Mol Gen Genet 232(2):221-230.

52.   Andersson CR, et al. (2000) Application of bioluminescence to the study of circadian rhythms in cyanobacteria. Bioluminescence and Chemiluminescence, Pt C 305:527-542.

53.   Gibson DG, et al. (2009) Enzymatic assembly of DNA molecules up to several hundred kilobases. Nat Methods 6(5):343-345.

54.   Nishimura T, Saito T, & Tomita K (1978) Purification and properties of beta-ketothiolase from Zoogloea ramigera. Arch Microbiol 116(1):21-27.

55.   Datsenko KA & Wanner BL (2000) One-step inactivation of chromosomal genes in Escherichia coli K-12 using PCR products. Proc Natl Acad Sci USA 97(12):6640-6645.

4. OXYGEN-TOLERANT COENZYME A-ACYLATING ALDEHYDE DEHYDROGENASE FACILITATES EFFICIENT PHOTOSYNTHETIC *N*-BUTANOL BIOSYNTHESIS IN CYANOBACTERIA

4.1. Introduction

While incorporation of ATP driving force successfully achieved direct photosynthetic production of n-butanol, the productivity of n-butanol is significantly less than that of isobutanol (8). In this chapter, we showed that oxygen sensitive CoA-acylating aldehyde dehydrogenase (Bldh) is the limiting step of the n-butanol pathway and achieved near 20-fold improvement of n-butanol productivity by replacing Bldh with an oxygen tolerant aldehyde dehydrogenase.

Cyanobacteria are currently being developed as microbial factories for production of renewable chemicals (1-9) by redirecting carbon fluxes from central metabolism into desirable products (Fig. 4.1A). However, metabolic engineering of cyanobacteria remain challenging because of their incompletely characterized physiology, limited genetic tools, and relatively low growth rate. In particular, pathways originated from anaerobes are often difficult to express in cyanobacteria due to enzyme oxygen sensitivity and difference in redox environment.

n-Butanol is an important chemical feedstock (Fig. 4.1B) used to produce solvents (butyl acetate, butyl glycol ethers), polymers (butyl acrylate, butyl methacrylate), and plasticizers (butyl phthalate, butylbenzyl phthalate). Derivatives of n-butanol including n-butene, butyraldehyde, and butyrate are also used to synthesize a wide array of chemical products. Furthermore n-butanol is a more efficient fuel additive or substitute than ethanol as it is higher in energy density and lower in hygroscopicity, allowing it to be compatible with existing infrastructure. Currently, global n-butanol consumption is 2.9 million metric tons, representing a $5.7 billion market, and continues to grow 4.7% a year (10).
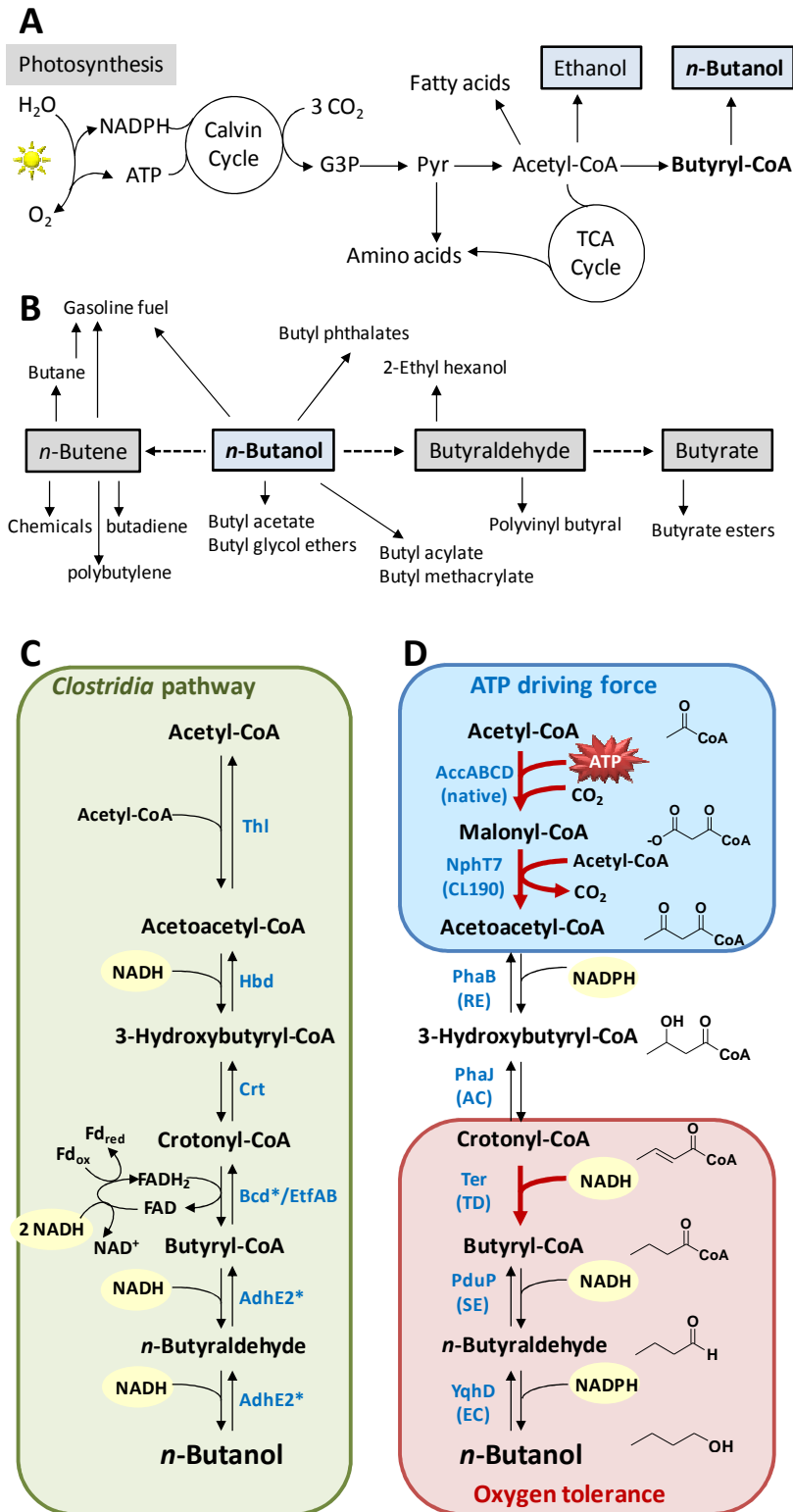
Figure 4.1. Schematics of *n*-butanol production from CO_2. Schematics for A) Cyanobacteria metabolism, B) Chemical derivatives of n-butanol, C) Native *Clostridium acetobutylicum* pathway for n-butanol production, and D) Synthetic n-butanol biosynthesis pathway designed

with ATP driving force and oxygen tolerance in this study. Abbreviations: Thl, thiolase; Hbd, 3-hydroxybutyryl-CoA dehydrogenase; crt, crotonase; Bcd/EtfAB, butyryl-CoA dehydrogenase electron transferring protein complex; AdhE2, bifunctional aldehyde/alcohol dehydrogenase; AccABCD, acetyl-CoA carboxylase; NphT7, acetoacetyl-CoA synthase; PhaB, acetoacetyl-CoA reductase; PhaJ, R-specific crotonase; Ter, trans-enoyl-CoA reductase; PduP, CoA-acylating propionaldehyde dehydrogenase; YqhD, NADPH dependent alcohol dehydrogenase; G3P, glyceraldehyde-3-phosphate; Pyr, pyruvate; Fd_{ox}, oxidized ferredoxin; Fd_{red}, reduced ferredoxin. * indicates oxygen sensitivity

Microbial n-butanol (11) is produced via natural metabolic pathway in selected species of *Clostridia* (12-14) and in recombinant organisms via synthetic pathways (15-17). The *Clostridium* Coenzyme A (CoA) dependent pathway is of particular interest for its efficient chain elongation which can be engineered to synthesize longer chain chemicals (18, 19). The native *Clostridium* pathway (Fig. 4.1C) proceeds by condensation of two acetyl-CoA and a series of reduction using NADH and dehydration to form n-butanol. The enzyme butyryl-CoA dehydrogenase complex (Bcd-EtfAB) has been difficult to express in heterologous organisms due to oxygen sensitivity (20) and potential requirement for accessory redox partners (21) which may not exist in heterologous organisms (Fig. 4.1C). Expression of a trans-2-enoyl-CoA reductase (Ter) using NADH for direct reduction of crotonyl-CoA efficiently avoided the need of Bcd/etfAB complex and achieved high flux production of n-butanol production in *Escherichia coli* (22, 23).

While the Ter-dependent pathway produces n-butanol well in *E. coli*, this performance is not directly transferable into cyanobacteria. We previously demonstrated that the Ter-dependent pathway in cyanobacterium *Synechococcus elongatus* PCC 7942 requires anaerobic treatment and inhibition of photosystem II to avoid oxygen evolution for the synthesis of n-butanol (24). Under these conditions, n-butanol production relies on internal storage of carbon. In contrast, isobutanol was produced in relatively high titer and productivity(8). Comparing the two pathways, we note that the first step in the isobutanol pathway evolves CO_2, which provides a

97

driving force, and that the isobutanol pathway does not involve any oxygen-sensitive enzymes. Thus, the difficulty of photosynthetic n-butanol production may be attributable to the lack of thermodynamic driving forces (3) and oxygen sensitivity of pathway enzymes. To solve the first problem, we engineered an ATP driving force (Fig. 4.1D boxed in blue) inspired by fatty acid biosynthesis and enabled the first demonstration of direct photosynthetic production of n-butanol (3). Activation of acetyl-CoA into malonyl-CoA with ATP provides the thermodynamic driving force necessary to overcome the energetic barrier of acetyl-CoA condensation. Utilizing this malonyl-CoA dependent pathway, the resulting *S. elongatus* strain produced 30 mg/L of n-butanol with peak productivity of 2 mg/L/d.

CoA-acylating butyraldehyde dehydrogenase (Bldh), which catalyzes the termination of CoA-dependent chain elongation by reducing butyryl-CoA into butyraldehyde, is an oxygen-sensitive enzyme which possibly limits the productivity of the pathway. Bldh from *Clostridium beijerinckii* has been characterized to lose activity upon exposure to oxygen (25). Similarly, AdhE2, a bifunctional aldehyde/alcohol dehydrogenase from traditional n-butanol producer *Clostridium acetobutylicum*, is also oxygen sensitive (26).

In this chapter, we address the oxygen sensitivity of Bldh by recruiting CoA-acylating propionaldehyde dehydrogenase (PduP) from coenzyme-B12-dependent 1,2-propanediol degradation pathway to substitute for Bldh. PduP from *Salmonella enterica* (27) has been shown to catalyze propionaldehyde oxidation to propionyl-CoA for detoxification of propionaldehyde, an intermediate formed from 1,2-propanediol degradation. We reasoned that since 1,2-propanediol degradation occurs under aerobic conditions, PduP is likely to be oxygen tolerant. Six different PduP homologues were cloned and purified with poly-His tags, and their kinetic properties were determined. We showed that these PduP homologues catalyze reversible

98

reduction of acyl-CoA of different carbon chain lengths. Expression of PduP with the enzymes of the n-butanol synthesis pathway in *S. elongatus* resulted in autotrophic n-butanol production to a cumulative titer of about 400 mg/L with peak productivity of 51 mg/L/d, exceeding the strain expressing Bldh by 20 fold. These results demonstrate that oxygen tolerance is an important factor for alcohol production under photosynthetic conditions.

4.2. Results

4.2.1. CoA-acylating aldehyde dehydrogenase PduP catalyzes butyryl-CoA reduction

To circumvent Bldh oxygen sensitivity in cyanobacteria, we searched for alternative CoA-acylating aldehyde dehydrogenases. PduP, an enzyme identified from *Salmonella enterica*, is responsible for catalyzing the oxidation of propionaldehyde to propionyl-CoA, an important detoxification step for 1,2-propanediol degradation pathway. This enzyme is expressed in *S. enterica* under aerobic condition and has been previously demonstrated with in vitro activity for the oxidation of propionaldehyde to propionyl-CoA (27). In addition to *S. enterica* PduP, we cloned five more PduP homologues identified by homology search with BLAST using *S. enterica* PduP protein sequence. It was unclear whether or not PduP is efficient at catalyzing the reduction of acyl-CoA to the corresponding aldehyde, the reverse of its natural direction. It was also uncertain whether or not PduP acts on butyl-CoA, the four carbon substrate.

We tested these PduP homologues for n-butanol production utilizing an anaerobic growth rescue assay previously described (22). *E. coli* strain JCL 166 ($\Delta adhE$, $\Delta ldhA$, $\Delta frdB$) contains gene knock-outs for mixed acid fermentation. Fermentation pathways are essential for *E. coli* to recycle NADH back into to NAD^+ for the Embden–Meyerhof–Parnas pathway to continue (Fig 4.2A). As a result of these knock-outs, strain JCL166 cannot grow anaerobically unless
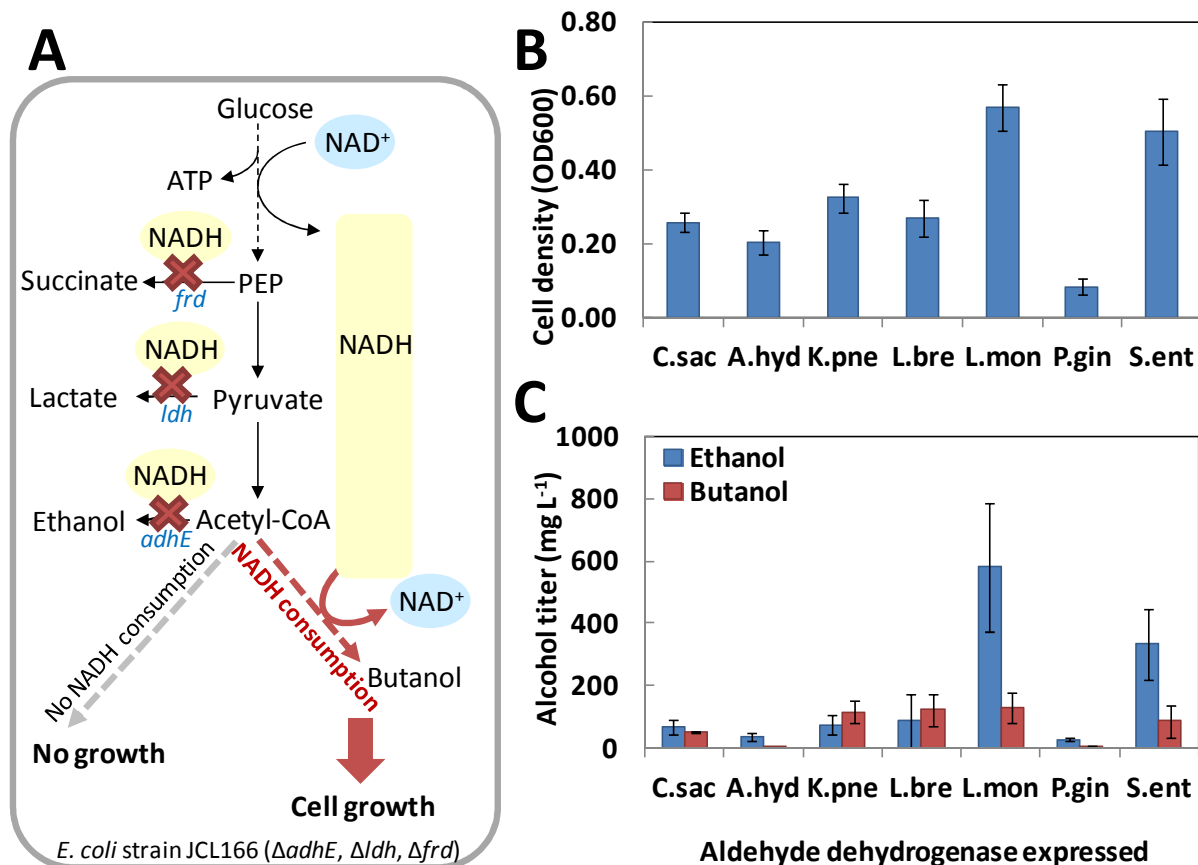
Figure 4.2. Anaerobic growth rescue of *E. coli* strain JCL166 by overexpression of *Clostridium* butanol pathway with different aldehyde dehydrogenases PduP. A) Schematics of anaerobic growth selection by *E. coli* strain JCL166. Genes for mixed acid fermentation (*adhE*, *ldhA*, *frdB*) were knocked out. As a result, *E. coli* strain JCL166 cannot recycle NADH back to NAD+. Cell growth of strain JCL166 is inhibited until a fermentation pathway consuming NADH is engineered into JCL166, establishing the basis of this anaerobic growth selection. B) Growth rescue of strain JCL166 by overexpression of different PduP with *Clostridium* butanol pathway. C) Alcohol production from the growth rescue broth.

complemented by an exogenous fermentation pathway such as n-butanol biosynthesis. We thus

expressed the PduP homologues together with the rest of the Ter dependent n-butanol

biosynthetic genes (22) using plasmids pEL179, pEL180, pEL181, pEL182, pEL183, and

pEL184 for expressing each *pduP* and *yqhD*, and pEL175 for expressing *atoB*, *hbd*, *crt*, and *ter*.

As shown in Fig 4.2B, all PduP, except the one from *P. gingivalis*, enabled anaerobic growth

rescue, and Bldh from *Clostridium saccharoperbutylacetonicum* was the positive control. We

100

analyzed the culture medium of these anaerobically grown cultures for alcohol production (Fig 4.2C) using gas chromatography (GC). PduP from *L. brevis* and *K. pneumoniae* produced more n-butanol than ethanol, while PduP from *L. monocytigenes* and *S. enterica* produced more ethanol than n-butanol at a ratio of 4:1. These results indicated that these PduP homologues catalyze the reduction of butyryl-CoA, in our desired and the non-native direction.

4.2.2. Substrate specificity of PduP

To characterize these PduP homologues, we constructed plasmids harboring individual *pduP* genes with a poly-His$_6$ tag (plasmids pCDF-pduP_ahyd, pCDF-pdup_kpne, pCDF-pdup_lbre, pCDF-pdup_lmon, pCDF-pdup_sent, and pCDF-pdup_pgin). PduP homologues were then purified under aerobic condition without cleaving off His tags. The activities of the enzymes were determined using acyl-CoA with different chain lengths, and the disappearance of NADH was monitored. As shown in Fig. 4.3A, PduP from *S. enterica, L. monocytigenes, and K. pneumoniae* exhibited higher activity than the other PduP homologues for carbon chain lengths ranging from 2 to 8. For butyryl-CoA reduction, *S. enterica* PduP was the most active (27 ± 14 µmol/min/mg) under the assayed condition, followed by PduP from *L. monocytigenes* (17 ± 2 µmol/min/mg), *K. pneumoniae* (8.9 ± 4.6 µmol/min/mg), L. brevis (2.5 ± 0.2 µmol/min/mg), *A. hydrophilia* (1.7 ± 0.6 µmol/min/mg), and *P. gingivalis* (0.49 ± 0.2 µmol/min/mg).

Specific activity was the highest for propionyl-CoA reduction compared to other acyl-CoAs for PduP from *S. enterica, L. monocytigenes, and K. pneumoniae* (Fig. 4.3B). This was expected since propionaldehyde is the natural substrate for PduP. Interestingly, PduP from *L. brevis*, *P. gingivalis*, and *A. hydrophilia* exhibited different substrate specificity. As shown in Fig. 4.3B, PduP from *L. brevis* and *P gingivalis* favors reduction of hexanoyl-CoA and
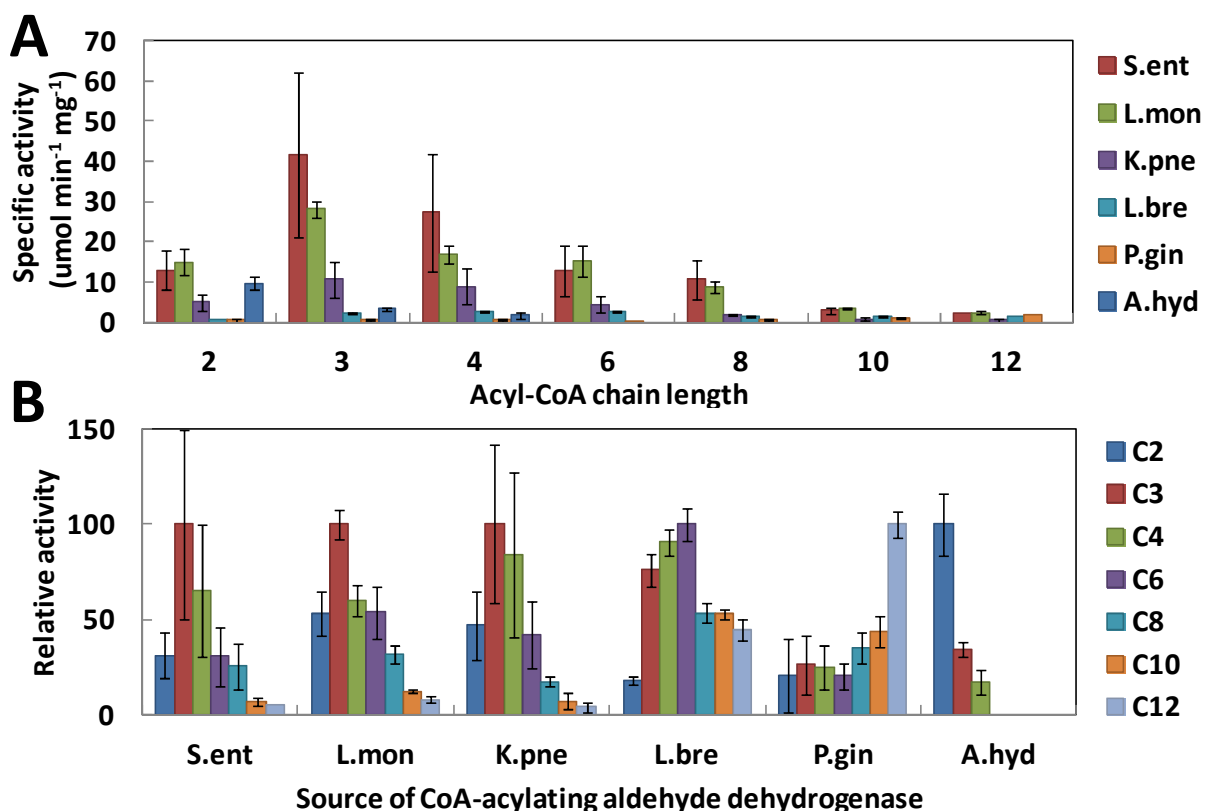
Figure 4.3. Substrate chain length specificity of CoA-acylating aldehyde dehydrogenases PduP. A) Specific activity of different PduP (umol min^{-1} mg^{-1}). B) Relative activity of PduP. Specific activity was determined with substrate concentration of 1 mM acyl-CoA, 500 uM NADH, 1 mM DTT in 50 mM potassium phosphate buffer at pH 7.15 at 30 °C

dodecanoyl-CoA, respectively, over other substrate lengths. These results are particularly useful when the synthesis of longer chain aldehydes and alcohols are desired.

4.2.3. Kinetic parameters of PduP

We further assessed the efficiency of these PduP homologues. Because these PduP enzymes act on both acetyl-CoA and butyryl-CoA, the ratio of their catalytic efficiency (k_{cat}/K_m) towards acetyl-CoA and butyryl-CoA is especially important for designing n-butanol production pathway. The kinetic parameters were measured for these PduP homologues by monitoring

Table 4.1. Kinetic parameters (k_{cat} and K_m) of CoA-acylating aldehyde dehydrogenase

Source Organism	Acetyl-CoA			Butyryl-CoA			Ratio C4:C2
	k_{cat} (s^{-1})	K_m (μM)	k_{cat}/K_m $(s^{-1}mM^{-1})$	k_{cat} (s^{-1})	K_m (μM)	k_{cat}/K_m $(s^{-1}mM^{-1})$	
C.sac	n.d[a]		–	n.d[a]		–	–
A.hyd	n.d[b]		–	n.d[b]		–	–
K.pne	4.63 ± 0.19	181.4 ± 25.1	25	7.02 ± 0.64	56.0 ± 25.9	125	**5**
L.bre	0.26 ± 0.10	76.0 ±38.2	3.0	3.37 ± 0.19	534.3 ± 59.8	6.0	**2**
L.mon	11.33 ± 0.97	92.6 ± 20.1	122	11.99 ± 1.56	71.7 ± 20.3	167	**1.4**
P.gin	0.08 ± 0.01	75.9 ± 25.1	1.1	0.19 ± 0.02	256.0 ± 40.5	0.7	**0.6**
S.ent	14.81 ± 1.00	342.1 ± 94.8	43	25.38 ± 1.81	87.0 ± 24.8	292	**6.8**

[a]not determined due to oxygen sensitivity
[b]not determined due to non-Michaelis-Menten behavior

NADH oxidation over a range of acetyl-CoA and butyryl-CoA concentrations. The K_m and k_{cat} values for acetyl-CoA and butyryl-CoA are summarized in Table 4.1. Kinetic parameters for PduP from *A. hydrophilia* and *Clostridium saccharoperbutylacetonicum* were not determined due to a non-Michealis-Menten behavior and oxygen sensitivity, respectively. PduP from *S. enterica* showed the highest butyryl-CoA to acetyl-CoA catalytic efficiency ratio of 6.8, followed by PduP from *K. pneumoniae* (5.0), *L. brevis* (2.0), *L. monocytigenes* (1.4), and *P. gingivalis* (0.6). These results indicated that PduP from *S. enterica*, *K. pneumoniae*, *L. brevis*, and *L. monocytigenes* are suitable for co-expression with the CoA-dependent pathway in cyanobacteria for n-butanol production.
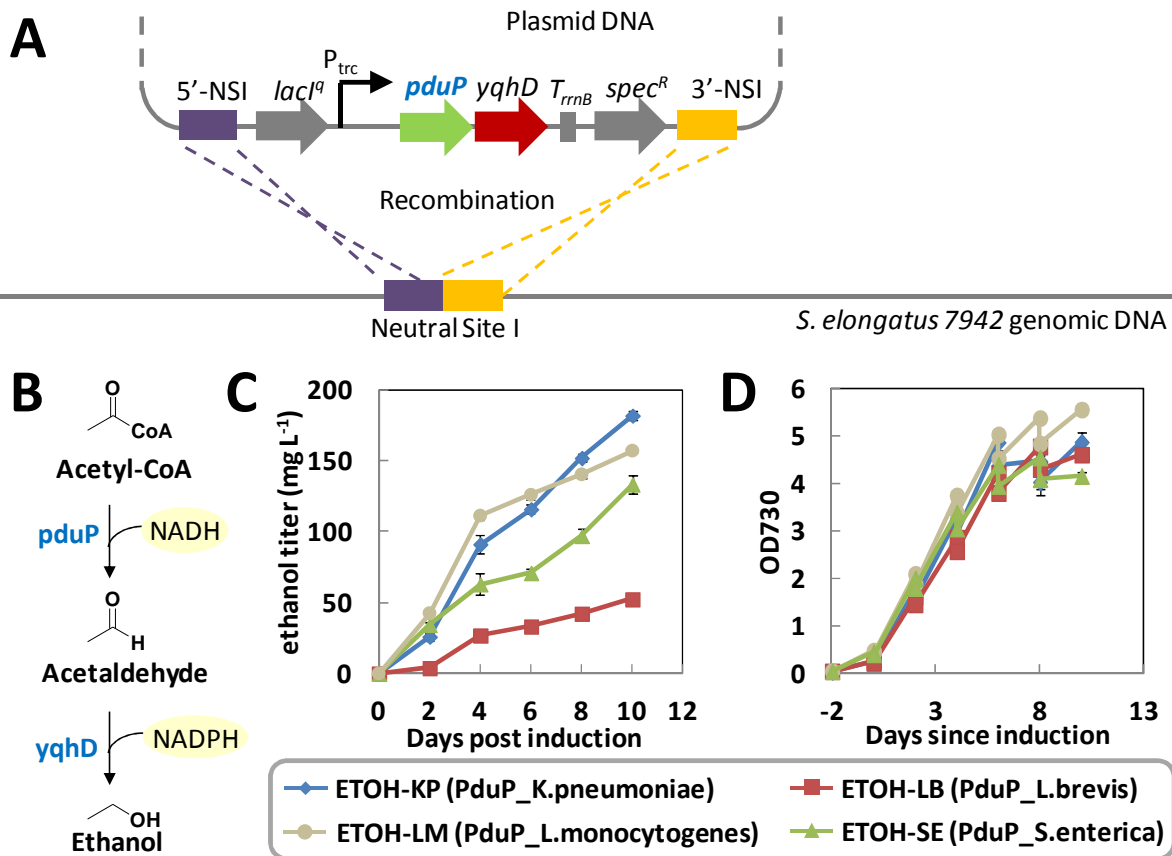
Figure 4.4. Ethanol biosynthesis from acetyl-CoA. A) Schematics of gene recombination of pduP and yqhD into neutral site I of S. elongatus PCC7942. B) Schematics of ethanol biosynthesis from acetyl-CoA using pduP and yqhD. C) Time course of cumulative ethanol production. Here cumulative titer takes into account the dilutions made to cyanobacteria culture by feeding. For detailed description, see Materials and Methods section. D) Cell density of S. elongatus strains ETOH-KP, ETOH-LB, ETOH-LM, and ETOH-SE.

4.2.4. Co-expression of PduP enables photosynthetic ethanol biosynthesis from acetyl-CoA

Next, we introduced the individual PduP enzymes with YqhD into *S. elongatus* PCC 7942 by homologous recombination (Fig. 4.4A) into Neutral Site (NS) I (28). We constructed plasmids harboring individual *pdup* genes and *yqhD* under an IPTG inducible Trc promoter. These plasmids were then individually used to transform *S. elongatus* PCC 7942. The resulting *S. elongatus* strains ETOH-KP, ETOH-LB, ETOH-LM, and ETOH-SE (Table 4.2) express YqhD and PduP from *K. pneumoniae, L. brevis, L. monocytigenes*, and *S. enterica*, respectively.

Expression of PduP and YqhD enabled photosynthetic ethanol production from acetyl-CoA (Fig. 4.4B). PduP reduces acetyl-CoA into acetaldehyde, which is then reduced to ethanol by YqhD.

As shown in Fig. 4.4C, all strains expressing PduP homologues with YqhD demonstrated ethanol production. Strain ETOH-KP produced the highest amount of ethanol, reaching a cumulative titer of 182 ± 4 mg/L after 10 days of cultivation with a peak productivity of 65 mg/L/d occurring between the Day 2 to 4. Strain ETOH-LM showed higher ethanol productivity than strain ETOH-KP for the first four days, after which production slowed down, reaching a cumulative titer of 157 ± 3 mg/L after 10 days. ETOH-LM exhibited highest cell growth (Fig. 4.4D), reaching OD730 of 5.56, which is about 15% higher than strain ETOH-KP and 30% higher than the slowest growing strain ETOH-SE. Strains ETOH-SE and ETOH-LB each produced 133 ± 7 mg/L and 53 ± 4 mg/L of ethanol, respectively after 10 days. Note that photosynthetic ethanol productions demonstrated previously (29, 30) were all from non-oxidative decarboxylation of pyruvate catalyzed by pyruvate decarboxylase (Pdc), which is not oxygen sensitive. Thus, the results shown here represent the first demonstration of photosynthetic ethanol biosynthesis from acetyl-CoA, and further indicated that PduP and YqhD were functional under oxygenated photosynthetic condition, which is a major step for n-butanol production.

4.2.5. PduP enables efficient n-butanol synthesis in cyanobacteria

To construct an oxygen tolerant n-butanol producing pathway in cyanobacteria, we introduced PduP homologues with the other enzymes of the malonyl-CoA dependent pathway (NphT7, PhaB, PhaJ, Ter, and YqhD) into *S. elongates* (Fig. 4.1). We first constructed synthetic operons expressing NphT7, PhaB, PhaJ, YqhD, and each individual PduP homologue under
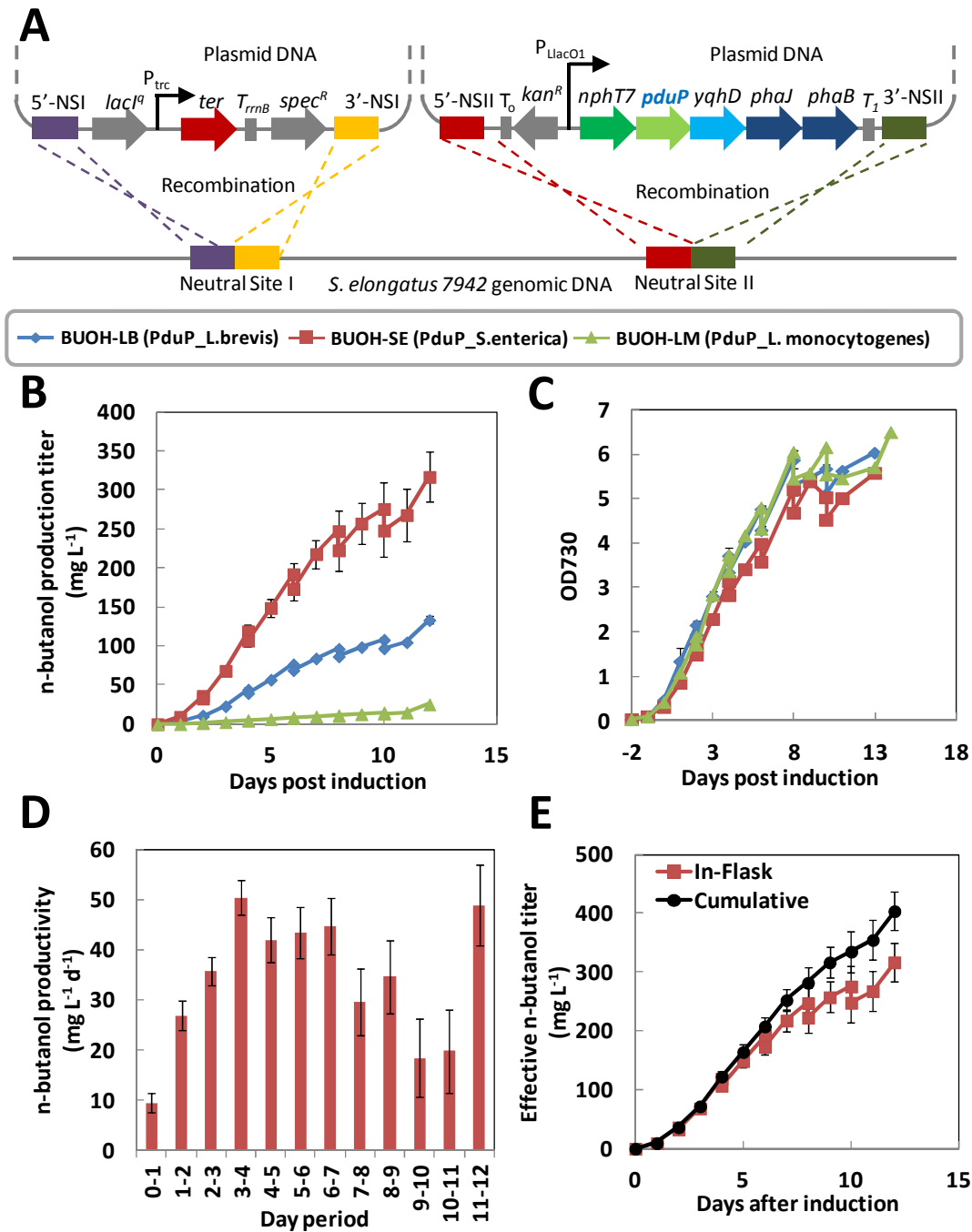
Figure 4.5. n-Butanol production by recombinant *S. elongatus*. A) Schematics of gene recombination into chromosomes of *S. elongatus* 7942. B) Time course of observed in-flask n-butanol titer by strains BUOH-LB, BUOH-SE, and BUOH-LM. C) Cell density. D) Daily productivity of n-butanol by *S. elongatus* strain BUOH-SE. E) Time course of in-flask and cumulative n-butanol produced by strain BUOH-SE. Here cumulative titer takes into account the dilutions made to cyanobacteria culture by feeding. For detailed description, see Materials and Methods section.

control of an IPTG inducible PL_{lacO1} promoter (Fig. 4.5A). These plasmids were then used to recombine the synthetic operons individually into NSII of *S. elongatus* EL9 (24) which expresses Ter at NSI. The resulting strains BUOH-LB, BUOH-LM, and BUOH-SE, expressing PduP from *L. brevis*, *L. monocytigenes*, and *S. enterica*, respectively, were genotypically verified by gene-specific PCR.

As shown in Fig. 4.5B, strain BUOH-SE produced the highest amount of n-butanol under photosynthetic conditions with an observed in-flask n-butanol titer of 317 mg/L in 12 days while BUOH-LB and BUOH-LM produced 134 mg/L and 25 mg/L, respectively. No detectable byproduct was observed in the culture medium, indicating the specificity of PduP for n-butanol production and the potential ease for product recovery. While these PduP homologues expressed by strains BUOH-LB, BUOH-LM, and BUOH-SE have higher catalytic efficiency towards butyryl-CoA than acetyl-CoA, it is interesting that no ethanol was detected in all three n-butanol producing strains. This result suggested that native *S. elongatus* acetyl-CoA carboxylase (Acc) and NphT7 efficiently channelled acetyl-CoA flux into n-butanol synthesis. Cell growth of strain BUOH-SE was slightly slower than that of the other strains (Fig. 4.5C). Daily productivity of strain BUOH-SE (Fig. 4.5D) increases with cell growth, reaching a maximum productivity of 51 mg/L/d between days 3 to 4. Daily productivity maintained around 40 mg/L/d until day 7, after which started to decline as culture entered stationary phase. The cumulative production titer (Fig. 4.5E) obtained from strain BUOH-SE was 404 mg/L in 12 days. Cumulative titer takes into account the dilutions made to cyanobacteria culture by feeding. Compared with *S. elongatus* expressing the malonyl-CoA dependent pathway using Bldh (3), strain BUOH-SE expressing PduP from *S. enterica* is a much more efficient n-butanol producer, exceeding the productivity of Bldh strain by 20 fold.

4.3. Discussion

Oxygen sensitivity is one of the major obstacles for designing synthetic pathways in cyanobacteria. Previously, we engineered an ATP driven malonyl-CoA dependent pathway in cyanobacteria and demonstrated the photosynthetic n-butanol production. However, the oxygen sensitivity of *Clostridium* Bldh severely limited the productivity of n-butanol. In this work, we showed that in addition to the ATP driving force, oxygen tolerance was essential for constructing a functional CoA-dependent n-butanol synthesis pathway in cyanobacteria. Oxygen sensitivity of *Clostridium* pathway was solved by substituting Bldh with the oxygen tolerant PduP from *S. enterica*. The resulting *S. elongatus* strain produced 404 mg/L of n-butanol (Fig. 4.5E), comparable to or higher than the level achieved in many heterotrophs. To our knowledge, this result represents the highest photosynthetic n-butanol production from CO_2 demonstrated to date.

Conversion between acyl-CoA and its corresponding aldehyde catalyzed by CoA-acylating aldehyde dehydrogenase is an important reaction occurring in both natural and synthetic pathways. For example, a synthetic 1,4-butanediol production pathway (31) utilizes two CoA-acylating aldehyde dehydrogenases for converting succinyl-CoA to succinate semialdehyde and 4-hydroxybutyryl-CoA to 4-hydroxybutyraldehyde. Similarly, CO_2 fixation utilizing the 3-hydroxypropionate cycle (32) also requires a CoA-acylating aldehyde dehydrogenases for converting malonyl-CoA to malonate semialdehyde. While CoA-acylating aldehyde dehydrogenases are ubiquitous, many of them from *Clostridium* are oxygen sensitive (25, 33, 34), prohibiting their use in photosynthetic microorganisms and other obligate aerobes. The oxygen tolerant PduP homologues that we characterized in this study are valuable for designing synthetic pathways requiring interconversion of acyl-CoA and its aldehyde. We showed that these PduPs have broad substrate specificity, ranging from C2 to C12. In particular,

PduP from *L. brevis* and *P. gingivalis* have higher specific activity towards longer chain acyl-CoAs (Fig. 4.3B), thus suitable for the synthesis of higher alcohols such as 1-hexanol and 1-octanol (19, 35).

Expression of PduP and YqhD alone enabled ethanol synthesis from acetyl-CoA. This pathway is different from the pyruvate dependent ethanol production demonstrated before (29, 30). Most of the PduP homologues characterized in this study exhibited a higher catalytic efficiency for butyryl-CoA over acetyl-CoA (Table 4.1). As a result, PduP selectively reacts with butyryl-CoA over acetyl-CoA when the CoA-dependent chain elongation is co-expressed. Co-expression of PduP and YqhD with the CoA-dependent chain elongation resulted in homo-butanol production in *S. elongatus* with no traces of ethanol or other detectable by-products in the culture medium, which is favorable for downstream product recovery.

Utilizing cyanobacteria as a catalyst to reduce CO_2 into usable chemicals is an attractive direction for sustainable chemistry and CO_2 mitigation. Specifically, *S. elongatus* PCC 7942 is a suitable host for n-butanol production because it does not have β-oxidation, thus cannot reuptake and metabolize n-butanol and preventing yield loss. The n-butanol productivity achieved in this study compares favorably to that of other acetyl-CoA derived products demonstrated in literature (Fig. 4.6A). With the exception of fatty acid production, the n-butanol productivity demonstrated here also compares favorably on the basis of carbon molar productivity, which is defined as molar productivity per carbon in the compound. However, several obstacles have to be overcome in order for it to be industrially feasible. One such challenge is the toxicity of n-butanol. As shown in Fig. 4.6B, at 750 mg/L of n-butanol in culture medium, *S. elongatus* strain BUOH-SE exhibited visible growth retardation. At 1 g/L of n-butanol, cell growth is inhibited. One approach to avoid product toxicity is to remove product *in situ* (8). Alternatively, directed
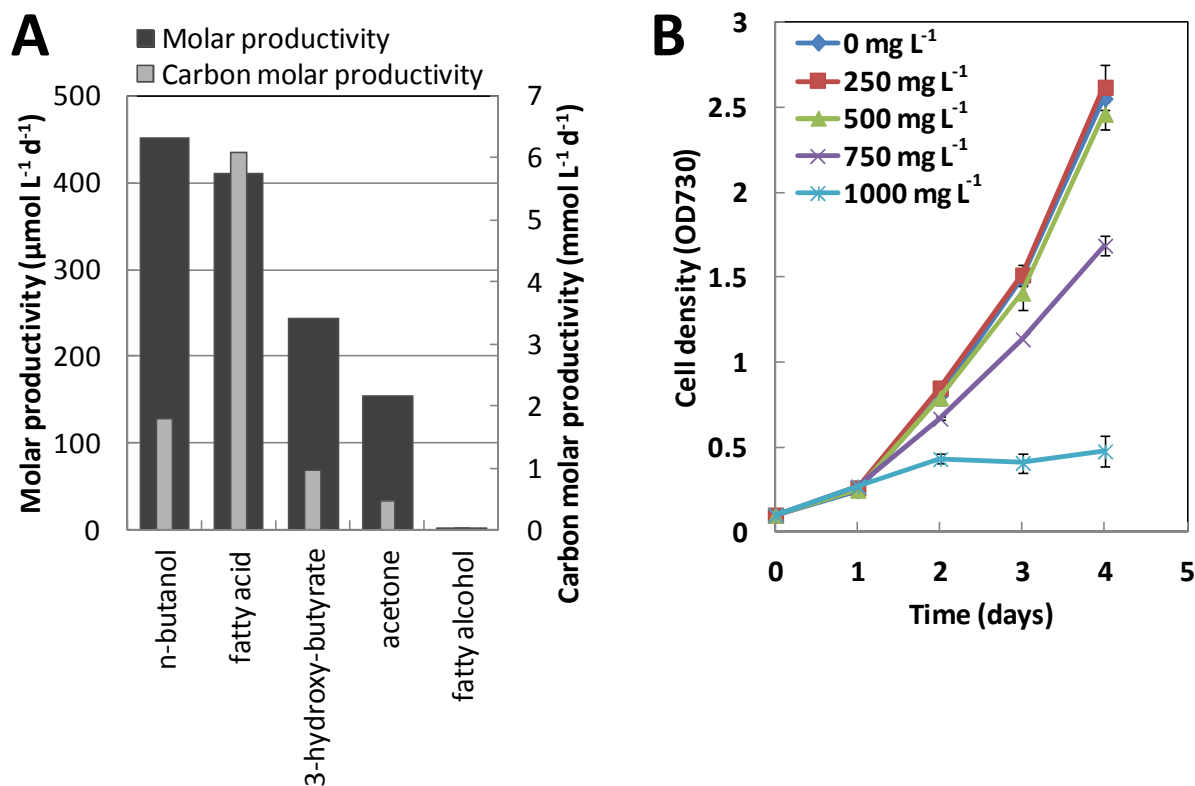
Figure 4.6. Productivity comparison and n-butanol toxicity level to *S. elongatus*. A) Comparison of molar productivities and carbon molar productivities of various acetyl-CoA based compounds produced by cyanobacteria. n-Butanol (This work), fatty acid (6), 3-hydroxybutyrate (39), acetone (40), fatty alcohol (41). Carbon molar productivity accounts for difference in number of carbons of the products and is calculated by multiplying molar productivity of the target compounds by its numbers of carbons. Detailed conversion of literature reported values into molar productivities is listed in supplementary material. B) n-Butanol toxicity to *S. elongatus* strain BUOH-SE.

evolution in combination with rational designs aided by systems analysis (36) may be useful to develop a higher butanol-tolerant host. Combining efforts of pathway engineering demonstrated here and future systems optimization, photosynthetic production of n-butanol is promising.

4.4. Materials and methods

4.4.1. Chemicals and reagents

All chemicals were purchased either from Sigma-Aldrich (St. Louis, MO) or Fisher Scientifics (Pittsburgh, PA) unless otherwise specified. iProof high-fidelity DNA polymerase was purchased from Bio-Rad (Hercules, CA). Restriction enzymes, Phusion DNA polymerase, and ligases were purchased from New England Biolabs (Ipswich, MA). T5-Exonuclease was purchased from Epicentre Biotechnologies (Madison, WI). KOD and KOD xtreme DNA polymerases were purchased from EMD biosciences (Gibbstown, NJ).

4.4.2. DNA manipulations

All chromosomal manipulations were carried out by homologous recombination of plasmid DNA into *S. elongatus* PCC 7942 genome at neutral site I (NSI) (28) and II (NSII) (37). All plasmids were constructed using Gibson isothermal DNA assembly method (38). Plasmids were constructed in *E. coli* XL-1 blue for propagation and storage (Table 4.3). Accession number for each enzyme used in this study is listed: NphT7 (BAJ10048), PhaB (AEI76813), PhaJ (O32472), Ter (Q73Q47), YqhD (AAC76047), PduP_A.hyd (YP_855873), PduP_K.pne (YP_001336844), PduP_L.bre (YP_795711), PduP_L.mon (NP_464690), PduP_P.gin (YP_001928839), PduP_S.ent (AAD39015)

4.4.3. Culture medium and condition

All *S. elongatus* PCC 7942 strains were grown in modified BG-11 (1.5 g/L $NaNO_3$, 0.0272 g/L $CaCl_2 \cdot 2H_2O$, 0.012 g/L ferric ammonium citrate, 0.001 g/L Na_2EDTA, 0.040 g/L K_2HPO_4, 0.0361 g/L $MgSO_4 \cdot 7H_2O$, 0.020 g/L Na_2CO_3, 1000x trace mineral (1.43 g H_3BO_3, 0.905 g/L $MnCl_2 \cdot 4H_2O$, 0.111 g/L $ZnSO_4 \cdot 7H_2O$, 0.195 g/L $Na_2MoO_4 \cdot 2H_2O$, 0.0395 g

$CuSO_4 \cdot 5H_2O$, 0.0245 g $Co(NO_3)2 \cdot 6H_2O$), 0.00882 g/L sodium citrate dihydrate) agar (1.5% w/v) plates. All *S. elongatus* PCC 7942 strains were cultured in BG-11 medium containing 50 mM $NaHCO_3$ in 250 mL screw cap flasks. Cultures were grown under 48 ± 2 μE/s/m^2 light measured by Licor quantum sensor (LI-250A equipped with LI-190 Quantum Sensor), supplied by 3 Lumichrome F30W-1XX 6500K 98CRI light tubes, at 29 ± 1 °C. Cell growth was monitored by measuring OD_{730} with Beckman Coulter DU800 spectrophotometer.

4.4.4. Strain construction and transformation

S. elongatus PCC 7942 strains were transformed by incubating cells at mid-log phase (OD_{730} of 0.4 to 0.6) with 2 μg of plasmid DNA overnight in the dark. The culture was then spread on BG-11 plates supplemented with appropriate antibiotics for selection of successful recombination. For selection and culture maintenance, 20 μg/ml spectinomycin and 10 μg/ml kanamycin were added into BG-11 agar plates and BG-11 medium where appropriate. Colony PCR was used to verify integration of inserted genes into the recombinant strain. In all cases, two or three individual colonies were analyzed and propagated for downstream tests. Genotypes of recombinant *S. elongatus* are listed in Table 4.3. *S. elongatus* strain ETOH-KP, ETOH-LB, ETOH-LM, and ETOH-SE were constructed by transforming strain PCC 7942 with plasmids pSR6, pSR7, pSR9, and pSR8, respectively. Strains BUOH-LB, BUOH-SE, and BUOH-LM were constructed by transforming strain EL9 with plasmids pSR2, pSR3, and pSR5, respectively.

4.4.5. *E. coli* anaerobic growth rescue

Cells of *E. coli* strain JCL166 and its derivatives were cultured overnight in LB with appropriate antibiotics at 37°C. Overnight cultures (3 μL) were used to inoculate 3 mL of fresh LB media supplemented with 1% glucose and appropriate antibiotics (100 μg/mL ampicillin and 50 μg/mL kanamycin) and 0.1 mM IPTG in 10 mL BD vacutainers. A needle with Millipore

PES filter was used to pierce through the rubber cap of the culture. The headspace of these cultures was then purged several times with 95% N_2/ 5% H_2 gas using an anaerobic chamber (Coy Lab Products, Grass Lake, MI). The needle with filter was removed in anaerobic chamber. These anaerobic cultures were then taken out of anaerobic chamber and incubated in 37°C rotary shaker. Culture was analyzed 24 hours later for cell density and alcohol content measurement.

4.4.6. CoA-acylating aldehyde dehydrogenase (PduP) assay

Protein purification was done by using His-Spin Protein miniprep purification kit from Zymo following manufacturer's manual. Overnight culture of *E. coli* strain BL-21(DE3) harboring different pCDF-pdup plasmid was used to inoculate fresh 20 ml LB. The newly inoculated culture was incubated at 37°C until OD_{600nm} reaches 0.6 which was then induced with 1 mM IPTG. The induced cultures were then incubated overnight in 30°C rotary shaker to allow protein expression. The cultures were then harvested by centrifugation at 4,300 x g for 20 min. The pellet was then resuspended with 1mL of Zymo His-binding buffer and mixed with 1mL of 0.1 mm glass beads (Biospec). The sample was then homogenated using TissueLyser II (Quiagen).

Enzyme assays were conducted by using Bio-Tek PowerWave XS microplate spectrophotometer. CoA-acylating aldehyde dehydrogenase activity was measured by the decrease of absorbance at 340 nm, corresponding to depletion of NADH. For determination of k_{cat} and K_m of the different aldehyde dehydrogenases, acetyl-CoA and butyryl-CoA concentrations were varied between 0.03 mM to 2 mM. The reaction mixture contained 50 mM potassium phosphate buffer at pH 7.15, 1 mM Dithiothreitol (DTT), 500 µM NADH, acetyl-CoA or butyryl-CoA at varying concentration, and enzyme. For determining specific activity for other chain length acyl-CoA, 500 µM was used. The mixture excluding acyl-CoA was incubated for 5

minutes at 30 °C. The addition of the acyl-CoA initiated the reaction. k_{cat} and K_m were determined by nonlinear regression fitting to Michaelis-Menten equation using graphing software Origin.

4.4.7. Production of ethanol and n-butanol in recombinant *S. elongatus*

A loopful of *S. elongatus* PCC 7942 was used to inoculate fresh 50 mL BG-11. Initial cell density of culture was typically OD_{730} 0.03 to 0.05. 500 mM IPTG was used to induce the growing culture at cell density OD_{730nm} of 0.4 to 0.6 with 1 mM IPTG as final concentration.

For n-butanol production, 1 mL of culture was removed from the culture daily for cell density measurement and quantification of n-butanol. Every two days, additional 3 mL of culture was removed from the flask, and 5 mL of fresh BG-11 with 500 mM $NaHCO_3$, appropriate antibiotics, and IPTG were added back to the culture. This procedure ensures the carbon supply for *S. elongatus*.

For ethanol production, 5 mL of culture was removed every two days from the flask for cell density measurement and quantification of ethanol. 5 mL of fresh BG-11 with 500 mM $NaHCO_3$, appropriate antibiotics, and IPTG were added back to the culture to supply nutrients necessary.

4.4.8. Alcohol quantification

Culture samples (1 mL) were centrifuged for 5 minutes at 15,000 x g. The supernatant (900 µL) was then mixed with 0.1% v/v 2-methyl-pentanol (100 µL) as internal standard. The mixture was then vortexed and directly analyzed on an Agilent GC 6850 system equipped with flame ionization detector and DB-FFAP capillary column (30m, 0.32mm i.d., 0.25 film thickness) from Agilent Technologies (Santa Clara, CA). Ethanol or n-butanol in the sample was identified and quantified by comparing to 0.1% v/v standard. The GC result was analyzed by

114

Agilent software Chem Station (Rev.B.04.01 SP1). Amount of alcohol in the sample was then calculated based on the ratio of its integrated area and that of the 0.1% v/v standard.

Helium was used as the carrier gas with 9.52 psi inlet pressure. The injector and detector temperatures were maintained at 225°C. Injection volume was 1 µL. For ethanol quantification, the GC over was initially held at 60°C for 2 minutes, and raised to 85°C with temperature ramp of 50°C/min and kept at 85°C for 2 minutes after which temperature was then raised to 235°C with ramp rate of 45°C/min and kept for 3 minutes. For n-butanol quantification, the GC oven temperature was initially held at 85°C for 3 minutes and then raised to 235°C with a temperature ramp of 45°C/min. The GC oven was then maintained at 235°C for 1 minute before completion of analysis. Column flow rate was 1.7 ml/min. DMF and water were used as organic and aqueous wash solvent, respectively.

Cumulative alcohol concentration is defined as the sum of daily productivities of the production period. Note that culture volume remained constant throughout production. 10% of alcohol was removed every two days due to nutrients replenishment. For example, feeding was done on day 2, therefore to calculate daily productivity of day 3, we took the difference between concentration of day 3 and 90% of day 2 as the daily productivity for day 3.

4.4.9. n-Butanol toxicity test

S. elongatus PCC7942 cells were grown according to the procedure in "culture medium and condition". Once growth reached OD_{730} about 2, the culture was diluted to OD_{730} of 0.1 with 50 mL fresh BG11 medium containing 50mM $NaHCO_3$ and appropriate antibiotics. Then, various amounts of n-Butanol were added into the culture to achieve the desired concentration (0, 250, 500, 750, and 1000 mg/L). Growth was measured daily. Every two days, 5 mL of culture was removed and 5 mL fresh BG-11 containing 500 mM NaHCO3, appropreiate amounts of

antibiotics and n-butanol was added back to the culture to ensure sufficient carbon supply.

Table 4.2. Cyanobacteria and *E. coli* strains used in this study

Strain	Relevant genotypes	Reference
	Cyanobacteria Strains	
PCC 7942	Wild-type *Synechococcus elongatus* PCC 7942	
EL9	P_{Trc}::His-tagged *ter* integrated at NSI	(24)
ETOH-KP	P_{Trc}::*pduP_K.pneumoniae, yqhD* integrated at NSI	This work
ETOH-LB	P_{Trc}::*pduP_ L.brevis, yqhD* integrated at NSI	This work
ETOH-LM	P_{Trc}::*pduP_ L.monocytigenes, yqhD* integrated at NSI	This work
ETOH-SE	P_{Trc}::*pduP_ S.enterica, yqhD* integrated at NSI	This work
BUOH-LB	P_{Trc}::His-tagged *ter* integrated at NSI and P_{LlacO1}::*nphT7, pduP_L.brevis, yqhD, crt, hbd* integrated at NSII	This work
BUOH-SE	P_{Trc}::His-tagged *ter* integrated at NSI and P_{LlacO1}::*nphT7, pduP_S.enterica, yqhD, crt, hbd* integrated at NSII	This work
BUOH-LM	P_{Trc}::His-tagged *ter* integrated at NSI and P_{LlacO1}::*nphT7, pduP_L.monocytigenes, yqhD, crt, hbd* integrated at NSII	This work
	E. coli strains	
XL-1 blue	*recA1 endA1 gyrA96 thi-1 hsdR17 supE44 relA1 lac* [F' *proAB lacI^{q}ZΔM15 Tn10* (Tet^R)]	Stratagene
JCL166	BW25113 $\Delta ldhA$ $\Delta adhE$ $\Delta frdBC$ / F' [*traD36, proAB+, lacI^q ZΔM15* (Tet^R)]	(22)
BL21(DE3)	F$^-$ *ompT hsdS*B (rB$^-$mB$^-$) *gal dcm rne131* (DE3)	In vitrogen

nphT7 (*Streptomyces* sp. strain CL190), acetoacetyl-CoA synthase; *phaB* (*R. Eutropha*), acetoacetyl-CoA reductase; *phaJ* (*A. caviae*), (R)-specific enoyl-CoA hydratase; *hbd* (*C. acetobutylicum*), 3-hydroxybutyryl-CoA dehydrogenase; *crt* (*C. acetobutylicum*), crotonase; *ter* (*T. denticola*), Trans-2-enoyl-CoA reductase; *yqhD* (*E. coli*), NADP-dependent alcohol dehydrogenase; *pduP* (*A. hydrophilia*, *K. pneumonia, L. brevis*, *L. monocytigenes*, *P. gingivalis,* or *S. enterica*), CoA-acylating aldehyde dehydrogenase.

Table 4.3. Plasmids used in this study

Plasmid	Genotypes	Reference
pCDFDuet	Spec^R; CDF ori; P$_{T7}$::MCS	Novagen
pEL54	Amp^R; ColE1 ori; P$_{LlacO1}$::*atoB,bldh,yqhD,crt,hbd*	(3)
pIM8	Kan^R; ColA ori; P$_{LlacO1}$::ter	(22)
pCDF-pduP _ahyd	Spec^R; CDF ori; P$_{T7}$::*pduP_A.hyd* (his tagged)	This work
pCDF-pduP _kpne	Spec^R; CDF ori; P$_{T7}$::*pduP_K.pne* (his tagged)	This work
pCDF-pduP _lbre	Spec^R; CDF ori; P$_{T7}$::*pduP_L.bre* (his tagged)	This work
pCDF-pduP _lmon	Spec^R; CDF ori; P$_{T7}$::*pduP_L.mon* (his tagged)	This work
pCDF-pduP _sent	Spec^R; CDF ori; P$_{T7}$::*pduP_P.gin* (his tagged)	This work
pCDF-pduP _pgin	Spec^R; CDF ori; P$_{T7}$::*pduP_ S.ent* (his tagged)	This work
pEL175	Amp^R; ColE1 ori; P$_{LlacO1}$::*atoB,ter,crt,hbd*	This work
pEL178	Kan^R; P15A ori; P$_{LlacO1}$::*bldh,yqhD*	This work
pEL179	Kan^R; P15A ori; P$_{LlacO1}$::*pduP_A.hyd,yqhD*	This work
pEL180	Kan^R; P15A ori; P$_{LlacO1}$::*pduP_K.pne,yqhD*	This work
pEL181	Kan^R; P15A ori; P$_{LlacO1}$::*pduP_L.bre,yqhD*	This work
pEL182	Kan^R; P15A ori; P$_{LlacO1}$::*pduP_L.mon,yqhD*	This work
pEL183	Kan^R; P15A ori; P$_{LlacO1}$::*pduP_P.gin,yqhD*	This work
pEL184	Kan^R; P15A ori; P$_{LlacO1}$::*pduP_ S.ent,yqhD*	This work
pSR2	Kan^R; NSII targeting; P$_{LlacO1}$::*nphT7,pduP_L.bre,crt,hbd*	This work
pSR3	Kan^R; NSII targeting; P$_{LlacO1}$::*nphT7,pduP_S.ent,crt,hbd*	This work
pSR5	Kan^R; NSII targeting; P$_{LlacO1}$::*nphT7,pduP_L.mon,crt,hbd*	This work
pSR6	Spec^R; NSI targeting; P$_{trc}$::*pduP_K.pne,yqhD*	This work
pSR7	Spec^R; NSI targeting; P$_{trc}$::*pduP_L.bre,yqhD*	This work
pSR8	Spec^R; NSI targeting; P$_{trc}$::*pduP_S.ent,yqhD*	This work
pSR9	Spec^R; NSI targeting; P$_{trc}$::*pduP_L.mon,yqhD*	This work

Kan^R, kanamycin resistance; Amp^R, ampicillin resistance; Spec^R, spectinomycin resistance
atoB (*E. coli*), thiolase; *nphT7* (*Streptomyces* sp. strain CL190), acetoacetyl-CoA synthase; *phaB* (*R. Eutropha*), acetoacetyl-CoA reductase; *phaJ* (*A. caviae*), (R)-specific enoyl-CoA hydratase; *hbd* (*C. acetobutylicum*), 3-hydroxybutyryl-CoA dehydrogenase; *crt* (*C. acetobutylicum*), crotonase; *ter* (*T. denticola*), Trans-2-enoyl-CoA reductase; *bldh* (*C. saccharoperbutylacetonicum*), butyraldehyde dehydrogenase; *yqhD* (*E. coli*), NADP-dependent alcohol dehydrogenase; *pduP* (*A. hydrophilia*, *K. pneumonia, L. brevis*, *L. monocytigenes*, *P. gingivalis,* or *S. enterica*), CoA-acylating aldehyde dehydrogenase.

4.5. Reference

1.   Oliver JW, Machado IM, Yoneda H, & Atsumi S (2013) Cyanobacterial conversion of carbon dioxide to 2,3-butanediol. Proc Natl Acad Sci USA 110(4):1249-1254.

2.   Li H & Liao JC (2013) Engineering a cyanobacterium as the catalyst for the photosynthetic conversion of CO2 to 1,2-propanediol. Microb Cell Fact 12.

3.   Lan EI & Liao JC (2012) ATP drives direct photosynthetic production of 1-butanol in cyanobacteria. Proc Natl Acad Sci USA 109(16):6018-6023.

4.   Shen CR & Liao JC (2012) Photosynthetic production of 2-methyl-1-butanol from CO2 in cyanobacterium Synechococcus elongatus PCC7942 and characterization of the native acetohydroxyacid synthase. Energy Environ Sci 5(11):9574-9583.

5.   Ducat DC, Avelar-Rivas JA, Way JC, & Silver PA (2012) Rerouting Carbon Flux To Enhance Photosynthetic Productivity. Appl Environ Microbiol 78(8):2660-2668.

6.   Liu XY, Sheng J, & Curtiss R (2011) Fatty acid production in genetically modified cyanobacteria. Proc Natl Acad Sci USA 108(17):6899-6904.

7.   Lindberg P, Park S, & Melis A (2010) Engineering a platform for photosynthetic isoprene production in cyanobacteria, using Synechocystis as the model organism. Metab Eng 12(1):70-79.

8.   Atsumi S, Higashide W, & Liao JC (2009) Direct photosynthetic recycling of carbon dioxide to isobutyraldehyde. Nat Biotechnol 27(12):1177-1180.

9.   Tyo KE, Jin YS, Espinoza FA, & Stephanopoulos G (2009) Identification of gene disruptions for increased poly-3-hydroxybutyrate accumulation in Synechocystis PCC 6803. Biotechnol Prog 25(5):1236-1243.

10.   Mascal M (2012) Chemicals from biobutanol: technologies and markets. Biofuel Bioprod Bior 6(4):483-493.

11.   Lan EI & Liao JC (2013) Microbial synthesis of n-butanol, isobutanol, and other higher alcohols from diverse resources. Bioresour Technol 135:339-349.

12.   Tracy BP, Jones SW, Fast AG, Indurthi DC, & Papoutsakis ET (2012) Clostridia: the importance of their exceptional substrate and metabolite diversity for biofuel and biorefinery applications. Curr Opin Biotechnol 23(3):364-381.

13.   Wang Y & Blaschek HP (2011) Optimization of butanol production from tropical maize stalk juice by fermentation with Clostridium beijerinckii NCIMB 8052. Bioresour Technol 102(21):9985-9990.

14.   Kopke M, et al. (2010) Clostridium ljungdahlii represents a microbial production platform based on syngas. Proc Natl Acad Sci USA 107(29):13087-13092.

15. Shen CR & Liao JC (2013) Synergy as design principle for metabolic engineering of 1-propanol production in Escherichia coli. Metab Eng 17C:12-22.

16. Atsumi S, Hanai T, & Liao JC (2008) Non-fermentative pathways for synthesis of branched-chain higher alcohols as biofuels. Nature 451(7174):86-89.

17. Shen CR & Liao JC (2008) Metabolic engineering of Escherichia coli for 1-butanol and 1-propanol production via the keto-acid pathways. Metab Eng 10(6):312-320.

18. Lan EI, Dekishima Y, Chuang DS, & Liao JC (2013) Metabolic engineering of 2-petanone synthesis in Escherichia coli. AICHE J:n/a-n/a.

19. Dekishima Y, Lan EI, Shen CR, Cho KM, & Liao JC (2011) Extending Carbon Chain Length of 1-Butanol Pathway for 1-Hexanol Synthesis from Glucose by Engineered Escherichia coli. J Am Chem Soc 133(30):11399-11401.

20. Atsumi S, et al. (2008) Metabolic engineering of Escherichia coli for 1-butanol production. Metab Eng 10(6):305-311.

21. Li F, et al. (2008) Coupled ferredoxin and crotonyl coenzyme a (CoA) reduction with NADH catalyzed by the butyryl-CoA dehydrogenase/Etf complex from Clostridium kluyveri. J Bacteriol 190(3):843-850.

22. Shen CR, et al. (2011) Driving forces enable high-titer anaerobic 1-butanol synthesis in Escherichia coli. Appl Environ Microbiol 77(9):2905-2915.

23. Bond-Watts BB, Bellerose RJ, & Chang MCY (2011) Enzyme mechanism as a kinetic control element for designing synthetic biofuel pathways. Nat Chem Biol 7(4):222-227.

24. Lan EI & Liao JC (2011) Metabolic engineering of cyanobacteria for 1-butanol production from carbon dioxide. Metab Eng 13(4):353-363.

25. Yan RT & Chen JS (1990) Coenzyme a-Acylating Aldehyde Dehydrogenase from Clostridium-Beijerinckii Nrrl-B592. Appl Environ Microbiol 56(9):2591-2599.

26. Fontaine L, et al. (2002) Molecular characterization and transcriptional analysis of adhE2, the gene encoding the NADH-dependent aldehyde/alcohol dehydrogenase responsible for butanol production in alcohologenic cultures of Clostridium acetobutylicum ATCC 824. J Bacteriol 184(3):821-830.

27. Leal NA, Havemann GD, & Bobik TA (2003) PduP is a coenzyme-a-acylating propionaldehyde dehydrogenase associated with the polyhedral bodies involved in B-12-dependent 1,2-propanediol degradation by Salmonella enterica serovar Typhimurium LT2. Arch Microbiol 180(5):353-361.

28. Bustos SA & Golden SS (1992) Light-Regulated Expression of the Psbd Gene Family in Synechococcus-Sp Strain Pcc-7942 - Evidence for the Role of Duplicated Psbd Genes in Cyanobacteria. Mol Gen Genet 232(2):221-230.

29. Gao ZX, Zhao H, Li ZM, Tan XM, & Lu XF (2012) Photosynthetic production of ethanol from carbon dioxide in genetically engineered cyanobacteria. Energy Environ Sci 5(12):9857-9865.

30. Dexter J & Fu PC (2009) Metabolic engineering of cyanobacteria for ethanol production. Energy Environ Sci 2(8):857-864.

31. Yim H, et al. (2011) Metabolic engineering of Escherichia coli for direct production of 1,4-butanediol. Nat Chem Biol 7(7):445-452.

32. Berg IA, Kockelkorn D, Buckel W, & Fuchs G (2007) A 3-hydroxypropionate/4-hydroxybutyrate autotrophic carbon dioxide assimilation pathway in archaea. Science 318(5857):1782-1786.

33. Wolff RA & Kenealy WR (1995) Purification and Characterization of the Oxygen-Sensitive 4-Hydroxybutanoate Dehydrogenase from Clostridium-Kluyveri. Protein Expression Purif 6(2):206-212.

34. Sohling B & Gottschalk G (1993) Purification and characterization of a coenzyme-A-dependent succinate-semialdehyde dehydrogenase from Clostridium kluyveri. Eur J Biochem 212(1):121-127.

35. Machado HB, Dekishima Y, Luo H, Lan EI, & Liao JC (2012) A selection platform for carbon chain elongation using the CoA-dependent pathway to produce linear higher alcohols. Metab Eng 14(5):504-511.

36. Jarboe LR, Liu P, & Royce LA (2011) Engineering inhibitor tolerance for the production of biorenewable fuels and chemicals. Current Opinion in Chemical Engineering 1(1):38-42.

37. Andersson CR, et al. (2000) Application of bioluminescence to the study of circadian rhythms in cyanobacteria. Bioluminescence and Chemiluminescence, Pt C 305:527-542.

38. Gibson DG, et al. (2009) Enzymatic assembly of DNA molecules up to several hundred kilobases. Nat Methods 6(5):343-345.

39. Wang B, Pugh S, Nielsen DR, Zhang W, & Meldrum DR (2013) Engineering cyanobacteria for photosynthetic production of 3-hydroxybutyrate directly from CO. Metab Eng 16C:68-77.

40. Zhou J, Zhang H, Zhang Y, Li Y, & Ma Y (2012) Designing and creating a modularized synthetic pathway in cyanobacterium Synechocystis enables production of acetone from carbon dioxide. Metab Eng 14(4):394-400.

41. Tan XM, et al. (2011) Photosynthesis driven conversion of carbon dioxide to fatty alcohols and hydrocarbons in cyanobacteria. Metab Eng 13(2):169-176.

5. REDESIGN OF MALONYL-COA BIOSYNTHESIS

5.1. Introduction

Malonyl-Coenzyme A (CoA), the starting substrate for n-butanol pathway, is naturally produced by acetyl-CoA carboxylase, which is a highly regulated protein and difficult to engineer. As such, in in this chapter, we designed at least five distinct pathways to synthesize malonyl-CoA from central metabolites such as phosphoenolpyruvate and pyruvate.

The first century of metabolic research has successfully discovered almost all of the enzymatic steps and mechanisms in metabolism that supports life. The study of metabolism is further enriched by genome sequencing that leads to rapid identification of genes coding for the enzymes. Meanwhile, genetic techniques and engineering principles have enabled modification and transferring foreign pathways to almost any organism to produce compounds for industrial purposes. After optimizing the terminal pathways for a specific product, the production is often limited by central metabolites that are produced from pathways optimized for cell's benefit rather than for production. As such, redesign of essential primary metabolic pathways for the purpose of production has become a priority.

Malonyl-CoAis an essential metabolite that serves as the common building block for fatty acids, polyketides, and flavonoids. Malonyl-CoA is synthesized via carboxylation of acetyl-CoA catalyzed by acetyl-CoA carboxylase (Acc) (Fig. 5.1A), which typically is a four subunit enzyme complex or a muti-domain enzyme. Biotin-carboxyl carrier protein (BCCP) domain is first biotinylated into active carboxyl-carrier. Biotin carboxylase then carboxylates BCCP-biotin complex while consuming ATP. Malonyl-CoA is subsequently produced upon transfer of the carboxyl group from AccB-biotin complex to acetyl-CoA by acetyl-CoA carboxyltransferase. Recently, the Acc-depdendent malonyl-CoA synthesis has also been used in an engineered
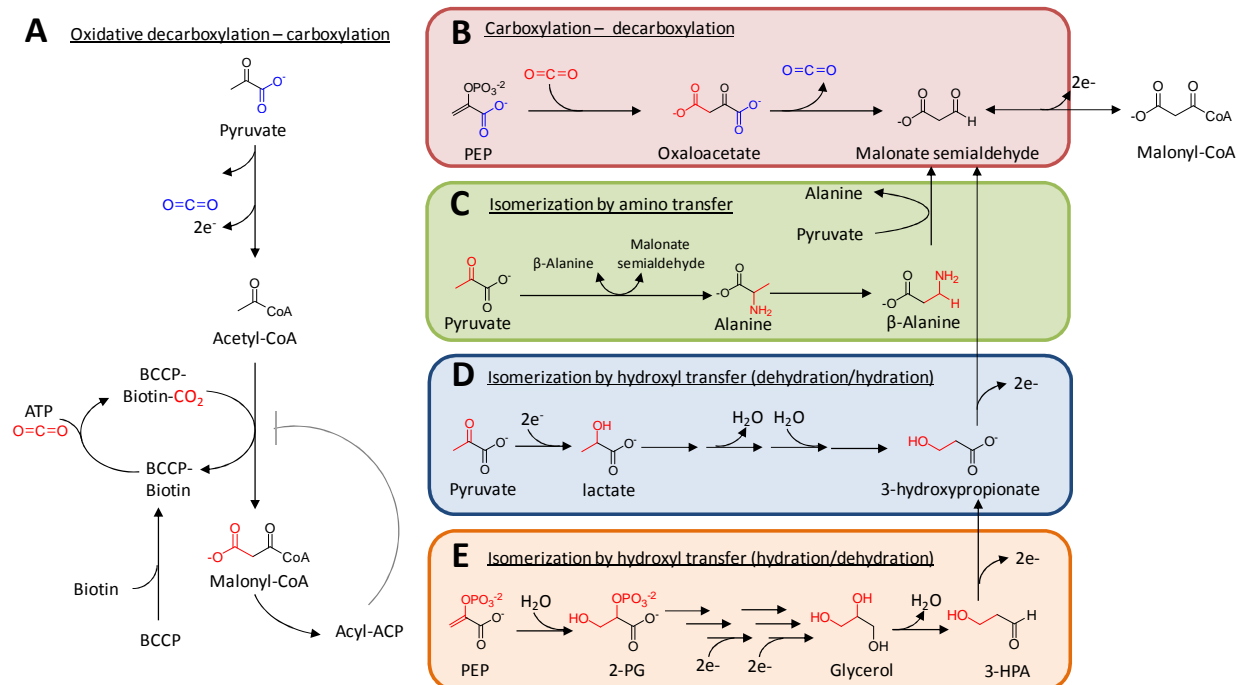
Figure 5.1. Schematics malonyl-CoA biosynthesis. A) Natural malonyl-CoA biosynthesis via acetyl-CoA. Synthetic malonyl-CoA biosynthesis pathway via malonate semialdehyde which can be produced by B) sequential carboxylation and decarboxylation of PEP, C) functionalization of α-keto to α-amino followed by α-amino transfer and regeneration of keto moiety, D) reduction of pyruvate to lactate in which net hydroxyl transfer can be achieved by sequential dehydration and hydration followed by re-oxidation of β-hydroxyl to β-keto, E) hydration of PEP to 2-phosphoglycerate and reduction to glycerol followed by dehydration of hydroxyl on carbon 2 of glycerol to 3-hydroxypropionaldehyde which can be oxidized to malonate semialdehyde. The detailed description of these reaction pathways are represented in Figure 5.S1.

pathway for acetoacetyl-CoA synthesis that leads to n-butanol production (1). Because Acc catalyzes the first step for directing acetyl-CoA flux towards secondary metabolite biosynthesis instead of amino acid biosynthesis or energy production, Acc expression is tightly regulated at all levels: transcriptional regulation by growth-rate (2), translational regulation by mRNA binding (3), and feedback inhibition by product acyl-ACP (4). As a result, biosynthesis of downstream products of malonyl-CoA is believed to be mainly controlled by Acc. Currently, almost all engineering approaches to increase malonyl-CoA flux are based on overexpression of Acc (5-8) or increasing acetyl-CoA flux (9, 10). Although these efforts achieved reasonable

success, Acc overexpression is not always effective and often results in conservative beneficial effects.

Decarboxylative Claisen condensation of malonyl-CoA and its derivative malonyl-acyl carrier protein (ACP) with Acyl-ACP is irreversible and provides the driving force necessary for iterative carbon chain elongation. β-Carboxylate of malonyl-CoA serves as a leaving group to facilitate this otherwise unfavorable condensation of two acetyl-CoA. Using pyruvate as a reference, nature's solution for achieving this β-carboxylate is by oxidative decarboxylation of pyruvate to acetyl-CoA and followed by an energy dependent carboxylation to malonyl-CoA (Fig. 5.1A). From a biochemical point of view, β-carboxylate of malonyl-CoA can also be achieved by CoA-acylating oxidation of malonate semialdehyde, a naturally occurring metabolite. Here we propose at least four general alternatives (Fig. 5.1B,C,D,E) and other variations thereof (Fig. 5.S1 for complete metabolic interconnections between the pathways) to achieve biosynthesis of malonyl-CoA via malonate semialdehyde, a structural isomer of pyruvate. The four general alternatives are: sequential carboxylation and decarboxylation (Fig. 5.1B), one step isomerization by amino transfer (Fig. 5.1C), and multi-step isomerization by hydroxyl transfer mediated by hydration and dehydration (Fig. 5.1D,E). Of these approaches, sequential carboxylation and decarboxylation is the most promising pathway to construct because it is thermodynamically favorable and requires fewer enzymatic steps. However, the key enzyme oxaloacetate 1-decarboxylase has not been found in nature. In particular, oxaloacetate, a β-keto acid, may favor decarboxylation of the β-carboxylate over the α-carboxylate. We solved this problem by creating a shunt utilizing aspartate decarboxylase. In this study, we demonstrated *in vitro* synthesis of malonyl-CoA from oxaloacetate. The limiting step, cofactor independent aspartate decarboxylase, was further solved by recruiting a PLP-dependent aspartate

124
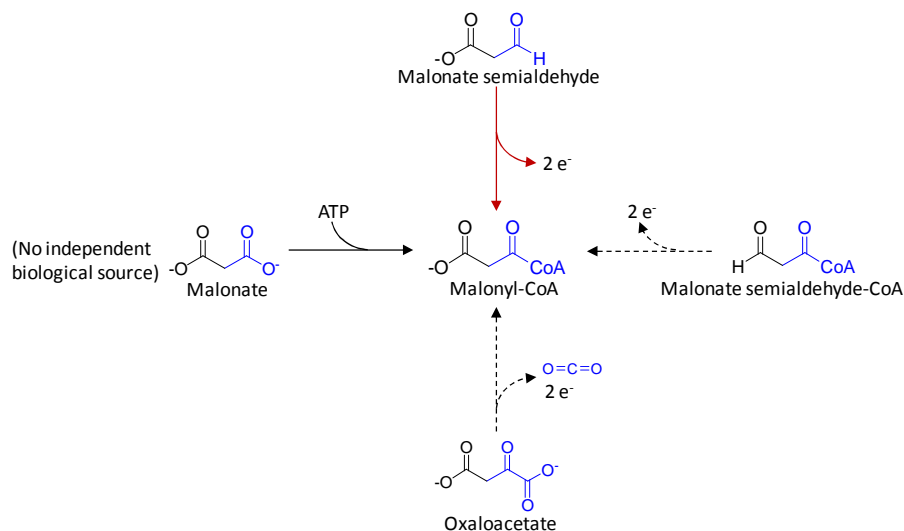
Figure 5.2. Possible direct precursors to malonate semialdehyde. Dashed lines represent enzymes not found in nature.

decarboxylase. Using this *in vitro* system, we were able to study the steady state kinetics of this synthetic pathway and effects of substrate concentration. These results represent the construction of the first synthetic malonyl-CoA biosynthesis and present an alternative method for increasing production of malonyl-CoA derived products.

5.2. Results

5.2.1. Design of synthetic malonyl-CoA biosynthesis

From a biochemical stand point, malonate, oxaloacetate, malonate semialdehyde-CoA, and malonate semialdehyde are the possible direct precursors to malonyl-CoA (Fig. 5.2). However, among them only malonate semialdehyde is biologically feasible. Malonate is not a feasible precursor because it is a product of malonyl-CoA or malonate semialdehyde. Oxaloacetate is also not feasible because direct conversion of oxaloacetate to malonyl-CoA requires a decarboxylative dehydrogenase which has not been found in nature. Similarly, malonate semialdehyde-CoA oxidation to malonyl-CoA requires a dehydrogenase not available

in nature. On the other hand, malonate semialdehyde is a naturally occurring metabolite found in 3-hydroxypropionate dependent CO_2 fixation pathway, indicating its intracellular stability.

Reversed reaction of malonyl-CoA reductase (Mcr), catalyzing the oxidation of malonyl-CoA to malonate semialdehyde using NADPH, converts malonate semialdehyde to malonyl-CoA. Two types of Mcr exist in nature: unifunctional and bifunctional. The reversibility of the unifunctional Mcr from *Sulfolobus tokodaii* (11) is uncertain and has not been reported. On the other hand, bifunctional Mcr from *Chloroflexus aurantiacus* (12), which catalyzes two step malonyl-CoA reduction to 3-hydroxypropionate, is reversible but with strong preference for malonyl-CoA reducing direction. Nevertheless, the calculated Gibbs free energy for malonate semialdehyde oxidation to malonyl-CoA under physiological conditions (1 mM concentration with 0.1M ionic strength at pH 7.0) is -7.5 kJ/mol, suggesting its likelihood of reaction.

Isomerization of pyruvate to malonate semialdehyde requires migration of the keto group from α-position to β-position. Because keto isomerization is not available, alternative reaction schemes are necessary to achieve this net isomerization. Four general solutions exist for this isomerization: 1) Carboxylation at β-position followed by α-decarboxylation (Fig. 5.1B), 2) transamination of α-keto into α-amino followed by amino transfer and re-transamination (Fig. 5.1C), and 3) Reduction of α-keto into α-hydroxyl followed by either dehydration and re-hydration (Fig. 5.1D) or 4) hydration and dehydration (Fig. 5.1E) and re-oxidation of β-hydroxyl.

PEP was chosen as a starting reference point for thermodynamics analysis because it is the common intermediate for all synthetic pathways for malonyl-CoA biosynthesis. The thermodynamics of these pathways were calculated based on physiological conditions and are shown in Fig. 5.3. These synthetic pathways can be divided into three groups based on their ATP yield. Group 1 pathways has an ATP yield of zero from either PEP or glucose and include
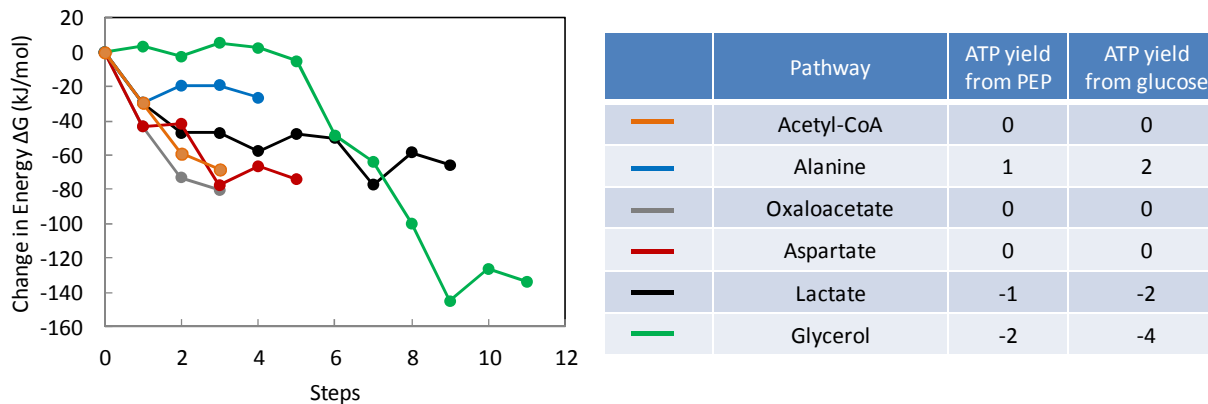
Figure 5.3. Thermodynamics of malonyl-CoA biosynthesis pathways. Change in energy was calculated using eQuilibrator with parameters of physiological conditions (See materials and methods). Each pathway is named based on their representative metabolite. ΔG′ and ΔG°′ are listed in Table 5.S1 and 5.S2.

Natural Acc dependent pathway (Fig. 5.1A), oxaloacetate (Fig. 5.1B), and aspartate (Fig. 5.4) dependent pathways. Group 2 pathway has ATP yield greater than zero and contains only represented by alanine (Fig. 5.1C) pathway. Group 3 pathways have ATP yield less than one, indicating extra energy cost, and include both the lactate (Fig. 5.1D) and glycerol (Fig. 5.1E) pathways.

Direct α-decarboxylation of oxaloacetate. Carboxylation of PEP at β-position followed by α-decarboxylation yielding malonate semialdehyde (Fig. 5.1B) is the shortest route, containing only two enzymatic steps, to achieve α to β keto-migration. Notably, this pathway has an overall thermodynamics similar to that of Acc dependent malonyl-CoA synthesis, where its ATP yield from both PEP and glucose is zero and all steps have negative ΔG′ (Fig. 5.3). However, the key enzyme oxaloacetate α-decarboxylase does not exist in nature, therefore hindering the construction of this route for malonyl-CoA biosynthesis. Nevertheless, α-decarboxylation occurs

127
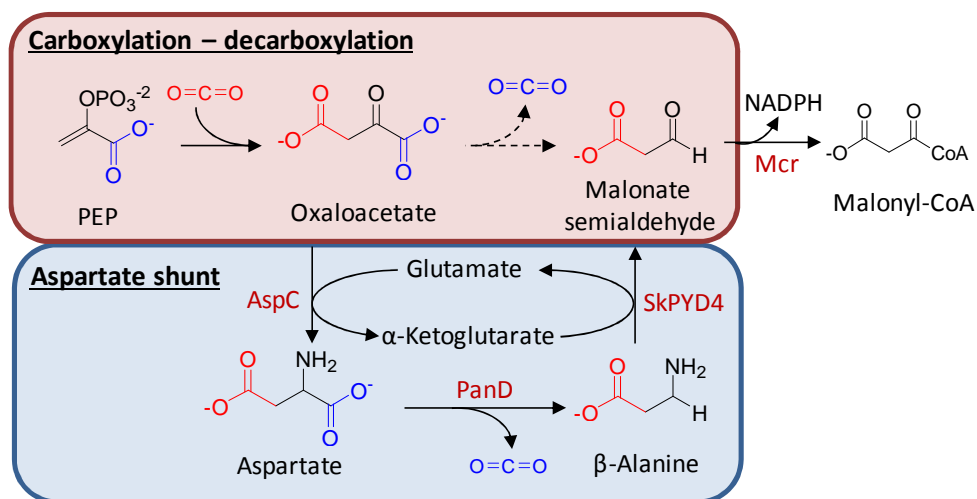
Figure 5.4. Aspartate shunt to bypass oxaloacetate 1-decarboxylase. Dash line represents that enzyme has not been found in nature.

naturally in many biological processes such as pyruvate decarboxylase in ethanol fermentation and α-ketoglutarate decarboxylase in cyanobacteria TCA cycle (13). Given their substrate structural similarity, it is therefore conceivable that these enzymes may be evolved into an oxaloacetate α-decarboxylase.

Aspartate shunt for α-decarboxylation. While the direct decarboxylation of oxaloacetate to malonate semialdehyde has not been found in nature, decarboxylation of aspartate, the transaminated form of oxaloacetate, has (Fig. 5.4). Oxaloacetate is transaminated into aspartate by aspartate aminotransferase (AspC) using glutamate as the amino donor. Aspartate then undergoes α-decarboxylation using aspartate 1-decarboxylase into β-alanine, a metabolite in panthothenate biosynthesis. Once β-alanine is formed, amino-group can then be transaminated back into keto functionality using α-ketoglutarate as the amino receptor to produce malonate semialdehyde. Transamination of β-alanine is catalyzed by β-Alanine aminotransferase (SkPYD4) found in *Saccharomyces kluyveri* (14). Effectively, transamination of oxaloacetate to

128

aspartate serves as a shunt to facilitate α-decarboxylation. All enzymes involved in this synthetic pathway are available from nature, suggesting its feasibility. However in bacteria, aspartate α-decarboxylase (PanD) is an unusual enzyme using pyruvate as a prosthetic group. PanD is translated as an inactive proenzyme, which after self-proteolysis forms two functional subunits and the pyruvyl-group. PanD may be a difficult enzyme to use for designing synthetic pathways because the rate of enzyme maturation depends on temperature and maturation factor (15). Nevertheless, decarboxylation of aspartate provides an irreversible trap for carbon flux, which serves as a driving force for this synthetic malonyl-CoA pathway.

Isomerization by amino transfer using Alanine. The least energy demanding and second shortest pathway for malonyl-CoA biosynthesis is mediated by amino transfer (Fig. 5.1C). Pyruvate is first transaminated into alanine, effectively converting α-keto to α-amino which is converted into β-amino by an alanine aminomutase. Subsequent transamination of β-alanine returns keto group by using either pyruvate or α-ketoglutarate as an amino receptor. This synthetic pathway has a net positive ATP yield. However, this synthetic pathway requires alanine aminomutase which has not been identified in nature. Enzymatic functional relatives of alanine aminomutase such as lysine 2,3-aminomutase (16) and glutamate 2,3-aminomutase (17) contains iron sulfur clusters for generating radical SAM, which facilitates amino transfer. While it is possible to evolve alanine aminomutase from these enzymatic relatives, their oxygen sensitive nature may be prohibitive for functionally constructing this synthetic pathway in aerobic systems.

Sequential dehydration and hydration of lactate enabled isomerization by hydroxyl transfer. Reduction of pyruvate yields lactate in which its α-hydroxyl can be removed by dehydration, resulting in formation of acrylate (Fig. 5.1D). Hydration at β-position of acrylate followed by oxidation returns keto functionality at the β-position, forming malonate semialdehyde. To facilitate dehydration of α-hydroxyl group, lactate is first activated into lactoyl-CoA using propionyl-CoA as CoA donor. Propionyl-CoA is synthesized from propionate, CoA, and ATP using AMP forming propionyl-CoA synthase. Two ATP are needed to convert AMP back into ATP, which increases ATP cost of this pathway and contributes to the net ATP deficiency of this pathway. Lactoyl-CoA dehydrates into acryloyl-CoA which is then rehydrated at the β-position, forming 3-hydroxypropionyl-CoA. 3-hydroxypropionyl-CoA is then hydrolyzed to 3-hydroxypropionate, structural isomer of lactate. Subsequent re-oxidation of β-hydroxyl group of 3-hydroxypropionate yields malonare semialdehyde. Alternatively, 3-hydroxypropionyl-CoA can be converted directly to malonyl-CoA In two reduction steps. However the enzymes necessary for these reductions have not been identified. While all enzymes of this synthetic pathway are available in nature, both the ATP demand and the number of enzymes required is larger than the aspartate dependent pathway which also has all enzymes available from nature, therefore lowering the feasibility of this pathway.

Hydration dehydration via glycerol pathway for hydroxyl transfer. Net hydroxyl transfer can also be achieved via a hydration pattern different from the lactate pathway. Here, utilizing gluconeogenesis, PEP is first hydrated at β-position to 2-phosphoglycerate (Fig. 5.1E). Following gluconeogenesis, glycerol is synthesized by reduction of dihydroxyacetone-phosphate using glycerol-3-phosphate dehydrogenase followed by dephosphorylation using glycerol

130

phosphatase. Subsequently, glycerol is dehydrated to 3-hydroxypropionaldehyde using glycerol dehydratase (Gdh). Two types of Gdh exist in nature. *Klebsiella* Gdh is composed of three subunits and utilizes coenzyme B12 as a prosthetic group (18). However, *Klebsiella* Gdh is irreversibly inactivated upon reaction with glycerol. A reactivating factor is necessary for subsequent glycerol dehydration. Glycerol dehydratase reactivating factor (Gdr) utilizes energy from ATP hydrolysis to reactivate Gdh (19), increasing additional ATP cost and contributing to the net ATP deficiency of this synthetic pathway. *Clostridium* Gdh on the other hand does not require Coenzyme B12 for catalysis. Instead, *Clostridium* Gdh requires an activation enzyme to introduce a glycyl radical required for catalysis (20). Similar to pyruvate:formate lyase, *Clostridium* Gdh is oxygen sensitive, prohibiting its function in many aerobic processes. While all enzymes of this synthetic pathway are available in nature, and overall thermodynamics is more favorable than all other pathways, both the ATP demand and the number of enzymes required are significantly larger than the other pathways.

5.2.2. In vitro biosynthesis of malonyl-CoA from β-alanine

From the thermodynamics and feasibility analysis, we proceeded with *in vitro* analysis of the aspartate dependent pathway. The first question is the reversibility of Mcr. While thermodynamics analysis suggests its reversibility, Mcr has not been demonstrated to function in the oxidative direction. Since malonate semialdehyde is not commercially available, we conducted a coupled reaction using SkPYD4 and Mcr (Fig. 5.5A) to convert β-alanine to malonyl-CoA. SkPYD4 and Mcr were individually purified using poly-His-tag. The results are shown in HPLC chromatogram (Fig. 5.5B). Malonyl-CoA is only synthesized upon presence of
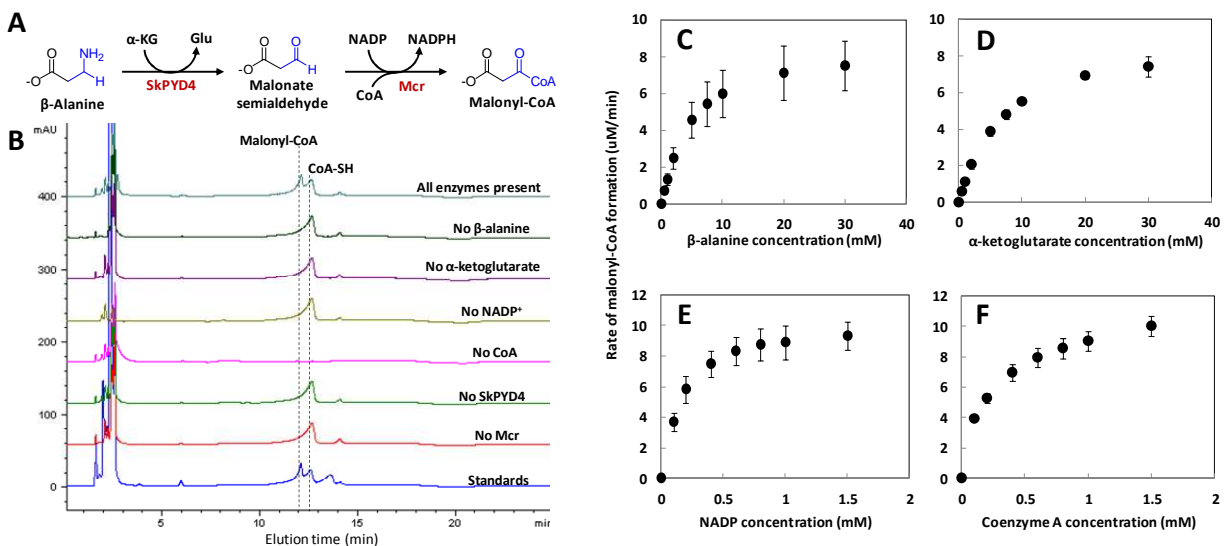
Figure 5.5. . Biosynthesis of malonyl-CoA from β-alanine. A) schematics of the coupled reaction containing SkPYD4 and Mcr. Titration of substrates and cofactors: B) β-alanine, C) α-ketoglutarate, D) NADP$^+$, and E) CoA. Except the substrate being titrated, concentrations of other substrates were: 1 mM of NADP$^+$, 1 mM of CoA, 30 mM β-alanine, and 30 mM α-ketoglutarate. Reaction was catalyzed using 200 nM of SkPYD4, and 200 nM of Mcr.

all components in the reaction, indicating both the reversibility of Mcr and the feasibility of malonyl-CoA biosynthesis from β-alanine.

To explore the dependence of this synthetic malonyl-CoA pathway on the substrate concentrations of these two steps, we titrated each reactant individually into the system and observed their effect on the rate of malonyl-CoA formation. Rate of malonyl-CoA synthesis reaches maximum at around 20 to 30 mM of β-alanine (Fig. 5.5C) and α-ketoglutarate (Fig. 5.5D). Both of these reactants achieve half-maximum rate around 4 to 5 mM which is consistent with the literature Km value of SkPYD4 for β-alanine and α-ketoglutarate (14). On the other hand, both NADP+ (Fig. 5.5E) and CoA (Fig. 5.5F) saturates rate of malonyl-CoA formation within concentration of 1.5 mM. These results indicated that rate of malonyl-CoA biosynthesis requires high concentration of β-alanine and α-ketoglutarate. Natural flux to
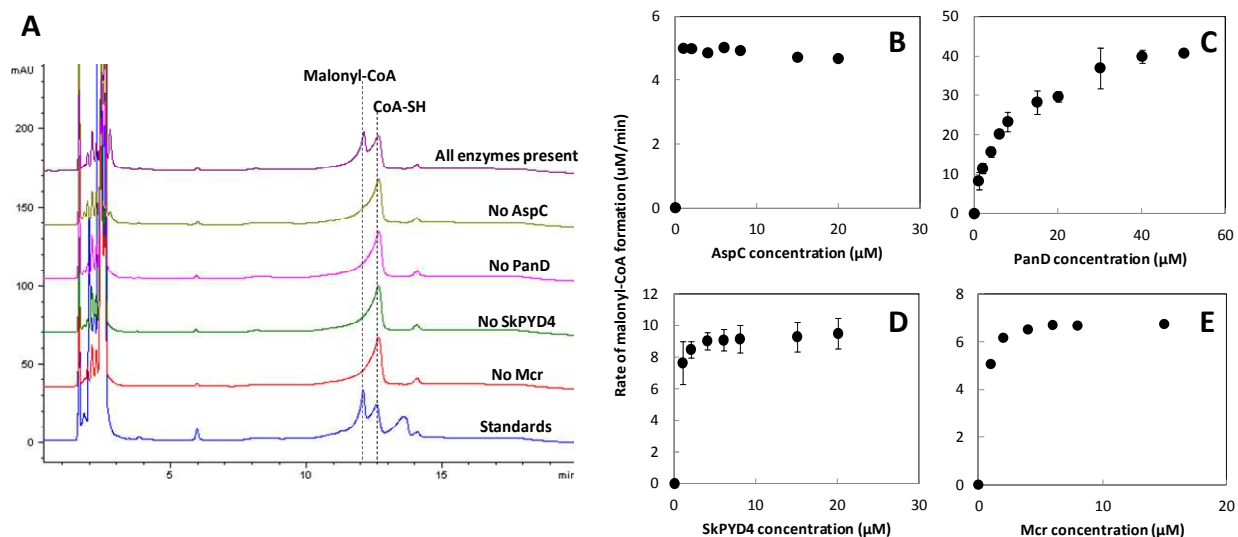
Figure 5.6. One pot biosynthesis of malonyl-CoA from oxaloacetate. A) HPLC chromatogram showing synthesis of malonyl-CoA only upon presence of all enzymes AspC, PanD, SkPYD4, and Mcr. Titration of individual enzymes in aspartate dependent biosynthesis of malonyl-CoA: B) AspC, C) PanD, D) SkPYD4, and E) Mcr. Reaction mixture contained at 1 mM of NADP$^+$, 1 mM of CoA, 20 mM oxaloacetate, 15 mM α-ketoglutarate, 15 mM glutamate, 100 µM of PLP. Except the enzyme being titrated, concentrations of other enzymes were kept constant at 1 µM.

β-alanine from aspartate is not expected to be large because its biosynthesis is mainly for synthesizing CoA, which only minor amounts are required. Therefore, it is likely that formation of β-alanine may be a limiting factor in this pathway.

5.2.3. Effect of individual enzyme concentration on rate of malonyl-CoA biosynthesis from oxaloacetate

To study the overall rate of malonyl-CoA biosynthesis using the aspartate dependent pathway, we constructed an *in vitro* system composed of AspC, PanD, SkPYD4, and Mcr to convert oxaloacetate to malonyl-CoA (Fig. 5.4). We chose to use PanD from *Corynebacterium glutamicum* for its more efficient maturation (21). As shown in HPLC chromatogram (Fig. 5.6A), malonyl-CoA is only synthesized upon presence of all four enzymes in the system, indicating the

functional constitution of this synthetic pathway. To analyze the concentration effect of each enzyme on the biosynthesis of malonyl-CoA from oxaloacetate, we individually titrated each enzyme in this four step reaction while keeping the concentration of other enzymes constant at 1 µM. No change in rate of malonyl-CoA formation was observed when the concentration of AspC was increased (Fig. 5.6B), indicating that AspC bares no bottleneck for this pathway. On the other hand, reaction rate increased with PanD concentration until 40 uM (Fig. 5.6C). This result indicated that PanD is the limiting step in this synthetic pathway, which is consistent with our expectation as β-alanine is not naturally produced at large flux. Both SkPYD4 (Fig. 5.6D) and Mcr (Fig. 5.6E) reaches maximum reaction rate at around 4 uM of enzyme concentration. From these results, we deduced that the optimum ratio of AspC:PanD:SkPYD4:Mcr for malonyl-CoA biosynthesis is 1:40:4:4.

5.2.4. PLP-dependent aspartate a-decarboxylase enhanced rate of malonyl-CoA biosynthesis

Considering the large concentration of PanD required to reach optimum rate of malonyl-CoA biosynthesis, we searched for alternative candidate enzyme for aspartate decarboxylation. Most amino acid α-decarboxylases such as glutamate decarboxylase and lysine decarboxylase use pyridoxal 5-phosphate (PLP) for catalysis. Turnover number of glutamate decarboxylase (22) (24.85 s^{-1}) and lysine decarboxylase (23) (30 s^{-1}) are both higher than that of PanD (24) (0.65 s^{-1}) in *E. coli,* indicating more efficient catalysis with PLP. Inspired by this observation, we searched for aspartate decarboxylase using PLP as a cofactor. Aspartate decarboxylase (ADC) from *Aedes aegypti* (25) is a structural homologue of glutamate decarboxylase using PLP as a cofactor. Therefore, we recruited ADC to replace PanD in our synthetic pathway.
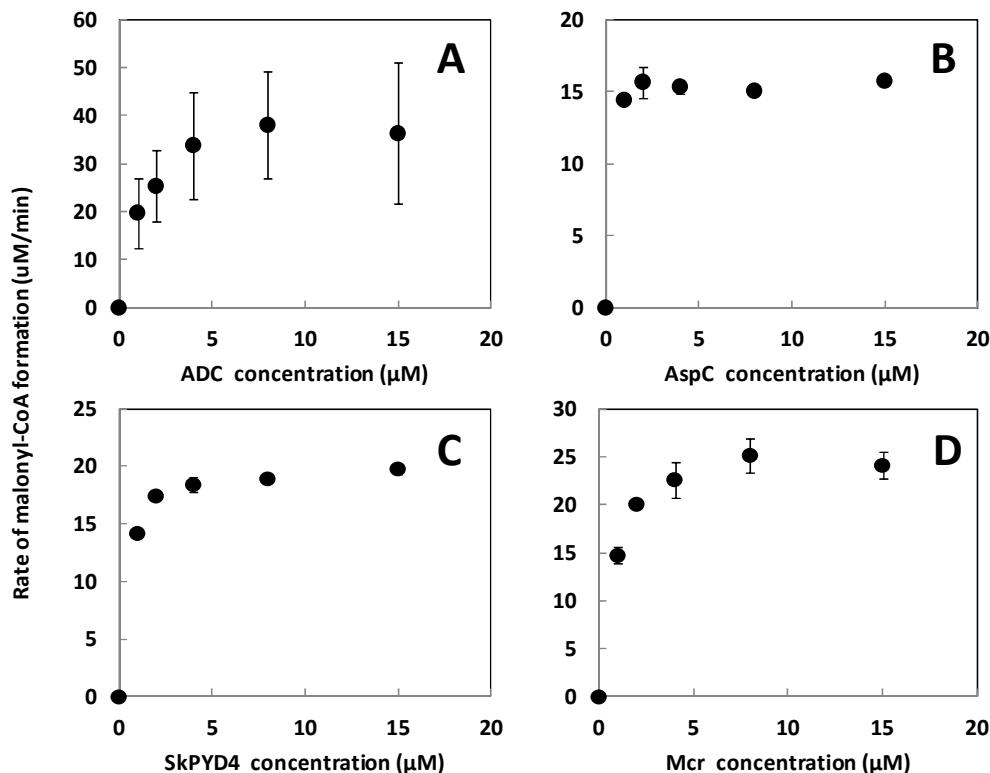
Figure 5.7. Titration of individual enzymes in malonyl-CoA biosynthesis with PLP-dependent aspartate decarboxylase. Titration of individual enzymes: B) ADC, C) AspC, D) SkPYD4, and E) Mcr. Mcr. Reaction mixture contained at 1 mM of NADP$^+$, 1 mM of CoA, 20 mM oxaloacetate, 15 mM α-ketoglutarate, 15 mM glutamate, and 100 µM of PLP. Except the enzyme being titrated, concentrations of other enzymes were kept constant at 1 µM.

Next, we again titrated each enzyme in the four step reaction with PLP dependent aspartate decarboxylase. Malonyl-CoA synthesis reaches maximum rate at 8 uM of ADC (Fig. 5.7A), which is significantly less than the 40 uM of PanD required for achieving maximum rate. AspC (Fig. 5.7B) and SkPYD4 (Fig. 5.7C) achieved highest rate at 1 uM and 4 uM, respectively, which is identical to the PanD dependent system. Mcr required 8 uM to reach highest rate in this system (Fig. 5.7D). Together, these results showed that using PLP dependent ADC, we are able to reduce the amount of enzyme required to achieve higher rate of malonyl-CoA synthesis. The optimum ratio of AspC:ADC:SkPYD4:Mcr is 1:8:4:8, which may be easier to implement *in vivo*.

5.3. Discussion

Synthetic metabolism enables biosynthesis of various valuable compounds and introduces new functions to cells. Nature uses limited sets of metabolites to construct a diverse space of complex molecules. Carbon chain elongation offers most diversity and complexity in molecules produced. Malonyl-CoA is one of the principle carbon extender for achieving this chemical diversity. In this study, we described the design and proof of concept demonstration of a synthetic malonyl-CoA biosynthesis pathway. We have shown the *in vitro* conversion of oxaloacetate to malonyl-CoA in four enzymatic steps. In particular, the rate of malonyl-CoA biosynthesis demonstrated is comparable to that of *in vitro* fatty acid biosynthesis (26), suggesting compatibility of this synthetic pathway for biofuel production.

Migration of the α-keto group of pyruvate to the β-position, forming malonate semialdehyde, is the major challenge for designing synthetic malonyl-CoA pathway. Because such isomerization is not available, alternative reaction schemes are necessary to achieve this result. Carboxylation of PEP to oxaloacetate introduces a carboxyl group at the γ-position of pyruvate. The original α-keto group of pyruvate therefore becomes β-keto relative to this new carboxyl group (Fig. 5.1B). Subsequent decarboxylation of the original pyruvate carboxyl group yields malonate semialdehyde. However, enzyme catalyzing this α-decarboxylation of oxaloacetate is not found in nature, therefore hindering the development of this pathway. Instead of decarboxylation of oxaloacetate, we utilized the decarboxylation of aspartate which is readily available in nature. In our synthetic pathway (Fig. 5.4), α-keto group of oxaloacetate is transaminated into amino group to facilitate the α-decarboxylation into β-alanine. Subsequent transamination returns keto functionality and forms malonate semialdehyde. Using this aspartate

shunt, we effectively converted oxaloacetate into malonate semialdehyde. This synthetic pathway has the same ATP cost as the natural Acc dependent pathway.

Recent advances (1, 27) have shown that malonyl-CoA can also be used for CoA-dependent chain elongation. Decarboxylative condensation of malonyl-CoA with acetyl-CoA is irreversible and thus provides driving force for downstream pathways, an important design principle for engineering photosynthetic organisms (1, 28). CoA dependent chain elongation includes *Clostridium* pathway for 1-butanol production (29) and mevalonate pathway for production of diverse downstream isoprenoids-based compounds (30). Incorporation of the synthetic malonyl-CoA pathway into *in vivo* systems would enahnce production of these diverse malonyl-CoA derived products.

5.4. Materials and methods

5.4.1. Chemicals and reagents

All chemicals were purchase from Sigma-Aldrich. KOD and KOD-extreme DNA polymerases were purchased from EMD Biosciences. Phusion DNA polymerase, and ligases were purchased from New England Biolabs (Ipswich, MA). T5-Exonuclease was purchased from Epicentre Biotechnologies. Oligonucleotides were obtained from IDT (San Diego, CA).

5.4.2. Plasmid constructions

A list of plasmids used in this work is presented in Table 5.S3. All plasmids were constructed by isothermal DNA assembly method (31). Plasmids were propagated and stored in *E. coli* strain XL-1 blue. Promoter and enzyme coding regions of all plasmids were verified by DNA sequencing performed by Genewiz (San Diego, CA). Gene *mcr* was synthesized by

Genewiz (South Plainfield, NJ) with codon optimization for *E. coli*. Genes *skpyd4* and *adc* were synthesized by DNA2.0 (Menlo Park, CA) with codon optimization for *E. coli*.

5.4.3. Protein expression and purification

All enzymes used in this study were expressed in BL21(DE3). Cells were inoculated from an overnight preculture at 100X dilution and grown in 2XYT rich medium containing 50 mg/L spectinomycin. At OD_{600} of 0.6, cell cultures were induced with 1 mM IPTG and incubated at 30 °C overnight. Cells were pelleted by centrifuging at 4300 x g for 20 minutes. Cell pellets were resuspended in His-Binding buffer (either from Zymo or EMD Millipore) and lysed either using TissueLyser II (Qiagen) or Sonicator (Branson Sonifier 250). Soluble proteins were separated from insoluble cell debris by centrifugation at 16,000 x g for 20 minutes. His-tagged enzymes were then purified using either His-Spin Protein Miniprep (Zymo) or Amicon® Pro Affinity Concentration Kit Ni-NTA (EMD Millipore) according to manufacturer's instruction. Purified enzymes were subjected to buffer exchange and stored in solution containing 50 mM Tris-HCl pH 8.5, 1mM DTT, and 20% glycerol at -80 °C. For AspC, SkPYD4, and ADC, additional 100 µM of PLP was added to storage buffer.

5.4.4. Analysis of synthetic malonyl-CoA pathways

Thermodynamics of each reaction step was calculated using eQuilibrator (32) with either standard condition ($\Delta G'^{\circ}$) or physiological relevant condition ($\Delta G'$ at 1 mM substrate and product concentration, pH 7.0, and ionic strength of 0.1 M).

5.4.5. Kinetic analysis of malonyl-CoA biosynthesis

Since NADPH is produced at 1 to 1 stoichiometric ratio with malonyl-CoA from either β-alanine or aspartate, spectrophotometeric assay monitoring the disappearance of NADPH corresponding to absorbance at 340 nm was used. Absorbance at 340 nm was monitored using Bio-TEK PowerWave XS microplate spectrophotometer. For determining the effect of substrate concentration on rate of malonyl-CoA biosynthesis from β-alanine, individual substrate was varied as indicated while keeping the concentration of other substrates constant at 1 mM of NADP+, 1 mM of CoA, 30 mM β-alanine, 30 mM α-ketoglutarate. α-Ketoglutarate was neutralized with NaOH prior to mixing with the enzymatic reaction. The reaction also contained 200 nM SkPYD4, and 200 nM Mcr in 50 mM Tris-HCl pH 8.5. reaction was started by addition of β-alanine.

For determining the effect of individual enzyme concentration on rate of malonyl-CoA biosynthesis from oxaloacetate, concentration of each enzyme was varied as indicated while keeping the concentration of other enzymes at 1 µM. The reaction mixture contained 20 mM oxaloacetate, 15 mM α-ketoglutrate, 15 mM glutamate, and 80 µM PLP in 50 mM Tris-HCl pH 8.5.

5.4.6. HPLC analysis of malonyl-CoA

Separation of CoA and malonyl-CoA was achieved using HPLC equipped with an autosampler and a C18 column (TOSOH, TSKgel ODS-100Z 4.6 x 150 mm, 5 µm). Product elution was carried out using gradient program with 50 mM sodium acetate pH 3.7 as aqueous solvent and acetonitrile as organic solvent with flow rate of 1 mL/min. The gradient program

used is summarized in Table 5.S4. Product elution was monitored at 254 nm using diode array detector. Injection volume was 20 µL. column temperature was kept at 30 °C.

Table 5.S1. Synthetic malonyl-CoA biosynthesis pathways with enzymes available in nature

Step	Enzyme	E.C number	Substrate	Product	$\Delta G'^o$	$\Delta G'$	Reversibility
			Aspartate pathway				
1	Phosphoenolpyruvate carboxylase	4.1.1.31	Phosphoenolpyruvate + CO_2	Oxaloacetate + phosphate	-43.2	-43.2	Irreversible
2	Aspartate aminotransferase	2.6.1.1	Oxaloacetate + glutamate	Aspartate + α-ketoglutarate	1.5	1.5	Reversible
3	Aspartate 1-decarboxylase	4.1.1.11	Aspartate	β-alanine + CO_2	-19.9	-35.8	Irreversible
4	β-Alanine aminotransferase	2.6.1.19	β-alanine + α-ketoglutarate	Malonate semialdehyde + glutamate	9.8	11	Reversible
5	Malonyl-CoA reductase	1.2.1.75	Malonate semialdehyde + CoA + $NADP^+$	Malonyl-CoA + NADPH	-14.9	-7.5	Reversible
			Glycerol pathway				
1	Enolase	4.2.1.11	Phosphoenolpyruvate + H_2O	2-phosphoglycerate	2.0	3.3	Reversible
2	Phosphoglycerate mutase	5.4.2.1	2-phosphoglycerate	3-phosphoglycerate	-5.7	-5.9	Reversible
3	Phosphoglycerate kinase	2.7.2.3	3-phosphoglycerate + ATP	1,3-bisphosphoglycerate + ADP + phosphate	7.8	8.1	Reversible
4	Glyceraldehyde-3-phosphate dehydrogenase	2.7.2.3	1,3-bisphosphoglycerate + NADH	glyceraldehyde 3-phosphate + NAD + phosphate	-7.8	-3.1	Reversible
5	Triosephosphate isomerase	5.3.1.1	glyceraldehyde 3-phosphate	Dihydroxyacetone phosphate	-7.7	-7.7	Reversible
6	Glycerol-3-phosphate dehydrogenase	1.1.1.8	Dihydroxyacetone phosphate + NADH	Glycerol-3-phosphate + NAD	-46.3	-43.3	Irreversible
7	Glycerol phosphatase	3.1.3.21	Glycerol-3-phosphate+ H_2O	Glycerol + phosphate	1.1	-15.3	Irreversible
8	Glycerol dehydratase	4.2.1.30	Glycerol	3-hydroxypropionaldehyde + H_2O	-36	-36	Irreversible
9	3-hydroxypropionaldehyde	1.2.1.-	3-hydroxypropionaldehyde + NAD	3-hydroxypropionate + NADH	-41.5	-45.2	Irreversible

	dehydrogenase						
10	3-hydroxypropionate dehydrogenase	1.1.1.59	3-hydroxypropionate + NADP	Malonate semialdehyde + NADPH	23.7	18.8	Reversible
11	Malonyl-CoA reductase	1.2.1.75	Malonate semialdehyde + CoA + NADP$^+$	Malonyl-CoA + NADPH	-14.9	-7.5	Reversible
	Lactate pathway						
1	Pyruvate kinase	2.7.1.40	Phosphoenolpyruvate + ADP + phosphate	Pyruvate + ATP	-30.6	-29.3	Irreversible
2	Lactate dehydrogenase	1.1.1.27	Pyruvate + NADH	Lactate + NAD	-20.2	-17.8	Reversible
3a	Propionyl-CoA transferase	2.8.3.1	Lactate + Propionyl-CoA	Lactoyl-CoA + Propionate	0	0	Reversible
3b	Propionate-CoA ligase	6.2.1.17	Propionate + ATP + CoA	Propionyl-CoA + AMP + PPi	-10.5	-10.4	Reversible
4	lactoyl-CoA dehydratase	4.2.1.54	Lactoyl-CoA	Acryloyl-CoA + H$_2$O	9.9	9.9	Reversible
5	3-hydroxypropionyl-CoA dehydratase	4.2.1.116	Acyloyl-CoA + H$_2$O	3-hydroxypropionyl-CoA	-2.4	-2.4	Reversible
6	3-hydroxypropionyl-CoA hydrolase	3.1.2.--	3-hydroxypropionyl-CoA + H$_2$O	3-hydroxypropionate + CoA	-25.8	-27.1	Irreversible
7	3-hydroxypropionate dehydrogenase	1.1.1.59	3-hydroxypropionate + NADP	Malonate semialdehyde + NADPH	23.7	18.8	Reversible
8	Malonyl-CoA reductase	1.2.1.75	Malonate semialdehyde + CoA + NADP$^+$	Malonyl-CoA + NADPH	-14.9	-7.5	Reversible

Table 5.S2. Synthetic malonyl-CoA biosynthesis pathways with enzymes not available in nature

Step	Enzyme	E.C number	Substrate	Product	$\Delta G'^o$	$\Delta G'$	Reversibility
α-Alanine pathway							
1	Pyruvate kinase	2.7.1.40	Phosphoenolpyruvate + ADP + phosphate	Pyruvate + ATP	-30.6	-29.3	Irreversible
2	β-alanine aminotransferase	2.6.1.18	Pyruvate + β-alanine	α-alanine + malonate semialdehyde	9.8	9.8	Reversible
3	Alanine aminomutase	---	α-alanine	β-alanine	0.4	0.4	Reversible
4	Malonyl-CoA reductase	1.2.1.75	Malonate semialdehyde + CoA + NADP$^+$	Malonyl-CoA + NADPH	-14.9	-7.5	Reversible
Oxaloacetate pathway							
1	Phosphoenolpyruvate carboxylase	4.1.1.31	Phosphoenolpyruvate + CO$_2$	Oxaloacetate + phosphate	-43.2	-43.2	Irreversible
2	Oxaloacetate	---	oxaloacetate	Malonate semialdehyde	-13.9	-29.7	Irreversible
3	Malonyl-CoA reductase	1.2.1.75	Malonate semialdehyde + CoA + NADP$^+$	Malonyl-CoA + NADPH	-14.9	-7.5	Reversible

Table 5.S3. Plasmids used in this study

Plasmid	Genotypes	Reference
pCDFDuet	Spec^R; CDF ori; P$_{T7}$::MCS (His tagged)	Novagen
pCDF-SkPYD4	Spec^R; CDF ori; P$_{T7}$::*Skpyd4* (His tagged)	This work
pCDF-AspC	Spec^R; CDF ori; P$_{T7}$::a*spC* (His tagged)	This work
pCDF-PanD	Spec^R; CDF ori; P$_{T7}$::*panD* (His tagged)	This work
pEL230	Kan^R; pUC ori; P$_{T5}$::*adc* (His tagged)	This work
pEL141	Amp^R; CDF ori; P$_{T5}$::*mcr* (His tagged)	This work

Table 5.S4. HPLC parameter for separation of malonyl-CoA

Buffer A	Buffer B	Gradient	
		Time (min)	%B
50 mM Sodium acetate pH 3.7	Acetonitrile	0	2
		4	2
		8	8
		12	20
		15	45
		20	2
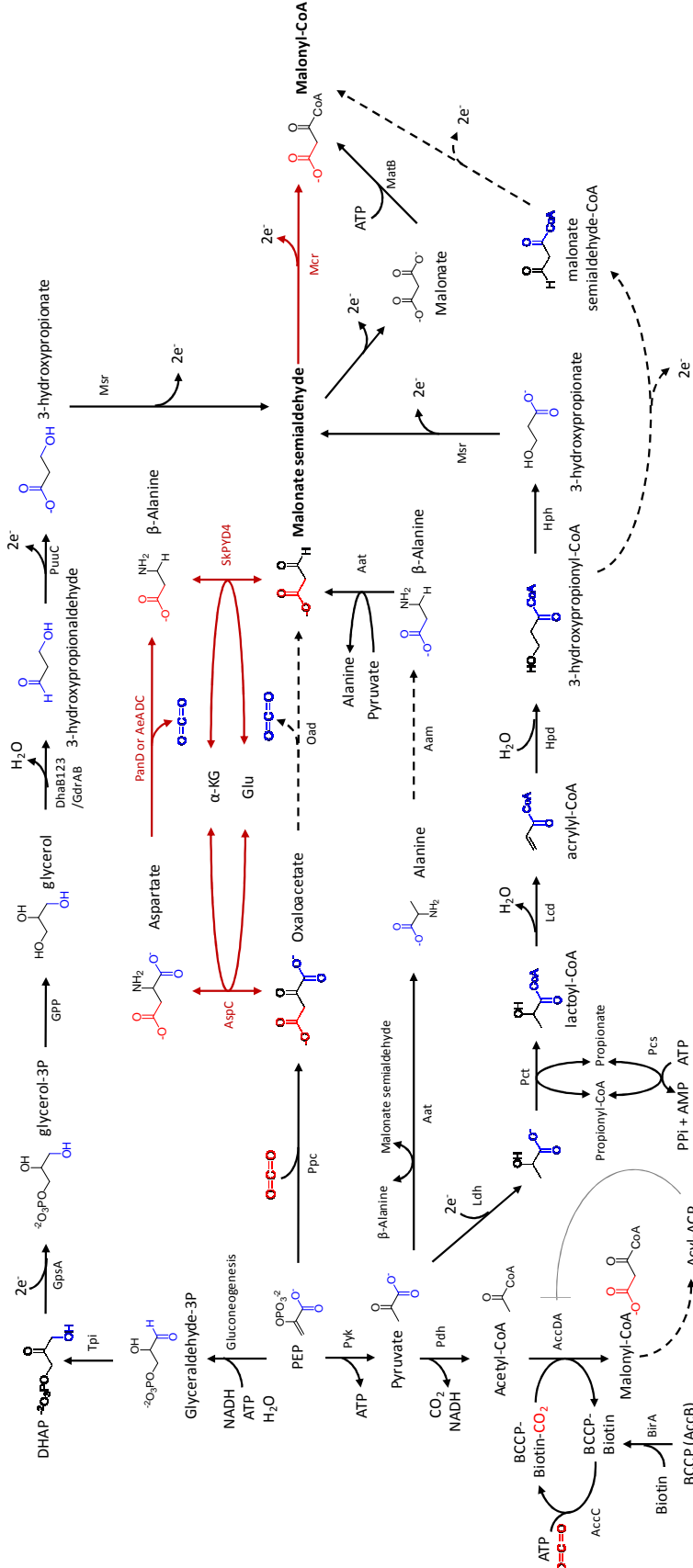
Figure 5.S1. Complete metabolic interconnections between the synthetic malonyl-CoA pathways. Dash lines represents enzymes not found in nature. Abbreviations: Tpi, triose phosphate isomerase; GpsA, glycerol-3-phosphate dehydrogenase; GPP, glycerol-3-phosphatase; DhaB123, glycerol dehydratase; GdrAB, glycerol dehratase reactivase; PuuC, aldehyde dehydrogenase; Msr, malonate semialdehyde dehydrogenase; Ppc, phosphoenolpyruvate carboxylase; AspC, aspartate transaminase; PanD, aspartate 1-decarboxylase; AeADC, PLP-dependent aspartate 1-decarboxylase; SkPYD4, β-alanine aminotransferase; Oad, oxaloacetate 1-decarboxylase; Mcr, malonyl-CoA reductase; Pyk, pyruvate kinase; Aat; alanine aminotransferase; Aam, alanine aminomutase; Pdh, pyruvate dehydrogenase; AccDA, acetyl-CoA carboxyltransferase; AccC, biotin carboxylase; Ldh, lactate dehydrogenase; Pct, lactoyl-CoA transferase; Pcs, propionyl-CoA synthase; Lcd, lactoyl-CoA dehyratase; Hpd, hydroxypropionyl-CoA dehydratase; Hph, hydroxypropionyl-CoA hydrolase; MatB, malonyl-CoA synthase.

145

5.5. Reference

1.   Lan EI & Liao JC (2012) ATP drives direct photosynthetic production of 1-butanol in cyanobacteria. Proc Natl Acad Sci USA 109(16):6018-6023.

2.   Li SJ & Cronan JE, Jr. (1993) Growth rate regulation of Escherichia coli acetyl coenzyme A carboxylase, which catalyzes the first committed step of lipid biosynthesis. J Bacteriol 175(2):332-340.

3.   Meades G, Jr., Benson BK, Grove A, & Waldrop GL (2010) A tale of two functions: enzymatic activity and translational repression by carboxyltransferase. Nucleic Acids Res 38(4):1217-1227.

4.   Davis MS & Cronan JE, Jr. (2001) Inhibition of Escherichia coli acetyl coenzyme A carboxylase by acyl-acyl carrier protein. J Bacteriol 183(4):1499-1503.

5.   Tai M & Stephanopoulos G (2013) Engineering the push and pull of lipid biosynthesis in oleaginous yeast Yarrowia lipolytica for biofuel production. Metab Eng 15:1-9.

6.   Shi S, Valle-Rodriguez JO, Khoomrung S, Siewers V, & Nielsen J (2012) Functional expression and characterization of five wax ester synthases in Saccharomyces cerevisiae and their utility for biodiesel production. Biotechnology for biofuels 5:7.

7.   Lu XF, Vora H, & Khosla C (2008) Overproduction of free fatty acids in E. coli: Implications for biodiesel production. Metab Eng 10(6):333-339.

8.   Davis MS, Solbiati J, & Cronan JE, Jr. (2000) Overproduction of acetyl-CoA carboxylase activity increases the rate of fatty acid biosynthesis in Escherichia coli. J Biol Chem 275(37):28593-28598.

9.   Zha WJ, Rubin-Pitel SB, Shao ZY, & Zhao HM (2009) Improving cellular malonyl-CoA level in Escherichia coli via metabolic engineering. Metab Eng 11(3):192-198.

10.   Xu P, Ranganathan S, Fowler ZL, Maranas CD, & Koffas MAG (2011) Genome-scale metabolic network modeling results in minimal interventions that cooperatively force carbon flux towards malonyl-CoA. Metab Eng 13(5):578-587.

11.   Alber B, et al. (2006) Malonyl-coenzyme A reductase in the modified 3-hydroxypropionate cycle for autotrophic carbon fixation in archaeal Metallosphaera and Sulfolobus spp. J Bacteriol 188(24):8551-8559.

12.   Hugler M, Menendez C, Schagger H, & Fuchs G (2002) Malonyl-coenzyme A reductase from Chloroflexus aurantiacus, a key enzyme of the 3-hydroxypropionate cycle for autotrophic CO(2) fixation. J Bacteriol 184(9):2404-2410.

146

13.   Zhang S & Bryant DA (2011) The tricarboxylic acid cycle in cyanobacteria. Science 334(6062):1551-1553.

14.   Andersen G, Andersen B, Dobritzsch D, Schnackerz KD, & Piškur J (2007) A gene duplication led to specialized γ-aminobutyrate and β-alanine aminotransferase in yeast. FEBS J 274(7):1804-1817.

15.   Nozaki S, Webb ME, & Niki H (2012) An activator for pyruvoyl-dependent l-aspartate alpha-decarboxylase is conserved in a small group of the gamma-proteobacteria including Escherichia coli. MicrobiologyOpen 1(3):298-310.

16.   Behshad E, et al. (2006) Enantiomeric free radicals and enzymatic control of stereochemistry in a radical mechanism: the case of lysine 2,3-aminomutases. Biochemistry (Mosc) 45(42):12639-12646.

17.   Ruzicka FJ & Frey PA (2007) Glutamate 2,3-aminomutase: a new member of the radical SAM superfamily of enzymes. Biochim Biophys Acta 1774(2):286-296.

18.   Toraya T, Shirakashi T, Kosuga T, & Fukui S (1976) Substrate specificity of coenzyme B12-dependent diol dehydrase: glycerol as both a good substrate and a potent inactivator. Biochem Biophys Res Commun 69(2):475-480.

19.   Mori K & Toraya T (1999) Mechanism of reactivation of coenzyme B12-dependent diol dehydratase by a molecular chaperone-like reactivating factor. Biochemistry (Mosc) 38(40):13170-13178.

20.   O'Brien JR, et al. (2004) Insight into the Mechanism of the B12-Independent Glycerol Dehydratase from Clostridium butyricum: Preliminary Biochemical and Structural Characterization‡. Biochemistry (Mosc) 43(16):4635-4645.

21.   Dusch N, Puhler A, & Kalinowski J (1999) Expression of the Corynebacterium glutamicum panD gene encoding L-aspartate-alpha-decarboxylase leads to pantothenate overproduction in Escherichia coli. Appl Environ Microbiol 65(4):1530-1539.

22.   Pennacchietti E, et al. (2009) Mutation of His465 alters the pH-dependent spectroscopic properties of Escherichia coli glutamate decarboxylase and broadens the range of its activity toward more alkaline pH. J Biol Chem 284(46):31587-31596.

23.   Kanjee U, et al. (2011) Linkage between the bacterial acid stress and stringent responses: the structure of the inducible lysine decarboxylase. EMBO J 30(5):931-944.

24.   Ramjee MK, Genschel U, Abell C, & Smith AG (1997) Escherichia coli L-aspartate-alpha-decarboxylase: preprotein processing and observation of reaction intermediates by electrospray mass spectrometry. Biochem J 323 (Pt 3):661-669.

25.   Richardson G, et al. (2010) An examination of aspartate decarboxylase and glutamate decarboxylase activity in mosquitoes. Mol Biol Rep 37(7):3199-3205.

26.   Yu X, Liu T, Zhu F, & Khosla C (2011) In vitro reconstitution and steady-state analysis of the fatty acid synthase from Escherichia coli. Proc Natl Acad Sci USA 108(46):18643-18648.

27.   Okamura E, Tomita T, Sawa R, Nishiyama M, & Kuzuyama T (2010) Unprecedented acetoacetyl-coenzyme A synthesizing enzyme of the thiolase superfamily involved in the mevalonate pathway. Proc Natl Acad Sci USA 107(25):11265-11270.

28.   Lan EI, Ro SY, & Liao JC (2013) Oxygen-tolerant coenzyme A-acylating aldehyde dehydrogenase facilitates efficient photosynthetic n-butanol biosynthesis in cyanobacteria. Energy Environ Sci.

29.   Shen CR, et al. (2011) Driving forces enable high-titer anaerobic 1-butanol synthesis in Escherichia coli. Appl Environ Microbiol 77(9):2905-2915.

30.   Paddon CJ, et al. (2013) High-level semi-synthetic production of the potent antimalarial artemisinin. Nature 496(7446):528-532.

31.   Gibson DG, et al. (2009) Enzymatic assembly of DNA molecules up to several hundred kilobases. Nat Methods 6(5):343-345.

32.   Flamholz A, Noor E, Bar-Even A, & Milo R (2012) eQuilibrator--the biochemical thermodynamics calculator. Nucleic Acids Res 40(Database issue):D770-775.

6. METABOLIC ENGINEERING OF 2-PENTANONE SYNTHESIS IN *ESCHERICHIA COLI*

6.1. Introduction

Building on the success of the *n*-butanol pthway, we also expand the chemical diversity of microbial products. We constructed a synthetic recursive chain elongation by expanding on the CoA-dependent pathway in *E. coli* and integrated it with acetone biosynthesis. In this chapter, we metabolically engineered *E. coli* for production of 2-pentanone, a methyl ketone with five carbons used as a solvent and flavor additive.

In the past century, the chemical industry relied almost exclusively on fossil resources such as petroleum, coal, and natural gas. Biological processes allow the use of renewable resources such as sugars (1), lignocellulose (2), waste proteins (3) or even CO_2 (4-6) as raw materials, and represent an important solution for energy and environmental problems (7). To achieve green manufacturing and to replace fossil raw materials in the chemical industry, expanding the chemical repertoire that a living organism can produce is essential. To meet this goal, microorganisms have been engineered to produce a wide array of products (8-11).

Ketones are an important class of solvents produced in large quantities. The simplest form, acetone, has been produced by microbial processes using *Clostridium* (12). To expand the chemical diversity of microbial synthesis, here we aim to produce a higher chain methyl ketone, 2-pentanone. Methyl ketones are used as solvents, and have been found in small quantities in microbial fermentation products (13). Methyl ketones are also used as food additives for providing scent and flavoring (14). In particular, 2-pentanone is a phytochemical naturally produced in banana and carrot, and has been demonstrated to inhibit cyclooxygenase 2 (COX-2) (15) which is involved in inflammatory processes and potentially associated with colon cancer.

Recently, *E. coli* has been engineered to produce long chain methyl ketones with 11-15 carbons by re-assimilating fatty acids into fatty acyl-coenzyme A (CoA) (16). Fatty acyl-CoA is then partially metabolized by β-oxidation to β-ketoacyl-CoA which is then hydrolyzed and decarboxylated to methyl ketone. Here we describe the engineering of *E. coli* to synthesize 2-pentanone without requiring fatty acid production.

To produce 2-pentanone, we extend the CoA dependent pathway (Fig. 6.1) that leads to acetone and n-butanol production (17, 18) for one more round of carbon chain elongation by applying the principle described for keto-acid chain elongation (19, 20). Note that the CoA dependent pathway resembles the reaction sequence of the β-oxidation in reverse (21). The CoA dependent pathway (Fig. 6.1) starts from acetyl-CoA, an essential metabolite in all organisms. The carbon number in acetyl-CoA can be increased to make acetoacetyl CoA, which after hydrolysis and decarboxylation produces acetone. If the chain length of acetoacetyl CoA is further increased to become 3-ketohexanoyl CoA (Fig. 6.1), similar biochemical transformations can be performed on this compound to produce 2-pentanone. To achieve this goal, efficient expression of the CoA dependent chain elongation pathway is essential.

Many groups have transferred the *Clostridium* n-butanol pathway into heterologous organisms as an alternative platform for n-butanol production (22-26). However, one of the enzymes, butyryl-CoA dehydrogenase electron transferring flavoprotein complex (Bcd/Etf), in the *Clostridium* CoA dependent pathway was not expressed well in heterologous organisms and resulted in low titers of butanol produced. This difficulty prevented further engineering of the CoA dependent pathway. To solve this problem, Bcd/Etf was replaced by *trans*-2-enoyl-CoA reductase (Ter). This replacement partially overcomes the difficulty of heterologous n-butanol production (1, 27). Further engineering of increasing acetyl-CoA and NADH concentration as

driving forces proved to be most effective to push the flux against the thermodynamic gradient of the condensation of two acetyl-CoA, a reaction with $\Delta G°'$ of 28.5 kJ/mol. Together, higher acetyl-CoA and NADH concentrations lower the energy barrier of the pathway and produce high titer and yield of n-butanol (1). These results paved the way for further engineering of the CoA-dependent pathway.

The native CoA-dependent pathway extends the carbon chain length from two (acetyl-CoA) to four (butyryl-CoA). This chain length extension enables the production of n-butanol, rather than ethanol. The same reaction sequence could be repeated to increase the carbon chain length by using enzymes that are active towards various chain lengths. For example, expression of a promiscuous thiolase, which catalyzes the first step of the chain elongation by condensation of acyl-CoA's, enables successive rounds of carbon chain elongation to produce 1-hexanol and 1-octanol (28, 29).

Here we constructed the CoA dependent chain elongation pathway for two rounds of acyl-CoA condensation and demonstrated for the first time the production of 2-pentanone in an engineered organism. We identified the acyl-CoA hydrolysis or thiol group transfer as a limiting step for 2-pentanone synthesis. After improving this step, the best strain produces 2-pentanone to 240 mg/L, representing an increase of 20 fold.

6.2. Results

6.2.1. Constructing the 2-pentanone production pathway

Previously, a modified CoA dependent chain elongation pathway (28) was constructed in *E. coli* by overexpression of a promiscuous β-keto-thiolase (BktB) from *Ralstonia eutropha* with rest of the CoA dependent pathway enzymes, thiolase (AtoB), 3-hydroxy butyryl-CoA
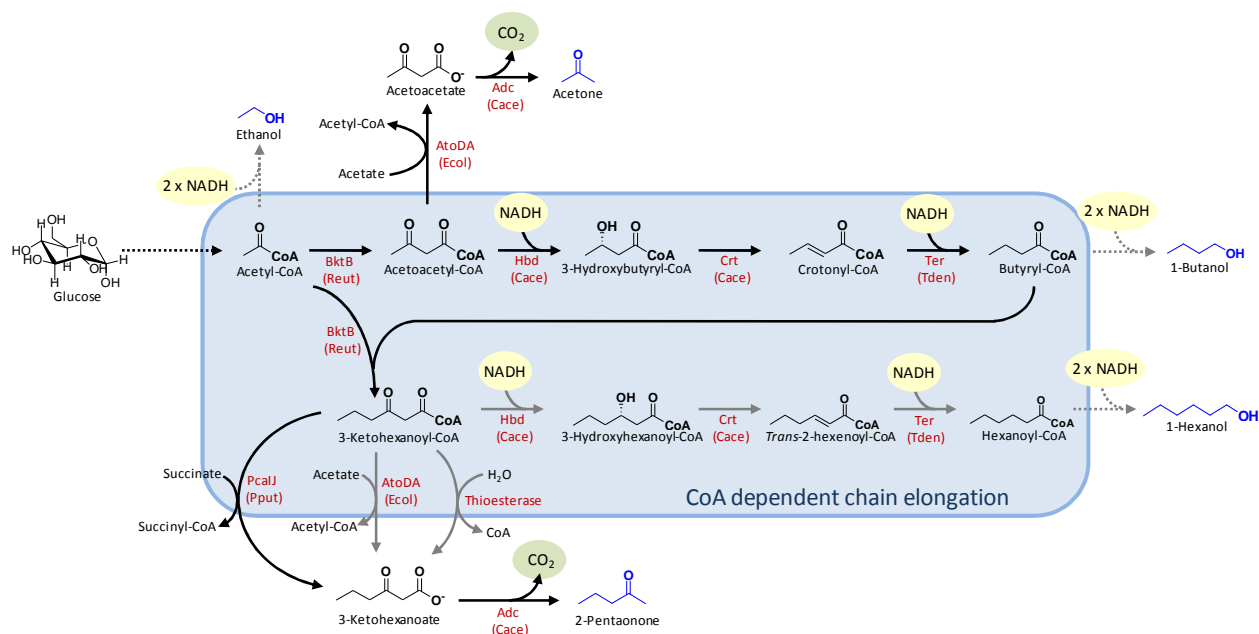
Figure 6.1. Schematic of 2-pentanone synthesis. Other products made from the CoA dependent pathway are also shown as references. Bktb, β-keto-thiolase; Hbd, hydroxybutyryl-CoA dehydrogenase; Crt, crotonase; Ter, *trans*-2-enoyl-CoA reductase; PcaIJ, 3-oxoadipate CoA-succinyl transferase; AtoDA, acetate CoA-transferase. Reut, *Ralstonia eutropha*; Cace, *Clostridium acetobutylicum*; Tden, *Treponema denticola*; Pput, *Pseudomonas putida*; Ecol, *Escherichia coli*.

dehydrogenase (Hbd), crotonase (Crt), and Ter. This synthetic pathway enabled the production of six carbon CoA intermediates as demonstrated by the synthesis of 1-hexanol. Since BktB also catalyzes the condensation of two acetyl-CoA into butyryl-CoA, AtoB was removed from the pathway in this work, reducing the enzymes required for CoA dependent chain elongation pathway to BktB, Crt, Hbd, and Ter.

Methyl ketones are produced from β-keto acids derived from β-ketoacyl-CoA. Acetone, the simplest ketone, is naturally produced by *Clostridia*. The *Clostridium* acetone production pathway branches out from the CoA-dependent pathway from the acetoacetyl-CoA node. Acetoacetyl-CoA goes through a transthiolation by reacting with acetate to form acetoacetate and acetyl-CoA using acetoacetyl-CoA transferase from *Clostridium acetobutylicum* (CtfAB) or from *E. coli* (AtoDA) (31, 32). Acetoacetate is then decarboxylated into acetone by acetoacetate
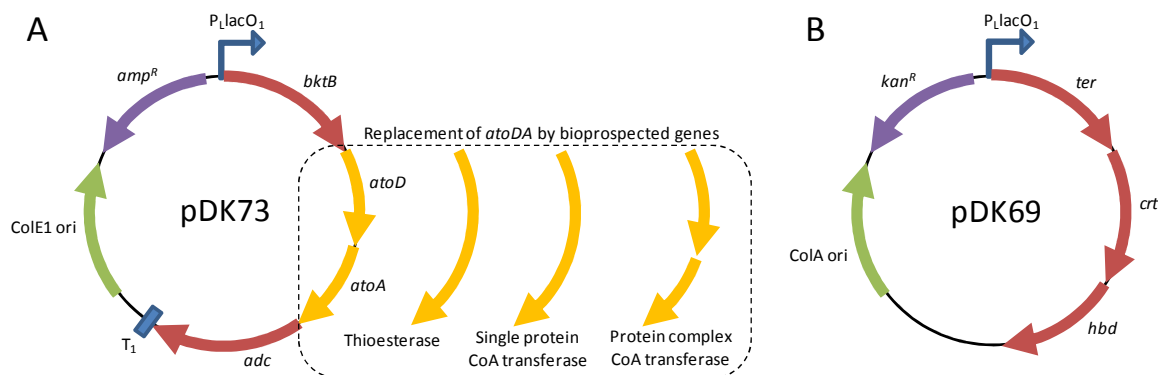
152

Figure 6.2. Plasmid maps for overexpressing 2-pentanone biosynthesis genes. Plasmid map of A) pDK73 and its derivatives, B) pDK69. Coexpression of these two plasmids enabled synthesis of 2-pentanone.

decarboxylase (Adc). By co-expressing the CoA dependent chain elongation (BktB, Crt, Hbd, and Ter) with AtoDA and Adc, we expected to synthesize 2-pentanone from 3-ketohexanoyl-CoA (Fig. 6.1).

To simultaneously express AtoDA, Adc, and the CoA dependent chain elongation pathway, we constructed two plasmids (Fig. 6.2) with different origins of replication. Plasmid pDK73 (Fig. 6.2A) harbored genes *bktB*, *atoDA*, and *adc* under an IPTG inducible promoter $P_L$lacO1. Plasmid pDK69 (Fig. 6.2B) harbored *ter*, *crt*, and *hbd,* which were also transcribed by promoter $P_L$lacO1. To minimize the formation of side products, mixed acid fermentation pathways were knocked out in the host strain JCL166 (Δldh, $\Delta frdB$, $\Delta adhE$). As shown in Fig. 6.3A, strain JCL166 expressing plasmid pTA30 (*atoB*, *atoDA*, *adc*) produced only acetone, and 2-pentanone was undetectable as expected. On the other hand, 6 mg/L of 2-pentanone (Fig. 6.3C) was produced by strain JCL166 expressing plasmid pDK73 (*bktB*, *atoDA*, *adc*) and pDK69 (*ter*, *crt*, *hbd*). Interestingly, 2 mg/L of 2-pentanone (Fig. 6.3B) was also produced by strain JCL166 expressing only plasmid pDK73, indicating that some native *E. coli* enzymes had the catalytic properties of the CoA dependent chain elongation. The identity of 2-pentanone produced was verified by GC-MS. The fragmentation pattern of the product (Fig. 6.3D) matched that of the 2-

acetone

A   No BktB

B   2-pentanone   BktB only
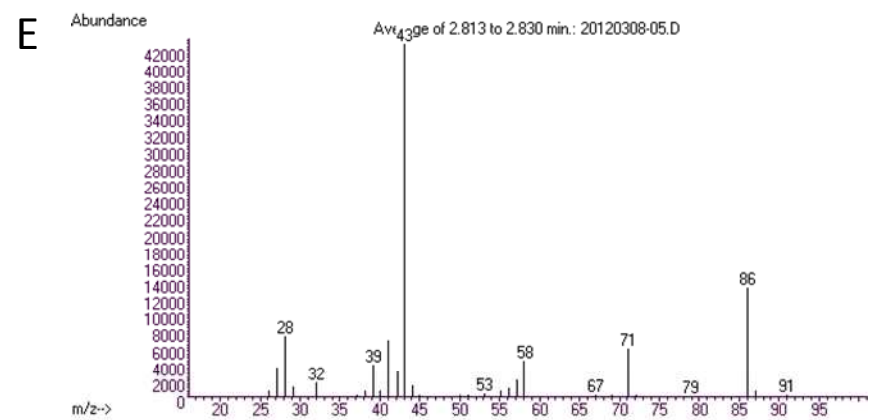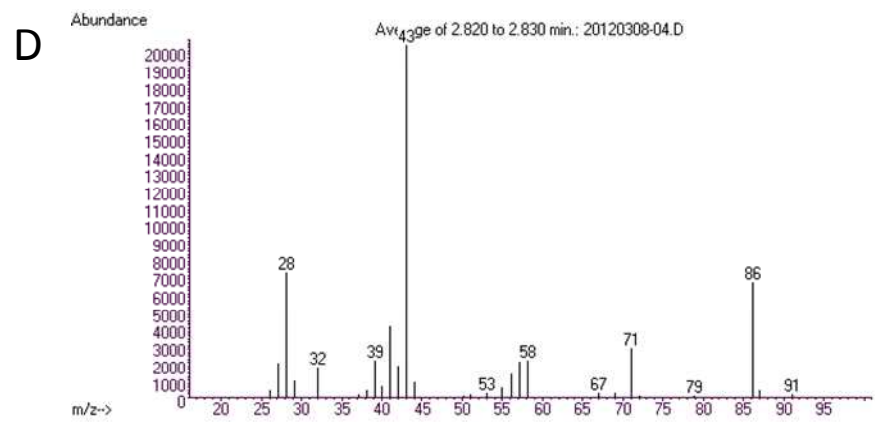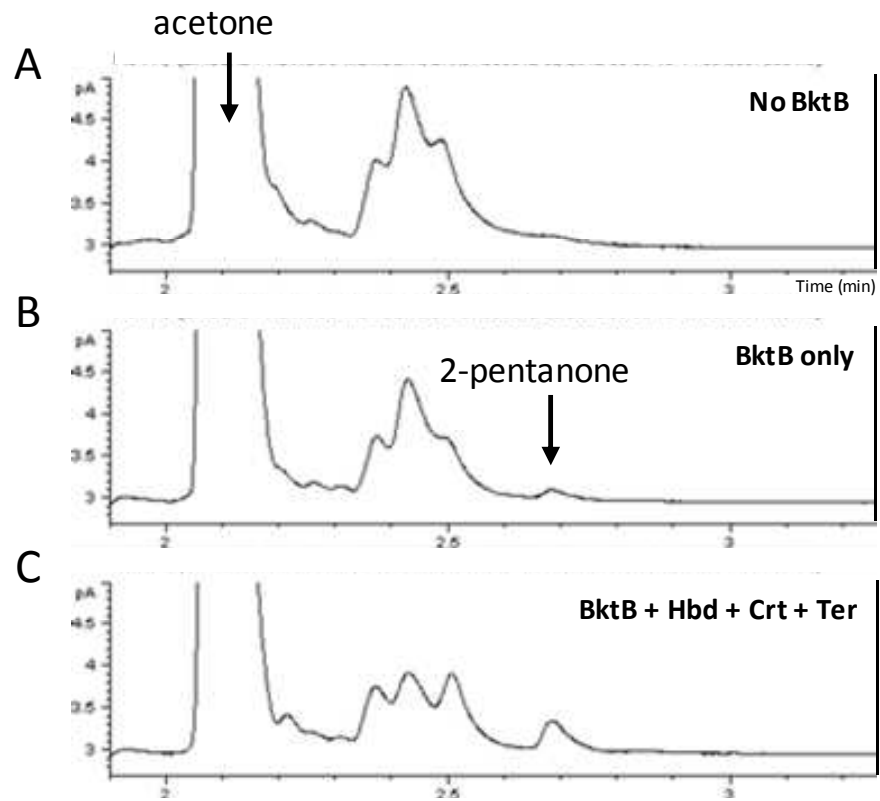
C   BktB + Hbd + Crt + Ter

D

E

Figure 6.3. Gas chromatogram of the 2-pentanone production. (A) JCL166/pTA30, (B) JCL166/pDK073 and (C) JCL166/pDK073/pDK069. Mass spectrum of (D) 2-pentanone produced by JCL166/pDK073/pDK069 and (E) 2-pentanone standard.

pentanone standard (Fig. 6.3E), confirming the compound produced by JCL166/pDK73/pDK69 was 2-pentanone. In all cases, the major product was acetone, indicating that either AtoDA and Adc were highly selective for four carbon substrates or they outcompeted chain elongation enzymes (BktB, Hbd, Crt, and Ter) in diverting carbon flux to acetone.

6.2.2. CoA transferase enables production

To determine the limiting step for 2-pentanone synthesis, we first compared 2-pentanone production pathway with that of the 1-hexanol production. The two pathways share the common intermediate 3-ketohexanoyl-CoA as the result of second round of carbon chain elongation. We previously demonstrated the production of 1-hexanol up to 500 mg/L (29), which is at least 2 orders of magnitude higher than the 2-pentanone produced. Therefore, the formation of 3-ketohexanoyl-CoA catalyzed by BktB is less likely to be the limiting step. Next, we rule out Adc as potential limiting step. Decarboxylation of β-keto acids to methyl-ketone is likely to occur spontaneously (16) and enables production of long chain methyl ketone up to 200 mg/L. Therefore we reasoned that the potential limiting step for 2-pentanone synthesis was AtoDA.

To search for a CoA transferase more suitable than AtoDA for 2-pentanone synthesis, we used the protein sequence of AtoD and BLAST to identify potential CoA transferases that are capable of removing CoA from 3-ketohexanoyl-CoA. We cloned CoA transferases from organisms including *Clostridium acetobutylicum*, *Clostridium beijerinckii*, *Clostridium difficile*, *Psudomonas putida*, *Helicobacter pylori*, *Xanthomonas campetris*, *Ralstonia eutropha*, and *Bacillus subtilis*. The identities of these homologues to AtoD range from 40% to 54%. CtfAB

155

from *C. acetobutylicum* (33) and *C. difficile* have been demonstrated and annotated, respectively, to catalyze the CoA transfer between acetate and acetoacetyl-CoA as well as between butyrate and acetoacetyl-CoA. On the other hand, the other transferases were annotated for catalyzing the CoA transfer between 3-keto acid and succinyl-CoA. To broaden our search for an enzyme efficient in converting 3-ketohexanoyl-CoA to 3-ketohexanoate, we cloned the single protein CoA transferase Cbei_2103 from *C. beijerinckii* and Cat1, Cat2, and Cat3 from *Clostridium kluyveri*. Additionally, we cloned thioesterases TesB, FadM, PaaI, and YbgC from *E. coli* to directly hydrolyze 3-ketohexanoyl-CoA.

The genes encoding for these CoA transferases and thioesterases were individually cloned to replace *atoDA* in plasmid pDK73 (Fig. 6.2A). These plasmids were transformed into *E. coli* with pDK69 to complete the pathway for 2-pentanone synthesis. The transformants vary greatly in colony size, indicating potential metabolic stress. Therefore, as a standard practice, we chose the smaller colonies to continue production assay. As shown in Fig. 6.4A, CoA transferase from *P. putida*, *H. pylori*, *X. campetris*, and *R. eutropha* increased the production of 2-pentanone as compared to AtoDA. In particular, PcaIJ of *P. putida* and Reut_1331_1332 of *R. eutropha* achieved the highest increase of 2-pentanone production to 99 ± 33 mg/L and 44 ± 9 mg/L respectively. The CoA transferases from *E. coli*, *C. acetobutylicum*, *C. beijerinckii* (*Cbei_2654_2653*), and *C. difficile* are selective for acetoacetyl-CoA as demonstrated by high acetone production (Fig. 6.4B) and minimal production of 2-pentanone. With the exception of PcaIJ from *P. putida* (34), the other enzymes demonstrated to aid 2-pentanone synthesis are uncharacterized proteins. Furthermore, enzymatic activities toward 3-ketohexanoyl-CoA of all enzymes tested were previously unknown. Therefore, the findings of this study may bring insights for the substrate specificity of these enzymes.
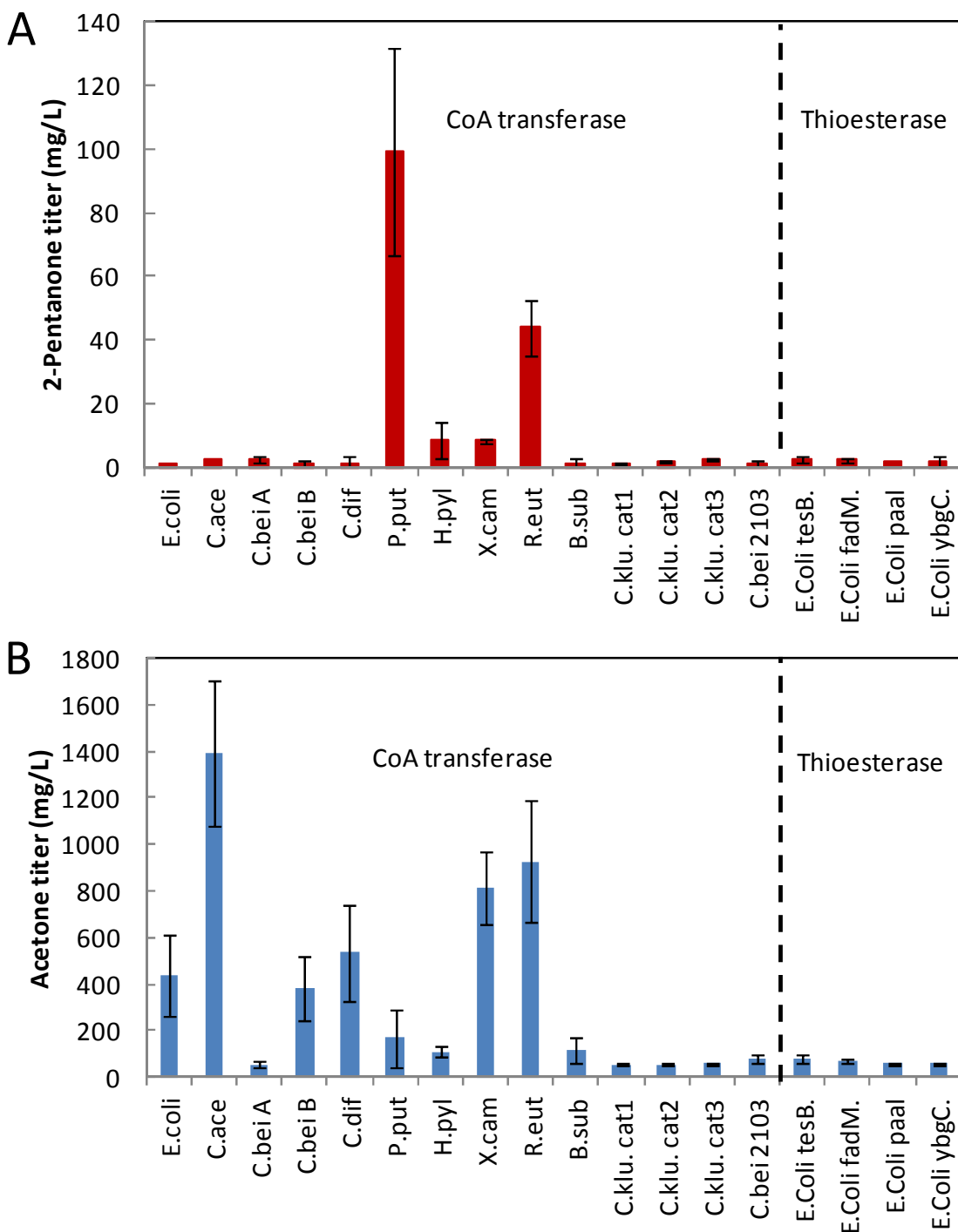
Figure 6.4. Production of 2-pentanone from expression CoA dependent chain elongation and bioprospected enzymes for converting 3-ketohexanoyl-CoA to 3-ketohexanoate. Host strain used was JCL166 ($\Delta adhE$, Δldh, $\Delta frdB$). Production was carried out in LB 1% glucose for 20 hours. Cbei A, 3833, 3834; Cbei B, 2654, 2653; gene names for other enzymes are listed in Table 6.1.

6.2.3. Time course of 2-pentanone production

The precursors for CoA dependent chain elongation and 2-pentanone production are acetyl-CoA and NADH. For each mole of 2-pentanone produced, three moles of acetyl-CoA and two moles of NADH are required. Glycolysis provides two acetyl-CoA and four NADH per mole of glucose consumed. Therefore, two moles of glucose can produce three moles of 2-pentanone, giving it a maximum theoretical yield of 67% molar conversion. However, for each mole of 2-pentanone produced, four moles of NADH are produced in excess. Therefore micro-aerobic environment was necessary for 2-pentanone production to avoid accumulation of NADH in strain JCL166. To increase the driving force for 2-pentanone production, we used *E. coli* strain JCL299 which is strain JCL166 with *pta* deleted to increase intracellular acetyl-CoA concentration. Accumulation of acetyl-CoA overcomes the large thermodynamic barrier (1)of the condensation reactions catalyzed by BktB.

To compare the effectiveness of different enzymes (PcaIJ vs *Reut_1331_1332) and acetyl-CoA driving force (with or without pta deletion),* plasmids pEL142 (harboring *bktB*, *pcaIJ*, and *adc*) and pEL145 (harboring *bktB*, *Reut_1331_1332*, *adc*) were individually transformed into JCL299 (Δ*ldhA* Δ*adhE* Δ*frdBC* Δ*pta*) and JCL166 (Δ*ldhA* Δ*adhE* Δ*frdBC*) with plasmid pDK69 (harboring *ter*, *crt*, and *hbd*). Time courses of the 2-pentanone and acetone productions in these strains are shown in Fig. 6.5. As expected, increasing intracellular acetyl-CoA by *pta* deletion (in JCL299) increased the production of 2-pentanone. 2-pentanone production (Fig 6.5A) by JCL299/pEL142/pDK69 (overexpressing PcaIJ) reached the highest titer of 240 mg/L. Strain JCL299/pEL145/pDK69 (overexpressing *Reut_1331_1332)* produced less 2-pentanone, reaching final titer of 110 mg/L. On the other hand, acetone production (Fig. 6.5B) from strain
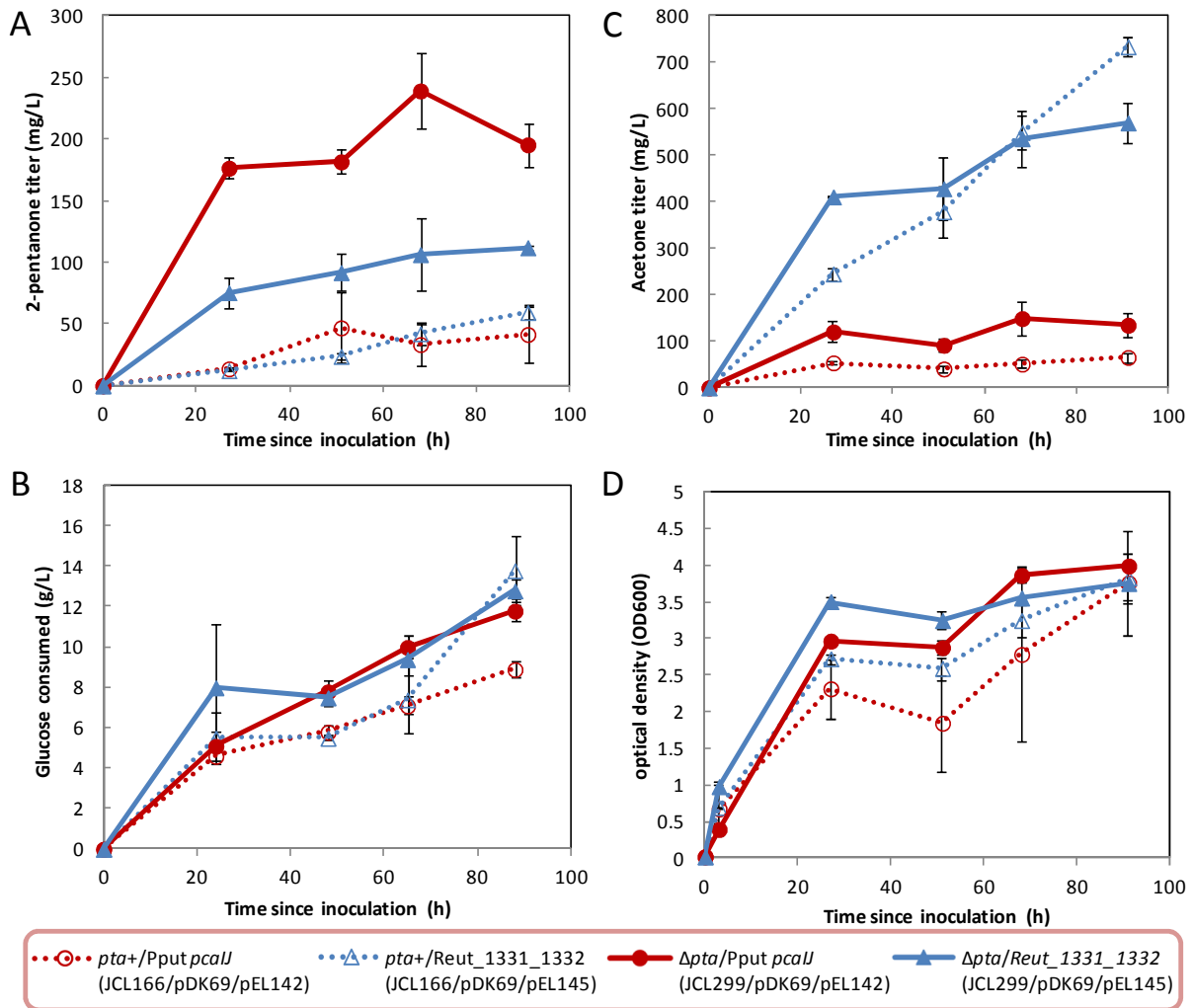
Figure 6.5. Time course for (A) production of 2-pentanone and (B) acetone, (C) glucose consumed, (D) cell density. *pta+* and Δ*pta* represent the presence and absence of pta on the chromosome, respectively.

JCL299/pEL145/pDK69 exceeded that from strain JCL299/pEL142/pDK69 by around 4 fold, indicating that *Reut_1331_1332* is more selective for acetoacetyl-CoA than PcaIJ.

To test if product toxicity inhibited production, we inoculated strain JCL299 into the TB medium supplemented with various concentrations of 2-pentanone and acetone. As shown in Fig. 6.6, 600 mg/L of 2-pentanone inhibits 50 % of the cell growth. At 5 g/L of 2-pentanone, growth was inhibited completely. On the other hand, acetone is much less toxic as 50% growth

Figure 6.6. Toxicity level of 2-pentanone and acetone to *E. coli*. Cell tolerance for 2-pentanone is significantly lower than that of acetone. 600 mg/L of 2-pentanone inhibited 50 % of growth.

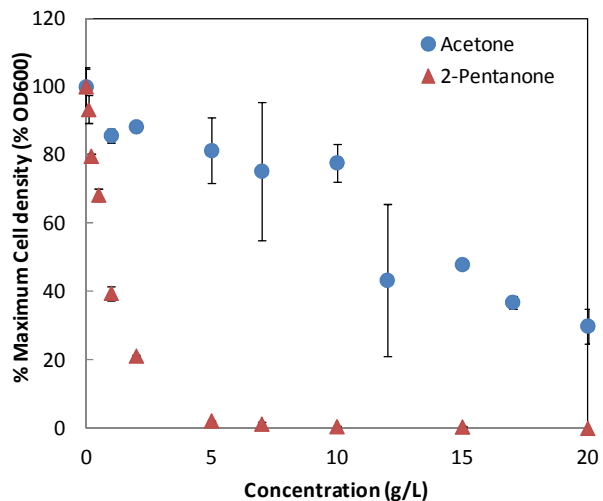inhibition occurs at 12 g/L of acetone. In our best producing strain JCL299/ pEL142/pDK69, the production of both 2-pentanone and acetone are below toxicity levels, indicating that the cease of production is unlikely due to toxicity, and further improvement is possible.

6.3. Discussion

Natural organisms use a finite set of pathways and chemistry to synthesize metabolites required for growth and survival. Some of these metabolites may serve as fuels, chemicals, and pharmaceuticals. To expand the chemical space available from microbes, synthetic biology and metabolic engineering methods are employed for designing new metabolic pathways. By hybridizing different pathway features, new chemicals are produced by recombinant microbes. These synthetic pathways can then be integrated into various microorganisms capable of utilizing a variety of resources such as CO_2 (35-37), syngas (38), and waste proteins (3), thus broadening the choice of green production strategies.

Here we engineered a strain of *E. coli* to produce 2-pentanone at 240 mg/L in 3 days by constructing a synthetic 2-pentanone production pathway based on CoA dependent chain elongation. CoA transferase step was identified as the potential limiting step for 2-pentanone synthesis as demonstrated by enhanced production upon expression of PcaIJ from *P. putida*. PcaIJ has been identified as β-ketoadipate:succinyl-CoA transferase (34) involved in the degradation of benzoate and 4-hydroxybenzoate. It is likely that PcaIJ outperformed the other CoA transferases and thioesterases for 2-pentanone synthesis because of the similarity between its natural substrate 3-ketoadipate and 3-ketohexanoate, the precursor for 2-pentanone (Fig. 6.1). It is also possible that a competition for carbon flux exists between carbon chain elongation and the synthesis of acetone. A less efficient enzyme for freeing the CoA from acetoacetyl-CoA may facilitate chain elongation, preferentially enabling the synthesis of 2-pentanone.

When compared to the fatty acid dependent synthesis of methyl ketones, the ATP requirement of the 2-pentanone production pathway presented here is lower. The CoA dependent chain elongation is more efficient in ATP conservation than fatty acid synthesis because it directly utilizes acetyl-CoA as carbon addition unit instead of having to activate acetyl-CoA into malonyl-CoA with ATP. Furthermore, CoA transferase conserves the chemical energy stored in thioester bond whereas the hydrolysis catalyzed by thioesterase does not.

With some notable exceptions (5, 39), minimizing ATP expenditure has been an important strategy for metabolic engineering, as increased ATP consumption from heterologous pathways may lead to adverse effects in the cell and reduce biomass formation. Thus, the pathway presented here may be particularly suitable for organisms where conserving ATP is beneficial and manipulating acetyl-coA driving force is possible.

6.4. Materials and methods

6.4.1. Chemicals and reagents

All chemicals were purchased from Fisher Scientifics (Pittsburgh, PA) or Sigma-Aldrich (St. Louis, MO). KOD (*Thermococcus kodakaraensis* KOD1) hot start and KOD-extreme hot start DNA polymerases were purchased from EMD Biosciences (San Diego, CA). Phusion DNA polymerase, and ligases were purchased from New England Biolabs (Ipswich, MA). T5-Exonuclease was purchased from Epicentre Biotechnologies (Madison, WI). Oligonucleotides were obtained from IDT (San Diego, CA).

6.4.2. Plasmid constructions

Plasmids used in this work are listed in Table 6.1. All plasmids were constructed by the isothermal DNA assembly method (30). Plasmids were propagated and stored in *E. coli* strain XL-1 blue. Promoter and enzyme coding regions of all plasmids were verified by DNA sequencing performed by Genewiz (San Diego, CA).

Plasmids pEL134, pEL135, pEL136, pEL137, pEL138, pEL139, pEL140, pEL142, pEL143, pEL144, pEL145, pEL146, pDC13, pDC14, pDC15, pDC16, pDC17, pDC18, pDC20, and pDC21 were constructed by replacing the *atoDA* gene (Fig. 6.2A) of pDK73 with individual genes listed in Table 6.1. These plasmids were constructed by DNA assembly of a linear DNA fragment containing *adc*, ColE1 origin, ampicillin resistance, $P_L$lacO$_1$ promoter, and *bktB* with individual genes listed in Table 6.1 for each plasmid. Primers used in this work are listed in Table 6.2.

6.4.3. Culture condition for 2-pentanone production

Production of 2-pentanone was either carried out in LB (10 g tryptone, 5 g yeast extract, and 5 g NaCl per liter of water) or in Terrific Broth (TB) (12 g tryptone, 24 g yeast extract, 2.31 g KH2PO4, 12.54 g K2HPO4, 4 ml glycerol per liter of water) supplemented with glucose (1% for LB and 4% for TB) . Pre-cultures were grown in LB overnight in 37 °C. 300 µL of the pre-cultures were then used to inoculate 3 mL of fresh medium in 15 mL BD vacutainer. Microaerobic condition was achieved by capping the BD vacutainer without anaerobic purging. The cultures were grown to OD630 of 0.4 to 0.6, which was then induced with 0.1 mM IPTG (Isopropyl β-D-1-thiogalactopyranoside). Induced cultures were then incubated in 37 °C shaker (250 rpm; New Brunswick Scientific, Enfield, CT) until sampling. For the bioprospecting enzymes capable of hydrolyzing CoA from 3-ketohexanoyl-CoA experiments, LB with 1 % (w/v) glucose was used as the culture medium. For time-course experiments, TB with 4 % (w/v) glucose was used.

6.4.4. Toxicity test for 2-pentanone and acetone

3 mL of Fresh TB supplemented with 4% glucose and varying concentration of 2-pentanone or acetone in BD vacutainer was inoculated at 0.1% (3 uL cell per 3mL medium) with strain JCL299 overnight preculture. Cultures were then incubated in 37 °C shaker at 250 rpm for 6 hours. After 6 hours of incubation, the cells were taken out for optical density measurement using Beckman Coulter DU 800.

6.4.5. Quantification of 2-pentanone

Culture samples were prepared by centrifuging (21,000 x g) the production cultures to separate the cell and supernatant. 200 µL of the supernatant was then mixed with 800 µL of 0.1% (v/v) 2-methyl-1-pentanol as the internal standard. The sample mixtures were then analyzed by gas chromatography equipped with flame ionization detector (Model 6850, Agilent Technologies, Santa Clara, CA). The separation of products was carried out with a DB-FFAP capillary column (Agilent Technologies, 30 m; 0.32 mm inner diameter; 0.25 µm film thickness). The GC result was analyzed by Agilent software Chem Station (Rev.B.04.01 SP1). The amount of 2-pentanone in the sample was then calculated based on the ratio of its integrated area and that of the 2-pentanone standard.

Helium was used as the carrier gas with 9.52 psi inlet pressure. The injector and detector temperatures were maintained at 225°C. Injection volume was 1 µL. Column flow rate was 1.7 ml/min. The oven program was as follows: 60 °C for 2 min, ramp to 85 °C at 45 °C/min, 85 °C for 2 min, ramp to 235 °C at 45 °C/min, 235 °C for 1 min.

6.4.6. GC-MS analysis

To analyze the supernatant of the production culture, 2-pentanone was extracted with n-hexane. 500 µL of supernatant was mixed with 200 µL of hexane. The organic layer was then Organic layer was analyzed by GC-MS system (model 6890N GC/5973N MSD, Agilent Technologies) equipped with a HP-5MS capillary column (Agilent Technologies, 30 m; 0.25 mm inner diameter; 0.25 µm film thickness). Helium (constant flow 1 mL/min) was used as a carrier gas. The temperature of the injector was 250 °C. The oven program was as follows: 50 °C for 3

min, ramp to 100 °C at 5 °C/min, 100 °C for 0 min, ramp to 250 °C at 50 °C/min, 250 °C for 1

min.

Table 6.1. Strain and plasmid list

Strain	Relevant genotypes	Reference
XL1-Blue	*recA1 endA1 gyrA96 thi-1 hsdR17 supE44 relA1 lac* [F' *proAB lacI^qZΔM15 Tn10* (Tet^R)]	Stratagene
BW25113	*rrnB*$_{T14}$ Δ*lacZ*$_{WJ16}$ *hsdR*514 Δ*araBAD*$_{AH33}$ Δ*rhaBAD*$_{LD78}$	1
JCL16	BW25113 / F' [*traD36, proAB+, lacI^q ZΔM15* (Tet^R)]	1
JCL166	JCL16 Δ*ldhA* Δ*adhE* Δ*frdBC*	1
JCL299	JCL16 Δ*ldhA* Δ*adhE* Δ*frdBC* Δ*pta*	1

Plasmid	genotypes	Reference
pTA30	*P*$_L$lacO$_1$::*atoB atoDA adc;* ColE1; Amp^R	24
pIM8	*P*$_L$lacO$_1$::*ter;* ColA; Kan^R	1
pDK69	*P*$_L$lacO$_1$::*ter crt hbd;* ColA; Kan^R	This work
pDK73	*P*$_L$lacO$_1$::*bktB atoDA adc;* ColE1; Amp^R	This work
pEL137	*P*$_L$lacO$_1$::*bktB ctfAB(C.ace) adc;* ColE1; Amp^R	This work
pEL138	*P*$_L$lacO$_1$::*bktB Cbei_3833 3834 adc;* ColE1; Amp^R	This work
pEL139	*P*$_L$lacO$_1$::*bktB Cbei_2654 2653 adc;* ColE1; Amp^R	This work
pEL140	*P*$_L$lacO$_1$::*bktB ctfAB(C.dif) adc;* ColE1; Amp^R	This work
pEL142	*P*$_L$lacO$_1$::*bktB pcaIJ(P.put) adc;* ColE1; Amp^R	This work
pEL143	*P*$_L$lacO$_1$::*bktB scoAB(H.pyl) adc;* ColE1; Amp^R	This work
pEL144	*P*$_L$lacO$_1$::*bktB IpsIJ(X.cam) adc;* ColE1; Amp^R	This work
pEL145	*P*$_L$lacO$_1$::*bktB R.eut_1331 1332 adc;* ColE1; Amp^R	This work
pEL146	*P*$_L$lacO$_1$::*bktB scoAB(B.sub) adc;* ColE1; Amp^R	This work
pDC13	*P*$_L$lacO$_1$::*bktB cat1(C.klu) adc;* ColE1; Amp^R	This work
pDC14	*P*$_L$lacO$_1$::*bktB cat2(C.klu) adc;* ColE1; Amp^R	This work
pDC15	*P*$_L$lacO$_1$::*bktB cat3(C.klu) adc;* ColE1; Amp^R	This work
pDC16	*P*$_L$lacO$_1$::*bktB Cbei_2103 adc;* ColE1; Amp^R	This work
pDC17	*P*$_L$lacO$_1$::*bktB tesB adc;* ColE1; Amp^R	This work
pDC18	*P*$_L$lacO$_1$::*bktB fadM adc;* ColE1; Amp^R	This work
pDC20	*P*$_L$lacO$_1$::*bktB paaI adc;* ColE1; Amp^R	This work
pDC21	*P*$_L$lacO$_1$::*bktB ybgC adc;* ColE1; Amp^R	This work

Kan^R, kanamycin resistance; Amp^R, ampicillin resistance.

atoB (*E. coli*), thiolase; *bktb* (*R. eutropha*), β-keto-thiolase; *hbd* (*C. acetobutylicum*), hydroxybutyryl-CoA dehydrogenase; *crt* (*C. acetobutylicum*), crotonase; *ter* (*T. denticola*), *trans*-2-enoyl-CoA reductase; *pcaIJ* (*P. putida*), 3-oxoadipate CoA-succinyl transferase; *atoDA* (*E. coli*), acetate CoA-transferase; R. eut, *Ralstonia eutropha*; C. ace, *Clostridium acetobutylicum*; T. den, *Treponema denticola*; P. put, *Pseudomonas putida*; E. col, *Escherichia coli*; C. bei, *Clostridium beijerinckii*; C. dif, *Clostridium difficile*; H. pyl, *Helicobacter pylori*; X. cam, *Xanthomonas campestris*; C. klu, *Clostridium kluyveri*.

Table 6.2. Primer Sequences

Primers	Sequence (5' -> 3')	Used for plasmid
rEL-556	TAATGATCTAGAAGGAGATATACCATGTTAAAGGA	pEL137, pEL138, pEL139 pEL140, pEL142, pEL143, pEL144, pEL145, pEL146, pDC13, pDC14, pDC15, pDC16, pDC17, pDC18, pDC20, pDC21
rEL-557	CATGGTACCTTTCTCCTGCATGCTTAGATAC	pEL137, pEL138, pEL139 pEL140, pEL142, pEL143, pEL144, pEL145, pEL146, pDC13, pDC14, pDC15, pDC16, pDC17, pDC18, pDC20, pDC21
rEL-558	TCTAAGCATGCAGGAGAAAGGTACCATGAACTCTAAAATAATTAGATTTGAAAATTTAAG	pEL137
rEL-559	TATCATTAATCATGGTATATCTCCTTTATGCAGGCTCCTTTACTATATAATTTATAAG	pEL137
rEL-560	CTGCATAAAGGAGATATACCATGATTAATGATAAAAACCTAGCGAAAGAAATAAT	pEL137
rEL-561	GTATATCTCCTTCTAGATCATTAAACAGCCATGGGTCTAAGTTCATTG	pEL137
rEL-562	TCTAAGCATGCAGGAGAAAGGTACCATGAATAAATTAGTAAAATTAACAGATTTAAAGCG	pEL138
rEL-563	AAGTAATGTTCATGGTATATCTCCTTTAAGCCGCCTCCTTAACGATATAATC	pEL138
rEL-564	AGGCGGCTTAAAGGAGATATACCATGAACATTACTTTTGAATCAGAAAATGGC	pEL138
rEL-565	GTATATCTCCTTCTAGATCATTATATATCCATAATCTTTAAGTTATCTGGAATAA	pEL138
rEL-566	TCTAAGCATGCAGGAGAAAGGTACCATGACAAAGATTAAGACAGTACAGGAAGCAG	pEL139
rEL-567	CATTTTCATGGTATATCTCCTTTATCTCATTTTATTAGTTCTTATCCATAAATCTT	pEL139
rEL-568	TGAGATAAAGGAGATATACCATGAAAATGATGAATGGTAAAGAGATAATTGC	pEL139
rEL-569	GTATATCTCCTTCTAGATCATTATATTTCCATTTCCTTAACATTATCAGCTATTA	pEL139
rEL-570	TCTAAGCATGCAGGAGAAAGGTACCATGAATAAAATAGTTAGCATTGATGAAGCTCTA	pEL140
rEL-571	ATTTATCCATGGTATATCTCCTTTATAAATTACCTCCTTCAACGATGTAATTC	pEL140
rEL-572	AATTTATAAAGGAGATATACCATGGATAAATTAGAAATGCAAGAATATATTGC	pEL140
rEL-573	GTATATCTCCTTCTAGATCATTAAACAACAGATATTTTTCCATTTAATGAATC	pEL140
rEL-578	TCTAAGCATGCAGGAGAAAGGTACCATGATCAATAAAACGTATGAGTCCATCG	pEL142
rEL-579	TGGTAATGGTCATGGTATATCTCCTTTAGACAGCGTTTGCGATCGAAGAA	pEL142
rEL-580	AAACGCTGTCTAAAGGAGATATACCATGACCATTACCACAAAACTTTCCC	pEL142
rEL-581	GTATATCTCCTTCTAGATCATTACTTGATCAGCGGCACACCACTG	pEL142
rEL-582	TCTAAGCATGCAGGAGAAAGGTACCATGAACAAGGTTATAACCGATTTAGACAAA	pEL143
rEL-583	CCTCTCTCATGGTATATCTCCTTTATTTCGCACTCCTTGTGGTGGTTT	pEL143
rEL-584	GTGCGAAATAAAGGAGATATACCATGAGAGAGGCTATCATTAAACGAGCG	pEL143
rEL-585	GTATATCTCCTTCTAGATCATTATAGATGCACTTCAAATTCAGCTTCTGT	pEL143
rEL-586	TCTAAGCATGCAGGAGAAAGGTACCATGGACAAGGTGGTCGCCACAGC	pEL144
rEL-587	GTGTCCAGGCCATGGTATATCTCCTTTAGCCGCTCACCGTCCCGGTT	pEL144
rEL-588	ACGGTGAGCGGCTAAAGGAGATATACCATGGCCTGGACACGCGAGGAGA	pEL144
rEL-589	GTATATCTCCTTCTAGATCATTACGAGCGGATCTCCTCCGGG	pEL144
rEL-590	TCTAAGCATGCAGGAGAAAGGTACCATGAACCAAGTTGCAAGGGG	pEL145
rEL-591	GGGTCCAGGCCATGGTATATCTCCTTTACTTGTCTCCCTGGCGCACGG	pEL145
rEL-592	GAGACAAGTAAAGGAGATATACCATGGCCTGGACCCGCGATCAGA	pEL145
rEL-593	GTATATCTCCTTCTAGATCATTAGCCTCTTGTTTGTACAACGAAC	pEL145
rEL-594	TCTAAGCATGCAGGAGAAAGGTACCATGAACAAGGTCTACGCCAGCGC	pEL146

rEL-595	CGTGTCCATGCCATGGTATATCTCCTTTAGCTGGCCGCGCGCACGGTG	pEL146
rEL-596	GCGGCCAGCTAAAGGAGATATACCATGGCATGGACACGTGACGAAATGG	pEL146
rEL-597	GTATATCTCCTTCTAGATCATTACAGCAGCGGAGCGCCAGTC	pEL146
rEL-598	TCTAAGCATGCAGGAGAAAGGTACCATGGGAAAAGTGCTGTCATCAAGC	pEL147
rEL-599	TCGCTTCCTTCATGGTATATCTCCTTTACTTGGCCTCACCCTTTCCC	pEL147
rEL-600	TGAGGCCAAGTAAAGGAGATATACCATGAAGGAAGCGAGAAAACGAATGG	pEL147
rEL-601	GTATATCTCCTTCTAGATCATTAAGAATTGAGTACAGACTGGCTTACAGC	pEL147
DC23-cat1-F	GAGCGTATCTAAGCATGCAGGAGAAAGGTACCATGAGTAAAGGGATAAGAATTC	pDC13
DC24-cat1-R	TAACATGGTATATCTCCTTCTAGATCATTATTTCATACTACCAGTTTTTATAA	pDC13
DC25-cat2-F	TTCGAGCGTATCTAAGCATGCAGGAGAAAGGTACCATGGAGTGGGAAGAGATATAT	pDC14
DC26-cat2-R	CTTTAACATGGTATATCTCCTTCTAGATCATTAAAATCTCTTTTTAAATTCATTCATT	pDC14
DC27-cat3-F	GCGTATCTAAGCATGCAGGAGAAAGGTACCATGGTTTTTAAAAATTGGCAGGATCT	pDC15
DC28-cat3-R	CATCCTTTAACATGGTATATCTCCTTCTAGATCATTAAAGCTTACAACTGAATCTT	pDC15
DC29-2103-F	AGCATGCAGGAGAAAGGTACCGTGTCTAAGATTAGCTGGAAAGATTTATACAAGAGTAA	pDC16
DC30-2103-R	CATGGTATATCTCCTTCTAGATCATTAAAATTTCACTTTAAACCTCTTTTCCCACTCTT	pDC16
DC31-tesB-F	GAGCGTATCTAAGCATGCAGGAGAAAGGTACCATGAGTCAGGCGCTAAAAAATTTAC	pDC17
DC32-tesB-R	CCTTTAACATGGTATATCTCCTTCTAGATCATTAATTGTGATTACGCATCACCCCT	pDC17
DC33-fadM-F	GAGCGTATCTAAGCATGCAGGAGAAAGGTACCATGCAAACACAAATCAAAGTTC	pDC18
DC34-fadM-R	ATGGTATATCTCCTTCTAGATCATTACTTAACCATCTGCTCCAGCTTTTCGCGC	pDC18
DC-37-paal-F	CGTATCTAAGCATGCAGGAGAAAGGTACCATGAGTCATAAGGCCTGGCAAAAT	pDC20
DC-38-paal-R	TCATCCTTTAACATGGTATATCTCCTTCTAGATCATTAGGCTTCTCCTGTAATGGTG	pDC20
DC-39-ybgC-F	CGAGCGTATCTAAGCATGCAGGAGAAAGGTACCGTGAATACAACGCTGTTTCGATGGC	pDC21
DC-40-ybgC-F	TCCTTTAACATGGTATATCTCCTTCTAGATCATTACTGCTTAAACTCCGCGACAAT	pDC21
pDK024 BB F2	CGACGGTATCGATAAGCTTGATATCGAATTCCTG	pDK69
pDK037 BB R1	GGTATATCTCCTTCTAGACTAAATCCTGTCGAACCTTTC	pDK69
pDK069 crt-hbd F1	GGATTTAGTCTAGAAGGAGATATACCATGGAACTAAACAATG	pDK69
pDK069 crt-hbd R1	CGATATCAAGCTTATCGATACCGTCGATTATTTTGAATAATCGTAGAAACC	pDK69
pDK062 BB F1	CTAGAGGCATCAAATAAAACGAAAGGC	pDK73
pDK006 BB R1	CCTCTTTAATGAATTCGGTCAGTGCGTCC	pDK73
pDK006 bktB F1	CGCACTGACCGAATTCATTAAAGAGGAGAAAGGTACCATGACGCGTGAAGTGGTAGTGG	pDK73
pDK049 fars BB R1	CTCCTGCATGCTTAGATACGCTCGAAG	pDK73
pDK072 atoDA F1	CGAGCGTATCTAAGCATGCAGGAGAAAGGTACCATGAAAACAAAATTGATGACATTAC	pDK73
pDK072 atoDA R1	CATCCTTTAACATGGTATATCTCCTTCTAGATCATAAATCACCCCGTTGCGTATTC	pDK73
pDK068 adc F1	GGAGATATACCATGTTAAAGGATGAAGTAATTAAAC	pDK73
pDK071 adc R1	GCCTTTCGTTTTATTTGATGCCTCTAGATTACTTAAGATAATCATATATAAC	pDK73

6.5. Reference

1. Shen CR, et al. (2011) Driving forces enable high-titer anaerobic 1-butanol synthesis in Escherichia coli. Appl Environ Microbiol 77(9):2905-2915.

2. Higashide W, Li Y, Yang Y, & Liao JC (2011) Metabolic engineering of Clostridium cellulolyticum for production of isobutanol from cellulose. Appl Environ Microbiol 77(8):2727-2733.

3. Huo YX, et al. (2011) Conversion of proteins into biofuels by engineering nitrogen flux. Nat Biotechnol 29(4):346-351.

4. Atsumi S, Higashide W, & Liao JC (2009) Direct photosynthetic recycling of carbon dioxide to isobutyraldehyde. Nat Biotechnol 27(12):1177-1180.

5. Lan EI & Liao JC (2012) ATP drives direct photosynthetic production of 1-butanol in cyanobacteria. Proc Natl Acad Sci USA 109(16):6018-6023.

6. Shen CR & Liao JC (2012) Photosynthetic production of 2-methyl-1-butanol from CO2 in cyanobacterium Synechococcus elongatus PCC7942 and characterization of the native acetohydroxyacid synthase. Energy Environ Sci 5(11):9574-9583.

7. Lan EI & Liao JC (2012) Microbial synthesis of n-butanol, isobutanol, and other higher alcohols from diverse resources. Bioresour Technol.

8. Atsumi S, Hanai T, & Liao JC (2008) Non-fermentative pathways for synthesis of branched-chain higher alcohols as biofuels. Nature 451(7174):86-89.

9. Yim H, et al. (2011) Metabolic engineering of Escherichia coli for direct production of 1,4-butanediol. Nat Chem Biol 7(7):445-452.

10. Ro DK, et al. (2006) Production of the antimalarial drug precursor artemisinic acid in engineered yeast. Nature 440(7086):940-943.

11. Xia XX, et al. (2010) Native-sized recombinant spider silk protein produced in metabolically engineered Escherichia coli results in a strong fiber. Proc Natl Acad Sci USA 107(32):14059-14063.

12. Jones DT & Woods DR (1986) Acetone-butanol fermentation revisited. Microbiol Rev 50(4):484-524.

13. Fadda S, Lebert A, Leroy-Setrin S, & Talon R (2002) Decarboxylase activity involved in methyl ketone production by Staphylococcus carnosus 833, a strain used in sausage fermentation. FEMS Microbiol Lett 210(2):209-214.

14. Forney FW & Markovetz AJ (1971) The biology of methyl ketones. J Lipid Res 12(4):383-395.

15. Pettersson J, Karlsson PC, Goransson U, Rafter JJ, & Bohlin L (2008) The flavouring phytochemical 2-pentanone reduces prostaglandin production and COX-2 expression in colon cancer cells. Biol Pharm Bull 31(3):534-537.

16. Goh EB, Baidoo EE, Keasling JD, & Beller HR (2012) Engineering of bacterial methyl ketone synthesis for biofuels. Appl Environ Microbiol 78(1):70-80.

17. Ezeji TC, Qureshi N, & Blaschek HP (2007) Bioproduction of butanol from biomass: from genes to bioreactors. Curr Opin Biotechnol 18(3):220-227.

18. Tracy BP, Jones SW, Fast AG, Indurthi DC, & Papoutsakis ET (2012) Clostridia: the importance of their exceptional substrate and metabolite diversity for biofuel and biorefinery applications. Curr Opin Biotechnol 23(3):364-381.

19. Shen CR & Liao JC (2011) A Synthetic Iterative Pathway for Ketoacid Elongation. Method Enzymol 497:469-481.

20. Felnagle EA, Chaubey A, Noey EL, Houk KN, & Liao JC (2012) Engineering synthetic recursive pathways to generate non-natural small molecules. Nat Chem Biol 8(6):518-526.

21. Dellomonaco C, Clomburg JM, Miller EN, & Gonzalez R (2011) Engineered reversal of the beta-oxidation cycle for the synthesis of fuels and chemicals. Nature 476(7360):355-359.

22. Atsumi S, et al. (2008) Metabolic engineering of Escherichia coli for 1-butanol production. Metab Eng 10(6):305-311.

23. Berezina OV, et al. (2010) Reconstructing the clostridial n-butanol metabolic pathway in Lactobacillus brevis. Appl Microbiol Biotechnol 87(2):635-646.

24. Inui M, et al. (2008) Expression of Clostridium acetobutylicum butanol synthetic genes in Escherichia coli. Appl Microbiol Biotechnol 77(6):1305-1316.

25. Nielsen DR, et al. (2009) Engineering alternative butanol production platforms in heterologous bacteria. Metab Eng 11(4-5):262-273.

26. Steen EJ, et al. (2008) Metabolic engineering of Saccharomyces cerevisiae for the production of n-butanol. Microb Cell Fact 7(36).

27. Bond-Watts BB, Bellerose RJ, & Chang MCY (2011) Enzyme mechanism as a kinetic control element for designing synthetic biofuel pathways. Nat Chem Biol 7(4):222-227.

28. Dekishima Y, Lan EI, Shen CR, Cho KM, & Liao JC (2011) Extending Carbon Chain Length of 1-Butanol Pathway for 1-Hexanol Synthesis from Glucose by Engineered Escherichia coli. J Am Chem Soc 133(30):11399-11401.

29. Machado HB, Dekishima Y, Luo H, Lan EI, & Liao JC (2012) A selection platform for carbon chain elongation using the CoA-dependent pathway to produce linear higher alcohols. Metab Eng.

30. Gibson DG, et al. (2009) Enzymatic assembly of DNA molecules up to several hundred kilobases. Nat Methods 6(5):343-345.

31. Hanai T, Atsumi S, & Liao JC (2007) Engineered synthetic pathway for isopropanol production in Escherichia coli. Appl Environ Microbiol 73(24):7814-7818.

32. Bermejo LL, Welker NE, & Papoutsakis ET (1998) Expression of Clostridium acetobutylicum ATCC 824 genes in Escherichia coli for acetone production and acetate detoxification. Appl Environ Microbiol 64(3):1079-1085.

33. Wiesenborn DP, Rudolph FB, & Papoutsakis ET (1989) Coenzyme A transferase from Clostridium acetobutylicum ATCC 824 and its role in the uptake of acids. Appl Environ Microbiol 55(2):323-329.

34. Parales RE & Harwood CS (1992) Characterization of the genes encoding beta-ketoadipate: succinyl-coenzyme A transferase in Pseudomonas putida. J Bacteriol 174(14):4657-4666.

35. Lan EI & Liao JC (2011) Metabolic engineering of cyanobacteria for 1-butanol production from carbon dioxide. Metab Eng 13(4):353-363.

36. Li H, et al. (2012) Integrated electromicrobial conversion of CO2 to higher alcohols. Science 335(6076):1596.

37. Shen CR & Liao JC (2012) Photosynthetic production of 2-methyl-1-butanol from CO2 in cyanobacteria Synechococcus elongatus PCC7942 and characterization of the native acetohydroxyacid synthase. Energy Environ Sci.

38. Kopke M, et al. (2010) Clostridium ljungdahlii represents a microbial production platform based on syngas. Proc Natl Acad Sci USA 107(29):13087-13092.

39. Causey TB, Zhou S, Shanmugam KT, & Ingram LO (2003) Engineering the metabolism of Escherichia coli W3110 for the conversion of sugar to redox-neutral and oxidized products: Homoacetate production. Proc Natl Acad Sci USA 100(3):825-832.